Development of bioprocess for treatment of Mn(II)-contaminated metal refinery wastewaters

サンティサック, ギッチャーヌギット

https://doi.org/10.15017/2534416

出版情報：Kyushu University, 2019, 博士（工学）, 課程博士
バージョン：
権利関係：

Development of bioprocess for treatment of Mn(II)-contaminated metal refinery wastewaters

By

Santisak Kitjanukit

A thesis submitted in partial fulfilment of the requirements for the degree of
DOCTOR OF ENGINEERING

Department of Earth Resources Engineering
Graduate School of Engineering
Kyushu University
Fukuoka, Japan

September 2019

Abstract

Contamination of manganese (Mn) in wastewaters, especially from metal-refinery industries, is a challenging problem. Since Mn^{2+} is thermodynamically stable over the wide range of pH (0-8) and its chemical oxidation promoted at alkaline pHs, a vast cost is needed for neutralizing-agents in conventional Mn-removal processes. On the other hand, microbiological (enzymatic) reactions enable oxidative precipitation of Mn^{2+} as biogenic birnessite at circumneutral pHs ($Mn^{2+} + 1/2O_2 + H_2O \rightarrow Mn^{III, IV}O_2 + 2H^+$; Eq. 1), even without the addition of chemical oxidizing-agents. Therefore, the development of bioprocess for Mn^{2+}-contaminating wastewater could become a more economical and environmentally feasible alternative. This study first analyzed the natural Mn^{2+} attenuation phenomena in the metal-refinery wastewater pipeline, from which a new Mn-oxidizing bacterium was isolated. The isolate was identified and further evaluated for its Mn-oxidation capability focusing on several metal-refinery water characteristics. Secondly, the individual contribution of biological (by bacteria) and chemical (by Mn-oxides) effect on Mn-oxidation was clarified. Lastly, the continuous biofilter column was constructed to test its feasibility for actual metal-refinery wastewater. Moreover, to find an additional value to the resultant biogenic Mn-oxide product, its potential utility for remediation of toxic arsenite (As(III)) was investigated.

In **chapter 1**, background information regarding the properties of Mn and its contamination problems were introduced. Previous studies related to the present work were reviewed and discussed in this chapter.

In **chapter 2**, methodologies used in this work were described.

Chapter 3 first described the phenomenon of natural Mn^{2+} attenuation observed in the actual metal-refinery wastewater pipeline, accompanied with extensive dark-brown-colored mineralization on the inner pipe surface (Mn^{2+} concentration

lowered from 1.n to 0.n mg/L after the wastewater traveled through a pipe). The dark-brown deposits taken from the pipe was characterized as mixed phases of crystalline $Mn^{IV}O_2$, $Mn^{III}_2O_3$, and Fe_2O_3 (the average oxidation state (AOS) of Mn was 3.75). Due to the high activation energy required for a spontaneous chemical Mn-oxidation, the involvement of microbiological activity was suspected. In fact, the Mn-deposit hosted the bacterial community comprised of *Hyphomicrobium* sp. (22.1%), *Magnetospirillum* sp. (3.2%), *Geobacter* sp. (0.3%), *Bacillus* sp. (0.18%), *Pseudomonas* sp. (0.03%), and non-metal-metabolizing bacteria (74.2%).

In **chapter 4**, culture enrichments of the Mn-deposit collected in chapter 3 was conducted. After selective screening on the solid agarose media, a Mn-oxidizing colony was isolated and named isolate SK3. Based on the 16S rRNA gene sequence analysis, the closest relative of isolate SK3 was *Pseudomonas* (*Ps.*) *resinovorans* (with 98.4% homology; 1398 bp), which is so far unknown as Mn-oxidizer. Next, isolate SK3 was tested for its Mn-oxidation ability under different conditions mimicking actual metal-refinery wastewater characteristics. When compared to the well-studied Mn-oxidizer *Ps. putida* MnB1, the superiority of isolate SK3 became noticeable: i.e. Oxidation of up to 100 mg/L Mn^{2+} readily progressed and completed by isolate SK3, even in the presence of high contents of $MgSO_4$ (up to 2400 mg/L; a typical solute in metal-refinery wastewaters). At this $MgSO_4$ concentration, *Ps. putida* MnB1 completely lost its Mn-oxidizing ability. Additional Cu^{2+} facilitated Mn-oxidation by isolate SK3 (implying the involvement of multicopper oxidase enzyme), allowing 2-fold greater Mn-removal rate, compared to the case of *Ps. putida* MnB1. Biogenic Mn-oxides formed by isolate SK3 was characterized by XRD as poorly-crystalline birnessite with high Mn^{IV} fraction of 0.86 and AOS of 3.8. Overall results in chapters 3-4 suggest that the natural Mn^{2+} attenuation phenomenon was featured by the robust

in-situ activity of Mn-oxidizers (including isolate SK3) for continuous generation of Mn^{IV}.

Mn-oxides produced by Mn-oxidizing bacteria are one of the strong chemical oxidants found in nature. From this point, Mn-oxidation in biological systems includes both direct enzymatic reaction (by microorganisms) and indirect chemical reaction (by Mn-oxides). Therefore, **chapter 5** aimed to clarify the individual contribution from the two. When only sterilized natural Mn-oxide (NMO) was provided, Mn-oxidation proceeded only to a limited extent by chemical synproportionation ($Mn^{2+} + Mn^{IV}O_2 + H_2O \rightarrow Mn^{III}{}_2O_3 + 2H^+$; Eq. 2). This was due to surface passivation of NMO with $Mn^{III}{}_2O_3$. When Mn-oxidizing SK3 cells were inoculated in addition to NMO, Mn-oxidation was significantly promoted, owing to the synergistic effect of chemical synproportionation and microbiological $Mn^{IV}O_2$ regeneration. The presence of NMO also likely provided the surface for bacterial colonization to support robust bacterial growth: This allowed isolate SK3 to oxidize Mn^{2+} even under originally inhibitory complex conditions such as at high $MgSO_4$ concentrations (2400 mg/L) and at a higher temperature (35°C).

Based on the fundamental knowledge obtained from the previous chapters, the continuous biofilter column tests were planned. Firstly, screening for the suitable column carrier (bacteria-supporting material) was conducted in **chapter 6**. Ten different SiO_2- or carbon-based materials were tested through the cycle Mn-oxidation test. The difference in the Mn-oxidation rate was noticed, especially in the first cycle. However, once Mn-oxides were attached to the support material, the difference gradually became smaller between the different materials. Nonetheless, generally greater effectiveness was noticed throughout the cycles with carbon-based materials, due to their higher affinity to both bacterial cells and Mn-oxides. Consequently,

activated carbon (AC) was chosen for further studies. While AC itself exhibited chemical Mn-oxidizing ability, its effect deteriorated after the second cycle (<40% Mn-removal) due to passivation of the product ($Mn^{III}_2O_3$). Overall, it was suggested that in the following AC-packed column test, the efficient Mn-removal would arise from synergistic interactions between; (i) active oxidation of Mn^{2+} by bacteria for continuous regeneration of $Mn^{IV}O_2$ (Eq. 1) (ii) chemical synproportionation effect of biogenic $Mn^{IV}O_2$ producing $Mn^{III}_2O_3$ from Mn^{2+} (Eq. 2) and (iii) chemical oxidation of Mn^{2+} by the AC surface, producing $Mn^{III}_2O_3$ (especially at the early-stage).

Finally, the laboratory-scale AC-packed biofilter column test was conducted in **chapter 7**, using two types of actual metal-refinery wastewaters (downstream water [Mn^{2+}] 2 mg/L, [SO_4^{2-}] 780 mg/L; upstream water [Mn^{2+}] 2-5 mg/L, [SO_4^{2-}] 1500 mg/L). The results obtained from this chapter were expected to offer improvement suggestions for the on-going pilot-scale test column constructed at the mental-refinery site. This *on-site* pilot-scale column was packed with zeolite with the current Mn-removal of around 40%. The advantage of using AC instead of SiO_2-based zeolite as column-carrier was reconfirmed in this test, as the contact time required for the complete Mn-removal was shortened with the former. Before starting the water flow (at the hydraulic retention time (HRT) of 20 min), AC granules pre-colonized with actively Mn-oxidizing SK3 cells were packed in the column, in order to kick-start the Mn-removal. The importance of organic supply was clearly indicated, since Mn-oxidation was catalyzed by heterotrophic bacteria: In fact, the addition of the minimum amount of yeast extract (0.01%) was essential to maintain high Mn-removal efficiency (65-90%, compared to 20-40% in control). For the treatment of upstream water with higher Mn^{2+} and SO_4^{2-} contents, the addition of pulverized AC to granule AC (at 3:7 ratio) promoted Mn-oxidation by 5-10%, resulting in about 85% final

Mn-removal at HRT 40 min, even after a harsh backwashing process. Overall results obtained in this chapter suggest that the following factors should be considered to improve performance of the *on-site* pilot-scale column; type of column-carrier, installation of pre-colonization step, the supply of suitable organic nutrient, optimization of HRT.

After the repeated use of the continuous biofilter column, the spent column carriers will be eventually produced. **Chapter 8** looked for a potential additional value of biogenic MnO_2 accumulated on the spent column carriers. Since groundwater contamination with As(III) is another significant problem associated with mining activity, biogenic MnO_2 was tested for its As(III) oxidation capability ($H_3As^{III}O_3 + Mn^{IV}O_2 + H^+ \rightarrow Mn^{2+} + H_2As^{V}O_4^- + H_2O$; Eq. 3). When synthetic As(III)-contaminated groundwater (pH 7) was tested, retaining active Mn-oxidizing SK3 cells on the MnO_2 surface enabled effective oxidation of As(III) to less toxic and mobile As(V). By so doing, it was possible to complete As(III) oxidation while no loss of Mn (as dissolved Mn^{2+}; Eq. 3) was made.

In **chapter 9**, conclusions and recommendations for future work were summarized.

要旨

金属製錬廃液を代表とするマンガン(Mn) による水質汚染は深刻な課題である。Mn^{2+} は広範囲の pH (0~8) 領域において熱力学的に安定に溶存するが、アルカリ pH でその化学的酸化が促進される。従来の Mn 除去法においては、酸性の製錬廃液に大量の中和剤を投入し、Mn 酸化物として沈殿除去するため、そのコストは膨大である。一方、微生物学的（酵素学的）Mn 酸化反応は化学的酸化剤の添加なくして中性 pH 域で促進され、Mn はﾊﾞｰﾈｻｲﾄなどの生体鉱物として析出する ($Mn^{2+} + 1/2O_2 + H_2O \rightarrow Mn^{III,IV}O_2 + 2H^+$; 式 1)。従って、Mn 汚染水処理のためのバイオプロセスは、より経済的かつ環境負荷の小さい代替法となり得る。本研究は、金属製錬現場における廃液パイプライン中で見られた Mn^{2+} の自然減衰現象の機構解明から始まった。現場の Mn スラッジから新たな Mn 酸化細菌株を単離・同定し、その Mn 酸化能について各種条件下で評価した。次に、Mn 酸化反応における、生物学的効果および化学的効果の個々の寄与を明らかにした。最後に、金属製錬現場へ導入可能なバイオプロセス構築を目指して、連続バイオフィルターカラム試験を行った。加えて、使用済カラムに残存する Mn 酸化物に対する付加価値として、亜ヒ酸 (As(III)) 酸化処理反応への応用可能性を見出した。

第 1 章では、Mn の化学特性と、その汚染問題の背景を紹介した。また文献調査を行った。

第 2 章では、実験方法および分析方法について記述した。

第 3 章では、まず、金属製錬現場の廃液パイプラインで観察された Mn^{2+} の自然減衰現象について説明した。このパイプ内管表面には濃暗褐色の鉱化作用が見られたため、堆積物を採取し分析したところ、結晶性の $Mn^{IV}O_2$、$Mn^{III}_2O_3$ 、および Fe_2O_3 が検出された。Mn の平均酸化数 (AOS) は 3.75 であった。自発的な化学的 Mn 酸化が起こる条件は見当たらなかったことから、微生物学的活性の関与が示唆された。DNA を抽出・分析したところ、Mn 堆積物から複雑な

微生物群集が検出された(*Hyphomicrobium* sp. 22.1%; *Magnetospirillum* sp. 3.2%; *Geobacter* sp. 0.3%; *Bacillus* sp. 0.18%; *Pseudomonas* sp. 0.03%; 非金属代謝細菌群 74.2%)。

第 4 章では、前章で採取した Mn 堆積物の集積培養を行った。固体アガロース選択培地上で暗褐色の Mn 酸化コロニーを単離し、SK3 株と命名した。16S rRNA 遺伝子配列解析結果に基づくと、SK3 単離株の最近縁種は *Pseudomonas* (*Ps*.) *resinovorans* (相同性 98.4%; 1398 bp) であったが、当該種における Mn 酸化能はこれまで報告はなく、更にその相同性の値より本単離株が新たな種に属する可能性も示唆された。次に、実際の製錬廃液特性を考慮した異なる条件下で SK3 単離株の Mn 酸化能を評価し、過去に研究例の多い *Pseudomonas* MnB1 株（カルチャーコレクションより入手）のそれと比較した。その結果、高濃度の $MgSO_4$ (2400 mg/L; 製錬廃液に特徴的な溶質）存在下においても、SK3 単離株は 100 mg/L の Mn^{2+}を速やかに酸化した。なお、比較対照である MnB1 株においては、同条件にて Mn 酸化能は完全に消失した。また、Cu^{2+}を微量添加することで両株の Mn 酸化効率は向上したが、特に SK3 単離株で顕著であり、その Mn 酸化速度は MnB1 株の 2 倍となった。これより、Mn 酸化反応における multicopper oxidase 酵素の関与が SK3 株においても示唆された。SK3 単離株の Mn^{2+}酸化反応によって生成した Mn 酸化物は、AOS を 3.8 とする低結晶性バーネサイト鉱であった。第 3、4 章の結果より、現場における Mn^{2+}自然減衰現象が、SK3 株を含む Mn 酸化細菌群による Mn 酸化物の連続再生活性に由来することが示唆された。

Mn 酸化細菌によって生成する Mn 酸化物は、自然界に見られる強力な化学酸化剤の 1 つと言われる。この点から、Mn 酸化反応には、直接的な酵素反応（微生物活性に起因）および間接的な化学反応（Mn 酸化物に起因）の両者が貢献するものと考えられる。したがって、**第 5 章**では、これら個々の関与を明確にすることを目的とした。滅菌済み天然 Mn 酸化物 (NMO) のみを添加した

場合、Mn 酸化は化学的な共均衡化 ($Mn^{2+} + Mn^{IV}O_2 + H_2O \rightarrow Mn^{III}_2O_3 + 2H^+$; 式 2) により、限られた程度しか進行しなかった。これは、産物である $Mn^{III}_2O_3$ による NMO の表面不動態化によるものと考えられる。NMO に SK3 単離株の細胞を接種すると、共均衡化と微生物学的 $Mn^{IV}O_2$再生による相乗効果のために、Mn 酸化反応が著しく促進された。 NMO はまた、コロニー形成の為の表面を供することで、細胞増殖を促したものと考えられる。これらの効果により、高 $MnSO_4$ 濃度（2400 mg / L）や高温（35℃）など、元々阻害性の高い複合条件下でも、SK3 単離株は効果的に Mn 酸化を示すことが可能であった。

前章までに得られた基礎知見に基づいて、連続的バイオフィルターカラム試験に進むこととした。まず、**第 6 章**でカラム充填材（細胞および Mn 酸化物の担持体）のスクリーニングを行った。10 種類の SiO_2 または炭素系の材料をサイクル Mn 酸化試験により比較評価した。特に 1 サイクル目において Mn 酸化速度の差が見られたものの、一旦 Mn 酸化物が担持体に付着してしまえば、異なる材料間における差は次第に小さくなった。しかし、全体的なサイクル試験を通して、炭素系材料においてより高い有効性が認められた。この理由として、微生物細胞と Mn 酸化物が炭素系材料に対してより付着し易いこと、更に、炭素材料が電子仲介媒体として機能していることが考えられた。最終的に担持体として活性炭を選択し、活性炭自身が示し得る化学的 Mn 酸化能についても評価した。その結果、Mn 酸化は 2 サイクル目以降に大きく低下することが分かった。これは、生成物（$Mn^{III}_2O_3$）による活性炭表面の不動態化に依るものであった。これらの結果より、次章の活性炭充填カラム内においては、Mn 酸化反応に次の 3 つの因子が同時に関与することが示唆された： (i) 微生物学的 Mn^{2+}酸化による $Mn^{IV}O_2$ の連続再生（式 1）、(ii) $Mn^{IV}O_2$ の化学的共均衡化による Mn^{2+}および $Mn^{III}_2O_3$ の生成（式 2）、(iii) 活性炭表面の化学的 Mn^{2+}酸化による $Mn^{III}_2O_3$ 生成（特に初期）。

第 7 章では、ラボスケールの活性炭充填バイオフィルターカラムを作製し、現場から入手した 2 種類の実廃液（下流廃液 [Mn^{2+}] 2 mg/L、[SO_4^{2-}] 780 mg/L; 上流廃液 [Mn^{2+}] 2-5 mg/L、[SO_4^{2-}] 1500 mg/L）をカラムに供した。現場にて現在進行中のパイロットスケールカラム試験（ゼオライト充填）では Mn 除去効率が 40%程度に留まっているため、これに対する改善策を提案することを期待して各種実験を行った。実廃液試験により、Mn の完全酸化に必要な接触時間は、ゼオライトより活性炭使用時の方が短縮されることが改めて確認された。カラムには予め SK3 株細胞を増殖させた活性炭（バイオ活性炭）を充填した上で、水理学的滞留時間 (HRT) 20 min にて下流廃液の通水を開始した。Mn 酸化細菌が従属栄養性であることから、有機物供給の重要性が明確に示された。酵母抽出物添加時 (65~90%) は、無添加時 (20~40%) と比較して高い Mn 除去効率が得られた。より高濃度の Mn^{2+}および SO_4^{2-}を含有する上流廃液の処理においては、顆粒状活性炭に粉砕活性炭を 7 : 3 の割合で混合することで、Mn 酸化が 5~10%程度促進された。結果として、逆洗後でも、Mn 酸化効率は順調に回復し、HRT 40 min にて約 85%の Mn 除去を達成した。本章の結果により、現場パイロット試験の性能を改善する為には、カラム担持体の変更、Mn 酸化細菌の事前集積培養、有機栄養素の持続的供給、HRT の最適化が必要であると考えられる。**第 8 章**では、カラム試験における使用済み担持体上に蓄積した Mn 酸化物の潜在的な付加価値を探索した。As(III) による地下水汚染は重大な鉱害問題の 1 つであることから、生物起源 Mn 酸化物の As(III) 酸化能について試験した($H_3As^{III}O_3 + Mn^{IV}O_2 + H^+ \rightarrow Mn^{2+} + H_2As^{V}O_4^- + H_2O$; 式 3)。模擬 As(III) 汚染水 (pH 7) に SK3 株が生成した MnO_2 を添加し、同時に SK3 株の活性を保持させたところ、As(III)を効果的により低毒性・低溶解性の As(V) に酸化することができた。この時、式 3 により生成した Mn^{2+} は SK3 株により素早く MnO_2 に再生したことから、実質的な Mn の溶出を伴わずに As(III)酸化を完了することが可能であった。

第 9 章では、実験結果の総括および今後の課題等について記述した。

Contents

List of Tables

List of Figures

Abbreviations

AC	Activated carbon
As(III)	arsenite (H_3AsO_3)
As(V)	arsenate ($H_2AsO_4^-$)
ATR-FTIR	attenuated total reflection-Fourier transform infrared spectroscopy
BET	Brunauer–Emmett–Teller
bioBir	Biogenic birnessite
EPA	environmental protection agency
EPS	extracellular polymeric substances
Fe(II)	ferrous iron (Fe^{2+})
Fe(III)	ferric iron (Fe^{3+})
FT-IR	Fourier transformed infrared spectroscopy
HBS	heterotrophic basal salts
IAP	ion activity products
ICP-OES	inductively coupled plasma optical emission spectrometry
NMO	Natural Mn-oxide
PCR	polymerase chain reaction
PlvAC	Pulverized acitivated carbon
SEM	scanning electron microscope
SSA	specific surface area
TCLP	toxicity characteristic leaching procedure
TG-DTA	thermo gravimetry differential thermal analysis
w/v	weight per volume
XRD	X-ray diffraction
XAFS	X-ray absorption fine structure
XANES	X-ray absorption near-edge structure
[ ]	concentration of ion species
$[\ ]_{ini}$	initial concentration of ion species in solution

Chapter 1

Introduction

1.1 Manganese (Mn)

Manganese is one of the first row of transition elements and can exist in the oxidation states 0, +2, +3, +6, and +7 attribute to the removal of electron from 4*s* and 3*d* orbitals. In nature, only +2, +3, and +4 oxidation states are commonly found. Of these three oxidation states, only Mn in +2 oxidation state can occur as a free ion in aqueous solution (both inorganic/organic complexes); as insoluble phosphates ($Mn_3(PO_4)_2$) or carbonates ($MnCO_3$); as a minor constituent in other minerals. Mn in +3 oxidation state can occur in aqueous solution only when it is complexed with organic ligands such as citrate, pyrophosphate, and pyoverdin.

1.1.1 Occurrence of Mn in Earth's crust

Mn is found in combination with another element instead of a free element in nature. For example, pyrolusite (MnO_2), psilomelane ($BaMn_9O_{16}(OH)_4$), and manganite ($Mn_2O_3H_2O$). These Mn oxides mostly originated formed by reprecipitation of dissolved manganese (Post, 1999).

1.1.2 Application of manganese

Most of Mn has been used in iron and steel making industries. Due to its sulfur-fixing, deoxidizing and alloying properties, it could remove excess dissolved oxygen, sulfur and phosphorus in order to improve the strength, hardness, and resistance to corrosion (Verhoeven, 2007).

1.1.3 Biological importance of manganese

Mn is an important trace element in a biological system. It participates in many

enzyme systems in microbial (glucose metabolism), plant (photosystem), and animal (glycogen metabolism) as a cofactor.

1.2 Biogeochemistry of Mn

1.2.1 Mn oxidation

In nature, Mn(II) is released through the weathering of igneous and metamorphic rock and is oxidized, forming more than 30 known Mn(II,III), Mn(III), Mn(IV), or mixed Mn(III,IV) oxide/hydroxide minerals (Post, 1999). Table 1.1 summarized the possible oxidation reaction of Mn ions and its oxides.

Table 1.1 Formation of Mn oxide mineral (amended from (Sasaki, 2005))

Reaction	AOS	Examples of Mn oxide mineral formed
$Mn^{2+} + 1/2O_2 + H_2O \rightarrow MnO_2 + 2H^+$	4	Pyrolusite (β-MnO_2), vernadite (δ-MnO_2) Ramsdellite (γ-MnO_2) Todorokite ([Ca, Na, K][Mg, Mn]Mn_5O_{12}・H_2O) Buserite ([Ca, Na, K][Mg, Mn]Mn_6O_{14}・$5H_2O$) Birnessite ([Ca, Na]Mn_7O_{14}・$2.8H_2O$)
$Mn^{2+} + 1/4\ O_2 + 3/2H_2O \rightarrow MnOOH + 2H^+$	3	Manganite (γ-MnOOH) Groutite (α-MnOOH) Feitnechtite (β-MnOOH)
$3Mn^{2+} + 1/2\ O_2 + 3H_2O \rightarrow Mn_3O_4 + 6H^+$	2.67	Hausmannite (Mn_3O_4)
$Mn_3O_4 + 2H^+ \rightarrow 2MnOOH + Mn^{2+}$	3	Manganite (γ-MnOOH) Groutite (α-MnOOH) Feitnechtite (β-MnOOH)
$Mn_3O_4 + 4H^+ \rightarrow MnO_2 + 2Mn^{2+} + 2H_2O$	4	Pyrolusite (β-MnO_2), vernadite (δ-MnO_2) Ramsdellite (γ-MnO_2) Todorokite ([Ca, Na, K][Mg, Mn]Mn_5O_{12}・H_2O) Buserite ([Ca, Na, K][Mg, Mn]Mn_6O_{14}・$5H_2O$) Birnessite ([Ca, Na]Mn_7O_{14}・$2.8H_2O$)
$2MnOOH + 2H^+ \rightarrow MnO_2 + Mn^{2+} + 2H_2O$	4	Pyrolusite (β-MnO_2), vernadite (δ-MnO_2) Ramsdellite (γ-MnO_2) Todorokite ([Ca, Na, K][Mg, Mn]Mn_5O_{12}・H_2O) Buserite ([Ca, Na, K][Mg, Mn]Mn_6O_{14}・$5H_2O$) Birnessite ([Ca, Na]Mn_7O_{14}・$2.8H_2O$)

*AOS: Average oxidation state

Owing to the high activation energy of Mn(II)-oxidation, the reaction mostly catalyzed by either mineral surfaces or enzymes. Many studies found that Mn biooxide produced in the laboratory have a similar structure to Mn oxides found in the environment. Table 1.2 showed examples of Mn-oxide found from the different natural environments such as terrestrial, freshwater, marine, and artificial structure. Variety of Mn-oxide phases was indicated but most of them categorized to high AOS oxide (i.e. vernadite, todorokite, buserite, and birnessite). Those finding lead to further support to the notion that most natural Mn oxides are of biological origin.

Table 1.2 Examples of naturally occurring Mn-oxide

Origin	Type of Mn-oxide	References
Lake sediment	Vernadite (α-MnO_2)	(Wehrli et al., 1995)
Eutrophic lake	H^+-birnessite	(Friedl et al., 1997)
Black sea	δ-MnO_2	(Tebo et al., 2004)
Pinal Creek	Todorokite and 7-Å phyllomanganate	(Lind and Hem, 1993)
Hot-spring deposit, Yuno-Taki falls	Buserite and 7-Å phyllomanganate	(Bilinski et al., 2002)
Hot-spring deposit, Yuno-Taki falls	Todorokite	(Mita et al., 1994)
Hot-spring, Sambe	Birnessite	(Okibe et al., 2013)
Hot-spring, Satsuma-Iwo Jima island	Buserite-like phyllomanganate	(Tazaki, 2000)
Hot-spring, Asahidake	Todorokite	(Mita and Miura, 2003)
Oceanic nodule	Birnessite, todorokite, and vernadite	(Burns et al., 1983)
Streambed, Kikukawa river	Buserite-like phyllomanganate	(Tani et al., 2003)
Galapagos mounds	Todorokite	(Lalou et al., 1983)
Tailing dam	Crystalline α-MnO_2	(Kitjanukit et al., 2019)

The following sections described how bacteria and fungi oxidize Mn(II).

1.2.1.1 Mn(II)-oxidizing bacteria

The existence of Mn-oxidizing bacteria was first described century ago (Jackson, 1901). Since their discovery, different kinds of bacteria and fungi with taxonomically related or unrelated have been reported in significant number.

Bacteria catalyze Mn(II) oxidation via direct and indirect pathways. For indirect pathway, this occurs when the bacteria (i) modify the pH and/or redox potential of the aqueous environment which will trigger chemical Mn(II)-oxidation, or (ii) secrete some metabolic products that can oxidize Mn(II) (Van Veen, 1972; Bromfield, 1979). The direct Mn(II)-oxidation pathway involved enzymatic reaction and on a molecular basis, some degree of commonality was found among several phylogenetically unrelated strain. The studied bacteria possess multicopper oxidase (MCO) enzyme-encoding genes with sequence similarity. Those genes included MnxG (*Bacillus* sp. SG-1 (Dick et al., 2008)), CopA (*Brevibacillus panacihumi* MK-8 (Zeng et al., 2018)), MofA (*Leptothrix discophora* SS-1 (Corstjens et al., 1997)), CumA (*Pseudomonas putida* GB-1 (Francis and Tebo, 2001)), MoxA (*Pedomicrobium* sp. ACM 3067 (Ridge et al., 2007)), and MopA (*Erythrobacter* sp. SD-21 (Nakama et al., 2014)). On a physiological basis, Mn(II)-oxidizing bacteria are divided into 3 groups. Group I; oxidize free Mn^{2+} ions by utilizing O_2 as a terminal electron acceptor, Group II; oxidize pre-bound Mn^{2+}, and Group III; oxidize Mn^{2+} with H_2O_2 as oxidant catalyzed by catalase. Some bacteria could conserve energy from Mn^{2+} (group I, subgroup Ia and group II). However, if MCO hypothesis is true, Mn(III) must be detected as an intermediate of Mn(II) oxidation to Mn(IV) since the enzyme all oxidize their substrates via one-electron transfer reaction (Solomon et al., 1996). Up to date, no MCO has been purified in quantities sufficient for biochemical study and

no MCO encoding gene has been successfully expressed in a foreign host.

Attempt to prove the existence of Mn(III) intermediate has been done using *In situ* XANES. Unfortunately, no Mn(III) was observed but just a simultaneous reduction of Mn(II) and increasing of Mn(IV) peaks (Bargar et al., 2000). Later in 2003, Mn(III)-PP (PP; pyrophosphate) was successfully detected (increase and decrease) during oxidation of Mn(II) to Mn(IV) by endospore of *Bacillus* sp. (Webb et al., 2005). There was no significant change in Mn(III)-PP concentration in the absence of endospore, indicating that the decreasing must be due to its further oxidized to Mn(IV) (Fig. 1.1).

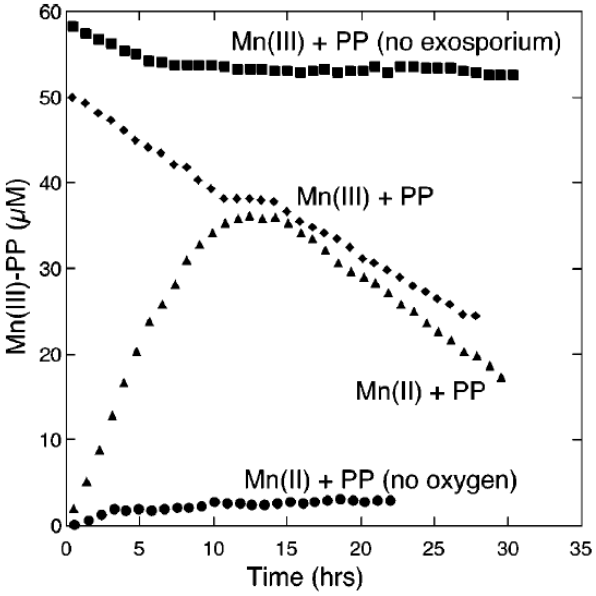

Figure 1.1 Measurement of Mn(III)-pyrophosphate complexes during bacterial Mn(II)-oxidation (Webb et al., 2005)

The importance of MCO encoding genes in Mn(II)-oxidation was exemplified using gene knockout method. A mutant strain of *Pseudomonas putida* GB-1 missing MofA and/or MnxG gave different Mn(II)-oxidation behavior. A mutant lack of both MofA and MnxG lost Mn(II)-oxidation activity; whereas a mutant lack of MofA or MnxG still can oxidize Mn(II) but in slower speed compared to wildtype (Geszvain et al., 2013).

1.2.1.2 Mn(II)-oxidizing fungi

Different form bacteria, fungi excrete Mn(II)-oxidizing enzyme (ex: Mn peroxidase) to catalyze Mn(II) oxidation. Commonly, Mn(II)-oxidizing fungi is known as lignin-degrading fungus, as they oxidize Mn(II) to Mn(III)-complex. The complex acts as an oxidant for organic materials to break down into smaller organic compounds which serve the fungus as nutrition (Glenn et al., 1986; Santelli et al., 2011). Although fungi are generally more robust than bacteria, but due to the slow growing and large biomass of fungi, it might be undesirable for some application.

Table 1.3 Examples of Mn(II)-oxidizing microorganisms, its origin, and location of Mn-oxide

Microorganism	Origin	Species name	Location and type of Mn-oxide	References
Bacteria	Soils and freshwater	*Pseudomonas putida* strain MnB1	Extracellularly, birnessite	(Villalobos et al., 2003; Villalobos et al., 2006)
	Marine	*Bacillus* sp.	Endospore, phyllomanganate oxide	(Webb et al., 2005)
	Freshwater	*Leptothrix cholodnii*	Extracellularly	(Takeda et al., 2012)
	Freshwater	*Pedomicrobium* sp. ACM 3067	Extracellularly	(Larsen et al., 1999)
Fungi	Isolated from acidic coal mine drainage	*Acremonium* sp. strain KR21-2	Hyphae, todorokite	(C. Santelli, 2012)
	Isolated from acidic coal mine drainage	*Pyrenochaeta* sp. strain DS3sAY3a	Hyphae, hexagonal birnessite	(C. Santelli, 2012)
	Soil	*Phanerochaete chrysosporium*	Hyphae, hexagonal birnessite	(J.K. Glenn, 1986)
	Isolated from stream-bed pebbles	*Acremonium* sp.	Hyphae, todorokite	(Saratovsky et al., 2009b)

1.2.2 Mn-reduction

Oxidized Mn can be served as a final electron acceptor in anoxic condition for some bacteria and fungi. Some bacteria can reduce the oxidized manganese both aerobic or anaerobically, whereas some of them can do it only in anaerobic condition. Mostly, Mn(IV)-reducing bacteria utilize reduced carbon (ex: glucose) as an electron donor but few of them can utilize H_2.

Bacteria that reduce manganese oxides (Mn^{III} or Mn^{IV} -oxide) include both gram-positive and gram-negative including *Geobacter metallireducens* (Lovley et al., 1993), *Pyrobaculum islandicum* (Kashefi and Lovley, 2000), and *Arthrobacter* sp. (Bromfield and David, 1976)

Both Mn(II) oxidizing- and Mn(IV) reducing microbes wide-spreading in terrestrial, freshwater, and marine environment are important for manganese geochemistry cycle in nature. Under circumneutral pH and anoxic conditions, Mn(II)-oxidizing microbes apparently important for the mineralization of Mn in soil, freshwater or ocean because of thermodynamically stability of Mn(II). Whereas under anoxic or anaerobic condition, Mn(III, IV)-oxide was solubilized back to Mn(II) enzymatically by Mn(IV) reducing microbes. This resulted in the biogeochemical cycle of Mn showed in Fig. 1.2.

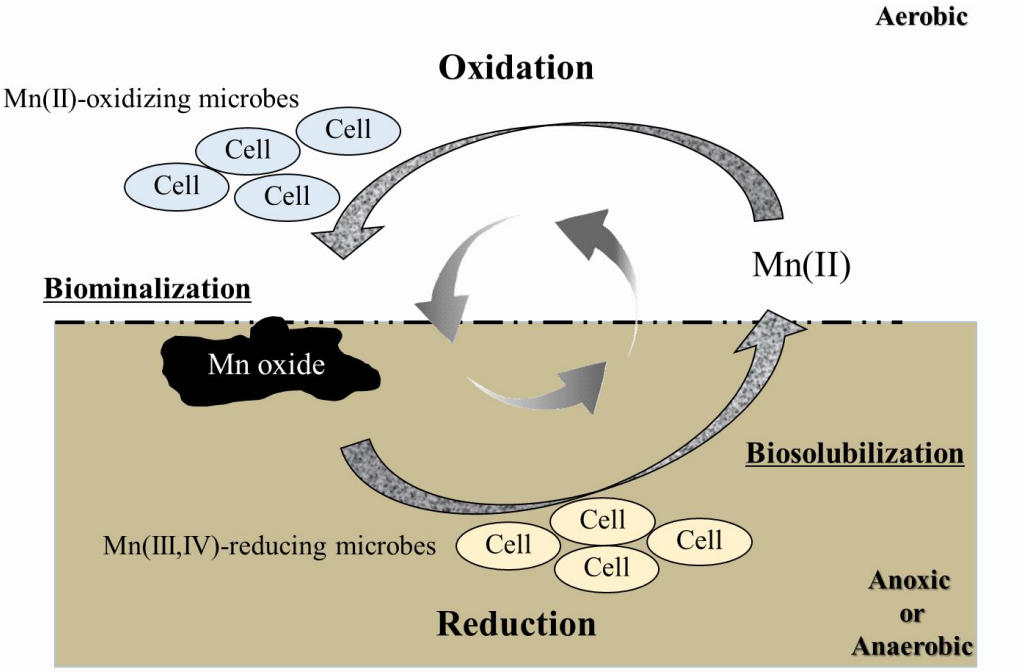

Figure 1.2 The manganese geochemistry cycle in nature

1.3 Contamination of Mn in aqueous solution

1.3.1 Aqueous speciation of manganese

As mentioned earlier, only divalent manganese (Mn^{2+}) can occur as a free ion in aqueous solution. As shown in Fig. 1.1, Mn^{2+} exists as a free ion under acidic to slightly alkaline pH and Eh range.

Owing to the high activation energy for the oxidation of Mn^{2+} to Mn^{3+} and Mn^{4+}

1.3.2 Sources and problems associated with Mn-contaminating wastewater

There are over 100 manganese-bearing minerals deposit around the world and most of them are associated with other metals. Deep sea polymetallic nodule is one of the most Mn-bearing deposit, it contained about 15-30% Mn, 5-22% Fe, and <1% of precious metals such as Co, Ni, and Cu (Sen, 2010).

The increasing demand for those metal resources and depletion of high-grade ores, Mn-bearing polymetallic nodules are being utilized in the metallurgical operation. Following the leaching processes, leachates containing desired metals and Mn were undergone extraction by electrowinning and left Mn in the waste stream. Contamination of Mn in acidic refinery wastewater is becoming a great concern in economical and environmental aspects.

Issues associated with Mn-contamination not only exemplified in the metallurgical industry, but also in groundwater, which is reported throughout the world especially in the middle of Asia where the majority of Mn took its place. Typical Mn-contamination problems could be observed in the household, which the water come with metallic taste and color or even clogging water pipe. The standard for soluble Mn in drinking water is set to lower than 0.1 mg/L in many countries (table 1.4).

Table 1.4 Standards for manganese levels in drinking water in selected countries

Country	Standard value in mg/L
Canada	0.05
Australia	0.05
Japan	0.05
South Africa	0.1
Taiwan	0.05
India	0.1
Brazil	0.1

1.4 Current techniques used for the removal of Mn

1.4.1 Ion exchange/adsorption and membrane filtration

Ion exchange is a physical treatment process in which toxic metal ions in liquid interchange with ions on a solid medium.

Utilization of polymer resins such as diethylene-glycol, triethylene-glycol, and propylene-glycol could remove more than 90% of the initial 5000 mg/L of $MnCl_2$ (Kononova et al., 2015).

Despite the high removal efficiency, the resins must be regenerated by a large volume of chemical reagents when they are exhausted. The regeneration process can cause serious secondary pollution. It is also costly, especially when used for the treatment of a large quantity of wastewater containing a low concentration of the contaminant.

Membrane filtration

In this technique,wastewater is passed through a semi-permeable membrane in which the contaminants (ions) were selectively trapped. Membrane filtration produces no solid waste, require no chemicals and has high efficiency. The main drawback for this technique is that the contaminants should be totally dissolvable because the filter media will get clogged.

1.4.2 Precipitation

1.4.2.1 Hydroxide precipitation

Precipitation of heavy metals as metal hydroxide is the most common treatment method. Either $Mg(OH)_2$ or $Ca(OH)_2$ is common reagent added to hydrometallurgical wastewater as a neutralizing agent. Both reagents could precipitate Mn^{2+} as shown in Eq. 1.1 and Eq. 1.2.

$$Mn^{2+} + Mg(OH)_2 \rightarrow Mn(OH)_2 + Mg^{2+} \quad Log\mathit{K} = 1.44 \qquad \text{(Eq. 1.1)}$$

$$Mn^{2+} + Ca(OH)_2 \rightarrow Mn(OH)_2 + Ca^{2+} \quad Log\mathit{K} = 7.36 \qquad \text{(Eq. 1.2)}$$

Based on Log*K* value, $Ca(OH)_2$ is better to drive the reaction toward the precipitation of $Mn(OH)_2$ (Zhang and Cheng, 2007). However, this technique is not a favorable option for the removal of Mn^{2+} to a very low level, as the pH is needed to be raised to >9.

1.4.2.2 Carbonate precipitation

This technique was carried out by the addition of Na_2CO_3 or limestone to hydrometallurgical wastewater. Mn^{2+} is precipitated as $MnCO_3$ at pH > 7.5 (60°C) and reached about >90% at pH 8.0 (eq. 1.3) (Zhang et al., 2010).

1.4.2.3 Oxidative precipitation

Either chlorine gas (Cl_2) or permanganate (MnO_4^-) is a common oxidant used to oxidize and precipitate Mn(II) as Mn(IV) oxide followed by sand filtration. Oxidation with chlorine gas requires alkaline pH, warm moderate temperature and 4-fold stoichiometric dosage for oxidation and removal of Mn(II) (Knocke et al., 1987).

1.5 Utilization of microbial Mn(II)-oxidation for Mn-contaminating wastewater treatment

Unnecessity of chemical oxidant, Mn(II) could be more effectively oxidized and precipitated by Mn(II)-oxidizing bacteria at circumneutral pH (6-8). Those microbial reactions could be used to replace conventional chemical process, which is costly and harmful to the environment. Following the neutralization, the wastewater could be treated with Mn(II)-oxidizing bacteria instead of further alkalization (Fig. 1.3).

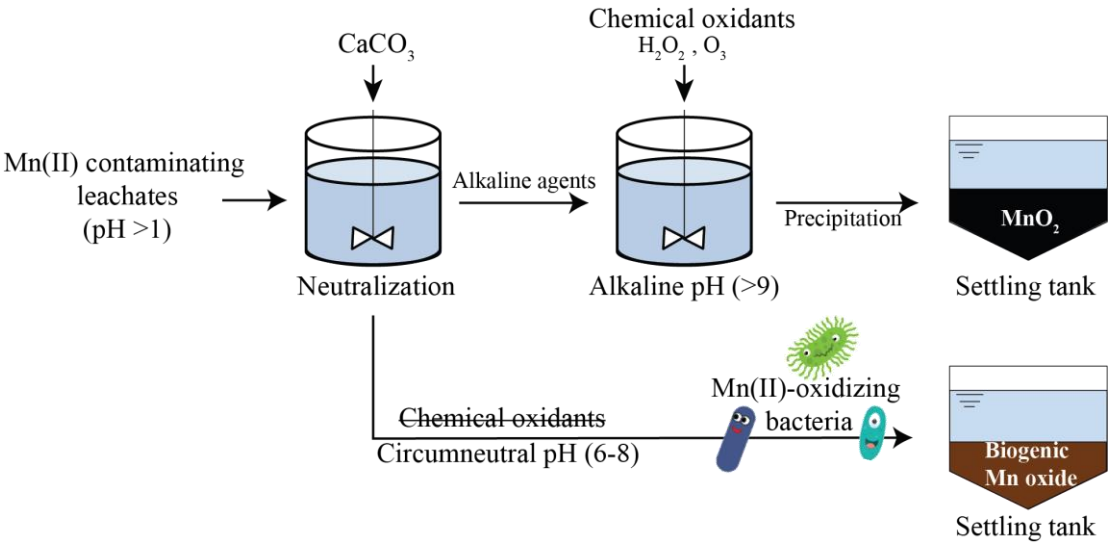

Figure 1.3 Comparison between conventional chemical and bioprocess for Mn(II)-contaminating wastewater treatment

Up till now, there are several Mn(II)-oxidizing microorganisms isolated and tested for Mn(II) oxidation activity. Table 1.5 showed an example of studies regarding the utilization of Mn(II)-oxidizing microorganisms for Mn(II)-contaminating wastewater treatment. Mostly, the oxidation took place at circumneutral pH with Mn(II) concentration ranging from 0.5 mM to few tens mM.

Ideally, those microbial reactions should be placed in upper stream of the treatment process to reduce the vast cost of alkaline/oxidizing agents required in the conventional process. Also, searching for robust Mn(II)-oxidizing bacteria that could actively oxidize Mn(II) in the harsh condition is necessary.

Table 1.5 Studies regarding utilization of Mn(II)-oxidizing microorganisms (bacteria and fungi) for Mn(II)-contaminating wastewater treatment.

No.	Microorganisms	Mn(II)-oxidizing enzyme encoding gene/ Mn(II) oxidation mechanism	Initial pH	Initial Mn(II) concentration	Temperature	Experimental condition	Removal efficiency	Types of biogenic Mn-oxide	References
Direct Mn(II) oxidation									
1	*Mesorhizobium australicum*		5.5	0.1-10 mM $MnCl_2$		Stationary		Bixbyite	(Bohu et al., 2015)
2	*Bacillus pumilus* WH4	CotA	8	5 mM $MnCl_2$	53℃	Shaking	18.2% (170 hours)	Mn_2O_3	(Su et al., 2013)
3	*Bacillus* sp.	MnxG	7.5	25 mM $MnCl_2$		Stationary		Hausmannite	(Mann et al., 1988)
4	*Pseudomonas putida*		6.6	1 mM $MnSO_4$	25℃	Shaking	220 h	Birnessite	(Okibe et al., 2013)
5	*Pseudomonas putida* MnB1	CumA		0.8 mM $MnCl_2$	30℃	Shaking		Birnessite	(Villalobos et al., 2003)
6	*Pseudomonas* sp. SK3		7	1.8 mM $MnSO_4$	25℃	Shaking	100% (48 hours)	Birnessite	(Kitjanukit et al., 2019)
7	*Pseudomonas putida* GB-1	CumA				Shaking			

Table 1.5 *(Continued)*

No.	Microorganisms	Mn(II)-oxidizing enzyme encoding gene/ Mn(II) oxidation mechanism	Initial pH	Initial Mn(II) concentration	Temperature	Experimental condition	Removal efficiency	Types of biogenic Mn-oxide	References
Direct Mn(II) oxidation									
8	*Leptothrix discophora* SP-6	MofA	7.2	1 mM $MnSO_4$	20℃	Shaking	92% (150 hours)		(Sasaki et al., 2002)
9	*Brevibacillus panacihumi* MK-8	CopA	8	1 mM $MnCl_2$	37℃	Shaking	100% (12 hours)	Mn_2O_3	(Zeng et al., 2018)
10	*Pedomicrobium sp.* ACM 3067	MoxA				Shaking		Not mentioned	(Ridge et al., 2007)
11	*Erythrobacter* sp. SD-21	MopA	8	1 mM $MnCl_2$		Shaking	24 h	Not mentioned	(Nakama et al., 2014)
12	*Acremonium* sp. KR21-2		6	275 mM $MnCl_2$		Agar surface		Todorokite	(Saratovsky et al., 2009a)
13	*Acremonium strictum* DS1bioAY4a		7	0.2 mM $MnCl_2$		Agar surface		Mixed birnessite and todorokite	(Santelli et al., 2011)

Table 1.5 *(continued)*

No.	Microorganisms	Mn(II)-oxidizing enzyme encoding gene/ Mn(II) oxidation mechanism	Initial pH	Initial Mn(II) concentration	Temperature	Experimental condition	Removal efficiency	Types of biogenic Mn-oxide	References
Direct Mn(II) oxidation									
14	*Phoma* sp.	Laccase	7.3	1.36 mM $MnSO_4$	25℃	Shaking	100% (75 h)	Ramsdellite (γ-MnO_2)	(Sasaki et al., 2004)
15	*Pyrenochaeta* sp. DS3sAY3a		7	0.2 mM $MnCl_2$					(Santelli et al., 2011)
16	*Escherichia coli* K-12	CueO	7.6-8.2	5 mM $MnCl_2$	28℃	Shaking	35.7% (190 hours)	Hausmannite	(Su et al., 2014)

Table 1.5 *(continued)*

No.	Microorganisms	Mn(II)-oxidizing enzyme encoding gene/ Mn(II) oxidation mechanism	Initial pH	Initial Mn(II) concentration	Temperature	Experimental condition	Removal efficiency	Types of biogenic Mn-oxide	References
Indirect Mn(II) oxidation									
18	*Aeromonas hydrophilia* DSo2		6	10-50 mM $MnCl_2$	35˚C	Shaking incubation	144 h	Hausmannite	(Zhang et al., 2019)
19	*Roseobacter* sp. AzwK-3b	Superoxide generation	7.2	0.1 mM $MnCl_2$	30˚C	Shaking incubation	90 h	Not mentioned	(Learman et al., 2011)

1.6 Bioprocesses for the treatment of Mn-contaminating wastewater (biofiltration)

Removal of Mn(II) in the filtration system, which based on the adsorption-oxidation process can be supported by microbial Mn(II)-oxidation by retaining Mn(II)-oxidizing bacteria on the surface of the solid filter media. After certain of time, biogenic Mn-oxide is deposited as layer coating the filter media. When fully coated, such filters are said to be matured and can efficiently catalyze Mn(II)-oxidation without additional chemical (Sahabi et al., 2009). This continuous technique is suitable to treat a large amount of wastewater. However, a lengthy period is commonly required to achieve high removal efficiency (Buamah et al., 2009).

1.6.1 Factor affecting the ripening time and efficiency of Mn removal biofilter

- Filter media

Ideally, filter media or supporting material should retain the activity of Mn(II)-oxidizing bacteria and promote Mn(II) removal via adsorption. Virgin quartz sand and anthracite are the most commonly used filter media. These materials do not have significant capacity to adsorb Mn(II). Some studies utilized MnO_x-coated filter media, which could promote Mn(II) removal through oxidation.

-Backwashing

A necessity of backwashing could not be avoided when the filter is clogged with particulate oxides, mostly iron oxides. Backwashing is done by flowing water upward at a higher speed in a short period to clean the filter. However, bacteria and Mn-oxide might be washed-out resulting in decreasing of Mn removal efficiency.

- Iron containing in the feed water

Iron is prone to precipitate as iron oxide (Fe_2O_3) upon aeration. When its concentration is high, the filter might be clogged and required backwashing more frequently. This negatively affected the filter efficiency. To avoid iron precipitation, pre-aeration and filtration of the wastewater in advance is commonly operated.

- pH and temperature

The efficiency of the enzyme-mediated reaction is strongly affected by pH and temperature. By adjusting the biofilter environment based on the optimal condition for indigenous Mn(II)-oxidizing microorganism could greatly improve the efficiency.

- Filtration rate and retention time

This factor dictated the amount of time for Mn(II)-oxidation to take place in the filter. Wastewater with higher Mn(II) concentration might require longer retention time to be completely removed.

- Nutrient enhancement

Most bacteria derived no energy from Mn(II)-oxidation, they require organic carbon to initiate the activity as well as to support the growth. Biofilter with nutrient enhancement showed greater improvement in Mn removal efficiency (Lauderdale et al., 2012). In addition, organic carbon could fasten the colonization of Mn(II)-oxidizing microbes leading to reduction of ripening time.

Studies regarding Mn(II) removal by biofiltration technique was summarized in table 1.6. Mostly, quartz sand and gravel are commonly used as filter media and indigenous microbe is used as inoculation material. Approximately more than 90% of Mn(II) was effectively removed after passed through biofilter.

Table 1.6 Studies regarding Mn(II)-removal by biofilter (modified from (Tekerlekopoulou et al., 2013))

No.	Type of filter	Type of wastewater	Support material	Inoculated material	Influent concentration (mg/L)		Removal efficiency (%)		Operation conditions			References
					[Mn]	[Fe]	[Mn]	[Fe]	Flow rate	pH	DO	
1	Full scale bio-sand filter	Drill water	Manganese sand	Isolated pure cultures	1.5-2.25	6 - 8	74.3	99	3.9 m/h	7.2	5	(Qin et al., 2009)
2	Pilot scale up-flow filter	Groundwater	Gravel	Indigenous bacteria	0.18-0.37	0.19-0.44	92	95	2.5 m/h	7-7.7	6-8.5	(Pacini et al., 2005)
3	Pilot plant trickling filter	Synthetic polluted water	Gravel	-	10	5	43-97	99	-	7.2	8	(Gouzinis et al., 1998)
4	Pilot plant trickling filter		Crushed foamed slag	Indigenous bacteria	0.7	2	100	100	3-10 m/h			(Frischherz et al., 1985)
5	Bench scale biological aerated filter	Water supply works	Lava rock	Indigenous bacteria	0.16-0.84		82		3.6 m/h	7.2-7.6		
6	Pilot plant	Synthetic polluted water	Ceramsite	Enrichment cultivation	2.5-3.2	1.2-4	99	95	0.744			(Tang et al., 2010)
7	Pilot plant pressurized filters	Groundwater	Sand	Indigenous bacteria	0.5-0.6	2.5-4	>95	100	26 m/h	6.7-7.5		(Bourgine et al., 1994)

Table 1.6 *(Continued)*

No.	Type of filter	Type of wastewater	Support material	Inoculated material	Influent concentration (mg/L)		Removal efficiency (%)		Operation conditions			References
					[Mn]	[Fe]	[Mn]	[Fe]	Flow rate	pH	DO	
8	Pilot plant pressurized filters	Groundwater	Quartz sand	Backwashed sludge	0.224	2.45	>78	100	10-22 m/h	7.48	-	(Štembal et al., 2005)
9	Lab-scale biofilter	Groundwater	Zeolite + Mn-sand	Mn(II)-oxidizer	1	3	>90	>90	4 m/h	-	-	(Li et al., 2016)
10	Lab-scale biofilter	Groundwater	Powdered activated carbon	Indigenous bacteria	0.8-1.4	10-17	>90	>90	5 m/h	6.7-7	5-9	(Du et al., 2017)
11	Lab-scale biofilter	Groundwater	Quartz sand	Bioaugmentation	2-4	5-6	80-100	100	-	-	3.5	(Bai et al., 2016)
12	Pilot plant up flow biofilter	Groundwater	Design by Anox AB	-	0.42	0.05	100	100	-	8	-	(Hedberg and Wahlberg, 1998)
13	Pilot plant bio-sand filter	Groundwater	Sand	Indigenous bacteria	11	9.5	99.2	94.3	38.2 m/h	7.4-7.8	-	

Table 1.6 *(Continued)*

No	Type of filter	Type of wastewater	Support material	Inoculated material	Influent concentration (mg/L)		Removal efficiency (%)		Operation conditions			References
					[Mn]	[Fe]	Mn	Fe	Flow rate	pH	DO	
14	Pilot plant bio-sand filter	Groundwater	Course sand	Indigenous bacteria	0.2-0.38	0.9-1.14	100	82.3	2.4 m/h	-	6.8-7.6	(Abramowski and Stoyanova, 2012)
15	Pilot plant pressurized filters	Groundwater	Quartz sand	Backwash sludge	0.147	1.04	>66	>81	-	7.3	-	(Štembal et al., 2004)
16	pilot-scale trickling filter	Synthetic polluted water	Silicit gravel	Media with immobilized bacteria	0.45	0.97	95	98	9.4 m/h	-	-	(Tekerlekopoulou and Vayenas, 2007)
17	Full scale trickling filter	Groundwater	Anthracite	Indigenous bacteria	0.54	5.4	96	98	2.2 m/h	7.2-7.4	-	(de Vet et al., 2009)
18	Pilot plant pressurized filters	Groundwater	Polystyrene bead	Indigenous bacteria	0.6	2.8	>90	>90	7 m/h	7.2	3.8	(Katsoyiannis and Zouboulis, 2004)
19	Rectangular bed (up-flow)	Coal mine drainage	Limestone	Indigenous bacteria	30	-	100	-	0.03 m/h	5.0	6	(Tan et al., 2010)
20	Rectangular bed (up-flow)	Coal mine drainage	Limestone	Indigenous bacteria	55.5	-	44	-	0.04 m/h	6.03	2.5	(Luan et al, 2012)

Table 1.6 *(Continued)*

No	Type of filter	Type of wastewater	Support material	Inoculated material	Influent concentration (mg/L)		Removal efficiency (%)		Operation conditions			References
					[Mn]	[Fe]	Mn	Fe	Flow rate	pH	DO	
21	Pilot plant up flow biofilter	Simulated contaminated water	Polypropylene	mixture of sewage activated sludge	0.6	-	95	-	5.94	5.94 - 6.84	0.5-2.15	(Hasan et al., 2011)
22	Full scale bio-sand filter	Groundwater	mixed sand	inoculation of native bacteria	0.57-3	0.01-0.5	80-100	80-100	4, 8 m/h	6.8	0.56	(Li et al., 2005)

1.7 Social acceptance for bioremediation technology

Bioremediation technology is considered as a new and complex technology compared with chemical treatment. Mostly, the development of these technology halted at industrialization step due to social factors such as social acceptance. Acceptance of new technology by the public is difficult to predict because people often being skeptical due to inadequate knowledge and information. As a result, installation of bioremediation-related technology is difficult and often introduce conflict with local residents. On a psychological basis, public acceptance often deals with attitude, which could be affected by several factors including perceived benefit, risk acceptance, familiarity and encouragement (Amin et al., 2007). Studies found that company social responsibility (CSR) could somehow conciliate the argument between the company and the consumer (society), and boost the positive image of the company. The questionnaire-based study revealed that peoples believe that bioremediation is an environmental-friendly approach and is a long-term solution for wastewater treatment. However, due to inadequate information, the technology being doubted when asked about the risks. Sample experienced in participating CSR activity tends to have higher positive perception toward bioremediation technology. The study also reviewed the example of CSR activity run by a major company in Japan (Kitjanukit, Evergreen (submitted)).

In order to industrialize bioremediation technology, we should not only focus on scientific but also on social science research.

1.8 Application of biogenic Mn-oxide

1.8.1 Adsorption of toxic metals

Several investigation on both field study and laboratory-scale indicated that Mn oxide minerals can bind to various cation such as $Zn^{2+,}$ Co^{2+}, Ce^{2+}, Ni^{2+}, and Pb^{2+} with high affinity (Loganathan and Burau, 1973; Golden et al., 1986; Takahashi et al., 2007; Yu et al., 2012; 2013). Generally, the structural O ions surrounding Mn(IV) vacant sites are believed as the hosts to most of the divalent ions.

Biogenic Mn oxides are characterized as poorly crystalline birnessite. Birnessite is a class of layer-type Mn (IV) oxides composed of edge-sharing MnO_6 octahedral with an interlayer of 7 Å. Compared to chemically synthesized counterparts (acid birnessite, alkaline birnessite, and H^+-exchanged birnessite), biogenic birnessite possesses more imperfect disordered structure resulted from the vacant site in its crystal structure (Bargar et al., 2005; Villalobos et al., 2006). This made biogenic birnessite a better adsorbent for divalent ions than synthesized birnessite.

1.8.2 Oxidation of toxic metals and organic wastes

Mn-oxide is a robust oxidant found in nature. Mn(IV)/Mn(II) couple have particularly high redox potentials making it a strong oxidant.

1.8.2.1 Arsenite (As(III)) oxidation

Arsenite (As(III)) and arsenate (As(V)) are two major species of arsenic in aqueous solution. The former is more toxic and has high mobility than the letter; thus, to immobilize As(III), the oxidation step is necessary. Conventionally, As(III) is oxidized to As(V) with chemical oxidants under neutral pH and coagulated with Fe(III) oxyhydroxide such as ferrihydrite ($FeO(OH)(H_2O)_{1+x}$). However, these

precipitations with Fe(III) requires high Fe/As molar ratio (>3) and resulted in a high volume of low-density sludge, which generates difficulty in disposal process (Riveros et al., 2001).

Scorodite ($FeAsO_4 \cdot 2H_2O$) is the orthorhombic compounds consisted of ferric iron (Fe(III)) and arsenate ((As(V)). This mineral is one of the effective arsenic immobilization phase owing to its thermodynamic stability, lower Fe/As molar ratio (lower iron demand), and high density (Krause and Ettel, 1988; Riveros et al., 2001; Langmuir et al., 2006; Bluteau and Demopoulos, 2007). Scorodite can be crystallized via elevated pressure in hydrothermal processes. Despite the advantages of the process such as simplicity and high efficiency, the cost for maintaining high temperature is an economical problem. Crystallization of scorodite under atmospheric pressure has been developed. Based on the supersaturation-control approach, neutralizing agents were added slowly to prevent the formation of amorphous compounds (Filippou and Demopoulos, 1997). This technique required a high concentration of As(V) and Fe(III) and undesirable for hydrometallurgical leachates because of the vast cost for neutralizing agents.

Recently, utilization of acidophilic Fe(II), As(III)-oxidizing microbes for crystallization of scorodite has been developed (Gonzalez-Contreras et al., 2010). This technique requires a lesser concentration of As(V) and Fe(III) to achieve high removal efficiency (>99%) (Gonzalez-Contreras et al., 2012; González-Contreras et al., 2012). Further study indicated that Thermo-acidophilic archaeon, *Acidianus brierleyi*, could facilitate crystallization of scorodite at dilute As(III) concentration (3.3-20 mM) by providing an excess Fe(II). Lengthy crystallization time required could be shortened by addition of bioscorodite seed crystals (Tanaka and Okibe,

2018). Moreover, sulfate ions were found as an importance factor for crystallization of scorodite at ambient pressure (Tanaka et al., 2018) which was previously considered as an inhibitor (Demopoulos et al., 1995). Nevertheless, those lengthy time required to immobilize arsenic as scorodite should be more shorten while maintaining high efficiency and stability of the product. Search for the catalyst to oxidize both As(III) and Fe(II) in the acidic condition is necessary.

Studies regarding As(III)-oxidation using Mn-oxide were summarized in table 1.7. Approximately 80-100% of 0.08-0.8 mM As(III) could be removed within a few minutes to few hours. Oxidation of As(III) by Mn-oxide is complex because it involves several simultaneous reactions. Upon oxidation of As(III) to As(V) or Fe(II) to Fe(III), Mn(II) is dissolved from Mn-oxide via a redox reaction. Those Mn(II) could also further reacted with Mn-oxide (synproportionation) or adsorbed into the vacancy site. Nevertheless, those Mn(II) should be ideally re-oxidized back to Mn-oxides for the recycling purpose. By so doing, biogenic Mn-oxide derived originally from Mn-contaminating wastewater treatment process could be utilized as the self-regenerating oxidants for As treatment. However, oxidation of As(III) and Fe(II) in extremely acidic condition by using Mn-oxide is challenging because of the acid dissolution.

1.8.2.2 Oxidation of organic compounds

Mn-oxides can transform numerous organic contaminants, such as antibacterial agents under environmentally friendly conditions to harmless small organic molecules. Mainly, the transformation involved a redox reaction in which Mn^{IV} is often considered to be the primary oxidant. However, Mn^{III} may play an important role and its activity needs further investigation. Upon oxidation of organic compounds, Mn(II) is reductively dissolved from Mn-oxide. In this case, Mn(II)-oxidizing microbes could be used to regenerate fresh reactive oxide to further make the process more cost-effective

Table 1.7 Studies regarding As(III)-oxidation by Mn-oxide

No.	Type of Mn-oxide	Mn oxide pulp density	As(III) initial concentration	Initial pH	Temperature	Oxidation/ Removal efficiency	Period	Immobilization phase	References
1	δ-MnO_2 + *P. fluorescences*	0.05 g/L	75 μM	7.2	RT	100%	2 hours	Adsorption onto Mn-oxide	(Jones et al., 2012)
2	δ-MnO_2 + *A. tumefaciens*					100%			
3	Biogenic Mn oxide	0.125-0.5 g/L	1.34 μM	7	RT	40-90%	18 hours		(Liang et al., 2017)
4	Synthetic birnessite	0.1, 0.25 g/L	100 μM	6.5	22℃	90, 100%	10 hours, 30 min	Adsorption onto Mn-oxide	(Manning et al., 2002)
5	δ -MnO_2	1.82 mM	100 μM	7.2	25℃	100%	15 min	Not mentioned	(Fischel et al., 2015)
	Random stacked birnessite					88%	8 hours		
	Acid birnessite					88%	8 hours		
	Biogenic Mn oxide					100%	6 hours		
	Hexagonal birnessite					36%	8 hours		
6	Nanoflower birnessite	0.6 g/L	0.1 mM	6	25℃	>98%	30 min	Adsorption onto Mn-oxide	(Hou et al., 2017)
	Nanowire birnessite					40%			
	Nanosheet birnessite					5%			
7	MnO_2 -loaded polystyrene resin	1.6 g/L	0.8 mM		20℃	90%	2 hours	Manganese arsenate	(Lenoble et al., 2004)

1.9 Objectives of the thesis

The main objective of the thesis is to develop bioprocess for the treatment of Mn(II)-contaminating metal-refinery wastewater. For that purpose, the work is divided into two parts; fundamental studies and application studies. Moreover, biogenic birnessite, a product from enzymatic Mn(II) oxidation was subjected to test for As(III) oxidation.

1.9.1 Fundamental studies

a) Investigate the natural attenuation of Mn level phenomenon in metal-refinery wastewater treatment facility (**chapter 3**)

b) Search for a new and robust Mn(II)-oxidizing bacteria (**chapter 4**)

c) Optimization of condition for Mn(II)-oxidative removal using Mn(II)-oxidizing bacteria in various complex conditions (**chapter 4**)

d) Investigate on the combination of abiotic and biotic Mn(II) oxidation reaction for the improvement of Mn(II)-oxidative removal efficiency in complex conditions (**chapter 5**)

1.9.2 Application studies

a) Search forsuitable bacterial-supporting materials for biofilter column application (**chapter 6**)

b) Optimization of condition for improving the Mn removal efficiency by means of biofilter column (**chapter 7**)

c) Investigation and optimization of condition for As(III) oxidation using biogenic birnessite (**chapter 8**)

1.10 Structure of the thesis

This thesis is divided into 8 chapters.

Chapter 1 mentions the background necessary to understand about manganese, its importance, and problem related to its contamination. Mechanism of bacterial Mn(II)-oxidation and its usage to treat Mn(II)-contaminating wastewater. Previous studies related to the present study are reviewed and discussed in this chapter.

Chapter 2 shows preparations of microbial culture media, microorganisms used in this work. Additionally, common experimental procedures and analytical methods used in this work, are described.

Chapter 3 and 4 present the study of the involvement of Mn(II)-oxidizing bacteria in the attenuation of Mn concentration and deposition of Mn-oxide inside metal-refinery wastewater treatment system water pipe.

In **chapter 3**, natural attenuation of dissolved Mn level phenomena in the metal-refinery wastewater treatment system and bacterial community structure of the Mn-oxide deposit were investigated in order to search for the useful Mn(II)-oxidizing bacteria, which could exhibit robust oxidation activity.

In **chapter 4**, Mn(II)-oxidizing bacteria were isolated from natural Mn-oxide (NMO) mentioned in chapter 3. The Mn(II)-oxidation activity of the isolate was tested in parallel with well-known *Pseudomonas putida* MnB1.

In **chapter 5**, NMO collected from metal-refinery wastewater was used to improve Mn(II)-oxidative removal efficiency.

In **chapter 6**, ten different water treatment/agricultural materials including SiO_2 and carbon-based materials were undergone evaluation for their bacteria-supporting properties.

In **chapter 7**, selected bacterial-supporting material was packed into a column and tested for continuous Mn(II)-removal from actual metal-refinery wastewater.

In **chapter 8**, birnessite produced enzymatically from Mn(II)-contaminating wastewater treatment was tested for its As(III)-oxidation capability.

Chapter 9 presents a summary of the general conclusions extracted from all the above chapters and the recommendation for further improvement.

References

Abramowski, T., and Stoyanova, V. (Year). "Deep-sea Polymetallic nodules: renewed interest as resources for environmentally sustainable development", in: *12th International Multidisciplinary Scientific GeoConference SGEM 2012*), 515-521.

Amin, L., Jahi, J.M., Nor, A.R.M., Osman, M., and Nor, M.M. (2007). Public Acceptance of Modern Biotechnology. *Asia Pac. J. Mol. Biol. Biotechnol.* 15(2), 39-51.

Bai, Y., Chang, Y., Liang, J., Chen, C., and Qu, J. (2016). Treatment of groundwater containing Mn(II), Fe(II), As(III) and Sb(III) by bioaugmented quartz-sand filters. *Water Res* 106, 126-134. doi: 10.1016/j.watres.2016.09.040.

Bargar, J.R., Tebo, B.M., and Villinski, J.E. (2000). In situ characterization of Mn(II) oxidation by spores of the marine Bacillus sp. strain SG-1. *Geochimica et Cosmochimica Acta* 64(16), 2775-2778. doi: https://doi.org/10.1016/S0016-7037(00)00368-9.

Bargar, J.R., Webb, S.M., and Tebo, B.M. (2005). Structural characterization of biogenic Mn oxides produced in seawater by the marine bacillus sp. strain SG-1. *American Mineralogist* 90(8-9), 1342-1357. doi: 10.2138/am.2005.1669.

Bilinski, H., Giovanoli, R., Usui, A., and Hanžel, D. (2002). Characterization of Mn oxides in cemented streambed crusts from Pinal Creek, Arizona, U.S.A., and in hot-spring deposits from Yuno-Taki Falls, Hokkaido, Japan. *American Mineralogist* 87(4), 580-591. doi: 10.2138/am-2002-0423.

Bluteau, M.-C., and Demopoulos, G.P. (2007). The incongruent dissolution of scorodite — Solubility, kinetics and mechanism. *Hydrometallurgy* 87(3), 163-177. doi: https://doi.org/10.1016/j.hydromet.2007.03.003.

Bohu, T., Santelli, C.M., Akob, D.M., Neu, T.R., Ciobota, V., Rosch, P., et al. (2015). Characterization of pH dependent Mn(II) oxidation strategies and formation of a bixbyite-like phase by Mesorhizobium australicum T-G1. *Front Microbiol* 6, 734. doi: 10.3389/fmicb.2015.00734.

Bourgine, F.P., Gennery, M., Chapman, J.I., Kerai, H., Green, J.G., Rap, R.J., et al. (1994). Biological Processes at Saints Hill Water-Treatment Plant, Kent - Discussion. *Journal of the Institution of Water and Environmental Management* 8(4), 379-392. doi: 10.1111/j.1747-6593.1994.tb01121.x.

Bromfield, S.M. (1979). Manganous ion oxidation at pH values below 5.0 by cell-free substances from streptomyces sp. Cultures. *Soil Biology and Biochemistry* 11(2), 115-118. doi: https://doi.org/10.1016/0038-0717(79)90086-5.

Bromfield, S.M., and David, D.J. (1976). Sorption and oxidation of manganous ions and reduction of manganese oxide by cell suspensions of a manganese oxidizing

bacterium. *Soil Biology and Biochemistry* 8(1), 37-43. doi: https://doi.org/10.1016/0038-0717(76)90019-5.

Buamah, R., Petrusevski, B., de Ridder, D., and van de Wetering, S. (2009). *Manganese removal in groundwater treatment: Practice, problems and probable solutions.*

Burns, R.G., Burns, V.M., and Stockman, H.W. (1983). A review of the todorokite-buserite problem; implications to the mineralogy of marine manganese nodules. *American Mineralogist* 68(9-10), 972-980.

C. Santelli, S.W., A. Dohnalcova, C. Hansel (2012). Diversity of Mn oxides produced by Mn(II)-oxidizing fungi. *Geochimica et Cosmochimica Acta* 75, 2762-2776.

Corstjens, P.L.A.M., de Vrind, J.P.M., Goosen, T., and Jong, E.W.d.V.d. (1997). Identification and molecular analysis of theLeptothrix discophoraSS - 1mofAgene, a gene putatively encoding a manganese - oxidizing protein with copper domains. *Geomicrobiology Journal* 14(2), 91-108. doi: 10.1080/01490459709378037.

de Vet, W.W.J.M., Rietveld, L.C., and van Loosdrecht, M.C.M. (2009). Influence of iron on nitrification in full-scale drinking water trickling filters. *Journal of Water Supply: Research and Technology-Aqua* 58(4), 247-256. doi: 10.2166/aqua.2009.115.

Demopoulos, G.P., Droppert, D.J., and Van Weert, G. (1995). Precipitation of crystalline scorodite (FeAsO4 · 2H2O) from chloride solutions. *Hydrometallurgy* 38(3), 245-261. doi: https://doi.org/10.1016/0304-386X(94)00062-8.

Dick, G.J., Torpey, J.W., Beveridge, T.J., and Tebo, B.M. (2008). Direct identification of a bacterial manganese(II) oxidase, the multicopper oxidase MnxG, from spores of several different marine Bacillus species. *Appl Environ Microbiol* 74(5), 1527-1534. doi: 10.1128/AEM.01240-07.

Du, X., Liu, G., Qu, F., Li, K., Shao, S., Li, G., et al. (2017). Removal of iron, manganese and ammonia from groundwater using a PAC-MBR system: The anti-pollution ability, microbial population and membrane fouling. *Desalination* 403, 97-106. doi: https://doi.org/10.1016/j.desal.2016.03.002.

Filippou, D., and Demopoulos, G.P. (1997). Arsenic immobilization by controlled scorodite precipitation. *JOM* 49(12), 52-55. doi: 10.1007/s11837-997-0034-3.

Fischel, M.H.H., Fischel, J.S., Lafferty, B.J., and Sparks, D.L. (2015). The influence of environmental conditions on kinetics of arsenite oxidation by manganese-oxides. *Geochemical Transactions* 16(1), 15. doi: 10.1186/s12932-015-0030-4.

Francis, C.A., and Tebo, B.M. (2001). cumA Multicopper Oxidase Genes from Diverse Mn(II)-Oxidizing and Non-Mn(II)-Oxidizing Pseudomonas Strains. *Applied and Environmental Microbiology* 67(9), 4272-4278. doi: 10.1128/aem.67.9.4272-4278.2001.

Friedl, G., Wehrli, B., and Manceau, A. (1997). Solid phases in the cycling of manganese in

eutrophic lakes: New insights from EXAFS spectroscopy. *Geochimica et Cosmochimica Acta* 61(2), 275-290. doi: https://doi.org/10.1016/S0016-7037(96)00316-X.

Frischherz, H., Zibuschka, F., Jung, H., and Zerobin, W. (1985). *Biological elimination of iron and manganese.*

Geszvain, K., McCarthy, J.K., and Tebo, B.M. (2013). Elimination of manganese(II,III) oxidation in Pseudomonas putida GB-1 by a double knockout of two putative multicopper oxidase genes. *Appl Environ Microbiol* 79(1), 357-366. doi: 10.1128/AEM.01850-12.

Glenn, J.K., Akileswaran, L., and Gold, M.H. (1986). Mn(II) oxidation is the principal function of the extracellular Mn-peroxidase from Phanerochaete chrysosporium. *Archives of Biochemistry and Biophysics* 251(2), 688-696. doi: https://doi.org/10.1016/0003-9861(86)90378-4.

Golden, D., Dixon, J., and Chen, C. (1986). *Ion exchange, thermal transformations, and oxidizing properties of birnessite.*

Gonzalez-Contreras, P., Weijma, J., and Buisman, C.J.N. (2012). Bioscorodite Crystallization in an Airlift Reactor for Arsenic Removal. *Crystal Growth & Design* 12(5), 2699-2706. doi: 10.1021/cg300319s.

González-Contreras, P., Weijma, J., and Buisman, C.J.N. (2012). Continuous bioscorodite crystallization in CSTRs for arsenic removal and disposal. *Water Research* 46(18), 5883-5892. doi: https://doi.org/10.1016/j.watres.2012.07.055.

Gonzalez-Contreras, P., Weijma, J., Weijden, R.v.d., and Buisman, C.J.N. (2010). Biogenic Scorodite Crystallization by Acidianus sulfidivorans for Arsenic Removal. *Environmental Science & Technology* 44(2), 675-680. doi: 10.1021/es902063t.

Gouzinis, A., Kosmidis, N., Vayenas, D.V., and Lyberatos, G. (1998). Removal of Mn and simultaneous removal of NH3, Fe and Mn from potable water using a trickling filter. *Water Research* 32(8), 2442-2450. doi: https://doi.org/10.1016/S0043-1354(97)00471-5.

Hasan, H.A., Abdullah, S.R.S., Kamarudin, S.K., and Kofli, N.T. (2011). Response surface methodology for optimization of simultaneous COD, NH4+–N and Mn2+ removal from drinking water by biological aerated filter. *Desalination* 275(1), 50-61. doi: https://doi.org/10.1016/j.desal.2011.02.028.

Hedberg, T., and Wahlberg, T.A. (1998). Upgrading of waterworks with a new biooxidation process for removal of manganese and iron. *Water Science and Technology* 37(9), 121-126. doi: https://doi.org/10.1016/S0273-1223(98)00279-0.

Hou, J., Xiang, Y., Zheng, D., Li, Y., Xue, S., Wu, C., et al. (2017). Morphology-dependent enhancement of arsenite oxidation to arsenate on birnessite-type manganese

oxide. *Chemical Engineering Journal* 327, 235-243. doi: https://doi.org/10.1016/j.cej.2017.06.102.

J.K. Glenn, L.A., M.H. Gold (1986). Mn(II) oxidation is the principal function of the extracellular Mn-Peroxidase from Phanerochaete chrysosporium. *Archives of Biochemistry and Biophysics* 251(2), 688-696.

Jackson, D. (1901). The precipitation of iron, manganese, and aluminum by bacterial action. *J Soc Chem Ind* 21, 681-684.

Jones, L.C., Lafferty, B.J., and Sparks, D.L. (2012). Additive and Competitive Effects of Bacteria and Mn Oxides on Arsenite Oxidation Kinetics. *Environmental Science & Technology* 46(12), 6548-6555. doi: 10.1021/es204252f.

Kashefi, K., and Lovley, D.R. (2000). Reduction of Fe(III), Mn(IV), and toxic metals at 100 degrees C by Pyrobaculum islandicum. *Applied and environmental microbiology* 66(3), 1050-1056.

Katsoyiannis, I.A., and Zouboulis, A.I. (2004). Biological treatment of Mn(II) and Fe(II) containing groundwater: kinetic considerations and product characterization. *Water Research* 38(7), 1922-1932. doi: https://doi.org/10.1016/j.watres.2004.01.014.

Kitjanukit, S., Takamatsu, K., and Okibe, N. (2019). Natural Attenuation of Mn(II) in Metal Refinery Wastewater: Microbial Community Structure Analysis and Isolation of a New Mn(II)-Oxidizing Bacterium Pseudomonas sp. SK3. *Water* 11(3), 507.

Knocke, W., Hoehn, R., and Sinsabaugh, R. (1987). *Using Alternative Oxidants to Remove Dissolved Manganese From Waters Laden With Organics.*

Kononova, O.N., Bryuzgina, G.L., Apchitaeva, O.V., and Kononov, Y.S. (2015). Ion exchange recovery of chromium (VI) and manganese (II) from aqueous solutions. *Arabian Journal of Chemistry*. doi: https://doi.org/10.1016/j.arabjc.2015.05.021.

Krause, E., and Ettel, V.A. (1988). Solubility and stability of scorodite, FeAsO4 .2H2 O; new data and further discussion. *American Mineralogist* 73(7-8), 850-854.

Lalou, C., Brichet, E., Jehanno, C., and Perez-Leclaire, H. (1983). Hydrothermal manganese oxide deposits from Galapagos mounds, DSDP Leg 70, hole 509B and "Alvin" dives 729 and 721. *Earth and Planetary Science Letters* 63(1), 63-75. doi: https://doi.org/10.1016/0012-821X(83)90022-5.

Langmuir, D., Mahoney, J., and Rowson, J. (2006). Solubility products of amorphous ferric arsenate and crystalline scorodite (FeAsO4·2H2O) and their application to arsenic behavior in buried mine tailings. *Geochimica et Cosmochimica Acta* 70(12), 2942-2956. doi: https://doi.org/10.1016/j.gca.2006.03.006.

Larsen, E., Sly, L., and McEwan, A. (1999). *Manganese(II) adsorption and oxidation by*

whole cells and a membrane fraction of Pedomicrobium sp. ACM 3067.

Lauderdale, C., Chadik, P., Kirisits, M.J., and Brown, J. (2012). Engineered biofiltration: Enhanced biofilter performance through nutrient and peroxide addition. *Journal - American Water Works Association* 104(5), E298-E309. doi: 10.5942/jawwa.2012.104.0073.

Learman, D.R., Voelker, B.M., Vazquez-Rodriguez, A.I., and Hansel, C.M. (2011). Formation of manganese oxides by bacterially generated superoxide. *Nature Geoscience* 4, 95. doi: 10.1038/ngeo1055

https://www.nature.com/articles/ngeo1055#supplementary-information.

Lenoble, V., Laclautre, C., Serpaud, B., Deluchat, V., and Bollinger, J.-C. (2004). As(V) retention and As(III) simultaneous oxidation and removal on a MnO2-loaded polystyrene resin. *Science of The Total Environment* 326(1), 197-207. doi: https://doi.org/10.1016/j.scitotenv.2003.12.012.

Li, C., Wang, S., Du, X., Cheng, X., Fu, M., Hou, N., et al. (2016). Immobilization of iron- and manganese-oxidizing bacteria with a biofilm-forming bacterium for the effective removal of iron and manganese from groundwater. *Bioresource Technology* 220, 76-84. doi: https://doi.org/10.1016/j.biortech.2016.08.020.

Li, D., Zhang, J., Wang, H., Yang, H., and Wang, B. (2005). Operational performance of biological treatment plant for iron and manganese removal. *Journal of Water Supply: Research and Technology-Aqua* 54(1), 15-24. doi: 10.2166/aqua.2005.0002.

Liang, G., Yang, Y., Wu, S., Jiang, Y., and Xu, Y. (2017). The generation of biogenic manganese oxides and its application in the removal of As(III) in groundwater. *Environmental Science and Pollution Research* 24(21), 17935-17944. doi: 10.1007/s11356-017-9476-5.

Lind, C.J., and Hem, J.D. (1993). Manganese minerals and associated fine particulates in the streambed of Pinal Creek, Arizona, U.S.A.: a mining-related acid drainage problem. *Applied Geochemistry* 8(1), 67-80. doi: 10.1016/0883-2927(93)90057-N.

Loganathan, P., and Burau, R.G. (1973). Sorption of heavy metal ions by a hydrous manganese oxide. *Geochimica et Cosmochimica Acta* 37(5), 1277-1293. doi: https://doi.org/10.1016/0016-7037(73)90061-6.

Lovley, D.R., Giovannoni, S.J., White, D.C., Champine, J.E., Phillips, E.J., Gorby, Y.A., et al. (1993). Geobacter metallireducens gen. nov. sp. nov., a microorganism capable of coupling the complete oxidation of organic compounds to the reduction of iron and other metals. *Arch Microbiol* 159(4), 336-344. doi: 10.1007/bf00290916.

Luan, F., Santelli, C.M., Hansel, C.M., Burgos, W.D. (2012). Defining manganese(II) removal processes in passive coal mine drainage treatment systems through laboratory incubation experiments. *Applied Geochemistry* 27, 1567-1578

Mann, S., Sparks, N.H., Scott, G.H., and de Vrind-de Jong, E.W. (1988). Oxidation of Manganese and Formation of Mn(3)O(4) (Hausmannite) by Spore Coats of a Marine Bacillus sp. *Appl Environ Microbiol* 54(8), 2140-2143.

Manning, B.A., Fendorf, S.E., Bostick, B., and Suarez, D.L. (2002). Arsenic(III) Oxidation and Arsenic(V) Adsorption Reactions on Synthetic Birnessite. *Environmental Science & Technology* 36(5), 976-981. doi: 10.1021/es0110170.

Mita, N., Maruyama, A., Usui, A., Higashihara, T., and Hariya, Y. (1994). A growing deposit of hydrous manganese oxide produced by microbial mediation at a hot spring, Japan. *GEOCHEMICAL JOURNAL* 28(2), 71-80. doi: 10.2343/geochemj.28.71.

Mita, N., and Miura, H. (2003). Evidence of Microbial Activity in the Formation of Manganese Wads at the Asahidake Hot Spring in Hokkaido, Japan. *Resource Geology* 53(3), 233-238. doi: 10.1111/j.1751-3928.2003.tb00173.x.

Nakama, K., Medina, M., Lien, A., Ruggieri, J., Collins, K., and Johnson, H.A. (2014). Heterologous Expression and Characterization of the Manganese-Oxidizing Protein from Erythrobacter sp. Strain SD21. *Applied and Environmental Microbiology* 80(21), 6837-6842. doi: 10.1128/aem.01873-14.

Okibe, N., Maki, M., Sasaki, K., and Hirajima, T. (2013). Mn(II)-Oxidizing Activity of Pseudomonas sp Strain MM1 is Involved in the Formation of Massive Mn Sediments around Sambe Hot Springs in Japan. *Materials Transactions* 54(10), 2027-2031. doi: 10.2320/matertrans.M-M2013825.

Pacini, V.A., María Ingallinella, A., and Sanguinetti, G. (2005). Removal of iron and manganese using biological roughing up flow filtration technology. *Water Research* 39(18), 4463-4475. doi: https://doi.org/10.1016/j.watres.2005.08.027.

Post, J.E. (1999). Manganese oxide minerals: Crystal structures and economic and environmental significance. *Proceedings of the National Academy of Sciences* 96(7), 3447-3454. doi: 10.1073/pnas.96.7.3447.

Qin, S., Ma, F., Huang, P., and Yang, J. (2009). Fe (II) and Mn (II) removal from drilled well water: A case study from a biological treatment unit in Harbin. *Desalination* 245(1), 183-193. doi: https://doi.org/10.1016/j.desal.2008.04.048.

Ridge, J.P., Lin, M., Larsen, E.I., Fegan, M., McEwan, A.G., and Sly, L.I. (2007). A multicopper oxidase is essential for manganese oxidation and laccase-like activity in Pedomicrobium sp. ACM 3067. *Environ Microbiol* 9(4), 944-953. doi: 10.1111/j.1462-2920.2006.01216.x.

Riveros, P.A., Dutrizac, J.E., and Spencer, P. (2001). Arsenic Disposal Practices in the Metallurgical Industry. *Canadian Metallurgical Quarterly* 40(4), 395-420. doi: 10.1179/cmq.2001.40.4.395.

Sahabi, D.M., Takeda, M., Suzuki, I., and Koizumi, J.-i. (2009). Removal of Mn2+ from water by "aged" biofilter media: The role of catalytic oxides layers. *Journal of Bioscience and Bioengineering* 107(2), 151-157. doi: https://doi.org/10.1016/j.jbiosc.2008.10.013.

Santelli, C.M., Webb, S.M., Dohnalkova, A.C., and Hansel, C.M. (2011). Diversity of Mn oxides produced by Mn(II)-oxidizing fungi. *Geochimica Et Cosmochimica Acta* 75(10), 2762-2776. doi: 10.1016/j.gca.2011.02.022.

Saratovsky, I., Gurr, S., and Hayward, M. (2009a). *The Structure of manganese oxide formed by the fungus Acremonium sp. strain KR21-2.*

Saratovsky, I., Gurr, S.J., and Hayward, M.A. (2009b). The Structure of manganese oxide formed by the fungus Acremonium sp strain KR21-2. *Geochimica Et Cosmochimica Acta* 73(11), 3291-3300. doi: 10.1016/j.gca.2009.03.005.

Sasaki, K. (2005). Biomineralization of manganese by microorganisms and its application to environmental remediation. *Shigen-Chishitsu* 55(2), 195-202. doi: 10.11456/shigenchishitsu1992.55.195.

Sasaki, K., Endo, M., Kurosawa, K., and Konno, H. (2002). Removal of Manganese(II) Ions from Water by <I>Leptothrix discophora</I> with Carbon Fiber. *MATERIALS TRANSACTIONS* 43(11), 2773-2777. doi: 10.2320/matertrans.43.2773.

Sasaki, K., Konno, H., Endo, M., and Takano, K. (2004). Removal of Mn(II) ions from aqueous neutral media by manganese-oxidizing fungus in the presence of carbon fiber. *Biotechnology and Bioengineering* 85(5), 489-496. doi: 10.1002/bit.10921.

Sen, P.K. (2010). Metals and materials from deep sea nodules: an outlook for the future. *International Materials Reviews* 55(6), 364-391. doi: 10.1179/095066010X12777205875714.

Solomon, E.I., Sundaram, U.M., and Machonkin, T.E. (1996). Multicopper Oxidases and Oxygenases. *Chem Rev* 96(7), 2563-2606. doi: 10.1021/cr950046o.

Štembal, T., Markić, M., Briški, F., and Sipos, L. (2004). Rapid start-up of biofilters for removal of ammonium, iron and manganese from ground water. *Journal of Water Supply: Research and Technology-Aqua* 53(7), 509-518. doi: 10.2166/aqua.2004.0040.

Štembal, T., Markić, M., Ribičić, N., Briski, F., and Sipos, L. (2005). *Removal of ammonia, iron and manganese from groundwaters of northern Croatia - Pilot plant studies.*

Su, J., Bao, P., Bai, T., Deng, L., Wu, H., Liu, F., et al. (2013). CotA, a Multicopper Oxidase from Bacillus pumilus WH4, Exhibits Manganese-Oxidase Activity. *PLOS ONE* 8(4), e60573. doi: 10.1371/journal.pone.0060573.

Su, J., Deng, L., Huang, L., Guo, S., Liu, F., and He, J. (2014). Catalytic oxidation of manganese(II) by multicopper oxidase CueO and characterization of the biogenic

Mn oxide. *Water Research* 56, 304-313. doi: https://doi.org/10.1016/j.watres.2014.03.013.

Takahashi, Y., Manceau, A., Geoffroy, N., Marcus, M.A., and Usui, A. (2007). Chemical and structural control of the partitioning of Co, Ce, and Pb in marine ferromanganese oxides. *Geochimica et Cosmochimica Acta* 71(4), 984-1008. doi: https://doi.org/10.1016/j.gca.2006.11.016.

Takeda, M., Kawasaki, Y., Umezu, T., Shimura, S., Hasegawa, M., and Koizumi, J. (2012). Patterns of sheath elongation, cell proliferation, and manganese(II) oxidation in Leptothrix cholodnii. *Arch Microbiol* 194(8), 667-673. doi: 10.1007/s00203-012-0801-6.

Tan, H., Zhang, G., Heaney, P.J., Webb, S.M., Burgos W.D. (2010). Characterization of manganese oxide precipitates from Appalachian coal mine drainage treatment systems. *Applied Geochemistry* 25, 389-399.

Tanaka, M., and Okibe, N. (2018). Factors to Enable Crystallization of Environmentally Stable Bioscorodite from Dilute As(III)-Contaminated Waters. *Minerals* 8(1), 23.

Tanaka, M., Sasaki, K., and Okibe, N. (2018). Behavior of sulfate ions during biogenic scorodite crystallization from dilute As(III)-bearing acidic waters. *Hydrometallurgy* 180, 144-152. doi: https://doi.org/10.1016/j.hydromet.2018.07.018.

Tang, Y., He, J., Ma, X., You, K., Zhang, R., Wu, W., et al. (Year). "Simultaneous Biological Removal of Iron, Manganese and Ammonium Nitrogen in Simulated Groundwater Using Biological Aerated Filter", in: *2010 4th International Conference on Bioinformatics and Biomedical Engineering*), 1-4.

Tani, Y., Miyata, N., Iwahori, K., Soma, M., Tokuda, S.-i., Seyama, H., et al. (2003). Biogeochemistry of manganese oxide coatings on pebble surfaces in the Kikukawa River System, Shizuoka, Japan. *Applied Geochemistry* 18(10), 1541-1554. doi: https://doi.org/10.1016/S0883-2927(03)00075-1.

Tazaki, K. (2000). *Formation of Banded Iron-Manganese Structures by Natural Microbial Communities.*

Tebo, B.M., Bargar, J.R., Clement, B.G., Dick, G.J., Murray, K.J., Parker, D., et al. (2004). Biogenic manganese oxides: Properties and mechanisms of formation. *Annual Review of Earth and Planetary Sciences* 32(1), 287-328. doi: 10.1146/annurev.earth.32.101802.120213.

Tekerlekopoulou, A.G., Pavlou, S., and Vayenas, D.V. (2013). Removal of ammonium, iron and manganese from potable water in biofiltration units: a review. *Journal of Chemical Technology & Biotechnology* 88(5), 751-773. doi: 10.1002/jctb.4031.

Tekerlekopoulou, A.G., and Vayenas, D.V. (2007). Ammonia, iron and manganese removal from potable water using trickling filters. *Desalination* 210(1), 225-235. doi: https://doi.org/10.1016/j.desal.2006.05.047.

Van Veen, W.L. (1972). Factors affecting the oxidation of manganese by Sphaerotilus discophorus. *Antonie Van Leeuwenhoek* 38, 623-626.

Verhoeven, J. (2007). *Steel Metallurgy for the Non-Metallurgist.*

Villalobos, M., Lanson, B., Manceau, A., Toner, B., and Sposito, G. (2006). Structural model for the biogenic Mn oxide produced by Pseudomonas putida. *American Mineralogist* 91(4), 489-502. doi: 10.2138/am.2006.1925.

Villalobos, M., Toner, B., Bargar, J., and Sposito, G. (2003). Characterization of the manganese oxide produced by Pseudomonas putida strain MnB1. *Geochimica Et Cosmochimica Acta* 67(14), 2649-2662. doi: 10.1016/S0016-7037(03)00217-5.

Webb, S.M., Dick, G.J., Bargar, J.R., and Tebo, B.M. (2005). Evidence for the presence of Mn(III) intermediates in the bacterial oxidation of Mn(II). *Proc Natl Acad Sci U S A* 102(15), 5558-5563. doi: 10.1073/pnas.0409119102.

Wehrli, B., Friedl, G., and Manceau, A. (1995). "Reaction Rates and Products of Manganese Oxidation at the Sediment-Water Interface," in *Aquatic Chemistry*. American Chemical Society), 111-134.

Yu, Q.Q., Sasaki, K., Tanaka, K., Ohnuki, T., and Hirajima, T. (2012). Structural factors of biogenic birnessite produced by fungus Paraconiothyrium sp WL-2 strain affecting sorption of Co2+. *Chemical Geology* 310, 106-113. doi: 10.1016/j.chemgeo.2012.03.029.

Yu, Q.Q., Sasaki, K., Tanaka, K., Ohnuki, T., and Hirajima, T. (2013). Zinc Sorption During Bio-oxidation and Precipitation of Manganese Modifies the Layer Stacking of Biogenic Birnessite. *Geomicrobiology Journal* 30(9), 829-839. doi: 10.1080/01490451.2013.774075.

Zeng, X., Zhang, M., Liu, Y., and Tang, W. (2018). Manganese(II) oxidation by the multi-copper oxidase CopA from Brevibacillus panacihumi MK-8. *Enzyme Microb Technol* 117, 79-83. doi: 10.1016/j.enzmictec.2018.04.011.

Zhang, W., and Cheng, C.Y. (2007). Manganese metallurgy review. Part II: Manganese separation and recovery from solution. *Hydrometallurgy* 89(3), 160-177. doi: https://doi.org/10.1016/j.hydromet.2007.08.009.

Zhang, W., Cheng, C.Y., and Pranolo, Y. (2010). Investigation of methods for removal and recovery of manganese in hydrometallurgical processes. *Hydrometallurgy* 101(1), 58-63. doi: https://doi.org/10.1016/j.hydromet.2009.11.018.

Zhang, Y., Tang, Y., Qin, Z., Luo, P., Ma, Z., Tan, M., et al. (2019). A novel manganese oxidizing bacterium-Aeromonas hydrophila strain DS02: Mn(II) oxidization and

biogenic Mn oxides generation. *Journal of Hazardous Materials* 367, 539-545. doi: https://doi.org/10.1016/j.jhazmat.2019.01.012.

Data shown in section 1.6 were partially included in the paper submitted to Evergreen (2019. June) entitled "Attitude toward bioremediation-related technology and relation with Company Social Responsibility"

Chapter 2

Methodology

2.1 Culture medium and chemical reagents used in this study

2.1.1 Culture media used for screening and isolation of Mn(II)-oxidizing bacteria

2.1.1.1 K-medium (pH 7.0)

Artificial seawater*

0.05% yeast extract

0.02% peptone

15 g/L Agarose

2.1.1.2 J-medium (pH 7.0)

1.5 mM NH_4Cl

2 mM $KHCO_3$

73 μM KH_2PO_4

Vitamin mix*[2]

0.5% Methanol

1.5 g/L Agarose

2.1.1.3 Yu-medium (pH 7.0)

2.43 mM $MgSO_4 \cdot 7H_2O$

0.48 mM $CaCl_2 \cdot 2H_2O$

4.5 g/L PIPES

0.005% Peptone

15 g/L Agarose

*Artificial seawater (2x)

24.7 g/L $MgSO_4 \cdot 7H_2O$

2.9 g/L $CaCl_2 \cdot 2H_2O$

35.1 g/L NaCl

1.5 g/L KCl

Dissolved each component completely in 250 mL of H_2O, the combine to make 1L solution.

*[2] Vitamin mix

Dissolve each of the following separately in 10 mL H_2O

40 mg Biotin in 40 mL H_2O (heat to dissolve)

4 mg Niacin

2 mg Thiamine

4 mg p-aminobenzoic acid

2 mg Pantothenic acid

20 mg Pyridoxine

2 mg Vitamin B12

4 mg Riboflavin

4 mg Folic acid

Combine all 9 solutions and make up to 200 mL using H_2O

2.1.2 Lysogeny (Luria) medium (LB)

Lysogeny is a nutritionally rich medium used for the growth of bacteria. The formula of LB medium (Luria) was as followed; (per litre) 5 g NaCl, 10 g yeast extract, and 10 g tryptone. pH of the medium was adjusted to desired value using HCl or NaOH before sterilized by autoclave (120℃, 20 min).

2.1.3 Modified peptone-yeast extract-glucose (PYG-1) medium

0.025% peptone, 0.025% yeast extract, 2.02 mM $MgSO_4 \cdot 7H_2O$, and 0.068 mM $CaCl_2 \cdot 2H_2O$ were added to the distilled water following by 15 mM PIPES (1,4-bis(2-etanesulfonic acid), a biological buffer. To dissolve PIPES, 5 M NaOH was slowly added and finally 1 M NaOH was used to adjust to desire pH. After autoclaved (120℃, 20 min), filter sterilized glucose (1 M stock solution) was added into PYG medium to the final concentration of 1 mM.

2.1.4 Acidophilic basal salt (ABS)

ABS stock solution (50X) composition

22.5 g/L $(NH_4)_2SO_4$

2.5 g/L KCl

2.5 g/L KH_2PO_4

25 g/L $MgSO_4 \cdot 7H_2O$

0.7 g/L $Ca(NO_3)_2 \cdot 4H_2O$

7.1 g/L Na_2SO_4

Solubilized into distilled water, filter-sterilized (0.22 μm polyethersulfone membranes (Steritop, Millipore) and stored in sterilized bottle at 4°C. To make 1 L of

ABS (1×) media, 20 mL of ABS stock solution (50×) was mixed with 900mL of distilled water and adjusted to desired pH (with H_2SO_4) before filled up to 1L with distilled water and sterilized by autoclave (120°C, 20 min).

2.1.5 Chemical reagents used in this study

10000 mg/L Mn(II) stock solution

$MnSO_4 \cdot 7H_2O$ (Wako pure chemicals) was solubilized into deionized water and adjusted to pH 6.5 (with NaOH), filtrated (0.02 μm), and stored in sterilized bottle at 4°C.

1 mM Cu(II) stock solution

$CuCl_2 \cdot 2H_2O$ (Wako pure chemicals) was solubilized into deionized water (pH 2.0 with H_2SO_4), filtrated (0.02 μm), and stored in sterilized bottle at 4°C.

1 M Glucose stock solution

Glucose (Wako pure chemicals) was solubilized into deionized water and adjusted to pH 7.0 (with NaOH), filtrated (0.02 μm), and stored in sterilized bottle at 4°C.

5% (w/v) Yeast extract stock solution

Yeast extract (Difco) was solubilized into acidic distilled water (pH 2.0 with H_2SO_4), filtrated (0.02 μm), and stored in sterilized bottle at 4°C.

Trace elements (1000×) stock solution

The following chemicals (Wako pure chemicals) were solubilized into acidified distilled water (pH 2.0 with H_2SO_4), filtrated (0.02 μm), and stored in sterilized bottle at 4°C

10 mg/L $ZnSO_4 \cdot 7H_2O$

1 mg/L $CuSO_4 \cdot 5H_2O$

1.09 mg/L $MnSO_4 \cdot 5H_2O$

1 mg/L $CoSO_4 \cdot 7H_2O$

0.39 mg/L $Cr_2(SO_4)_3 \cdot 7H_2O$

0.6 mg/L H_3BO_3

0.5 mg/L $Na_2MoO_4 \cdot 2H_2O$

0.1 mg/L $NaVO_3$

1 mg/L $NiSO_4 \cdot 6H_2O$

0.51 mg/L Na_2SeO_4

0.1 mg/L $Na_2WO_4 \cdot 2H_2O$

Sterilized elemental sulfur powder

Powder of elemental sulfur (Wako pure chemicals) was sterilized in oven (100°C, overnight, twice) and stored in sterilized bottle at 4°C.

2.2 Microorganisms used in this study

2.2.1 Culture maintenances

Table 2.1 Microbial culture maintenances.

Microorganisms	pH	Temp.	Medium	
Pseudomonas putida MnB1 (ATCC 23483)	7.0	25°C	LB medium pH 7.0	
Microorganisms	pH	Temp.	e^- donor	Others
Sulfobacillus sp. YTF1	2.0	45°C	10 mM Glucose	0.01% (w/v) y.e.
Sulfobacillus Thermotolerans Kr1	1.5	45°C	10 mM Fe(II)	0.01% (w/v) y.e. 0.005% (w/v) pyrite
Sulfobacillus sibiricus N1 (AY079150)	1.5	45°C	10 mM Fe(II)	0.01% (w/v) y.e. 0.005% (w/v) pyrite
Acidithiobacillus caldus KU (Z29975)	2.0	45°C	0.01% (w/v) S^0	TES (1x)

* TES: Trace element solution

All the cultures were maintained in 300 mL Erlenmeyer flask containing 100 mL HBS media (pH adjusted as the above) supplemented with the electron donors and yeast extract or trace elements, as is described in table 2.1. The flasks were maintained at the temperatures (table 2.1) on an orbital rotary shaker at 100-150 rpm.

2.2.2 Sub-culturing

All the sub-culturing was carried out using 500 mL Erlenmeyer flask containing 200 mL HBS media: Media composition was same as that of the stock culture.

2.3 Experimental conditions

Aerobic conditions

Aerobic conditions were established using air permeable silicon caps for Erlenmeyer flasks.

2.4 Sampling procedures

2.4.1 Liquid samples

Liquid samples taken from the experimental cultures after compensation of water evaporated with pure water, and then used for cell counting using microscope, filtered using 0.20-μm cartridge filters, and used for measurements of metal concentrations, pH values and solution redox potential values.

2.4.2 Solid samples

At the end of the experiments, solid samples were collected by filtration (0.45 μm) using vacuum pump, and freeze-dried overnight. Procedure for special samples such as cell and mineral/cell will be mentioned in respective chapter.

2.5 Analytical methods: Liquid analysis

2.5.1 pH and solution redox potential values measurements

Solution pH and redox potential values (Ag/AgCl reference electrode) were measured using pH-Eh meter (MM-60R, TOADKK). The measured solution redox potential values were automatically converted to values vs. SHE as follows;

"*E* vs. SHE" = "*E* vs. Ag/AgCl" + 206 - 0.7 ("Solution Temp." - 25) (Eq. 2.1)

E: Solution redox potentials (mV)

2.5.2 Cell density

Cell density was determined by counting the living cells on bacteria counting chamber (Thoma counting chamber) under phase contrast light microscope (Olympus BX51) with 40x objective lens.

2.5.3 Storage of sample

Samples withdrawn from experiments were acidified with 0.1 M HCl before store at 4℃ prior to further analysis (eg. total dissolved metal)

2.5.4 Determination of As(V) and As(III) using molybdenum blue method

Molybdenum blue method was used in this study as a As(III) assay. The procedures are described below (K. Oyama, unpublished data)

1. Add 30 μL of 1 M H_2SO_4 into the wells of 96-well plate
2. Add 30 μL of liquid samples to the wells. Note that all samples were filtered (0.22 μm) and subsequently diluted if needed. (The concentration should not exceed 1 mM)
3. Add 30 μL of 1 mM of $KMnO_4$ (in the case of total As)
4. Add 30 μL of ascorbic acid solution. Note that ascorbic acid solution was made fresh prior to measurement (3 spoons of ascorbic acid powder (Wako pure chemical) solubilized in 5 mL of deionized water)
5. Add 30 μL of Mo-Sb solution (1% (w/v) $(NH_4)_6Mo^{VI}_7O_{24}\cdot 4H_2O$) and 0.02% (w/v) $K_2(Sb^{III}O)_2C_8H_4O_{10}\cdot 3H_2O$)
6. Add deionized water to make up each well to 300 μL
7. Left for 15 min to reach equilibrium

8. Measure absorbance at 880 nm
9. As(III) concentration can be calculated by subtraction of total As with As(V) concentration

2.5.5 Determination of Fe(II) concentration using *O*-phenanthroline method

O-phenanthroline method was used in this study as a Fe(II) assay. The procedures are described below (Caldwell and Adams, 1946).

1. Add 30 μL of 1 M HCl to the wells of 96-well plate.

2. Add 30 μL of liquid samples to the wells. Note that all samples were centrifuged (12,000 rpm, 8 min) using Bio Shaker G·BR-200 (TAITEC), and subsequently diluted (e.g., ×10, etc.) using 1 M HCl if needed.

3. Add 30 μL of ascorbic acid solution to the wells in the case of total soluble Fe measurements. Note that ascorbic acid solution was made on all such occasions since the chemical is unstable in solution (one spoon of ascorbic acid powder (Wako pure chemicals) solubilized into 5 mL of distilled water).

4. Give 5 min to react Fe(III) ions and ascorbic acid.

5. Add 30 μL of 5 mM *o*-phenanthroline solution (solubilized in distilled water) to the wells in order to form $[Fe(phenanthoroline)_3]^{2+}$ complex.

6. Add 30 μL of 2 M sodium acetate solution (solubilized in distilled water) to the wells.

7. Add distilled water until total volume of 300 μL.

8. Left for 10 min to reach equilibrium

9. Measure absorbance at 510 nm using spectrophotometer (Multiskan Go, Thermo Scientific).

A standard curve used is shown in Fig. 2.2. Note that calibration curve was redrawn every time new chemical reagents were made.

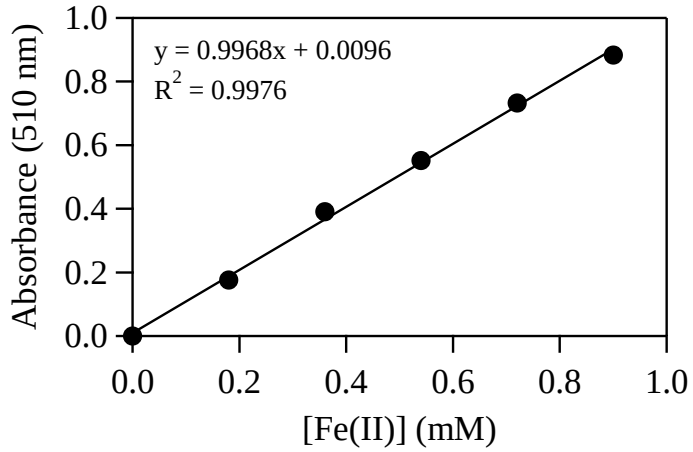

Figure 2.1 Standard curve of Fe(II) concentration using *o*-phenanthroline method

2.5.6 Determination of total soluble metal concentration

Concentrations of total soluble metal ions (e.g., Fe, Cr, Cu, Ni, Ca, Mg, Al, Co) in acid solution samples were measured using ICP-OES (Optima 8300, PerkinElmer). Standard solutions of total soluble metal ions were made by appropriate dilution of standard 1000 ppm solution (Wako chemical) in 0.1 M HCl matrix. The standard solutions were kept at 4℃ and re-make every 2 months.

Stored liquid samples (section 2.6.1.2) was appropriately diluted (x10, x50, etc.) to estimated concentrations of target metal ions in them (e.g., ×25, 100, 250, etc.) using 0.5 M HCl. All the measurements using ICP-AES were carried out in duplicates: The average values were used for the results.

Wavelengths measured for each metal are described as follows:

Fe: 238.204, 239.562, 259.939 nm (Wavelength of 238.204 nm was used for calculations of Fe concentrations.)

Cr: 267.716, 205.560, 283.563 nm (Wavelength of 267.716 nm was used for

calculations of Cr concentrations.)

Cu: 327.393, 324.752, 224.700 nm (Wavelength of 327.393 nm was used for calculations of Cu concentrations.)

Ni: 231.604, 221.648, 232.003 nm (Wavelength of 231.604 nm was used for calculations of Ni concentrations.)

Ca: 317.933, 315.887, 393.366 nm (Wavelength of 317.933 nm was used for calculations of Ca concentrations.)

Mg: 285.213, 279.077, 280.271 nm (Wavelength of 285.213 nm was used for calculations of Mg concentrations.)

Al: 396.153, 308.215, 394.401 nm (Wavelength of 396.153 nm was used for calculations of Al concentrations.)

Co: 228.616, 238.892, 230.786 nm (Wavelength of 228.616 nm was used for calculations of Co concentrations.)

2.6 Analytical methods: Solid analysis

2.6.1 X-ray fluorescence (XRF)

Elemental compositions of freeze-dried sediment samples collected from Chinoike-Jigoku hot spring, were analyzed using ZSX Primus II (Rigaku). Measurement were carried out with oxide mode (diameter irradiated X-ray was 10 mm) under vacuum conditions. The calculation was conducted using fundamental parameter (FP) method.

2.6.2 X-ray diffraction (XRD)

XRD measurement (Ultima IV, Rigaku) was performed with Cu-Kα radiation as an X-ray source. The accelerating voltage and current were 40 kV and 40 mA, with a scanning speed of 2°/min and scanning step of 0.02°. Peak assignment was done based on International Centre for Diffraction Data (ICDD) using powder diffraction analysis software PDXL (Rigaku).

2.6.3 X-ray absorption near edge structure (XANES)

Samples for XAFS measurement were prepared by using a tablet press machine at 10 MPa for 5 min. X-ray absorption spectra were collected on Kyushu University beam line (BL06) at Kyushu Synchrotron Light Research Center (SAGA-LS; 1.4 GeV storage ring with a circumference of 75.6 m). The measurements were conducted at the Cu K-edge (with the energy range from 8,650 to 10,500 eV) and Cr K-edge (with the energy range from 5,660 to 7.500 eV) and experimental data were collected in transmission mode. Energy selection was accomplished by a double crystal Si (1, 1, 1) monochromator. Intensities of incident and transmitted X-ray were recorded by using ionization chambers. Standard chemicals and samples were uniformly mixed with boron nitride (BN; Wako pure chemicals) in appropriate ratios for XAFS measurement.

2.6.4 Scanning electron microscope (SEM)

Overnight freeze-dried samples were fixed on SEM stub using carbon tape and Au-Pd magnetron-sputtered (MSP-1S, Vacuum Device). SEM images were collected using VE-9800 (Keyence) at accelerated voltage of 5-10 keV. Special pre-treatment for

biological samples (eg: bacteria cells and bacteria-mineral) will be mentioned in section 4.2.2 and *4.2.4.3*.

2.6.5 Microwave treatment

Teflon vessels containing a known amount of solid samples and 60% HNO_3 solution or aqua regia (37% HCl and 60% HNO_3 are mixed in a volume ratio 3:1) were placed in the microwave digestion system (Ethos Plus, Milestone) and heated to 230°C with 7°C /min increments, kept for 15 min at 230°C, and finally allowed to cool to room temperature.

2.6.6 Specific surface area (BET method)

Specific surface area of bacterial support materials was measured using BET (Brunauer-Emmett-Teller) theory (BEL-Max, MicrotracBEL) based on adsorption isotherms using N_2 gas at −196℃. Samples were dewatered and degassed under vacuum at 80℃ for 50 hours prior to measurement.

2.6.7 Zeta-potential measurement

Zeta-potential measurement of bacteria cells ($5x10^7$ cells/mL) or solid samples (0.2% (w/v)) were measured in 10^{-3} KCl solution using Zetasizer Nano ZS (Malvern) at pH values ranging from 5.0-8.0 (adjusted with HCl and KOH). All measurements were conducted at least in triplicate. Special pre-treatment for each sample will be mentioned later.

2.6.8 Fourier transforms infrared spectroscopy (FT-IR)

FT-IR spectra of the samples were obtained by KBr and ATR (attenuated total reflection) methods using FT-IR-670 (JASCO). For KBr method, sample was mixed quantitatively the KBr (FT-IR grade) and pressed into transparent pellet. The spectra was collected

2.6.9 Estimation of average oxidation state of Mn in Mn-oxide

Average oxidation state (AOS) of Mn in Mn-oxide dictated the oxidation power of Mn-oxide. High AOS Mn-oxide (>3.6) usually consisted of majority Mn(IV) proportion.

Two-step colorimetric method was used in this study as AOS determination assay. The procedures are described below (Zhu et al., 2017).

2.6.9.1 Total Mn

2.6.9.1.1 Chemical reagents

- Formaldoxime

  Dissolve 20 g of hydroxylamine hydrochloride () in 450 mL H_2O then add 10 mL formaldehyde and make up to 500 mL

- 10% hydroxylamine hydrochloride
- 0.1M EDTA solution
- Ammonia

2.6.9.1.2 Protocol

1) Dissolve Mn oxide sample in 10% hydroxylamine hydrochloride solution
2) Dilute into appropriate concentration

3) Mix ammonia and formaldoxime solution (1:1)
4) Add 2 mL of the mixture to the unknown sample
5) Add 2 mL of EDTA solution
6) Left for 20 min to reach equilibrium
7) Measure absorbance at 450 nm using spectrophotometer (Multiskan Go, Thermo Scientific).

A standard curve used is shown in Fig. 2. Note that calibration curve was redrawn every time new chemical reagents were made.

2.6.9.2 A_{620}-Transfer electron concentration (TEC)

2.6.9.2.1 Chemical reagents

- 0.04% Leucoberbelin solution (LBB)

Dissolve 0.1 g Leucoberberlin in 250 mL of 45 mM acetic acid

- 10% hydroxylamine hydrochloride

2.6.9.2.2 Protocol

1) Disperse Mn-oxide sample using sonicator
2) Mix 100 μL of the suspension with 500 μL of LBB solution
3) Incubate in the dark for 15-20 min
4) Measure absorbance at 620 nm

For calibration curve, known concentration $KMnO_4$ was used as a standard. Concentration of $KMnO_4$ was converted into CTE (concentration of transfer electron) by multiply by factor of 5. Average oxidation state (AOS) of Mn was calculate using the following equation (Eq. 2.2)

$AOS = n_{(CTE)} / n_{(Mn\ total)} + 2$

Where; $n_{(CTE)} = C_{(CTE)}$ x V/1000 (V= total volume of mineral suspension)

$$n_{(Mn\ total)} = \text{Mn oxide weight x } Mn_{total}\,\%/\ mw_{(Mn)} \quad \text{(Eq. 2.2)}$$

2.6.10 Stability evaluation for As immobilized product

Toxicity characteristic leaching procedure (TCLP) was conduction by following EPA method 1311 (EPA, 1994). Arsenic immobilized products (scorodite or birnessite) were transferred into 25 mL vials containing 10 mL acetate buffer pH (4.93) at a pulp density of 5% (w/v) (solid:liquid = 1:20) and incubated at 25°C, rotated at 30 rpm for 18 hours. Liquid samples were filtered (0.45 μm) to measure total soluble Fe, As, and Mn concentrations (ICP-OES). Tests were conducted in duplicates.

Acetate buffer at pH 4.93 was prepared as followed; 5.7 mL glacial acetic acid (CH_3COOH) and 64.3 mL of 1 N NaOH were added to 500 mL of distilled water and diluted to 1 L.

References

Caldwell, D.H., and Adams, R.B. (1946). Colorimetric Determination of Iron in Water With o-Phenanthroline. *Journal (American Water Works Association)* 38(6)**,** 727-730.

EPA (1994). "Toxicity Characteristic Leaching Procedure. Test methods for evaluating solid wastes physical/chemical methods". (Washington DC).

Zhu, Y., Liang, X., Zhao, H., Yin, H., Liu, M., Liu, F., et al. (2017). Rapid determination of the Mn average oxidation state of Mn oxides with a novel two-step colorimetric method. *Analytical Methods* 9(1)**,** 103-109. doi: 10.1039/C6AY02472F.

Chapter 3

Natural attenuation of dissolved Mn level in the metal-refinery wastewater treatment system

Abstract

In this chapter, natural attenuation of Mn(II) concentration inside metal-refinery wastewater treatment was investigated. The phenomena accompanied with the dark-brown-colored mineralization (mostly $Mn^{IV}O_2$ with some $Mn^{III}_2O_3$ and Fe_2O_3) on the inner pipe surface. The Mn-deposit hosted the bacterial community comprised of *Hyphomicrobium* sp. (22.1%), *Magnetospirillum* sp. (3.2%), *Geobacter* sp. (0.3%), *Bacillus* sp. (0.18%), *Pseudomonas* sp. (0.03%) and non-metal-metabolizing bacteria (74.2%). Autotrophic growth capability of the budding bacteria, *Hyphomicrobium* sp., was speculated for its important role in primary colonization in the water pipe. This enables structural and nutritional support for the heterotrophic Mn(II)-oxidizer to colonize and deposit Mn-oxide. Even though the primary products were poorly-crystalline, transformation or crystallization of biogenic Mn-oxide

Natural Mn-oxide could oxidize and remove Mn^{2+} via synproportionation reaction (Mn(II)/Mn(IV)) producing Mn(III)-oxide, on it on the surface. That passivation layer greatly lower Mn(II) removal efficiency. However, the active microbial reaction could further oxidize residual Mn(II), resulting in better removal efficiency compared with autoclaved natural Mn-oxide.

3.1 Introduction

Mn-oxide deposition by microorganism via enzymatic reaction was believed to occur in nature since the Mn(II)-oxidation is thermodynamically stable (Morgan, 2005). Obviously, there is no direct evidence linking Mn(II) oxidation to energy conservation even though the oxidation of Mn(II) to Mn(III) or Mn(IV) is thermodynamically favorable. Nevertheless, the activity of such Mn(II)-oxidizing bacteria have been widely observed not only in natural open environments but also within artificial man-made structures such as freshwater pipelines and sewage treatment plants (Tyler, 1970; Sly et al., 1988; Holm et al., 1996; Okibe et al., 2013). The majority of naturally occurring Mn oxides in these environments are considered originating directly from microbial Mn(II) oxidation or from the subsequent alteration of biogenic Mn-oxides (Tebo et al., 2005). This indicates the ubiquitous and robust nature of these Mn(II)-oxidizing bacteria providing an extensive impact on Mn geochemistry on the earth's crust.

Natural attenuation of Mn(II) inside water pipes of the metal-refinery wastewater treatment system, which was accompanied by extensive mineralization on its inner surface. Based on the pH and ORP values of the wastewater, this phenomenon appeared to involve biological intervention, rather than spontaneous chemical Mn(II) oxidations. In this chapter, bacterial community analysis was conducted in order to clarify the mechanism of this natural Mn(II) attenuation as well as to search for Mn(II)-oxidizing bacteria responsible for this phenomena. The understanding could be reconstituted as a bioprocess to be introduced in wastewater treatment facilities.

3.2 Materials and methods

3.2.1 Collection and analysis of on-site samples

3.2.1.1 Water sample

Mn(II) containing wastewater samples were collected at the inlet and outlet of the 10 km-long wastewater pipe at the metallurgical wastewater treatment facility. The pH and ORP values were measured on-site. Concentrations of metals, NO_3^- and TOC (Total Organic Carbon) were determined by ICP-OES (iCAP 6500, Thermo Scientific), ion chromatography (Dionex ICS1000, Thermo Scientific) and TOC analyzer (TOC-5000A, Shimadzu), respectively.

3.2.1.2 Mn-deposit sample

Blackish-brown-colored precipitates accumulated on the inner wall of the wastewater pipe were collected. The pH and ORP values of the slurry were measured. An aliquot of the freeze-dried sample was digested with 60% HNO_3 (for TOC analysis), or with aqua regia (HNO_3:HCl = 3:1, for metal composition) in teflon vessels placed in the microwave digestion system (Ethos Plus, Milestone) (heated to 210℃ with 7℃/min increments, kept for 15 min at 210℃, and finally allowed to cool to room temperature). The sample was then filtered (0.22 μm) and diluted (with deionized water) for the TOC (TOC-VCHS, Shimadzu) and ICP-OES (Optima 8300DV, PerkinElmer) analyses. For comparison, the sample was mixed with poly powder and pressed into a pellet for X-ray fluorescence (XRF; ZSX Primus II, Rigaku) analysis.

The freeze-dried Mn-deposit sample was also analyzed by X-ray diffraction (XRD; Ultima IV, Rigaku; CuKα 40 mA, 40 kV) and by X-ray absorption near edge structure (XANES) to calculate the ratios of Mn oxidation states (as described in 2.4.2). Genomic DNA was extracted from the raw Mn-deposit sample and the next

generation sequencing was performed to analyze the microbial community structure based on the 16S rRNA gene sequence (Techno Suruga Lab. Co., Ltd. Japan).

3.2.2 Mn(II) removal using natural occurring Mn-oxide

Natural occurring Mn-oxide collected from metal-refinery wastewater treatment system was tested for their Mn(II)-oxidizing activity. Mn-oxide sample (0.5%) were added into 300 mL Erlenmeyer flasks containing 100 mL of modified PYG medium (1 mM glucose, 0.025% yeast extract, 0.025% peptone, 2.02 mM $MgSO_4 \cdot 7H_2O$, 0.068 mM $CaCl_2 \cdot 2H_2O$, 15 mM PIPES). The initial Mn(II) concentration was set at 100 mg/L (added as $MnSO_4$). Autoclaved Mn-oxide sample (120℃, 20 min) was also tested in parallel to test the influence of active microbial reaction.

The experiment was conducted in duplicate, incubated shaking at 120 rpm. Sample was routinely withdrawn to monitor pH and the Mn(II) concentration (ICP-OES).

3.3 Results and discussion

3.3.1 Water chemistry of metal-refinery wastewater treatment system

The physicochemical characteristics of the wastewater and Mn-deposit samples are shown in table 3.1. Compared to other solutes, the Mn(II) concentration was noticeably lowered from 1.5 mg/L to 0.48 mg/L as the water traveled through wastewater pipe (table 3.1). The inner pipe surface was found heavily encrusted with dark-brown precipitates, typical color of Mn-oxide. In fact, the main metal constituent of the precipitate was Mn with less abundant metals such as Fe, Ca and Mg (table 3.1) and XRD detected crystalline $Mn^{IV}O_2$, $Mn^{III}{}_2O_3$, and Fe_2O_3 . Owing to the circumneutral pH and low ORP values of the water samples (table 3.1), spontaneous chemical Mn oxidation was unlikely to be triggered, and it was suspected that microbiological interaction was involved in this natural attenuation phenomenon.

Based on LCF fitting of Mn-K edge XANES spectrum (Fig 3.2), the ratio of Mn species of the Mn-deposit is Mn(IV) 84%, Mn(III) 13%, and Mn(II) 3% with the average oxidation state (AOS) of 3.75.

Naturally occurring biogenic Mn-oxide are generally formed as poorly-crystalline birnessite, as observed in environments such as hot spring, streambed crusts and eutrophic lake (Lind and Hem, 1993; Friedl et al., 1997; Bilinski et al., 2002; Okibe et al., 2013). These primary biogenic Mn-oxides were reported to transform into different crystalline Mn-oxides (e.g., todorokite), through prolonged exposure to high enthalpy of hydration cations (e.g. Ca^{2+}, Mg^{2+}, and Zn^{2+}) (Bodei et al., 2007; Feng et al., 2010; Cheng et al., 2017). The reaction of primary biogenic Mn-oxides (by *Bacillus* sp. SG-1) with Mn(II) was also shown to result in the abiotic formation of secondary feitknechtite ($Mn^{III}OOH$) or phyllomanganate, depending on the Mn(II) concentration (Bargar et al., 2005). Based on the water characteristics shown in table 3.1, such natural transformation reactions also likely took place in the wastewater pipe during years of operation to produce crystalline Mn-oxides deposits even though the primary products were poorly-crystalline.

Table 3.1 Characteristics of the wastewater and Mn-deposit samples (taken from the inlet and outlet of the wastewater pipe)

	Wastewater samples		**Mn-deposit sample**	
	Inlet	**Outlet**		
pH	7.9	7.6	7.3 (slurry)	
ORP (mV)	100	105	231 (slurry)	
	(mg/L)		(mg/g)	mass%*[1]
TOC	4	N.D.	2.5	
Metal composition				
Ca	389	386	59±4.3	6.6
Mg	280	276	51±4.3	1.97
Si	5.3	5.3	N.D.	-
Mn	1.n	0.n	617±46	28.2
Pb	0.26	0.25	0.056±0.002	-
Al	0.18	0.16	11±0.72	0.92
Cr	0.03	0.03	<0.01	-
Zn	<0.01	<0.01	1.0±0.05	0.04
Ni	<0.01	<0.01	2.7±0.17	0.28
Fe	<0.01	<0.01	121±6.8	6.95
Cu	<0.01	<0.01	0.06±0.005	0.02
Co	<0.01	<0.01	0.47±0.024	0.04
O	N.D	N.D.	N.D.	47.25
C	N.D.	N.D.	N.D.	4.86

N.D.: Not Determined

*1: Determined by XRF

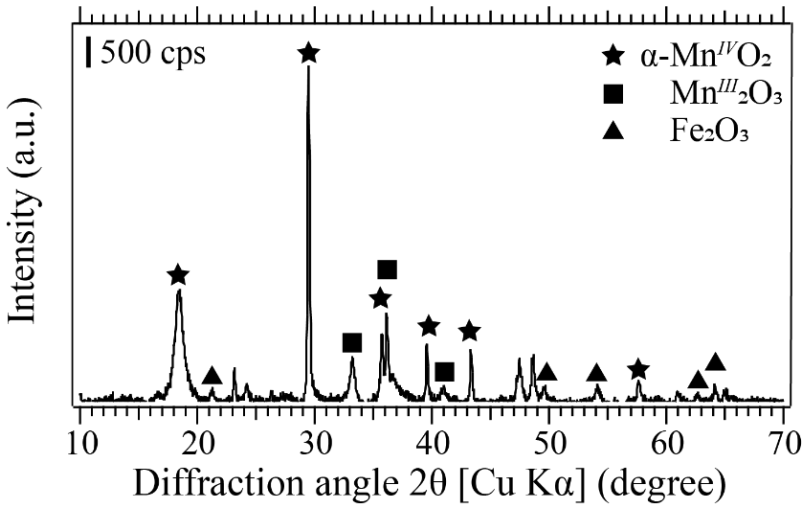

Figure 3.1 X-ray diffraction patterns of the Mn-deposit collected from the metal-refinery wastewater pipe. ★; α-$Mn^{IV}O_2$ (JCPDS 44-141), ■; $Mn^{III}{}_2O_3$ (JCPDS 41-1442), ▲; Fe_2O_3 (JCPDS 39-1346).

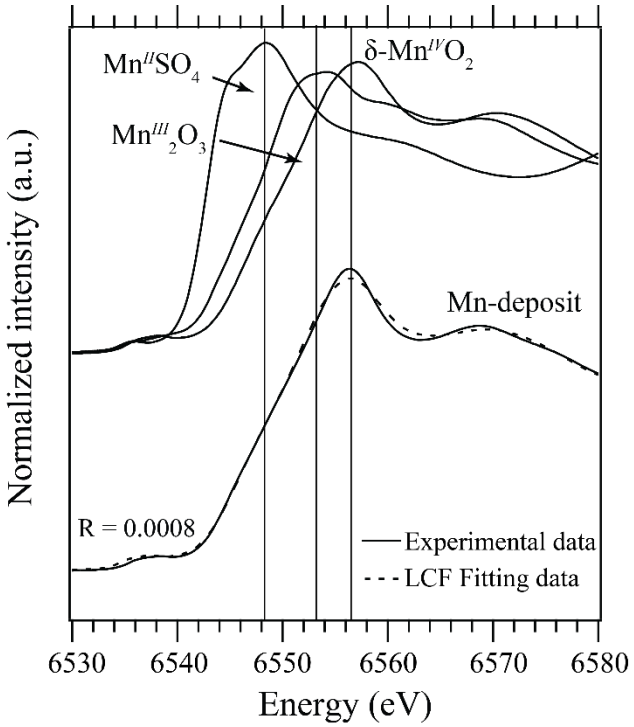

Figure 3.2 Mn K-edge spectra of Mn-deposit sample collected from metal-refinery wastewater treatment system (solid line). Linear combination fitting results (broken line). As Mn standards, $Mn^{II}SO_4$, $Mn^{III}{}_2O_3$ and δ-$Mn^{IV}O_2$ were used.

3.3.2 Bacterial community analysis and proposed mechanism of Mn-deposit formation process in the wastewater pipe

The bacterial community structure in the Mn-deposit was analyzed in order to search for the Mn(II)-oxidizing bacteria responsible for its formation in the wastewater pipe. The number of gene sequences analyzed was 22733, from which 18605 (81.8%) were unclassified and 352 (1.5%) did not match database entries. Fig. 3.3 shows full analysis of the bacterial community structure (genus-level) and based on the remaining 3776 (16.6%) classified sequences and Mn (metal)-metabolizing genera were shows in Fig 3.4.

Around 74.2% of the community was unknown as metal-metabolizing bacteria, the majority (52%) of which were *Porphyrobacter* spp. (Fig. 3.3; mostly *P. sanguineus*): these bacteria receive light energy with bacteriochlorophyll but perform aerobic photoheterotrophic metabolism requiring organic substrates for growth (Hiraishi et al., 2002). Since the wastewater was once pooled in open storage before entering the pipe, the photoheterotrophs may have taken advantages of the light to dominate the community in such an oligotrophic environment in the wastewater treatment system.

The second dominant genus (22.1%) was aerobic, methylotrophic budding bacteria *Hyphomicrobium* (Fig. 3.4) (mostly *H. zavarzinii* and *H. hollandicum*; Table 3.2), characteristic in producing hyphal filament during growth and budding reproduction. This genus of budding bacteria is lack of enzyme pyruvate dehydrogenase, they are examined as methylotroph utilizing one-carbon compound for reproduction (Harder et al., 1975). *Hyphomicrobium* has been widely detected as a dominant member in Mn-deposits from worldwide locations, including freshwater pipeline (Tyler, 1970) and sewage treatment plant (Holm et al., 1996). Despite its abundance in Mn-deposits,

the difficulty in its isolation and steady maintenance makes it still unclear whether or not *Hyphomicrobium* is indeed directly responsible for Mn(II) oxidation (Tyler and Marshall, 1967; Tyler, 1970). The observation that *Hyphomicrobium* is capable of autotrophic growth (Uebayasi et al., 2014), lead us to speculate its important role in primary colonization via unique hyphae-network onto the pipeline surface, establishing the structural and nutritional scaffolds to support secondary colonization of heterotrophic Mn(II)-oxidizers against a continuous water flow (Fig 3.5).

Micro-aerobic magnetotactic bacteria, *Magnetospirillum* spp. (all *Ms. gryphiswaldense*: table 3.2) accounted for 3.2% of the community (Fig 3.4). *Ms. gryphiswaldense* synthesizes nano-sized magnetosomes (Fe_3O_4) by active uptake and reduction of Fe^{3+} through ferric reductase (Zhang et al., 2013). The Mn concentration in the wastewater may have been affected by this bacterium to some extent since Mn can be incorporated into the magnetite crystal (Prozorov et al., 2014).

Facultative anaerobes, *Geobacter* spp. (mostly *Gb. sulfurreducens*; table 3.2), comprised 0.3% of the community (Fig 3.4). These Fe(III)-reducing bacteria may adversely affect Mn(II) oxidation in the wastewater pipe, as they may reduce Mn-oxides in anaerobic respiration in the event of oxygen depletion (Zacharoff et al., 2017). The genus *Bacillus* and *Pseudomonas* accounted for a minor portion of the community structure (0.18% and 0.03%, respectively; Fig 3.4). Mn(II) oxidation is well-studied in some *Bacillus* and *Pseudomonas* strains, such as *Bacillus* sp. SG-1 (Francis and Tebo, 2002), *Ps. putida* MnB1 (Villalobos et al., 2003), and *Ps. putida* GB-1 (Geszvain et al., 2013). From the Mn-deposit in this study, six different *Bacillus* spp. and *Ps. resinovorans* were detected (Fig. 3.3, table 3.2). However, Mn(II)-oxidizing ability is yet unknown in these species. As was proposed in Fig 3.5,

growth of these possible heterotrophic Mn(II) oxidizers perhaps as well as non-Mn-metabolizing *Porphyrobacter* may depend on the growing biofilms of *Hyphomicrobium*, by scavenging organic exudates deriving from these primary colonizers.

In diverse species microbial community, the order of colonization on the surface is strongly depending on water velocity and nutrient condition. In high water velocity, attraction force non-budding bacteria to the surface obviously not enough to compete the shear forces of turbulent flow in high water velocity. On the other hand, colonization of hyphomicrobia at high water velocity was not observed at a lower velocity and this still remained unclear (Sly et al., 1988).

Apart from Mn(II)-containing water distribution system, Hyphomicrobia also found in other systems such as biological denitrification system (Fan et al., 2018; Li et al., 2018), biological pesticide wastewater treatment system (Fang et al., 2018), and fine chemical wastewater treatment system (Zhang et al., 2018). These illustrated the presence of Hyphomicrobia as one of the dominated species, which may more or less contribute to the successful colonization in the water distribution system.

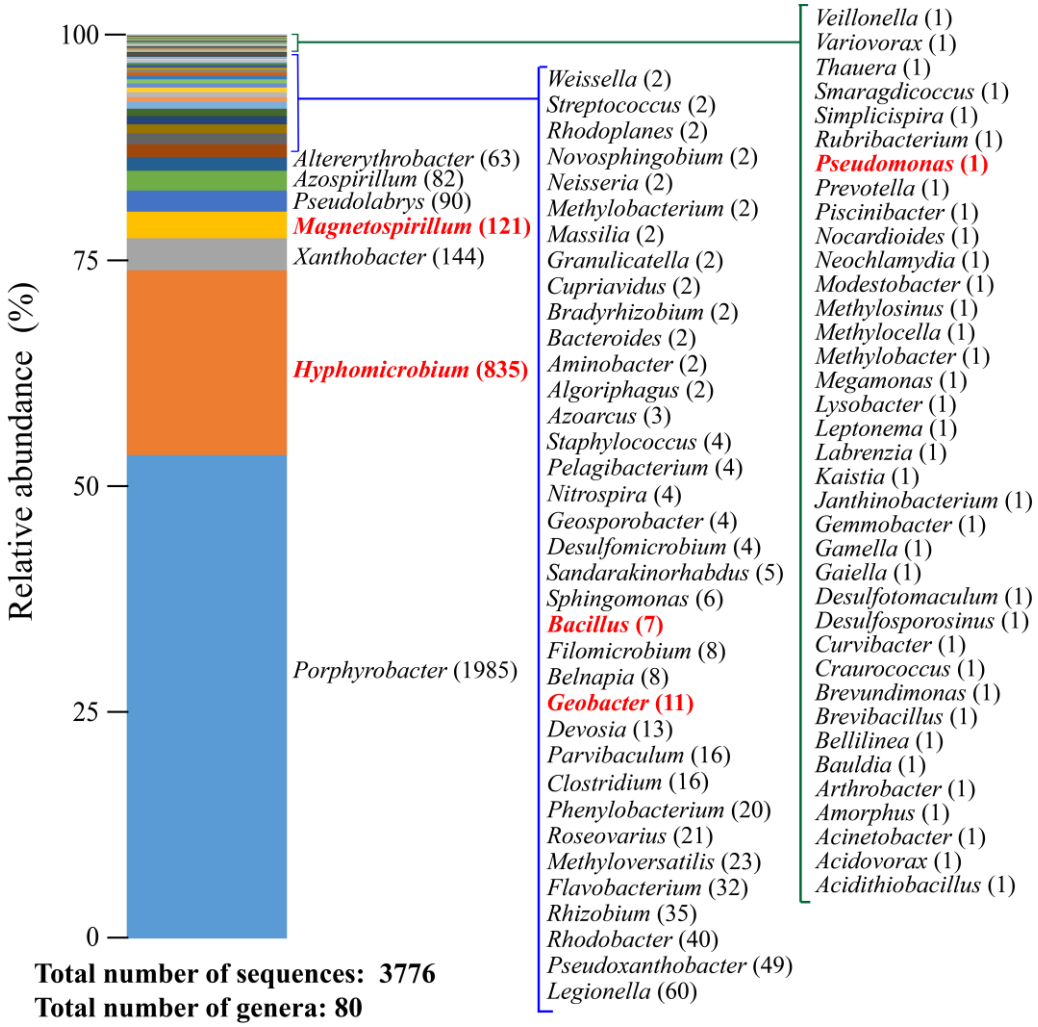

Figure 3.3 Bacteria community structure (genus level) in Mn-deposits collected from the metal-refinery wastewater treatment system (full data). Putative Mn-metabolizing genera were highlighted in red.

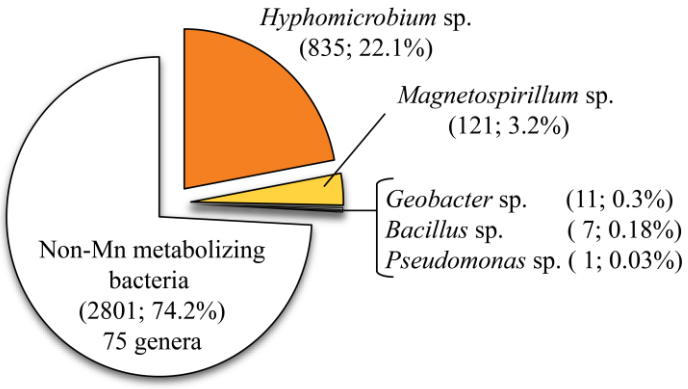

Figure 3.4 Bacterial community structure in the Mn-deposit collected from the metal-refinery wastewater pipe. Values in brackets indicate the total number of sequences and its percentage.

Table 3.2 Species names under the genera *Hyphomicrobium*, *Magnetospirillum*, *Geobacter*, *Bacillus* and *Pseudomonas* detected in the bacterial community structure shown in fig 3.4.

Species	Number of sequences
***Hyphomicrobium* sp.**	**835 (total)**
H. zavarzinii	655
H. hollandicum	118
H. facile	57
H. vulgare	5
***Magnetospirillum* sp.**	**121 (total)**
Ms. gryphiswaldense	121
***Geobacter* sp.**	**11 (total)**
Gb. sulfurreducens	6
Gb. bremensis	2
Gb. bemidjiensis	1
Gb. luticola	1
Gb. toluenoxydans	1
***Bacillus* sp.**	**7 (total)**
B. aryabhattai	2
B. asahii	1
B. funiculus	1
B. graminis	1
B. indicus	1
B. solisalsi	1
***Pseudomonas* sp.**	**1 (total)**
Ps. resinovorans	1

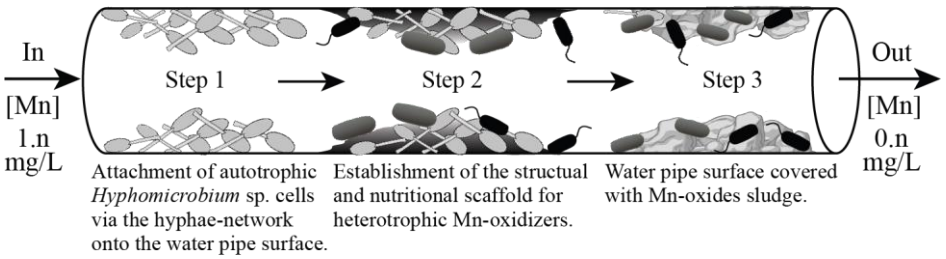

Figure 3.5 Schematic image of the proposed Mn-deposit formation process in the water pipe

3.3.3 Oxidative removal of Mn(II) using natural occurring Mn oxide

Mn(II) initially 100 mg/L was oxidized and removed in the presence of natural Mn-oxide (no oxidation in sterile control (data not shown)). The advantage of the active microbial reaction was illustrated by the difference in Mn(II) oxidative removal efficiency (Fig. 3.6). Solution pH dropped owing to the proton-generating Mn(II) oxidation reaction (Fig. 3.7). Dissolved Mn^{2+} and Mn^{IV}-oxide were reported to undergo synproportionation reaction, leading to Mn(III) formation (Zhao et al., 2016). Since natural Mn-oxide contained both MnO_2 and Mn_2O_3, chemically-synthesized MnO_2 was used to confirm the phenomena. After synproportionation, Mn(III) as Mn_2O_3 was clearly detected by X-ray diffraction (fig. 3.8). Passivation of Mn_2O_3 on the MnO_2 surface slowed down the speed of the reaction since it cannot oxidize Mn^{2+}. The presence of active microbial reaction (perhaps indigenous Mn(II)-oxidizing bacteria) could oxidize the residue Mn^{2+}.

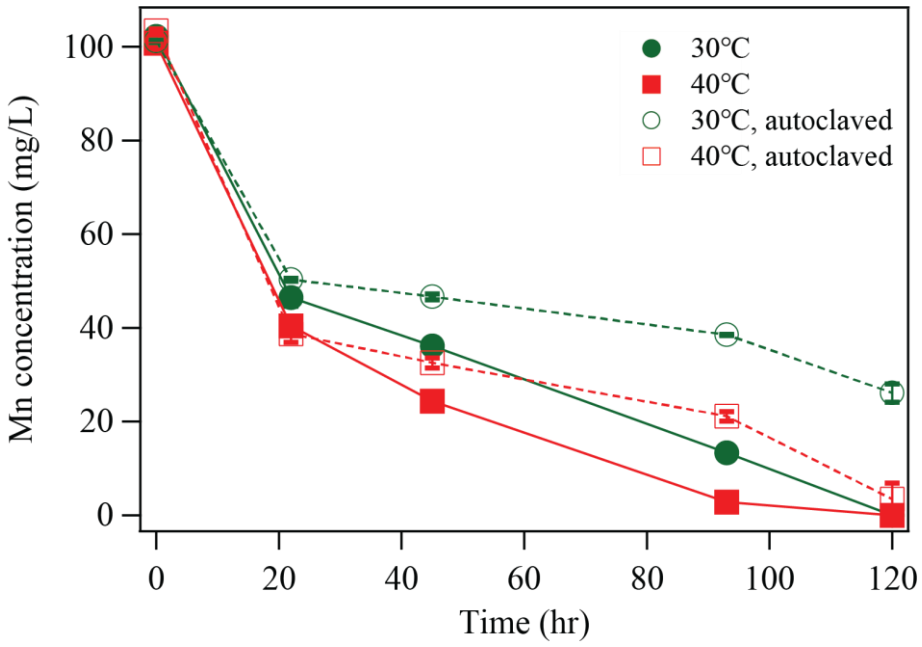

Figure 3.6 Mn(II)-oxidative removal by raw (solid symbols with solid line) and autoclaved (open symbols with broken lines) Mn-deposit collected from wastewater pipe under different temperature of 30°C and 40°C.

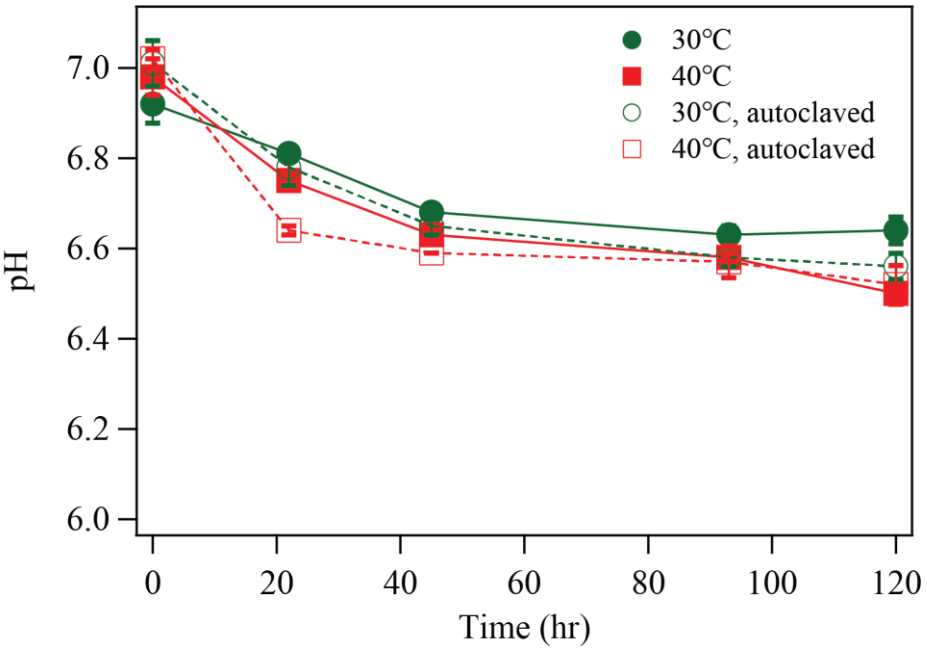

Figure 3.7 The changes in pH during Mn(II) oxidative removal by raw (solid symbols with solid line) and autoclaved (open symbols with broken lines) Mn-deposit collected from wastewater pipe under different temperature of 30°C and 40°C.

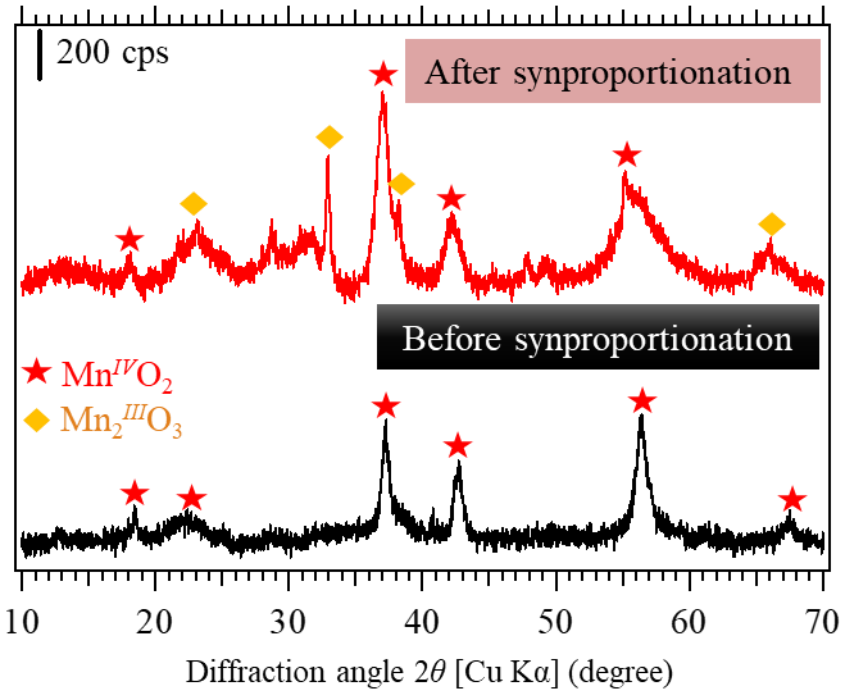

Figure 3.8 X-ray diffraction patterns of the $Mn^{IV}O_2$. ★; α-$Mn^{IV}O_2$ (JCPDS 44-141), ♦; $Mn^{III}_2O_3$ (JCPDS 41-1442)

3.4 Conclusions

- Natural Mn(II) attenuation was found inside an industrial metal-refinery wastewater pipeline, coincided with extensive brown-colored Mn-mineralization (mostly crystalline $Mn^{IV}O_2$ with some $Mn^{III}{}_2O_3$ and Fe_2O_3) of the inner pipe surface.

- Nearly 82% of the microbial community in the Mn-deposit was unclassified. The rest (18%) comprised of *Hyphomicrobium* sp. (22.1%), *Magnetospirillum* sp. (3.2%), *Geobacter* sp. (0.3%), *Bacillus* sp. (0.18%), *Pseudomonas* sp. (0.03%) and non-metal-metabolizing bacteria (74.2%). The methylotrophic budding bacteria, *Hyphomicrobium* sp. was proposed to be the first colonizer in the water pipe, whereas putative heterotrophic Mn(II)-oxidizer, *Bacillus* sp. and *Pseudomonas* sp. took the advantages of structural and nutritional scaffolds supported by the former against continuous water flow.

- Poorly-crystalline Mn-oxide (such as birnessite and vernadite) was thought to be initially formed biogenically. Through several years of operation, those poorly-crystalline Mn-oxides were undergone structural transformation or crystallization by reaction with other contaminants in the wastewater.

- Active indigenous Mn(II)-oxidizer was suspected to improve the Mn(II)-oxidative removal efficiency by natural Mn-oxide.

References

Bargar, J.R., Tebo, B.M., Bergmann, U., Webb, S.M., Glatzel, P., Chiu, V.Q., et al. (2005). Biotic and abiotic products of Mn(II) oxidation by spores of the marine *Bacillus* sp. strain SG-1. *American Mineralogist* 90(1), 143-154. doi: 10.2138/am.2005.1557.

Bilinski, H., Giovanoli, R., Usui, A., and Hanzel, D. (2002). Characterization of Mn oxides in cemented streambed crusts from Pinal Creek, Arizona, USA, and in hot-spring deposits from Yuno-Taki falls, Hokkaido, Japan. *American Mineralogist* 87(4), 580-591.

Bodei, S., Manceau, A., Geoffroy, N., Baronnet, A., and Buatier, M. (2007). Formation of todorokite from vernadite in Ni-rich hemipelagic sediments. *Geochimica Et Cosmochimica Acta* 71(23), 5698-5716. doi: 10.1016/j.gca.2007.07.020.

Cheng, Y., Huang, T.L., Sun, Y.K., and Shi, X.X. (2017). Catalytic oxidation removal of ammonium from groundwater by manganese oxides filter: Performance and mechanisms. *Chemical Engineering Journal* 322, 82-89. doi: 10.1016/j.cej.2017.04.010.

Fan, X.Y., Gao, J.F., Pan, K.L., Li, D.C., Dai, H.H., and Li, X. (2018). Functional genera, potential pathogens and predicted antibiotic resistance genes in 16 full-scale wastewater treatment plants treating different types of wastewater. *Bioresour Technol* 268, 97-106. doi: 10.1016/j.biortech.2018.07.118.

Fang, H., Zhang, H., Han, L., Mei, J., Ge, Q., Long, Z., et al. (2018). Exploring bacterial communities and biodegradation genes in activated sludge from pesticide wastewater treatment plants via metagenomic analysis. *Environ Pollut* 243(Pt B), 1206-1216. doi: 10.1016/j.envpol.2018.09.080.

Feng, X.H., Zhu, M.Q., Ginder-Vogel, M., Ni, C.Y., Parikh, S.J., and Sparks, D.L. (2010). Formation of nano-crystalline todorokite from biogenic Mn oxides. *Geochimica Et Cosmochimica Acta* 74(11), 3232-3245. doi: 10.1016/j.gca.2010.03.005.

Francis, C.A., and Tebo, B.M. (2002). Enzymatic Manganese(II) Oxidation by Metabolically Dormant Spores of Diverse Bacillus Species. *Applied and Environmental Microbiology* 68(2), 874-880. doi: 10.1128/aem.68.2.874-880.2002.

Friedl, G., Wehrli, B., and Manceau, A. (1997). Solid phases in the cycling of manganese in

eutrophic lakes: New insights from EXAFS spectroscopy (vol 61, pg 275, 1997). *Geochimica Et Cosmochimica Acta* 61(15), 3277-3277. doi: Doi 10.1016/S0016-7037(97)00178-6.

Geszvain, K., McCarthy, J.K., and Tebo, B.M. (2013). Elimination of manganese(II,III) oxidation in *Pseudomonas putida* GB-1 by a double knockout of two putative multicopper oxidase genes. *Appl Environ Microbiol* 79(1), 357-366. doi: 10.1128/AEM.01850-12.

Harder, W., Matin, A., and M. Attwood, M. (1975). Studies on the Physiological Significance of the Lack of a Pyruvate Dehydrogenase Complex in *Hyphomicrobium* sp.. *J Gen Microbiol* 86(2), 319-326.

Hiraishi, A., Yonemitsu, Y., Matsushita, M., Shin, Y.K., Kuraishi, H., and Kawahara, K. (2002). Characterization of *Porphyrobacter sanguineus* sp. nov., an aerobic bacteriochlorophyll-containing bacterium capable of degrading biphenyl and dibenzofuran. *Arch Microbiol* 178(1), 45-52. doi: 10.1007/s00203-002-0423-5.

Holm, N.C., Gliesche, C.G., and Hirsch, P. (1996). Diversity and structure of hyphomicrobium populations in a sewage treatment plant and its adjacent receiving lake. *Appl Environ Microbiol* 62(2), 522-528.

Li, E.C., Jin, X.W., and Lu, S.G. (2018). Microbial communities in biological denitrification system using methanol as carbon source for treatment of reverse osmosis concentrate from coking wastewater. *Journal of Water Reuse and Desalination* 8(3), 360-371. doi: 10.2166/wrd.2017.024.

Lind, C.J., and Hem, J.D. (1993). Manganese Minerals and Associated Fine Particulates in the Streambed of Pinal Creek, Arizona, USA - a Mining-Related Acid Drainage Problem. *Applied Geochemistry* 8(1), 67-80. doi: Doi 10.1016/0883-2927(93)90057-N.

Morgan, J.J. (2005). Kinetics of reaction between O_2 and Mn(II) species in aqueous solutions. *Geochimica et Cosmochimica Acta* 69(1), 35-48. doi: 10.1016/j.gca.2004.06.013.

Okibe, N., Maki, M., Sasaki, K., and Hirajima, T. (2013). Mn(II)-Oxidizing Activity of *Pseudomonas* sp. Strain MM1 is Involved in the Formation of Massive Mn Sediments around Sambe Hot Springs in Japan. *Materials Transactions* 54(10), 2027-2031. doi: 10.2320/matertrans.M-M2013825.

Prozorov, T., Perez Gonzalez, T., Valverde-Tercedor, C., Jimenez-Lopez, C., Yebra-Rodriguez, A., Körnig, A., Faivre, D., Mallapragada, S.K., Howse, P.A., Bazylinski, D.A., Prozorov, R. (2014). Manganese Incorporation into Magnetosome Magnetite: Magnetic Signature of Doping. *European Journal of Mineralogy* 26, 457-471.

Sly, L.I., Hodgkidon, M.C., Arunpairojana V. (1988). Effect of water velocity on the early development of manganese-depositing biofilm in a drinking-water distribution-system. *Fems Microbiology Ecology* 53(3-4), 175-186. doi: 10.1111/j.1574-6968.1988.tb02662.x.

Tebo, B.M., Johnson, H.A., McCarthy, J.K., and Templeton, A.S. (2005). Geomicrobiology of manganese(II) oxidation. *Trends Microbiol* 13(9), 421-428. doi: 10.1016/j.tim.2005.07.009.

Tyler, P.A. (1970). Hyphomicrobia and the oxidation of manganesse in aquatic ecosystems. *Antonie Van Leeuwenhoek* 36(4), 567-578. doi: 10.1007/bf02069059.

Tyler, P.A., and Marshall, K.C. (1967). Microbial oxidation of manganese in hydro-electric pipelines. *Antonie Van Leeuwenhoek* 33(2), 171-183. doi: Doi 10.1007/Bf02045548.

Uebayasi, M., Tomizuka, N., Kamibayashi, A., and Tonomura, K. (2014). Autotrophic Growth of a *Hyphomicrobium* sp. and Its Hydrogenase Activity. *Agricultural and Biological Chemistry* 45(8), 1783-1790. doi: 10.1080/00021369.1981.10864795.

Villalobos, M., Toner, B., Bargar, J., and Sposito, G. (2003). Characterization of the manganese oxide produced by *Pseudomonas putida* strain MnB1. *Geochimica Et Cosmochimica Acta* 67(14), 2649-2662. doi: 10.1016/S0016-7037(03)00217-5.

Zacharoff, L.A., Morrone, D.J., and Bond, D.R. (2017). *Geobacter sulfurreducens* Extracellular Multiheme Cytochrome PgcA Facilitates Respiration to Fe(III) Oxides But Not Electrodes. *Front Microbiol* 8, 2481. doi:

10.3389/fmicb.2017.02481.

Zhang, B., Yu, Q., Yan, G., Zhu, H., Xu, X.Y., and Zhu, L. (2018). Seasonal bacterial community succession in four typical wastewater treatment plants: correlations between core microbes and process performance. *Sci Rep* 8(1), 4566. doi: 10.1038/s41598-018-22683-1.

Zhang, C., Meng, X., Li, N., Wang, W., Sun, Y., Jiang, W., et al. (2013). Two bifunctional enzymes with ferric reduction ability play complementary roles during magnetosome synthesis in *Magnetospirillum gryphiswaldense* MSR-1. *J Bacteriol* 195(4), 876-885. doi: 10.1128/JB.01750-12.

Zhao, H., Zhu, M., Li, W., Elzinga, E.J., Villalobos, M., Liu, F., et al. (2016). Redox Reactions between Mn(II) and Hexagonal Birnessite Change Its Layer Symmetry. *Environ Sci Technol* 50(4), 1750-1758. doi: 10.1021/acs.est.5b04436.

The results in this chapter were partially cooperated by Mr. Kyohei Takamatsu (bachelor 4th year student in fiscal year 2016).

Data shown in this chapter were partially included in the paper submitted to Water (2019, 11(3)) entitled "Natural attenuation of Mn(II) in metal refinery wastewater: Microbial community structure analysis and isolation of a new Mn(II)-oxidizing bacterium *Pseudomonas* sp. SK3*"*

Chapter 4

Isolation, characterization of *Pseudomonas* sp. SK3 and its robust Mn(II)-oxidation activity

Abstract

With the aim to search for a robust Mn(II)-oxidizing bacteria, natural Mn-oxide collected from metal-refinery wastewater facility was subjected to selective enrichment and screening.

Black-brown colonies (indicator for Mn(II)-oxidation activity) resulted from enrichment of natural Mn-oxide on Mn(II)-containing media were purified via single colony isolation several times. Among isolates, SK3 showed the most stable and strongest Mn(II)-oxidation activity. Phylogenetic tree analysis indicated that the closest relative of the isolate SK3 is *Pseudomonas resinovorans* (98.4% (1398 bp) 16S rRNA gene sequence identity). Mostly, Mn(II)-oxidization activity was reported mainly in *Ps. putida* group and *Ps. resinovorans* is unknown to possess it. Interestingly, oxidation of up to 100 mg/L Mn(II) was readily initiated and completed by the isolate, even in the presence of high contents of $MgSO_4$ (a typical solute in metal-refinery wastewater). Additional of Cu(II) facilitated Mn(II) oxidation by isolate SK3 (implying the involvement of multicopper oxidase enzyme), allowing a 2-fold greater Mn removal rate. High Mn AOS biogenic birnessite produced by isolate SK3 exemplified the its involvement in the formation of natural Mn-oxide inside the wastewater pipeline. Overall, the potential utility of isolate SK3 is illustrated for further industrial application in metal-refinery wastewater treatment processes.

4.1 Introduction

Mn(II)-oxidizing bacteria are phylogenetically diverse including Firmicutes (*Bacillus* sp. *Brevibacillus* sp.), Proteobacteria (*Leptothrix* sp., *Pseudomonas* sp., *Erythrobacter* sp., *Pedomicrobium* sp.) and Actinobacteria (*Arthrobacter* sp.) (Tebo et al., 2004; Tebo et al., 2005). The presence of multicopper oxidase (MCO; at least four copper atoms present as cofactor) was reported in these bacteria as Mn(II) oxidase enzyme, exemplified by MnxG (*Bacillus* sp. SG-1 (Dick et al., 2008)), CopA (*Brevibacillus panacihumi* MK-8 (Zeng et al., 2018)), MofA (*Leptothrix discophora* SS-1 (Corstjens et al., 1997)), CumA (*Ps. putida* GB-1 (Francis and Tebo, 2001)) and MoxA (*Pedomicrobium* sp. ACM 3067 (Ridge et al., 2007)). More recently, the involvement of an animal heme peroxidase (AHP) in Mn(II) oxidation was found in *Ps. putida* GB-1, showing the first example of an Mn(II)-oxidizing bacterium utilizing both MCO and AHP enzymes (Geszvain et al., 2016).

Different types of Mn-oxides were reported as a result of microbial Mn(II) oxidation, including birnessite ($(Na, Ca)_{0.5}(Mn^{IV}, Mn^{III})_2O_4 \cdot 1.5H_2O$), todorokite ($(Mn^{II}, Ca, Na, K)(Mn^{IV}, Mn^{II}, Mg)_6O_{12} \cdot 3H_2O$), bixbyite ($(Mn^{III}, Fe^{III})_2O_3$) and hausmannite ($Mn^{II}, Mn^{III}{}_2O_4$) formed by bacteria and fungi (Mann et al., 1988; Tebo et al., 2005; Saratovsky et al., 2009; Santelli et al., 2011; Bohu et al., 2015). It was suggested that birnessite-like biogenic Mn-oxides are initially formed enzymatically and later transformed into lower AOS Mn-oxides such as hausmannite due to reaction with the remaining Mn(II) or crystallized to todorokite (Feng et al., 2010; Lefkowitz et al., 2013).

Unlike Fe(II)-oxidizing bacteria, the reason is yet unclear why Mn(II)-oxidizing bacteria oxidize Mn(II). Although the oxidation of Mn(II) to Mn(III) or Mn(IV) is thermodynamically favorable, there is no direct evidence linking Mn(II) oxidation to energy conservation (Tebo et al., 2005). The possible advantages of microbial Mn(II) oxidation could include storage of Mn-oxides as an electron acceptor and self-protection by Mn-oxide armoring from environmental insults (e.g., UV, predation, toxic heavy metals). Also, since Mn-oxide is one of strongest oxidants found in nature, Mn(II)-oxidizing bacteria may benefit from its capability to degrade recalcitrant humic

substances into low molecular organic compounds for feeding (Tebo et al., 2004; Tebo et al., 2005).

For this aim, it was necessary to find an isolate which withstands high Mn(II) concentration and displays robust Mn(II) oxidation, especially in the presence of $MgSO_4$ as a typical major component in refinery wastewaters. In this chapter, a new Mn(II)-oxidizing bacterium with a robust Mn(II)-oxidizing capability was isolated from natural Mn-oxide collected from metal-refinery wastewater treatment system mentioned in **chapter 3**.

4.2 Materials and methods

4.2.1 Screening for Mn(II)-oxidizing bacteria

An aliquot of the Mn-deposit sample was diluted 10 times with 0.85% (w/v) NaCl, 100 μL of which was spread on the following solid media containing 10 mg/L Mn(II) (as $MnCl_2$); Yu medium, K- medium, and J-medium (refer to section 2.1.1 for medium composition). Plates were incubated at 25℃ for 3 days until black colonies appeared (indicator for Mn(II)-oxidizing activity). After repeating single-isolation four times, four isolates (SK1 from K medium; SK2-3 from Yu medium, SK4 from J medium) were tested for Mn(II)-oxidation ability in respective liquid media containing 100 mg/L Mn(II). As a result, only isolate SK3 exhibited stable Mn(II)-oxidizing ability during subculturing. Other than in Mn(II) oxidation tests, isolate SK3 was maintained in Luria-Bertani (LB) medium.

4.2.2 Identification of isolated Mn(II)-oxidizing bacteria

Genomic DNA was extracted from strain SK3 cells using the Ultraclean microbial DNA isolation kit (MO-BIO) and the partial 16S rRNA gene was amplified by Touchdown PCR (Premix Taq, TaKaRa BIO) using universal 27F (5'-AGAGTTTGATCMTGGCTCAG-3') and 1492R (5'-TACGGYTACCTTGTTACGACTT-3') primers. The concentration of template DNA was varied. The PCR product was checked by gel electrophoresis (100V, 30 min) along with smart ladder (Nippon gene; 0.2-10 kbp) . The PCR product was purified (Mono FAS, GL-Sciences), sequenced (Research Support Center, Graduate School of Medical Sciences, Kyushu University) and analyzed by BLAST (http://blast.ncbi.nlm.nih.gov/Blast.cgi). The phylogenetic tree was constructed by the neighbor-joining method with a bootstrap value of 1,000 using ClustalX v2.0 and

visualized by NJplot software. NCBI accession numbers of bacteria used to construct phylogenetics tree are summarized separately in Table 4.2

For the morphological study, SK3 cells were fixed (with a mixture of 2% glutaraldehyde and 2.5% formaldehyde), dehydrated (with ascending concentration of ethanol; 70, 80, 90, and 99.5% for 5 min each, and 100% (for 10 min)), dried in vacuum desiccator for 24 h, and finally magnetron-sputter coated with Au-Pd (MSP-1S, Vacuum Device), prior to observe by scanning electron microscope (SEM; Keyence VE-9800) at an accelerated voltage of 5 keV.

Table 4.1 Touchdown PCR protocol

Temperature	Duration	Cycle time
95°C	5 min	1 Cycle
95°C	30 sec	20 cycles (temperature increment of 0.5°C/cycle)
57°C	30 sec	
72°C	90 sec	
95°C	30 sec	15 cycles
47°C	30 sec	
72°C	90 sec	
72°C	10 min	
4°C	Keep	Keep

4.2.3 Mn(II) oxidation test

In addition to the new isolate *Pseudomonas* sp. SK3, the well-studied Mn(II)-oxidizing relative, *Ps. putida* MnB1 (ATCC 23483) was also tested as a comparison. Each strain was pre-grown overnight in LB medium (pH 7.0), washed, harvested by centrifugation prior to use in the following Mn(II) oxidation experiments.

In all cases, duplicate flasks were set up, incubated shaking at 120 rpm. Samples were routinely withdrawn to monitor cell density (bacterial counting chamber), pH, and the Mn(II) concentration (ICP-OES).

4.2.3.1 Effect of initial Mn(II), Cu(II), and $MgSO_4$ concentration

Pre-grown cells were re-suspended (1 x 10^9 cells/mL) into 300 mL Erlenmeyer flasks containing 100 mL of PYG-1 medium (1 mM glucose, 0.025% yeast extract, 0.025% peptone, 2.02 mM $MgSO_4 \cdot 7H_2O$, 0.068 mM $CaCl_2 \cdot 2H_2O$, 15 mM PIPES). The initial Mn(II) concentration was set at 100 or 200 mg/L (added as $MnSO_4$), both plus or minus 3 μM Cu(II) (added as $CuCl_2$). Next, in addition to 24 mg/L $MgSO_4$ present originally in PYG-1 medium, its initial concentration was raised to 240, 1200 or 2400 mg/L to see the effect of excess $MgSO_4$ on microbial Mn(II) oxidation (3 μM Cu(II) was added in all cases). The initial pH value was set to 7.0 and temperature at 25℃

4.2.3.2 Effects of pH and temperature

Pre-grown cells were re-suspended (1 x 10^9 cells/mL) into 300 mL Erlenmeyer flasks containing 100 mL of PYG-1 medium.

The initial Mn(II) concentration was set at 100 mg/L, plus 3 μM Cu(II). The initial pH was set at 6.0, 6.5, 7.0, 7.5 or 8.0 (25℃), and temperature at 20, 25, 30, 35 or

40°C (pH 7.0). Cu(II) was added in all cases). The initial pH value was set to 7.0 and temperature at 25°C.

4.2.3.3 Effect of individual PYG-1 medium components (test for isolate SK3 only)

In order to investigate durability of microbial Mn(II) oxidation in oligotrophic medium, pre-grown SK3 cells were re-suspended (1 x 10^9 cells/mL) into 300 mL flasks containing 100 mL of PYG-1 medium lacking single/multiple organic components as follows: -Glu, -YE/Pep, -Glu/YE/Pep, -Pep (YE 0.01% instead of 0.025%) (Glu; glucose, YE; yeast extract, Pep; peptone). In addition, the effect of the absence of PIPES was also evaluated (-PIPES). The initial Mn(II) concentration was set at 100 mg/L plus 3 μM Cu(II). The initial pH value was set at 7.0 and temperature at 25°C.

4.2.4. Characterization of biogenic Mn-precipitates

4.2.4.1 X-ray diffraction (XRD)

Biogenic Mn-precipitates were periodically collected by centrifugation during Mn(II)-oxidation by isolate SK3 (at 0, 24, 48 and 72 h; corresponding to Fig 4.4a +Cu(II); ■). The precipitates were washed with deionized water twice and freeze-dried overnight for XRD analysis (Rigaku UltimaIV; CuKα 40 mA, 40 kV). Standard acid birnessite sample was chemically synthesized as described in (Villalobos et al., 2003).

4.2.4.2 X-ray absorption near edge structure (XANES)

Biogenic Mn-precipitates were collected during Mn(II) oxidation by isolate SK3 (as described in section 4.2.4.1) as well as by *Ps. putida* MnB1 (at 0, 24, 48, 72 and 120 h; Fig. 4.4a +Cu(II); □). Each sample was quantitatively mixed with boron nitride and

pressed into a tablet. The Mn K-edge XANES spectra were collected (transmission mode; 6200-8500 eV) at SAGA-LS (1.4 GeV, 75.6 m; Kyushu University Beam Line 06), using standard chemicals $Mn^{II}SO_4$, $Mn^{III}_2O_3$ and δ-$Mn^{IV}O_2$ (Wako pure chemicals). The ratio of Mn species and the average oxidation states (AOS) were calculated based on the linear combination fitting of Mn-K edge XANES spectra (6200-6600 eV), using the Athena program (Demeter version 0.9.24) (Ravel and Newville, 2005).

4.2.4.3 Scanning electron microscope (SEM)

Biogenic Mn-precipitates were fixed with a mixture of 2% glutaraldehyde and 2.5% formaldehyde in 0.1 M phosphate buffer solution (PBS; pH 7.6) (4℃, 30 min), washed twice with 0.1 M PBS, dehydrated with ascending concentration of ethanol (70, 80, 90, and 99.5% for 5 min each, and 100% for 10 min), dried in vacuum desiccator for 24 h, and finally magnetron-sputter coated with Au-Pd (MSP-1S, Vacuum Device), prior to SEM observation (SEM; Keyence VE-9800; 5 kV).

Table 4.2 NCBI accession numbers used to construct the phylogenetic tree

Species	Strain	Accession no.
***Pseudomonas syringae* group**		
Pseudomonas avellanae	P90	U49384
Pseudomonas syringae	ATCC 19310^T	D84026
Pseudomonas mandelii	CIP 105273^T	AF058286
Pseudomonas caricapapayae	ATCC 33615^T	D84010
Pseudomonas ficuserectae	JCM 2400^T	AB021378
Pseudomonas savastano	ATCC 13522^T	AB21402
Pseudomonas syringae	LMG 13190^T	Z76660
Pseudomonas amygdali	ATCC 33614^T	D84007
Pseudomonas meliae	MAFF 301463^T	AB021382
Pseudomonas cichorii	ATCC 10857^T	AB021398
Pseudomonas viridiflava	LGM 2352^T	Z76671
***Pseudomonas chlororaphis* group**		
Pseudomonas chlororaphis	IAM 12354^T	D84011
Pseudomonas aurantiaca	ATCC 33663^T	AB021412
Pseudomonas chlororaphis	IAM 12353^T	D84008
Pseudomonas taetrolens	IAM 1653^T	D84027
Pseudomonas fragi	IFO 3458^T	AB021413
Pseudomonas lundensis	ATCC 49968^T	AB21395
***Pseudomonas fluorescens* group**		
Pseudomonas corrugata	ATCC 29736^T	D84012
Pseudomonas tolaasii	ATCC 33618^T	D84028
Pseudomonas fluorescens	IAM 12022^T	D84013
Pseudomonas orientalis	CFML 96-170	AF064457
Pseudomonas cedrella	CFML 96-198	AF064461
Pseudomonas azotoformans	IAM 1603^T	D84009
Pseudomonas gessardii	CIP 105469	AF074384
Pseudomonas mucidolens	IAM 12406^T	D84017
Pseudomonas synxantha	IAM 12356^T	D84025
Pseudomonas libaniensis	CIP 105460	AF057645
Pseudomonas veronii	CIP 104663^T	AB21411
Pseudomonas rhodesiae	CIP 104664^T	AB021410
Pseudomonas marginalis	ATCC 10844^T	AB021401
Pseudomonas migulae	CIP 105470	AF074383

Table 4.2 Continued

Species	Strain	Accession no.
***Pseudomonas putida* group**		
Pseudomonas sp.	PCP	AF326381
Pseudomonas sp.	ISO6	AF326377
Pseudomonas sp.	MM1	KF366422
Pseudomonas jessenii	CIP 105274	AF068259
Pseudomonas agarici	ATCC 25941^T	D84005
Pseudomonas asplenii	ATCC 23835^T	A021397
Pseudomonas fuscovaginae	MAFF 301177^T	AF068259
Pseudomonas putida	IAM 1236^T	D84020
Pseudomonas oryzihabitans	IAM 1568^T	D84004
Pseudomonas fulva	IAM 1529^T	D84015
Pseudomonas mosselii	CIP 105259	AF072688
Pseudomonas putida	MnB1	U70977
Pseudomonas putida	GB-1	CP000926
Pseudomonas monteilii	CIP	AB021409
Pseudomonas plecoglossicida	FPC951	AB009457
***Pseudomonas aeruginosa* group**		
Pseudomonas anguilliseptica	NCMB 1949^T	AB021376
Pseudomonas flavescens	B62^T	U01916
Pseudomonas straminae	IAM 1598^T	D84023
Pseudomonas mendocina	ATCC 25411^T	M59154
Pseudomonas pseudoalcaligenes	JCM 5968^T	AB021379
Pseudomonas alcaligenes	IAM 12411^T	D84006
Pseudomonas nitroreducens	IAM 1439^T	D84021
Pseudomonas citronellolis	ATCC 13674^T	AB021396
Pseudomonas luteola	IAM 13000^T	D84002
Pseudomonas oleovorans	IAM 1508^T	D84018
Pseudomonas stutzeri	CCUG 11256^T	U26262
Pseudomonas balearica	SP 1402^T	U26418
Pseudomonas aeruginosa	LMG 1242^T	Z76651
Pseudomonas resinovorans	ATCC 14235^T	AB021373
***Pseudomonas petucinogena* group**		
Pseudomonas denitrificans	IAM 12023^T	AB021419
Pseudomonas pertucinogena	IFO 14163^T	AB021380
Bacillus sp.	SG-1	AF326373

4.3 Results and discussion

4.3.1 Screening of Mn(II)-oxidizing bacteria from Mn-deposit

After 3 days of incubation, black-brown (Mn(II)-oxidizer) and white colony (non-Mn(II)-oxidizer) were appeared. Three Mn(II)-oxidizing isolates (SK1, 2, and 3) were obtained after repeated single colony isolation (Fig 4.1). Following several-times sub-culturing and Mn(II)-oxidation tests at 100 mg/L Mn(II), isolate SK3 was selected as the most stable and strongest Mn(II)-oxidizer for further studies.

4.3.2 Identification of isolate SK3

Following genomic DNA extraction, the partial 16S rRNA gene was amplified by touchdown PCR using universal 27F and 1492R primers. PCR products were checked with gel electrophoresis and condition (E) was selected (less smear) for further process (Fig. 4.2). Based on the 16S rRNA gene sequence of isolate SK3 (1398 bp), its closest relative was shown to be *Pseudomonas resinovorans* ATCC 14235T [AB021373] with a similarity of 98.4% (Fig. 4.3). So far several Mn(II)-oxidizing strains have been reported from *Ps. putida* group (Francis and Tebo, 2001; Villalobos et al., 2003; Geszvain et al., 2013; Geszvain et al., 2016). However, the presence of Mn(II) oxidation ability is so far unknown in *Ps. resinovorans* (Fig. 4.3). Identification of *Pseudomonas* sp. SK3, phylogenetically far-related with *Ps. putida* group, implies that Mn(II)-oxidizing ability may be more diversely present across the genus *Pseudomonas* (Fig. 4.3 and table 4.4).

Table 4.3 PCR condition for 16s rRNA amplication

Condition	DNA template concentration	PCR method
A	0.5x	PCR
B		PCR
C		Touchdown PCR
D	0.1x	PCR
E		Touchdown PCR
F	0.2x	PCR
G		Touchdown PCR

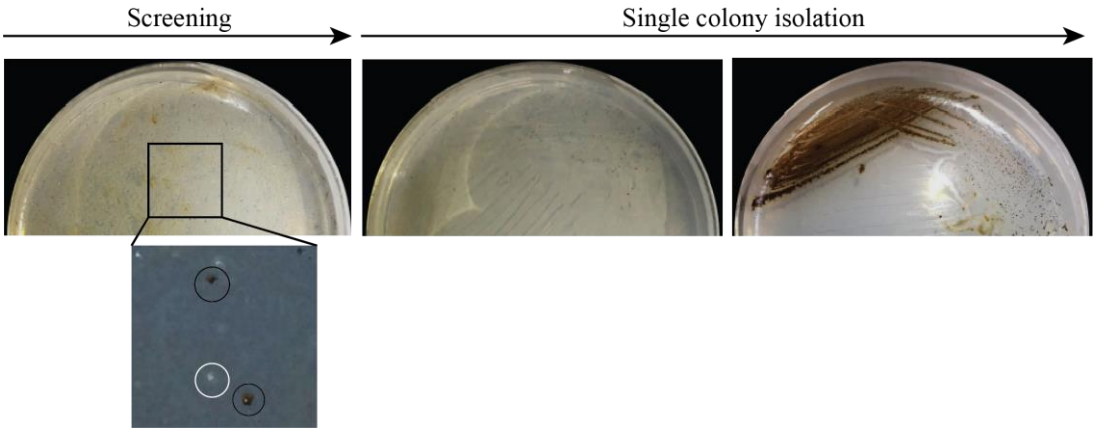

Figure 4.1 Screening of Mn(II)-oxidizing bacteria from Mn-deposit. Black-brown colonies indicate Mn(II)-oxidizing activity. Single colony isolation was repeated for four times.

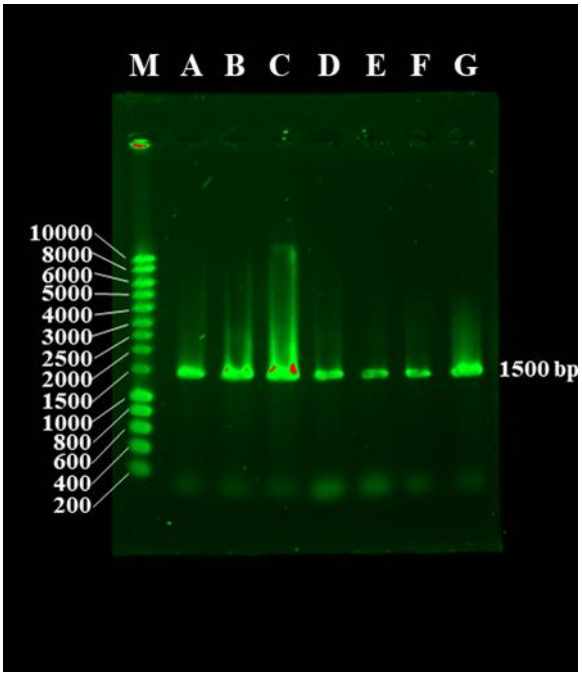

Figure 4.2 Gel electrophoresis of PCR product showing the size 1400-1500 bp, a typical size for 16S rRNA. A-G indicated the variation of template concentration showed in table 4.3

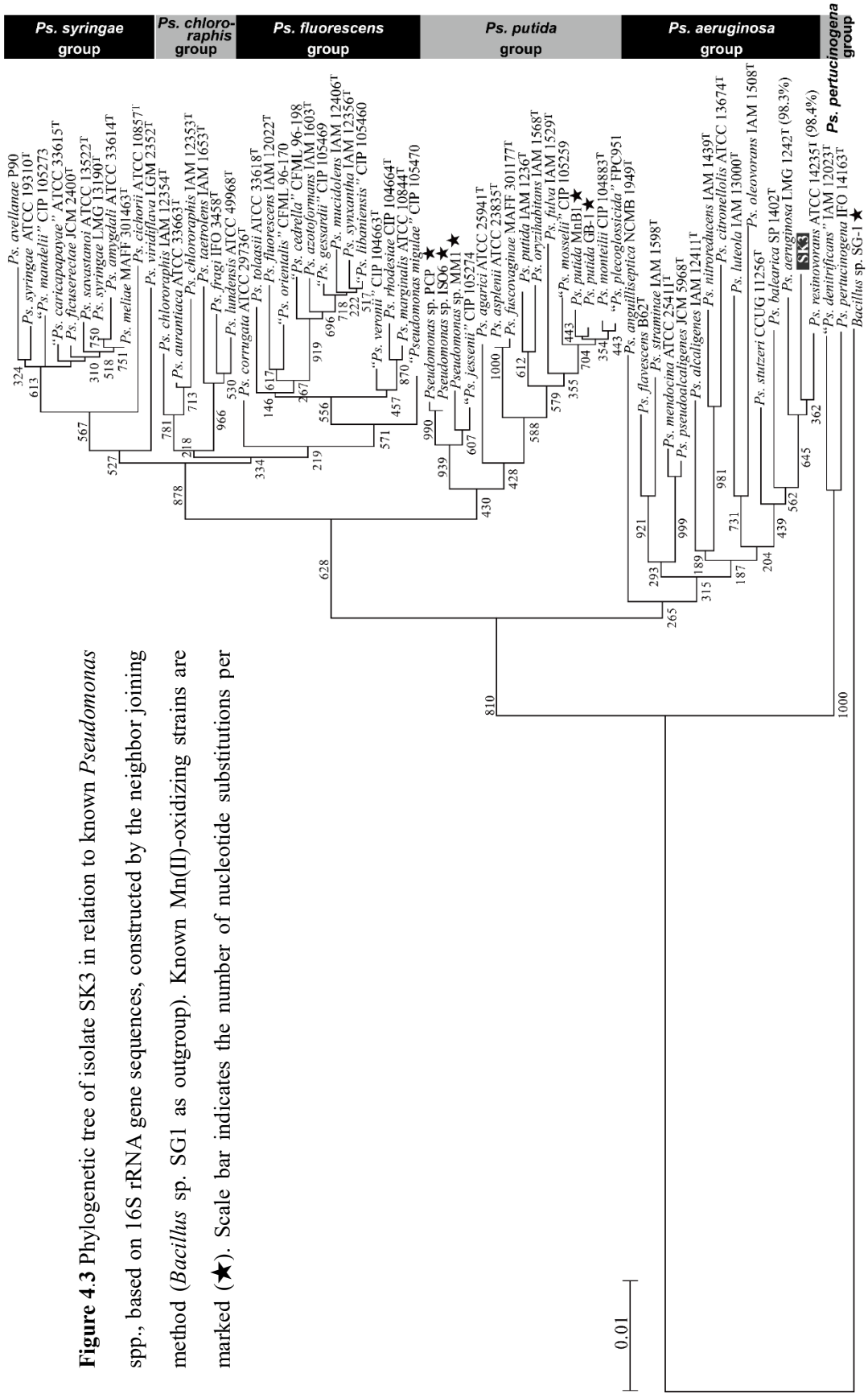

Figure 4.3 Phylogenetic tree of isolate SK3 in relation to known *Pseudomonas* spp., based on 16S rRNA gene sequences, constructed by the neighbor joining method (*Bacillus* sp. SG1 as outgroup). Known Mn(II)-oxidizing strains are marked (★). Scale bar indicates the number of nucleotide substitutions per

Table 4.4 Relatedness of 16S rRNA genes from some type strains of the genus *Pseudomonas* and isolate SK3

Strain	**% Identity of 16S rRNA gene sequence**					
	(1)	(2)	(3)	(4)	(5)	(6)
Ps. resinovorans ATCC 14235 (1)						
Ps. aeruginosa LMG 1242^{T} (2)	97.4%					
Ps. putida IAM 1236^{T} (3)	94.6%	94.9%				
Ps. putida MnB1 (4)	94.6%	95.6%				
MM1 (5)	95%	94.7%	97%	97.7%		
SK3 (6)	98.4%	98.3%	94.9%	95.5%	95.2%	

4.3.3 Mn(II) oxidation by *Pseudomonas* sp. SK3

4.3.3.1 Effect of initial [Mn(II)]. [Cu^{2+}] and [$MnSO_4$]

Our challenge in this study was to find a robust Mn(II)-oxidizer which can be potentially utilized in an industrial Mn(II) treatment process. Ideally, the new bioprocess can be placed in further upstream of the metal-refinery wastewater system to deal with a few tens of mg/L Mn(II) contaminant coexisting with $MgSO_4$ at neutral or slightly acidic pH values.

First, pre-grown cells of isolate SK3 (as well as *Ps. putida* MnB1; a well-studied Mn(II)-oxidizer for comparison) were tested for Mn(II) oxidation at 100 mg/L and 200 mg/L (each plus or minus 3 μM Cu(II)). As shown in Fig 4.4a, isolate SK3 completely oxidized 100 mg/L Mn(II) by 48 h (plus Cu(II)), while the **a**bsence of

Cu(II) clearly slowed down its Mn(II) oxidation. The similar effect of Cu(II) was apparent with *Ps. putida* MnB1, but its Mn(II) oxidation was generally slower, compared to isolate SK3 (Fig. 5a). When the initial Mn(II) concentration was raised to 200 mg/L, Mn(II) oxidation by *Ps. putida* MnB1 became negligible, while isolate SK3 managed to partially oxidize Mn(II), especially in the presence of Cu(II) (37 mg/L of Mn(II) was oxidized in 70 h; Fig 4.4a). The presence of 3 μM Cu(II) was found sufficient, since the addition of Cu(II) at higher concentrations (5 μM or 10 μM) resulted in similar Mn(II) oxidation removal efficiencies by isolate SK3 (data not shown). The results here support the hypothesis that isolate SK3 also shares the activity of MCO enzyme in Mn(II) oxidation, as was reported with *Ps. putida* GB-1 (Francis and Tebo, 2001) as well as in other genera such as *Bacillus* (Dick et al., 2008), *Brevibacillus* (Zeng et al., 2018) and *Leptothrix* (Corstjens et al., 1997).

Isolate SK3 exhibited remarkable resistance to high $MgSO_4$ doses. Although an increasingly longer delay in Mn(II) oxidation, due to inhibitory effect from SO_4^{2-} ,was noticed corresponding to higher $MgSO_4$ doses, isolate SK3 still managed to effectively oxidize Mn(II) nearly to completion by 120 h (Fig. 5b). On the other hand, the presence of 1200 mg/L or 2400 mg/L $MgSO_4$ mostly or completely stopped Mn(II) oxidation by *Ps. putida* MnB1, respectively (Fig. 5b) even in the presence of Cu(II).

4.3.3.2 Effect of pH and temperature

Mn(II) oxidation activity by isolate SK3 peaked over the relatively wider pH range (pH 7.0-8.0) when 3 μM Cu(II) was present, whereas the activity of *Ps. putida* MnB1 peaked at pH 7.0 and a slight pH shift especially to alkali caused a detrimental effect

(Fig 4.5a). Chemical Mn(II) oxidation is thermodynamically unfavorable at acidic pHs for initiation of Mn(II) oxidation coupled with O_2 (Morgan, 2005). However, even at slightly acidic pH 6.5, Mn(II) oxidation by isolate SK3 persisted even with a greater Mn removal rate than that by *Ps. putida* MnB1 at its optimal pH 7.0. Both strains lost their Mn(II) oxidation activity at pH 6.0 (Fig. 4.5a). Interestingly, however, the absence of Cu(II) (Fig. 4.5a) resulted in total deactivation of Mn(II) oxidation by isolate SK3 at pH 7.5 and 8.0. Isolate SK3 showed a clear preference for the temperature of 25℃, while lower (20℃) or higher (30℃) temperatures slowed down Mn(II) oxidation by one-fourth (Fig. 4.5b). On the other hand, Mn(II) oxidation rate by *Ps. putida* MnB1 was nearly stable over 20-30℃. Both strains lost Mn(II) oxidation ability at 35℃ (Fig. 4.5b), although no decrease in the cell density was observed (data not shown). Overall, it was clearly shown that under optimal conditions, Mn(II) oxidative removal by isolate SK3 was shown significantly greater than *Ps. putida* MnB1 (Fig. 4.5a,b). The positive effect of Cu(II) in Mn(II) oxidation by isolate SK3 again emphasized here. Although under the detection limit (table 3.1 in **chapter 3**), a small amount of available Cu(II) ions might have facilitated on-site Mn deposition in the wastewater pipe.

4.3.3.3 Effect of medium components

The above Mn(II) oxidation tests under different conditions indicated the potential effectiveness of isolate SK3 (also in relative to the representative Mn(II)-oxidizing *Pseudomonas* strain) for industrial application. Therefore, isolate SK3 was further tested for its persistence in the oligotrophic medium by omitting one or more organic components from the PYG-1 medium (Fig. 4.6). Removing glucose caused some

delay in Mn(II) oxidation, but no severe effect was seen as long as complex nutrients were provided (Fig. 4.6a). The amount of complex nutrients could be lowered (by removing peptone at the same time halving yeast extract) without altering Mn(II) oxidation activity. However, the total absence of complex nutrients led to a severe decline in cell densities (Fig. 4.6c) and thus no Mn(II) oxidation was achieved (Fig. 4.6a). These results indicated that in actual industrial operation, feeding a minimum amount of complex nutrients would be essential to promote Mn(II) oxidative removal. The absence of buffering agent (PIPES) caused a pH drop from 7.0 to 6.0, owing to the proton-generating Mn(II) oxidation reaction (Mn^{2+} + 1/2 O_2 + H_2O → MnO_2 + $2H^+$) consequently to halt microbial activity. This suggests that addition of a buffering effect would be necessary to maintain microbial activity when applying to actual industrial wastewaters.

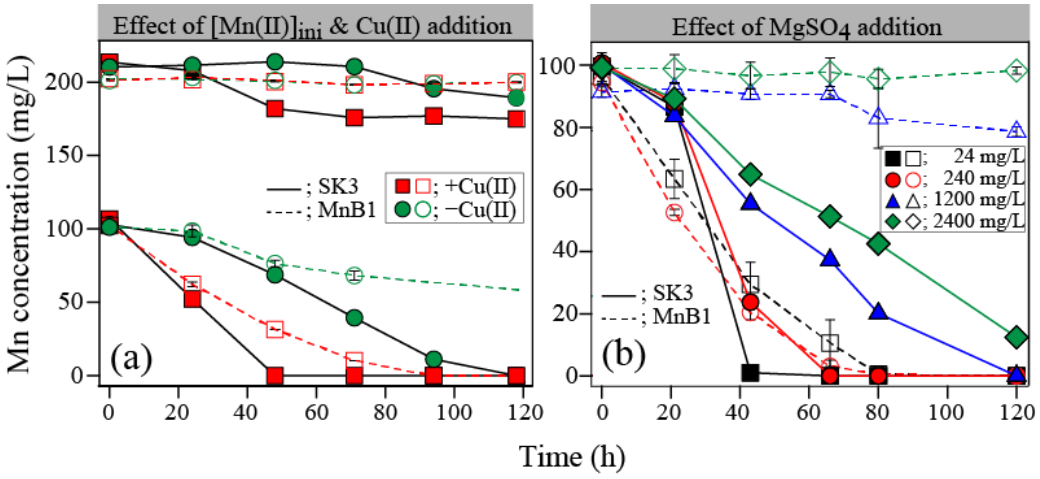

Figure 4.4 Mn(II) oxidative removal by isolate SK3 (solid symbols with solid lines) in comparison with *Ps. putida* MnB1 (open symbols with broken lines) under different conditions (pH_{ini} 7.0, 25°C). (a) Effects of the initial Mn(II) concentration (100 mg/L or 200 mg/L) was tested in the presence (■,□) or absence (●,○) of 3 µM Cu(II). [$MgSO_4$] = 24 mg/L (present originally in PYG-1 medium). (b) Effects of increasing dose of $MgSO_4$ was tested by adding extra MgSO4 to the final concentration of 240 mg/L (●, ○), 1200 mg/L (▲,△) or 2400 mg/L (♦,◇), in comparison with the controls (■,□; 24 mg/L $MgSO_4$ originally present in PYG-1 medium). [Mn^{2+}] = 100 mg/L. [Cu(II)] = 3 µM.

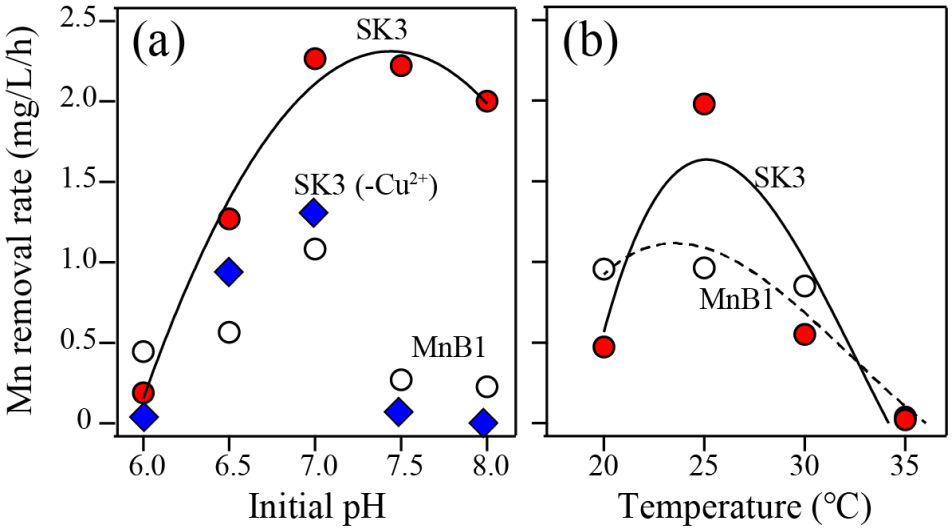

Figure 4.5 Mn(II) oxidative removal rates at different initial pHs (a) and temperatures (b). ●; isolate SK3 with 3 μM Cu(II) (calculated for the time period of 0-48 h). ♦; isolate SK3 without Cu(II) (calculated for the time period of 0-63 h). ○; *Ps. putida* MnB1 with 3 μM Cu(II) (calculated for the time period of 0-72 h). Initial conditions: [Mn(II)]=100 mg/L; [$MgSO_4$] = 24 mg/L (originally present in PYG-1 medium). (a) Temperature was set at 25°C. (b) The initial pH was set at 7.0. Fitting curves were drawn only for isolate SK3 with 3 μM Cu(II).

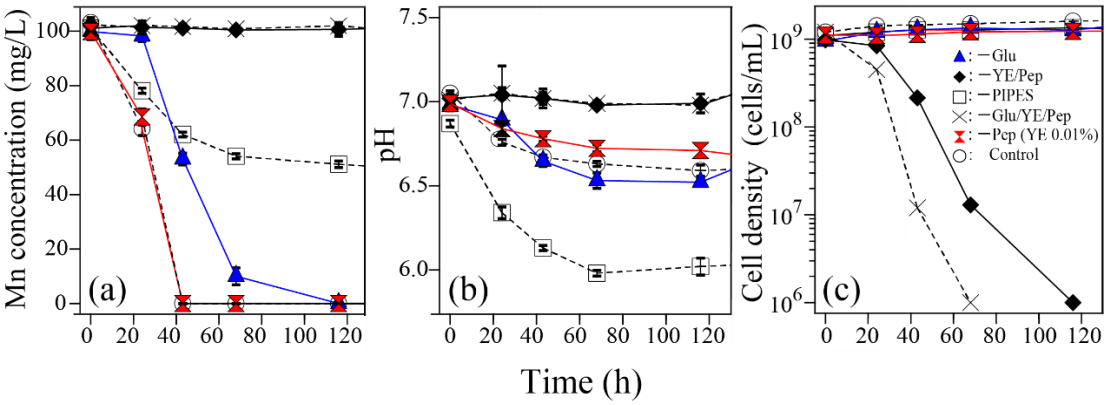

Figure 4.6 Effect of individual PYG-1 medium components on Mn(II) oxidative removal. Changes in the (a) Mn concentration, (b) pH value and (c) cell density during Mn(II) oxidation are shown. The following components were omitted from PYG-1 medium: ▲; -Glu, ♦; -YE/Peptone, □; -PIPES, ×; -Glu/YE/Peptone, ⧗; -Peptone (YE lowered to 0.01%), ○; Control. Initial conditions: [Mn(II)]=100 mg/L; [Cu(II)] = 3 μM; [$MgSO_4$]=24 mg/L (originally present in PYG-1 medium) at pH 7.0, 25°C.

4.3.4 Analysis of biogenic Mn-oxides produced by *Pseudomonas* sp. SK3

The over-time change in XRD peaks of biogenic Mn-oxide precipitates is shown in Fig. 4.7. The broad peak at around 20° deriving from cellular carbon (Fig. 4.7a) gradually became unnoticeable, accompanied by the emergence of increasingly evident birnessite peaks (Fig. 4.7b-d). The mineral surface morphology of biogenic birnessite (Fig.4.7d') and chemically-synthesized acid birnessite (Fig. 4.7e') are compared. A number of bacterial cells were found attached onto the biogenic birnessite surface, hidden in the mineral pores, or encrusted by self-produced Mn-oxides. The surface of biogenic birnessite was coated with string-like biofilm structures (Fig. 4.7d'). Types of biogenic Mn-oxides are diverse depending on several factors such as pH, initial Mn(II) concentration and DO level. For examples; bixbyite (*Mesorhizobium australicum* T-G1, pH 5.5, 0.1-10 mM $MnCl_2$, unshaken incubation) (Bohu et al., 2015), hausmannite (*Bacillus* sp. spore, pH 7.5, 1375 mg/L $MnCl_2$, unshaken incubation) (Mann et al., 1988), mixed hexagonal birnessite and todorokite (*Acremonium strictum* DS1bioAY4a, pH 7.0, 11 mg/L $MnCl_2$, agar surface) (Santelli et al., 2011), birnessite (*Pseudomonas putida* MM1, 50 mg/L $MnSO_4$, pH 7.0, shaken incubation) (Okibe et al., 2013), and todorokite (*Acremonium* sp. KR21-2, pH 6.0, 275 mM $MnCl_2$, agar surface) (Saratovsky et al., 2009). Birnessite-like type of biogenic Mn-oxide was believed to be initially formed enzymatically and later transformed into lower AOS Mn-oxide (hausmannite) due to reaction with the remained Mn(II) or crystallized to todorokite (indicated by sharpened of peaks around 12º and 23º).

The XANES LCF fitting indicated that the over-time maturation of biogenic birnessite (Fig. 4.8 a-d) is accompanied with the change in the Mn oxidation states (Fig. 4.8a). The ratio of Mn(II) and Mn(III) in the birnessite structure steadily

decreased during Mn(II) oxidation by isolate SK3, altering the AOS from 3.5 (at 24 h) to 3.8 (at 72 h). A slower Mn(II) oxidation by *Ps. putida* MnB1 compared to isolate SK3 (Fig. 4.4a) was accompanied by a slower change in the Mn AOS (from 3.5 at 24 h to 3.73 at 120 h; Fig. 4.8b). The enhancing effect of Cu(II) on Mn(II) oxidation (observed in section 4.3.3.1-4.3.3.2) together with the sequential change in the Mn oxidation state of biogenic birnessite observed here in fact support the one-electron Mn(II) oxidation reaction suggested for MCO enzymes (Webb et al., 2005; Zhao et al., 2016).

Chemically-synthesized birnessite (so as biogenic birnessite) were reported to undergo structural transformation via the synproportionation reaction between adsorbed Mn(II) and the surrounding Mn(IV), leading to Mn(III) formation, with the Mn AOC shifting from 3.7 to 3.5 in 20 days (Zhao et al., 2016). This decrease in the Mn AOS of birnessite during the mineral ripening results in its deactivation as the chemical oxidant. The oxidative removal of Mn(II) from wastewaters would rely both on microbial (enzymatic) Mn(II) oxidation and chemical Mn(II) oxidation by Mn(IV). Therefore, accumulation and passivation of Mn(III) onto Mn^{IV}-oxides needs to be avoided in order to maintain effective and continuous Mn removal.

The ability of isolate SK3 to effectively raise the Mn AOS to 3.8 (Fig.4.8a) would be therefore advantageous for steady and continuous water treatment. Together with the efficient in-vitro Mn(II)-oxidation displayed by isolate SK3, the high Mn AOS level of 3.75 observed with the in-situ pipeline Mn-deposit suggests that continuous generation of Mn(IV) was promoted via the robust in-situ activity of indigenous Mn(II) oxidizers (including strain SK3). This microbial reaction also likely pushed the chemical Mn(II)/Mn(IV) synproportionation reaction, resulting in synergistic Mn

oxidative removal within the complex ecosystem established in this artificial pipeline structure.

Biogenic birnessite produced by strain SK3 have high Mn(IV) proportion (approximately 86%, collected after 72 hours (Fig. 4.8)), this enables it to be used in various application such as As(III)-oxidation (Jones et al., 2012), and organic waste oxidation (Zhang and Huang, 2003; Jiang et al., 2009; Tu et al., 2014) since, Mn(IV)/Mn(II) couple have particularly high redox potentials making it a strong oxidant (Tebo et al., 2004). Interestingly, Mn^{IV}-oxide produced enzymatically from the treatment Mn-contaminating wastewater could be further utilized in bioremediation of toxic metals and organic wastes application, which will be mention in **chapter 8**.

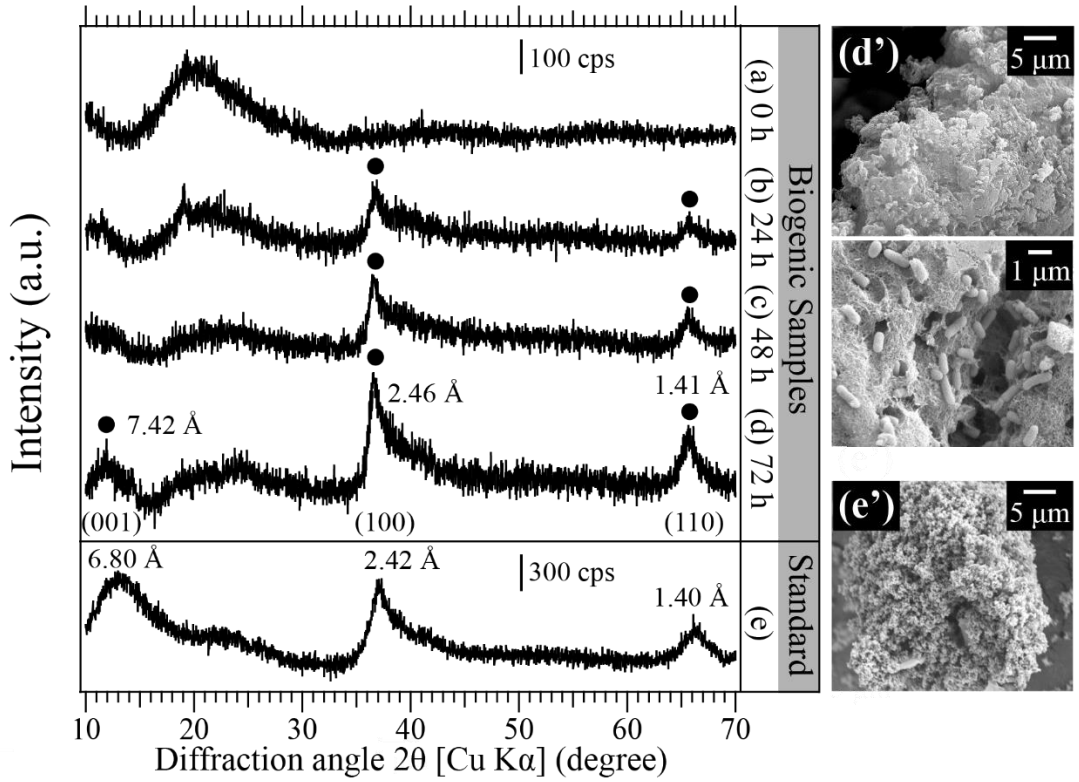

Figure 4.7 XRD diffraction patterns of Mn-precipitates recovered during Mn(II) oxidation by isolate SK3 at 0 h (a), 24 h (b), 48 h (c) and 72 h (d), in comparison with chemically synthesized acid birnessite (e). ●; birnessite (JCDD 43-1456). Sampling times of the Mn-precipitates correspond to those shown in Fig. 4.4 (a) (■; +Cu(II)). SEM images of the sample (d) and (e) are shown in (d') and (e'), respectively.

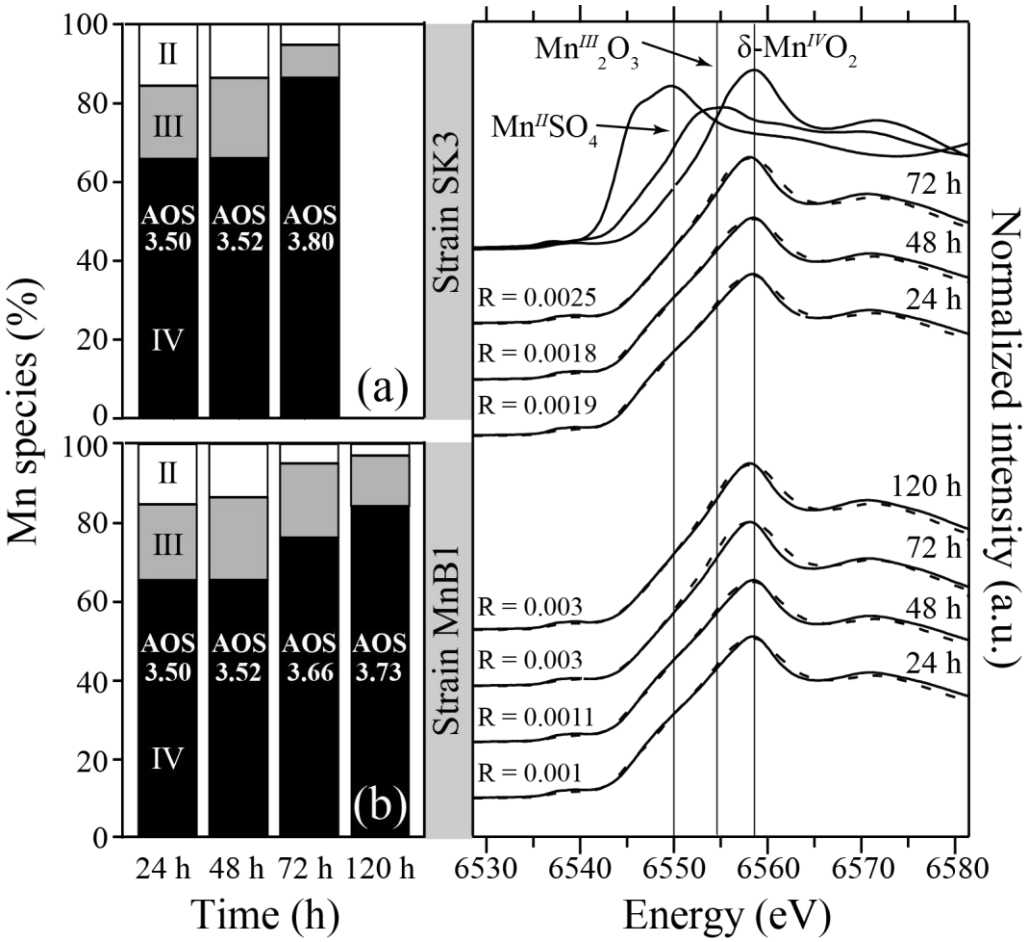

Figure 4.8 Changes in the Mn AOS of Mn-precipitates produced by isolate SK3 (a) or *Ps. putida* MnB1 (b). The ratios of Mn(II) (white), Mn(III) (grey) and Mn(IV) (black) were calculated from the linear combination fitting result (broken lines) of Mn K-edge XANES spectra (solid lines). Sampling points (24, 48, 72 and 120 h) of the Mn-precipitates correspond to those shown in fig. 4.4 (a) (■ □; +Cu^{2+}). As Mn standards, $Mn^{II}SO_4$, $Mn^{III}_2O_3$ and δ-$Mn^{IV}O_2$ were used. AOS stands for average oxidation state. Fitting results with R-factors < 0.003 were considered reliable.

4.4 Conclusions

- A heterotrophic Mn(II)-oxidizer *Pseudomonas* sp. SK3 (with 98.4% 16S rRNA gene sequence identity with *Ps. resinovorans*, previously unknown as Mn(II)-oxidizer) was isolated from the Mn-deposit.
- Isolate SK3 readily catalyzed oxidation of 100 mg/L Mn(II), even in the presence of 2.4 g/L $MgSO_4$ (a typical co-existing solute in metal-refinery wastewaters). Additional Cu^{2+} ions positively affected Mn(II) oxidation efficiency.
- Under the optimal conditions (pH 7.0-8.0; 25°C), the Mn removal rate of isolate SK3 was 2-fold greater than that of the well-studied Mn(II)-oxidizer *Ps. putida* MnB1 (the latter also did not withstand high $MgSO_4$ contents).
- Poorly crystalline biogenic birnessite was formed by isolate SK3 via one-electron transfer oxidation, increasingly shifting the Mn AOS from 3.50 (24 h) to 3.80 (72 h).
- The overall robust Mn(II)-oxidizing ability of isolate SK3 likely contributed the natural Mn(II) attenuation via formation of extensive Mn-deposits in the wastewater pipeline.
- The Mn AOC of Mn-deposits was maintained as high as 3.75, against naturally-occurring chemical Mn(II)/Mn(IV) synproportionation reaction to form Mn(III) in the wastewater pipeline. This suggests that Mn(II)-oxidizers including *Pseudomonas* sp. SK3 actively inhabit the ecosystem created in the pipeline (even though their overall percentage in the microbial community is minor). Active and continuous generation of Mn(IV) by Mn(II)-oxidizing microbes together with

chemical synproportionation of Mn(II)/Mn(IV) likely enabled efficient synergism of biological and chemical Mn(II) oxidative removal.

References

Bohu, T., Santelli, C.M., Akob, D.M., Neu, T.R., Ciobota, V., Rosch, P., et al. (2015). Characterization of pH dependent Mn(II) oxidation strategies and formation of a bixbyite-like phase by Mesorhizobium australicum T-G1. *Front Microbiol* 6, 734. doi: 10.3389/fmicb.2015.00734.

Corstjens, P.L.A.M., de Vrind, J.P.M., Goosen, T., and Jong, E.W.d.V.d. (1997). Identification and molecular analysis of theLeptothrix discophoraSS - 1mofAgene, a gene putatively encoding a manganese - oxidizing protein with copper domains. *Geomicrobiology Journal* 14(2), 91-108. doi: 10.1080/01490459709378037.

Dick, G.J., Torpey, J.W., Beveridge, T.J., and Tebo, B.M. (2008). Direct identification of a bacterial manganese(II) oxidase, the multicopper oxidase MnxG, from spores of several different marine Bacillus species. *Appl Environ Microbiol* 74(5), 1527-1534. doi: 10.1128/AEM.01240-07.

Feng, X.H., Zhu, M.Q., Ginder-Vogel, M., Ni, C.Y., Parikh, S.J., and Sparks, D.L. (2010). Formation of nano-crystalline todorokite from biogenic Mn oxides. *Geochimica Et Cosmochimica Acta* 74(11), 3232-3245. doi: 10.1016/j.gca.2010.03.005.

Francis, C.A., and Tebo, B.M. (2001). cumA Multicopper Oxidase Genes from Diverse Mn(II)-Oxidizing and Non-Mn(II)-Oxidizing Pseudomonas Strains. *Applied and Environmental Microbiology* 67(9), 4272-4278. doi: 10.1128/aem.67.9.4272-4278.2001.

Geszvain, K., McCarthy, J.K., and Tebo, B.M. (2013). Elimination of manganese(II,III) oxidation in Pseudomonas putida GB-1 by a double knockout of two putative multicopper oxidase genes. *Appl Environ Microbiol* 79(1), 357-366. doi: 10.1128/AEM.01850-12.

Geszvain, K., Smesrud, L., and Tebo, B.M. (2016). Identification of a Third Mn(II) Oxidase Enzyme in Pseudomonas putida GB-1. *Appl Environ Microbiol* 82(13), 3774-3782. doi: 10.1128/AEM.00046-16.

Jiang, L., Huang, C., Chen, J., and Chen, X. (2009). Oxidative transformation of 17beta-estradiol by MnO2) in aqueous solution. *Arch Environ Contam Toxicol* 57(2), 221-229. doi: 10.1007/s00244-008-9257-8.

Jones, L.C., Lafferty, B.J., and Sparks, D.L. (2012). Additive and competitive effects of bacteria and Mn oxides on arsenite oxidation kinetics. *Environ Sci Technol* 46(12), 6548-6555. doi: 10.1021/es204252f.

Lefkowitz, J.P., Rouff, A.A., and Elzinga, E.J. (2013). Influence of pH on the reductive transformation of birnessite by aqueous Mn(II). *Environ Sci Technol* 47(18), 10364-10371. doi: 10.1021/es402108d.

Mann, S., Sparks, N.H., Scott, G.H., and de Vrind-de Jong, E.W. (1988). Oxidation of

Manganese and Formation of Mn(3)O(4) (Hausmannite) by Spore Coats of a Marine Bacillus sp. *Appl Environ Microbiol* 54(8), 2140-2143.

Morgan, J.J. (2005). Kinetics of reaction between O2 and Mn(II) species in aqueous solutions. *Geochimica et Cosmochimica Acta* 69(1), 35-48. doi: 10.1016/j.gca.2004.06.013.

Okibe, N., Maki, M., Sasaki, K., and Hirajima, T. (2013). Mn(II)-Oxidizing Activity of Pseudomonas sp Strain MM1 is Involved in the Formation of Massive Mn Sediments around Sambe Hot Springs in Japan. *Materials Transactions* 54(10), 2027-2031. doi: 10.2320/matertrans.M-M2013825.

Ravel, B., and Newville, M. (2005). ATHENA, ARTEMIS, HEPHAESTUS: data analysis for X-ray absorption spectroscopy using IFEFFIT. *J Synchrotron Radiat* 12(Pt 4), 537-541. doi: 10.1107/S0909049505012719.

Ridge, J.P., Lin, M., Larsen, E.I., Fegan, M., McEwan, A.G., and Sly, L.I. (2007). A multicopper oxidase is essential for manganese oxidation and laccase-like activity in Pedomicrobium sp. ACM 3067. *Environ Microbiol* 9(4), 944-953. doi: 10.1111/j.1462-2920.2006.01216.x.

Santelli, C.M., Webb, S.M., Dohnalkova, A.C., and Hansel, C.M. (2011). Diversity of Mn oxides produced by Mn(II)-oxidizing fungi. *Geochimica Et Cosmochimica Acta* 75(10), 2762-2776. doi: 10.1016/j.gca.2011.02.022.

Saratovsky, I., Gurr, S.J., and Hayward, M.A. (2009). The Structure of manganese oxide formed by the fungus Acremonium sp strain KR21-2. *Geochimica Et Cosmochimica Acta* 73(11), 3291-3300. doi: 10.1016/j.gca.2009.03.005.

Tebo, B.M., Bargar, J.R., Clement, B.G., Dick, G.J., Murray, K.J., Parker, D., et al. (2004). Biogenic manganese oxides: Properties and mechanisms of formation. *Annual Review of Earth and Planetary Sciences* 32(1), 287-328. doi: 10.1146/annurev.earth.32.101802.120213.

Tebo, B.M., Johnson, H.A., McCarthy, J.K., and Templeton, A.S. (2005). Geomicrobiology of manganese(II) oxidation. *Trends Microbiol* 13(9), 421-428. doi: 10.1016/j.tim.2005.07.009.

Tu, J., Yang, Z., Hu, C., and Qu, J. (2014). Characterization and reactivity of biogenic manganese oxides for ciprofloxacin oxidation. *J Environ Sci (China)* 26(5), 1154-1161. doi: 10.1016/S1001-0742(13)60505-7.

Villalobos, M., Toner, B., Bargar, J., and Sposito, G. (2003). Characterization of the manganese oxide produced by Pseudomonas putida strain MnB1. *Geochimica Et Cosmochimica Acta* 67(14), 2649-2662. doi: 10.1016/S0016-7037(03)00217-5.

Webb, S.M., Dick, G.J., Bargar, J.R., and Tebo, B.M. (2005). Evidence for the presence of Mn(III) intermediates in the bacterial oxidation of Mn(II). *Proc Natl Acad Sci U S*

A 102(15), 5558-5563. doi: 10.1073/pnas.0409119102.

Zeng, X., Zhang, M., Liu, Y., and Tang, W. (2018). Manganese(II) oxidation by the multi-copper oxidase CopA from Brevibacillus panacihumi MK-8. *Enzyme Microb Technol* 117, 79-83. doi: 10.1016/j.enzmictec.2018.04.011.

Zhang, H., and Huang, C.H. (2003). Oxidative transformation of triclosan and chlorophene by manganese oxides. *Environ Sci Technol* 37(11), 2421-2430. doi: 10.1021/es026190q.

Zhao, H., Zhu, M., Li, W., Elzinga, E.J., Villalobos, M., Liu, F., et al. (2016). Redox Reactions between Mn(II) and Hexagonal Birnessite Change Its Layer Symmetry. *Environ Sci Technol* 50(4), 1750-1758. doi: 10.1021/acs.est.5b04436.

The results in this chapter were partially cooperated by Mr. Kyohei Takamatsu (Bachelor 4th year student in fiscal year 2016).

Data shown in this chapter were partially included in the paper submitted to Water (2019, 11(3), 507) entitled “Natural attenuation of Mn(II) in metal-refinery wastewater: Microbial community structure analysis and isolation of a new Mn(II)-oxidizing bacterium *Pseudomonas* sp. SK3”

Chapter 5

Synergistic effect of natural Mn oxide and Mn(II)-oxidizing bacteria on oxidative removal of Mn(II) from wastewater

Abstract

In this chapter, a combination of chemical Mn(II)-oxidation (synproportionation) by natural Mn-oxide (NMO) and enzymatic Mn(II)-oxidation by *Pseudomonas* sp. SK3 was tested for Mn removal efficiency under various conditions.

Synproprotionation is the reaction between Mn^{IV} and Mn(II) resulted in the formation of Mn_2O_3, which will passivate on the surface of NMO leading to incomplete Mn(II)-removal (about 50%) even though 2.5 times of the required NMO amount was added. Interestingly, the presence of strain SK3 synergistically oxidized Mn(II), resulting in complete oxidation of Mn(II) with higher efficiency as the biogenic Mn-oxide (birnessite) could further catalyze the synproprotionation reaction. Colonization of strain SK3 on NMO surface via biofilm enabled it to exhibited Mn(II) oxidation activity even under originally inhibited conditions (moderate temperature; 35℃ and high $MgSO_4$ concentration; 2400 mg/L) (Sutherland, 2001; Wang et al., 2009). Addition of NMO in acidic Mn(II)-containing medium (pH 3.0-5.0) resulting in the releasing of alkaline substances, which brought the pH up and consequently triggered Mn(II) oxidation activity of strain SK3 (pH >6.5). Moreover, NMO could oxidize and remove the toxicity from organic contaminants in tailing dam wastewater, which formerly inhibited Mn(II) oxidation by planktonic strain SK3 cells.

Overall, the potential utility of the synergistic Mn(II)-oxidative removal is illustrated for further industrial wastewater treatment.

5.1 Introduction

A new Mn(II)-oxidizing bacterium, *Pseudomonas* sp. SK3 has been isolated from natural Mn-oxide (NMO) and displayed robust oxidation activity under conditions where *Pseudomonas putida* MnB1 was inhibited (Kitjanukit et al., 2019). However, the reaction speed is needed to be improved for industrial application. Previously, active enzymatic Mn(II) oxidation by indigenous bacteria was showed as an important factor to completely remove Mn(II) by NMO (in **chapter 3**). Combination of biogenic Mn-oxide and Mn(II)-oxidizing bacteria has been studied for the application like oxidative removal of toxic organic compounds and arsenite (Matsushita et al., 2018; Tran et al., 2018; He et al., 2019). The role of Mn(II)-oxidizing bacteria is to regenerate Mn^{III} or Mn^{IV} from Mn^{II} dissolution from Mn-oxide upon redox reaction with those toxic compounds; thus, promoting synergistic effect. Despite those extensive studies, synergistic Mn(II)-oxidative removal by Mn-oxide and Mn(II)-oxidizer is still limited. Mn-oxide is known as one of the strongest oxidants found in nature which could oxidized various heavy metals including Mn itself. Redox reaction between Mn^{IV} in Mn-oxide and Mn^{2+} in solution resulted in formation of $Mn^{III}_2O_3$ called synproportionation (Zhao et al., 2016).

The objective of this study is to investigate the contribution of Mn(II)-oxidizing bacteria to the Mn(II)-oxidative removal by NMO and vice versa.

5.2 Materials and methods

5.2.1 Mn(II)-oxidizing bacteria

Pseudomonas sp. SK3 isolated from metal-refinery wastewater treatment facility (Kitjanukit et al., 2019) was pre-grown overnight in LB medium (pH 7.0), washed, and harvested by centrifugation prior to use.

5.2.2 Preparation of natural Mn-oxide

Crystalline MnO_2 collected from metal-refinery wastewater treatment facility contained mainly Mn(IV) 84% (with minor of 13% Mn(III) and 3% Mn(II)) and has an average oxidation state of 3.75 (Kitjanukit et al., 2019). To prevent the effects of indigenous microbial activity, the oxide was washed with ethanol followed by deionized water and freeze-dried overnight. Mn-oxide was kept in sterilized brown bottle prior to further use.

5.2.3 Synergistic Mn(II) removal using natural Mn-oxide and Mn(II)-oxidizing bacteria

In all cases, duplicate flasks were set up and incubated with shaking at 120 rpm. The sample was routinely withdrawn to monitor cell density (bacterial counting chamber), pH, and Mn(II) concentration (ICP-OES).

5.2.3.1 Effect of initial [Mn(II)] and [$MgSO_4$]

Sterilized natural Mn-oxide (0.5% (w/v)) and *Pseudomonas* sp. SK3 cell suspension (10^9 cells/mL) were added into 300 mL Erlenmeyer flask containing pre-sterilized 100 mL PYG-1 medium omitting PIPES (section 2.1.3) containing 100, 200, or 400

mg/L Mn(II) (added as $MnSO_4$), plus 3 μM Cu(II) (added as $CuCl_2$). In addition to 24 mg/L $MgSO_4$ originally presented in PYG-1 medium, its concentration was raised to 4800 mg/L. The initial pH value was set to 8.0 and temperature at 25℃.

5.2.3.2 Effects of elevated temperature

Sterilized natural Mn-oxide (0.5% (w/v)) and *Pseudomonas* sp. SK3 cell suspension (10^9 cells/mL) were added into 300 mL Erlenmeyer flask containing pre-sterilized 100 mL PYG-1 medium omitting PIPES (section 2.1.3) containing 100 mg/L Mn(II) (added as $MnSO_4$), plus 3 μM Cu(II) (added as $CuCl_2$). In addition to 24 mg/L $MgSO_4$ originally presented in PYG-1 medium, its concentration was raised to 2400 or 4800 mg/L. The initial pH value was set to 8.0 and temperature at 30, 35, or 40℃.

5.2.3.3 Mn(II) oxidative removal in acidic condition

Sterilized natural Mn-oxide (0.5% (w/v)) and *Pseudomonas* sp. SK3 cell suspension (10^9 cells/mL) were added into 300 mL Erlenmeyer flask containing pre-sterilized 100 mL PYG-1 medium omitting PIPES (section 2.1.3) containing 100 mg/L Mn(II) (added as $MnSO_4$), plus 3 μM Cu(II) (added as $CuCl_2$). The initial pH value was set to 4.0, 5.0, 6.0, or 7.0 and temperature at 25℃.

5.2.4 Application study of synergistic Mn(II)-oxidative removal from tailing dam wastewater

Sterilized natural Mn-oxide (0.5% (w/v)) and *Pseudomonas* sp. SK3 cell suspension (10^9 cells/mL) were added into 300 mL Erlenmeyer flask containing pre-sterilized 100 mL tailing dam wastewater (table 5.1). In addition to approximately 2 mg/L

Mn(II) originally presented in the wastewater, initial Mn(II) concentration was set to 100 mg/L (added as $MnSO_4$), plus 3 μM Cu(II) (added as $CuCl_2$). Yeast extract concentration was set to 0, 0.0025, 0.005, or 0.01% (w/v).

Table 5.1 Composition of tailing dam wastewater collected from the metal-refinery wastewater treatment facility

Composition	
Mn	1.n ~ 2.3 mg/L
Cu	0.008 mg/L
Ni	0.035 mg/L
Ca	510 mg/L
Si	5.1 mg/L
Mg	150 mg/L
S (as SO_4^{2-})	780 mg/L
pH	6.9-7.3

5.2.5 Solid characterization

X-ray diffraction

Newly formed Mn-oxide were collected after Mn(II) oxidative removal test by short spin (3000 rpm, 5 seconds) to separate it from natural Mn-oxide. The solid samples were freeze-dried overnight and analyzed with X-ray diffraction (XRD; Rigaku UltimaIV; CuKα 40 mA, 40 kV).

Scanning electron microscope (SEM)

Solid residues were fixed with a fixing reagent (2% glutaraldehyde and 2.5% formaldehyde in 0.1 M phosphate buffer solution (PBS; pH 7.6) at 4℃ for 30 min, washed twice with 0.1 M PBS, followed by dehydration using ascending concentration of ethanol (70, 80, 90, and 99.5% for 5 min each, and 100% for 10 min)

and dried in vacuum desiccator for 24 h. The pre-treated sample was sputter coated with Au-Pd (MSP-1S, Vacuum Device) and observed with SEM (Keyence VE-9800; 5keV).

5.3 Results and discussion

5.3.1 Synergistic Mn(II) removal using natural Mn-oxide and Mn(II)-oxidizing bacteria

5.3.1.1 High [Mn(II)] and [$MgSO_4$]

Our challenge in this study is to improve Mn oxidative removal efficiency. Ideally, the new bioprocess would be placed further upstream of the metal refinery wastewater treatment system to deal with a few hundreds of mg/L Mn(II) contaminant coexisting with a high concentration of $MgSO_4$.

First, pre-grown cells of *Pseudomonas* sp. SK3 together with natural Mn-oxide (NMO) was tested for Mn(II) oxidation at 100, 200, and 400 mg/L coexisting with 200 mM $MgSO_4$.

As shown in Fig. 5.1, the combination of NMO and *Pseudomonas* sp. SK3 apparently oxidized Mn(II) with more efficiently than NMO alone. Mn(II) was first oxidized and immobilized via synproportionation reaction producing $Mn^{III}_2O_3$ mineral (Eq. 5.1) (Zhao et al., 2016).

$$Mn^{IV}O_2(s) + Mn^{2+} + H_2O \rightarrow Mn^{III}_2O_3(s) + 2H^+ \text{ (Eq. 5.1)}$$

The rate of the reaction is rapid at the early stage, gradually slowed down and eventually ceased. According to the proportion of Mn^{IV} species in the NMO (about 80%), 0.5% (w/v) is a stoichiometrically excess amount (approximately 2.5 fold) for complete oxidation of 100 mg/L Mn(II). The $Mn^{III}_2O_3$ mineral resulted from

synproportionation, was passivated on the surface of NMO could not further catalyze Mn(II)-oxidation.

The presence of Mn(II)-oxidizing bacteria (in this case; *Pseudomonas* sp. SK3) could regenerate fresh Mn^{IV}-oxide as birnessite via enzymatic activity, which could further catalyzed synproportionation. XRD pattern of precipitates selectively collected after the experiment indicated that the birnessite peak appeared only in the presence of Mn(II)-oxidizing bacteria (Fig. 5.3).

This phenomenon was also studied in other aspects such as regeneration of Mn^{III} and Mn^{IV} for the oxidation of organic waste (Matsushita et al., 2018; Tran et al., 2018).

An equal amount of NMO fed (0.5%) is 1.2 and 0.6 fold of the amount of Mn^{IV} required to completely oxidize 200 and 400 mg/L Mn(II), respectively. Strain SK3 together with NMO promoted synergistic Mn(II)-oxidative removal, which improved the removal efficiency from 39.6% to 88.35% and 24.2% to 58.2%, at 200 and 400 mg/L initial Mn(II), respectively within 120 hours of incubation (Fig. 5.1a).

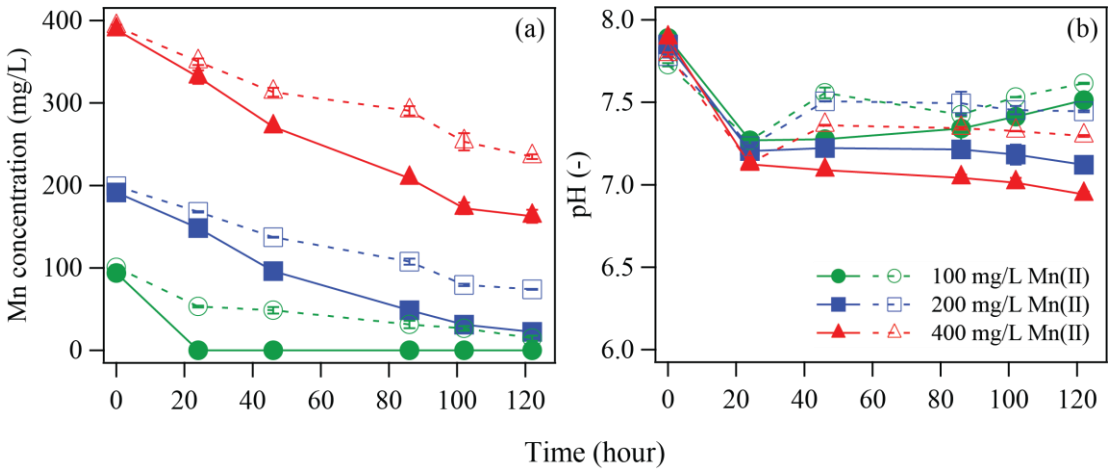

Figure 5.1 Changes in Mn concentration (a) and pH (b) during Mn(II)-oxidative removal in the presence of sterilized natural Mn oxide (0.5% (w/v)) and *Pseudomonas* sp. SK3 at different initial Mn(II) concentration of 100, 200, and 400 mg/L. Closed and opened symbols indicated NMO/SK3 and NMO only, respectively.

5.3.1.2 Effect of temperature

In **chapter 3**, Mn(II)-oxidative removal by NMO was improved in elevated temperature and indigenous microbes were found to play an important role in facilitating the Mn(II) removal. To test the broad applicability of the combination of strain SK3 and NMO in the treatment of Mn(II)-contaminating wastewater, the test was further conducted at elevated temperature (30-40℃).

At 30℃, planktonic cells of strain SK3 could oxidize 80% Mn(II) within 120 hours whereas 60% was oxidized in the case of NMO only. Obviously, a combination of them synergistically enhanced Mn(II)-oxidative removal efficiency; 100% of Mn(II) was oxidized within 40 and 62 hours, in the presence of 1200 and 2400 mg/L $MgSO_4$, respectively (Fig. 5.2a). In the case of 35℃, planktonic strain SK3 cells could not oxidize Mn(II) at 35℃ due to enzyme inactivation (Kitjanukit et al., 2019), while NMO managed to oxidized about 65% (with higher speed compared with 30℃). Interestingly, the combination of strain SK3 and NMO enabled completed oxidation of Mn(II) with higher speed even in the presence of high $MgSO_4$; within 20 and 40 hours at 1200 and 2400 mg/L $MgSO_4$, respectively. No synergistic effect was observed when the temperature was raised to 40℃ (data not shown) since there is no significant difference with sterile control.

Addition of NMO could have provided a site for strain SK3 to colonize via biofilm. This may have enabled cells to be less affected by the inhibitory effect, high concentration of $MgSO_4$ and moderate temperature in this case.

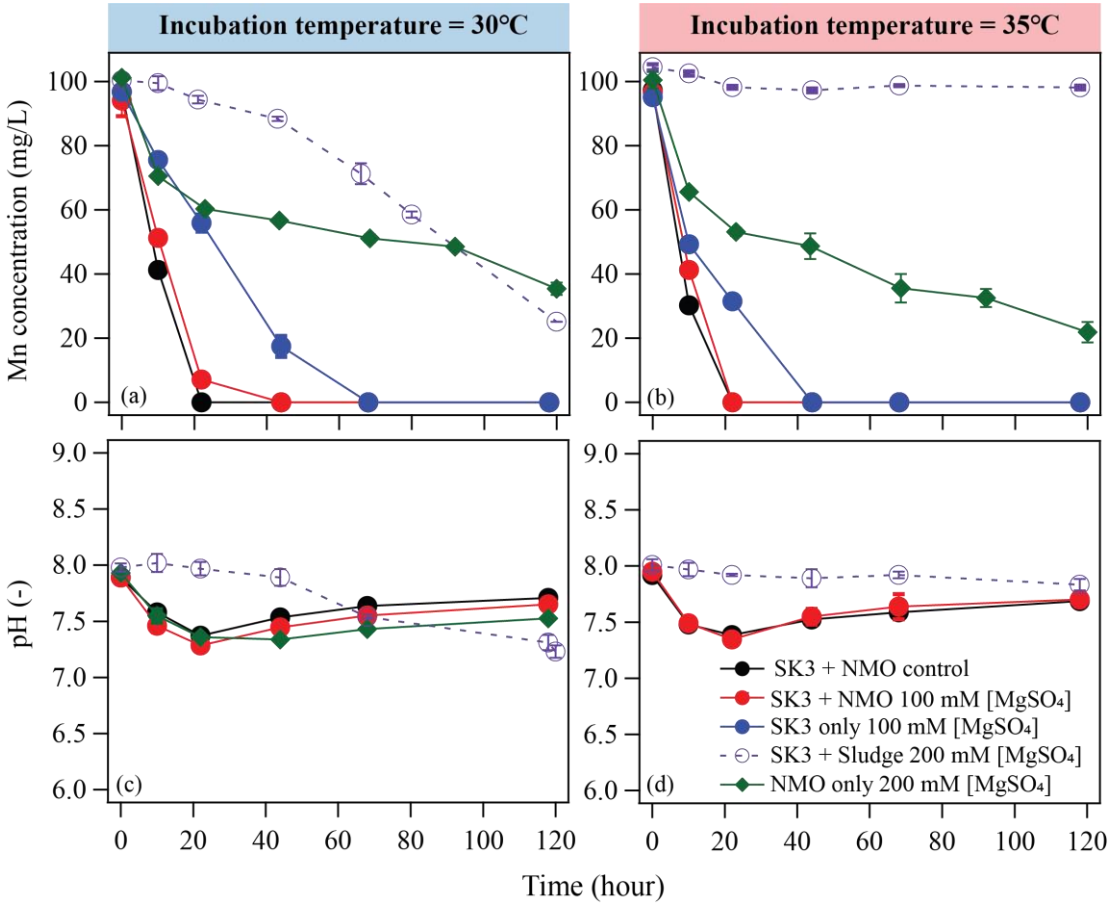

Figure 5.2 Changes in Mn concentration (a,b) and pH (c,d) during Mn(II)-oxidative removal in the presence of sterilized natural Mn oxide (0.5% (w/v)) and *Pseudomonas* sp. SK3 at an incubation temperature of 30°C (a,c) and 35°C (b,d). Initial $MnSO_4$ concentration was set to 2400 mg/L (100 mM) and 4800 mg/L (200 mM) in addition to 24 mg/L presented originally in PYG-1 medium.

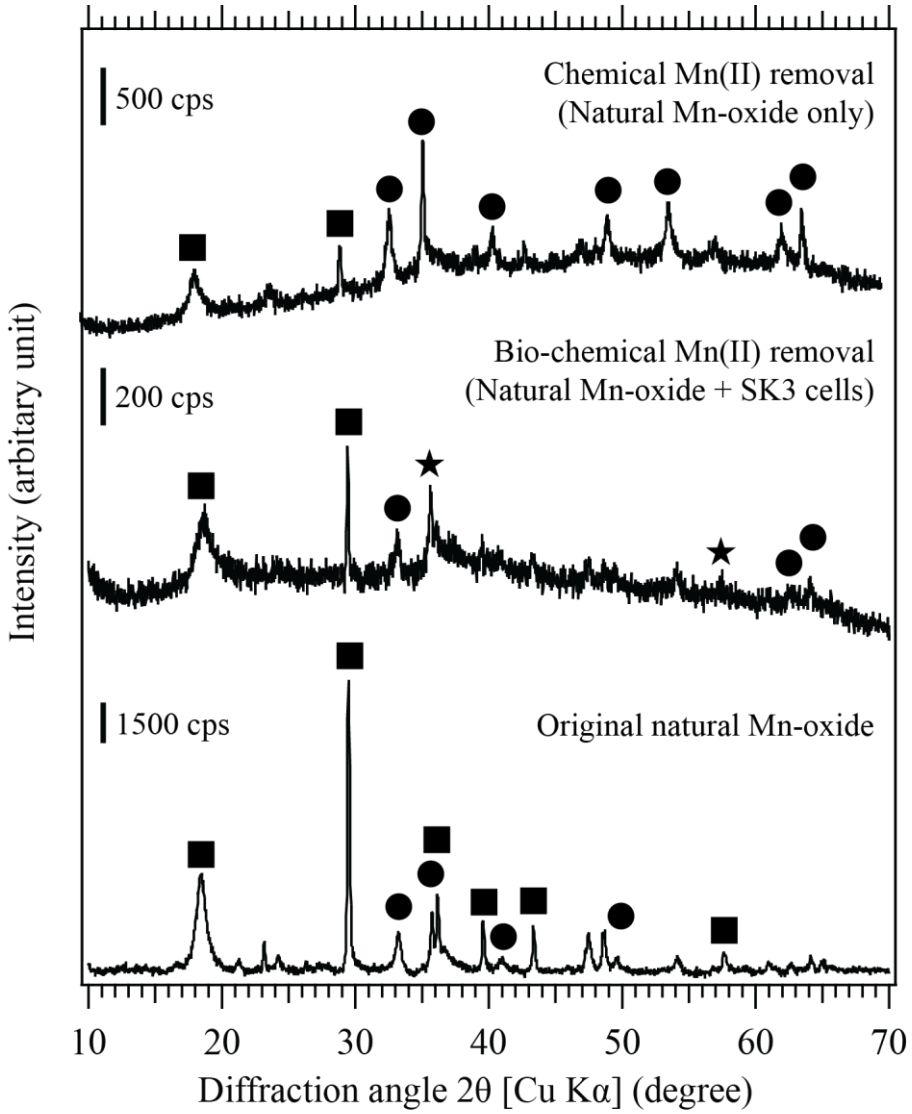

Figure 5.3 X-ray diffraction pattern of original natural Mn-oxide and precipitates after selective collection after Mn(II) oxidative removal using natural Mn oxide/SK3 cells and natural Mn oxide. ■: MnO_2, ●: Mn_2O_3 JCPDS 41-1442, ★: birnessite JCDD 43-1456.

5.3.1.3 Mn(II)-oxidative removal in acidic pH

Our main challenge was to develop bioprocess to deal with the treatment of Mn(II)-contaminating metal-refinery wastewater, which is acidic. Up till now, acidophilic Mn(II)-oxidizing bacteria has not been discovered yet. Nevertheless, the new bioprocess should ideally be placed further upstream of the treatment system to deal with acidic wastewater.

Mn(II)-oxidative removal test by planktonic SK3 cells in **chapter 4** indicated that it could not oxidize Mn(II) at pH below 6.5 (Kitjanukit et al., 2019). Combination of NMO and strain SK3 synergistically oxidized and removed Mn(II) effectively under complex conditions earlier in this chapter. Hence, Mn(II)-oxidative removal under acidic pH (4.0-7.0) was investigated.

In all conditions, solution pH was increased upon addition of pre-sterilized NMO and this may due to the dissolution of alkaline components (Fig. 5.4 b,e). After pH increased beyond 6.5, enzymatic Mn(II)-oxidation was triggered. The combination of NMO and strain SK3 again exhibited remarkable Mn(II) removal efficiency. Although it required a longer time to completely oxidized Mn(II), which corresponding to lower pH values (Fig. 5.4a). Similar to the previous experiment, only 50% of Mn(II) was removed in the case of NMO only (Fig. 5.4d).

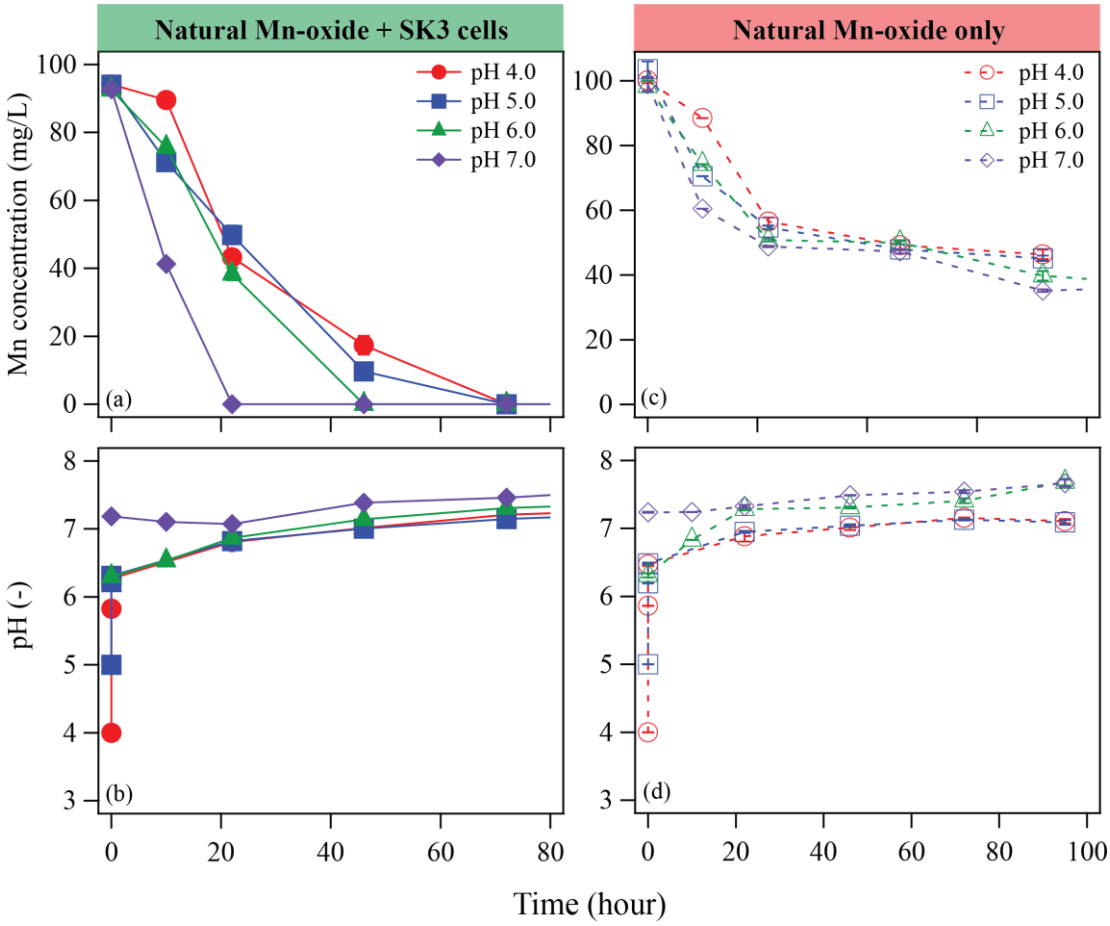

Figure 5.4 Changes in Mn concentration (a, c) and pH (b, d) during Mn(II) oxidative removal in the presence of natural Mn-oxide/*Pseudomonas* sp. SK3 cells (solid symbols) and natural Mn oxide only (open symbol) at different initial pH of 4.0-7.0.

5.3.2 Mn(II)-oxidative removal from tailing dam wastewater

Tailing dam wastewater collected from metal-refinery wastewater treatment facility contained mainly Mn (~2 mg/L) as heavy metal and high concentration of SO_4^{2-} ion (780 mg/L). To study the applicability of strain SK3 to oxidize Mn(II) from tailing dam wastewater, initial Mn(II) concentration was adjusted to 100 mg/L.

Planktonic cells of SK3 could not manage to initiate Mn(II) oxidation activity in all conditions (Fig. 5.5a and b). In fact, this tailing dam wastewater might contain some organic contaminants (ex: flocculants) which inhibited Mn(II)-oxidation activity.

Previously, strain SK3 could readily initiated and oxidized Mn(II) completely, even under high concentration of $MgSO_4$ (1200-2400 mg/L) (Kitjanukit et al., 2019). Although cell death was not observed (except for 0% yeast extract), some component in the tailing dam wastewater might inhibit the enzymatic activity (Fig. 5.5c).

Addition of NMO chemically oxidized about 50% of Mn(II) (Fig. 5.5a; 0% y.e.) and the contribution from strain SK3 was apparently showed (Fig. 5.5a; 0.005% y.e.). Double the yeast extract concentration has improved the removal of Mn(II) from 75% to 85%. Mn-oxide both synthetic and biogenic have been widely used for oxidation of trace organic contaminants (Remucal and Ginder-Vogel, 2014). NMO might oxidize those contaminants and allowed strain SK3 to exhibit Mn(II) oxidation activity.

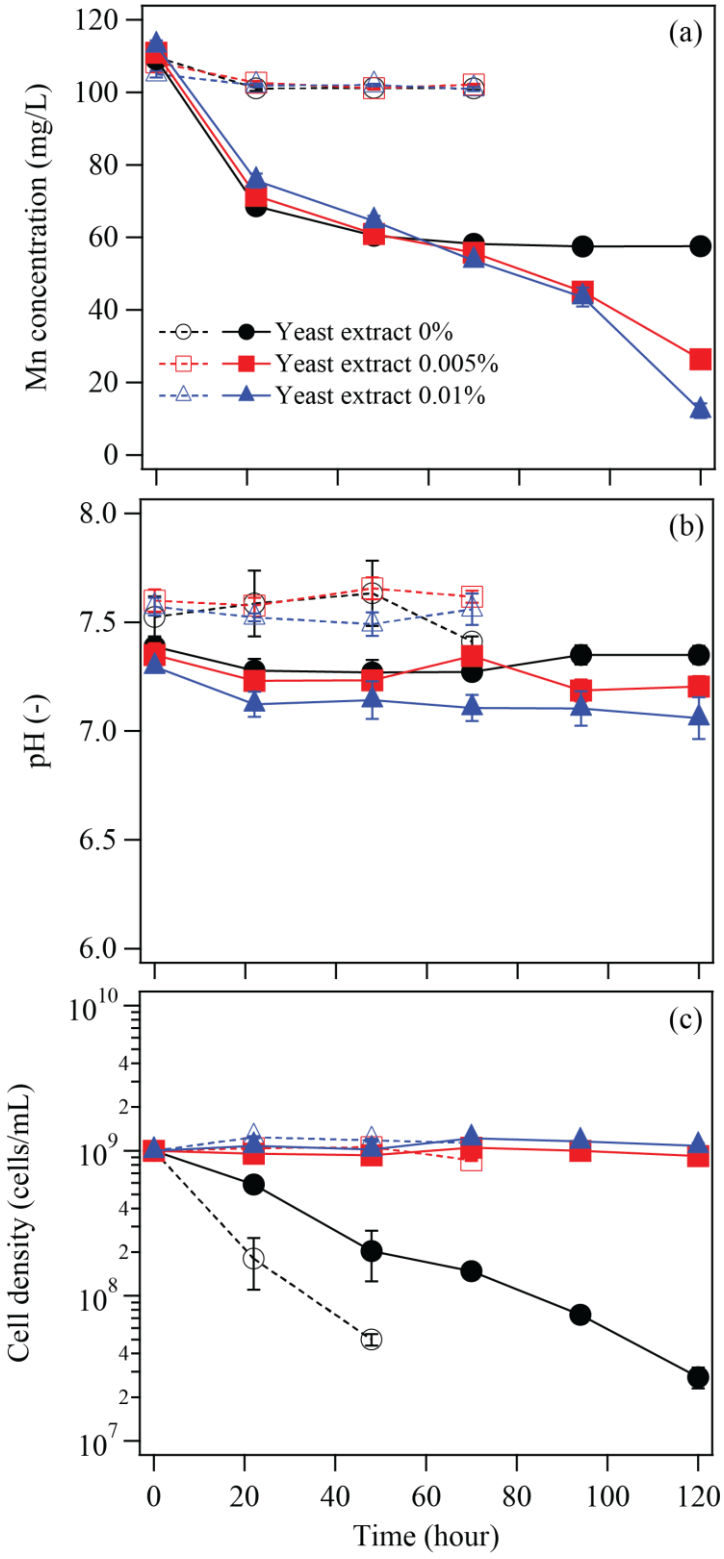

Figure 5.5 Changes in Mn concentration (a), pH (b), and cell density (c) during Mn(II) oxidative removal from tailing dam wastewater in the presence of natural Mn-oxide/*Pseudomonas* sp. SK3 cells (solid symbols) or planktonic cells only (open symbol) at different yeast extract concentration of 0, 0.005, or 0.01% (w/v).

5.4 Conclusions

- Natural Mn-oxide (NMO) facilitated Mn(II)-oxidative removal via synproportionation reaction (Mn^{IV} and Mn^{2+}) resulted in the formation of Mn_2O_3.
- Mn(II) removal proceeded rapidly at the early stage and then slowed down due to passivation of Mn_2O_3
- The presence of Mn(II)-oxidizing bacteria synergistically oxidized Mn(II) enzymatically producing biogenic birnessite. Those biogenic Mn-oxide could further catalyze Mn(II) via synproportionation (Fig. 5.6)
- Colonization of strain SK3 via biofilm on the surface provided by NMO enabled them to alleviate the inhibitory factors such as $MgSO_4$ and high temperature.
- Releasing of alkaline substances from NMO caused the rising of pH in acidic solution and consequently triggered Mn(II)-oxidation activity of strain SK3.
- Some trace organic contaminants originally presented in tailing dam wastewater might inhibit Mn(II)-oxidation activity of planktonic strain SK3 cells rather than those minor heavy metals (i.e. Ni and Cu).
- NMO might contribute to the oxidation of trace organic contaminants and allowed strain SK3 to exhibit its Mn(II) oxidation activity.

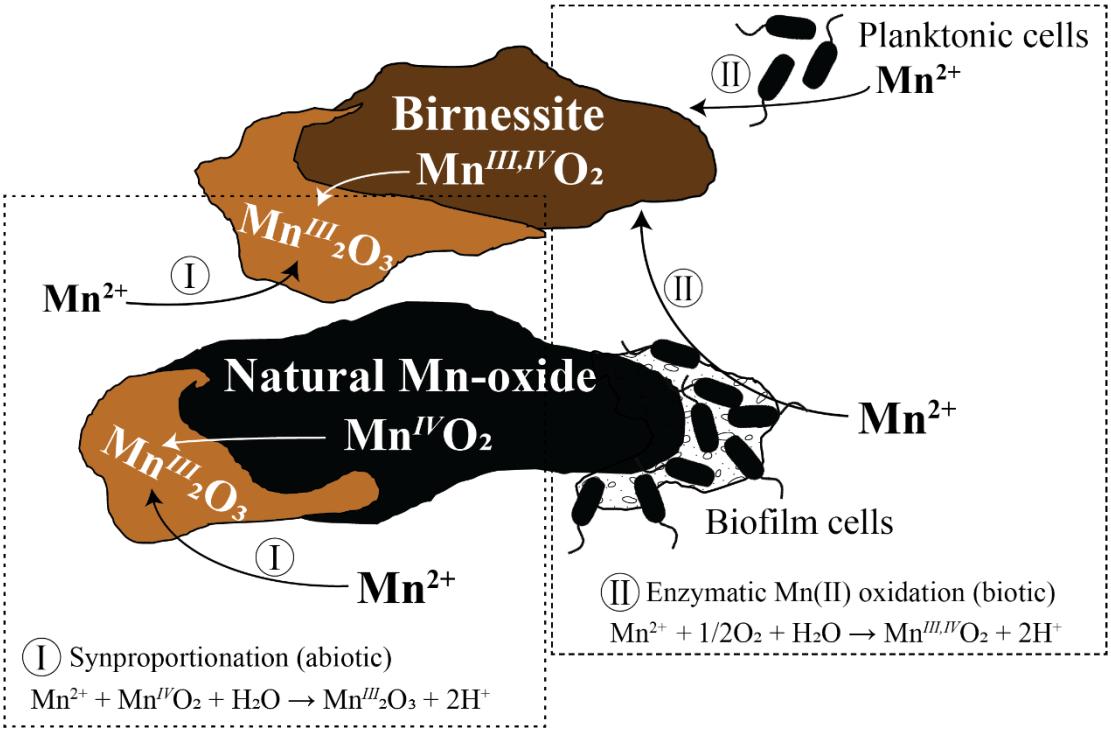

Figure 5.6 Purpose mechanism for synergistic Mn(II)-oxidative removal by natural Mn-oxide and Mn(II)-oxidizing bacteria (*Pseudomonas* sp. SK3)

References

He, Z., Li, Z., Zhang, Q., Wei, Z., Duo, J., and Pan, X. (2019). Simultaneous remediation of As(III) and dibutyl phthalate (DBP) in soil by a manganese-oxidizing bacterium and its mechanisms. *Chemosphere* 220, 837-844. doi: https://doi.org/10.1016/j.chemosphere.2018.12.213.

Kitjanukit, S., Takamatsu, K., and Okibe, N. (2019). Natural Attenuation of Mn(II) in Metal Refinery Wastewater: Microbial Community Structure Analysis and Isolation of a New Mn(II)-Oxidizing Bacterium Pseudomonas sp. SK3. *Water* 11(3), 507.

Matsushita, S., Komizo, D., Cao, L.T.T., Aoi, Y., Kindaichi, T., Ozaki, N., et al. (2018). Production of biogenic manganese oxides coupled with methane oxidation in a bioreactor for removing metals from wastewater. *Water Research* 130, 224-233. doi: https://doi.org/10.1016/j.watres.2017.11.063.

Remucal, C.K., and Ginder-Vogel, M. (2014). A critical review of the reactivity of manganese oxides with organic contaminants. *Environmental Science: Processes & Impacts* 16(6), 1247-1266. doi: 10.1039/C3EM00703K.

Sutherland, I.W. (2001). Exopolysaccharides in biofilms, flocs and related structures. *Water Science and Technology* 43(6), 77-86. doi: 10.2166/wst.2001.0345.

Tran, T.N., Kim, D.G., and Ko, S.O. (2018). Synergistic effects of biogenic manganese oxide and Mn(II)-oxidizing bacterium Pseudomonas putida strain MnB1 on the degradation of 17 alpha-ethinylestradiol. *J Hazard Mater* 344, 350-359. doi: 10.1016/j.jhazmat.2017.10.045.

Wang, Z., Wu, Z., and Tang, S. (2009). Extracellular polymeric substances (EPS) properties and their effects on membrane fouling in a submerged membrane bioreactor. *Water Research* 43(9), 2504-2512. doi: https://doi.org/10.1016/j.watres.2009.02.026.

Zhao, H., Zhu, M., Li, W., Elzinga, E.J., Villalobos, M., Liu, F., et al. (2016). Redox Reactions between Mn(II) and Hexagonal Birnessite Change Its Layer Symmetry. *Environ Sci Technol* 50(4), 1750-1758. doi: 10.1021/acs.est.5b04436.

Chapter 6

Searching for bacteria-supporting materials for Mn(II) removal using biofilter column

Abstract

In this chapter, 10 different materials including SiO_2-based (fuji sand, pumice, black sand, porous ceramic, hydroculture, natural zeolite, gravel, and perlite) and carbon-based (smoked rice husk and activated carbon) were undergone evaluation for their bacteria-supporting properties.

Cycle Mn(II)-oxidative removal in the presence of those materials and Mn(II)-oxidizing bacterium, *Pseudomonas* sp. strain SK3 was conducted in order to evaluate the bacteria and its biogenic birnessite supporting properties.

According to the results, natural zeolite, perlite, smoked rice husk, and activated carbon was evaluated as suitable bacterial-supporting materials to be utilized in further biofilter application. Additional sterile control cycle experiment for AC indicated that it could promote chemical Mn(II)-oxidation and also marked the importance of the presence of active Mn(II)-oxidizing bacteria. Thus, three Mn(II)-oxidative removal including, (1) chemical Mn(II) oxidation by AC, (2) enzymatic Mn(II) oxidation, and (3) synproportionation could be expected by the combination of AC and Mn(II)-oxidizing bacteria.

The biofilter column filled with bio-AC for Mn(II)-oxidative removal from metal-refinery wastewater will be tested and discussed in the next chapter.

6.1 Introduction

In a practical application for Mn-contaminating wastewater treatment, a continuous process is preferred over batch process due to the amount of wastewater generated.

Mn removal by means of the continuous process is commonly achieved through filtration. This technique column requires filler which could retain and support active Mn(II)-oxidizing bacteria (Pujol et al., 1994; Wang et al., 1995).

The main drawbacks for this technique are unavoidably long start-up period and washed out of Mn(II)-oxidizing bacteria during operation or backwashing. Therefore, pre-colonization of Mn(II)-oxidizing bacteria onto an ideal supporting material has been suggested as a strategy to accelerate the start-up period as well as to prevent bacterial washout. Immobilization of bacteria in alginate beads have been developed for wastewater treatment application (Pluemsab et al., 2007; Cruz et al., 2013).

It would also be worthy to investigate the attachment of biogenic birnessite ($Mn^{III,IV}O_2$) on bacterial-supporting material since it could further catalyze chemical Mn(II)-oxidative removal via synproportionation (Zhao et al., 2016). In this case, three Mn(II)-oxidative removal reaction could be expected.

6.2 Materials and methods

Mn(II)-oxidizing bacteria, *Pseudomonas* sp. SK3 (Kitjanukit et al., 2019) was pre-grown overnight in LB medium (pH 7.0), washed, and harvested by centrifugation prior to use in the following experiments. In all cases, duplicate flasks were set up and incubated with shaking at 120 rpm. The sample was routinely withdrawn to monitor cell density (bacterial counting chamber), pH, and Mn(II) concentration (ICP-OES).

6.2.1 Characterization of bacteria-supporting materials

Water treatment/agricultural materials including SiO_2-based materials; fuji sand, pumice, black sand, porous ceramic, hydroculture, natural zeolite, gravel, and perlite, carbon-based materials; smoked rice husk, and activated carbon with particle sizes of 1.0-2.0 mm (fig. 6.1) were washed with water and dried. All materials were characterized for their physical properties including surface area (BET), zeta-potential measurement, morphology (SEM) and solid phase (XRD). The sample preparation was mentioned in chapter 2.

6.2.2 Cycle Mn(II)-oxidative removal experiment

Bacteria-supporting materials (10% (v/v)) were added into modified PYG medium (pH 7.0) and autoclaved (120°C, 20 min). Mn(II) (100 mg/L), Cu(II) (3 μM) (added as $CuCl_2$) and glucose (1 mM) were aseptically added prior to inoculation of *Pseudomonas* sp. strain SK3 to the final cell density of 10^9 cells/mL. After 3 days, the spent medium was replaced with fresh sterilized PYG-1 medium (section 2.1.3) containing 100 mg/L Mn(II), Cu(II) 3 μM without re-inoculation of bacteria cells. The cycles were repeated for 3 times for evaluation of bacteria supporting properties.

6.2.3 Characterization of bacteria-supporting materials after cycle Mn(II)-oxidative removal experiment

The supporting materials were collected from the spent medium and washed thoroughly with sterile distilled water (centrifugation, 8000 rpm for 10 min).

6.2.3.1 Scanning electron microscope (SEM)

The sample was freeze-dried overnight, sputter coated and observed with a scanning electron microscope (KEYENCE; VE-9800)

6.2.3.2 Zeta potential measurement

The sample was crushed and ground before suspended in 0.1 M KCl solution and sonicated for 20 min. The pH value was set to 6.0 and 7.0 using HCl and KOH. All measurements were conducted at least in triplicate.

6.2.4 Mn(II)-oxidative removal using activated carbon

6.2.4.1 Single batch experiments

Activated carbon (Kuraray) 0.25, 0.5, 1, 1.25, 2.5, 5, 10% (w/v) was added into Erlenmeyer flask containing 100 mL PYG-1 medium (section 2.1.3) . At lower AC pulp densities (0.25-1%), pre-grown cells of *Pseudomonas* sp. SK3 (10^9 cells/mL) were suspended in addition. The initial Mn(II) concentration was set at 100 mg/L (added as $MnSO_4$). The initial pH value was set to 7.0 and temperature at 25℃.

6.2.4.2 Cycle experiment

Activated carbon 5% (w/v) was added into Erlenmeyer flask containing 100 mL PYG-1 medium. The initial Mn(II) concentration was set at 100 mg/L, plus 3 μM Cu(II) (added as $CuCl_2$). Initial cell density was set to 10^9 cells/mL. After 72 hours

(1^{st} cycle), the spent medium was replaced with fresh pre-sterilized PYG-1 medium (containing 100 mg/L Mn(II) and 3 μM Cu(II)) without re-inoculation of bacteria cells. The cycles were repeated for another 2 times after 48 hours incubation each.

6.2.4.3 Solid characterization

For batch experiment (section 6.2.4.1), spent AC was collected after the experiment. For cycle experiment (section 6.2.4.2), an aliquot amount of spent AC was collected after each cycle. The sample was washed thoroughly using deionized water, freeze-dried overnight and crushed into powder. The powdered samples were analyzed for Mn-oxide phase using XRD. After the 3^{rd} cycle, spent activated carbon was collected and fixed with a mixture of 2% glutaraldehyde and 2.5% formaldehyde in 0.1 M phosphate buffer solution (PBS; pH 7.6) (4℃, 30 min), washed twice with 0.1 M PBS. The samples were then undergo dehydration process using an ascending concentration of ethanol (70%, 80%, 90%, and 99.5% for 5 min each, and 100% for 10 min) and dried in a vacuum desiccator for 48 hours. After sputter coated with Au-Pd, the bio-AC pellet was cut to observe its cross-section surface with SEM (KEYENCE VE-9800).

Figure 6.1 Bacteria-supporting materials used in this study

6.3 Results and discussion

6.3.1 Characterization of bacteria-supporting materials

The materials are different in shape, color, and density based on the composition. SEM images revealed that mostly the morphology of the materials was porous with a variety of pore size. Natural zeolite has a smaller pore size compared with other materials and smoked rice husk has distinguished shape (Fig 6.1). XRD pattern shown in Fig. 6.2 indicated that the main composition of most materials are crystalline quartz and anorthite ($CaAl_2Si_2O_8$) except for gravel (amorphous silica), perlite (amorphous silica), and smoked rice husk (carbon). All materials have a negative surface charge at neutral pH (7.0), perlite with the most negative and activated carbon with the least negative charge. The materials tested have variety of surface area in the following order: activated carbon > natural zeolite > smoked rice husk > pumice > perlite > porous ceramic > fuji sand > hydroculture > black sand > gravel (Table 6.1). Water uptake: activated carbon > smoked rice husk > perlite > natural zeolite > black sand > porous cermic > fuji sand > gravel > pumice > hydroculture.

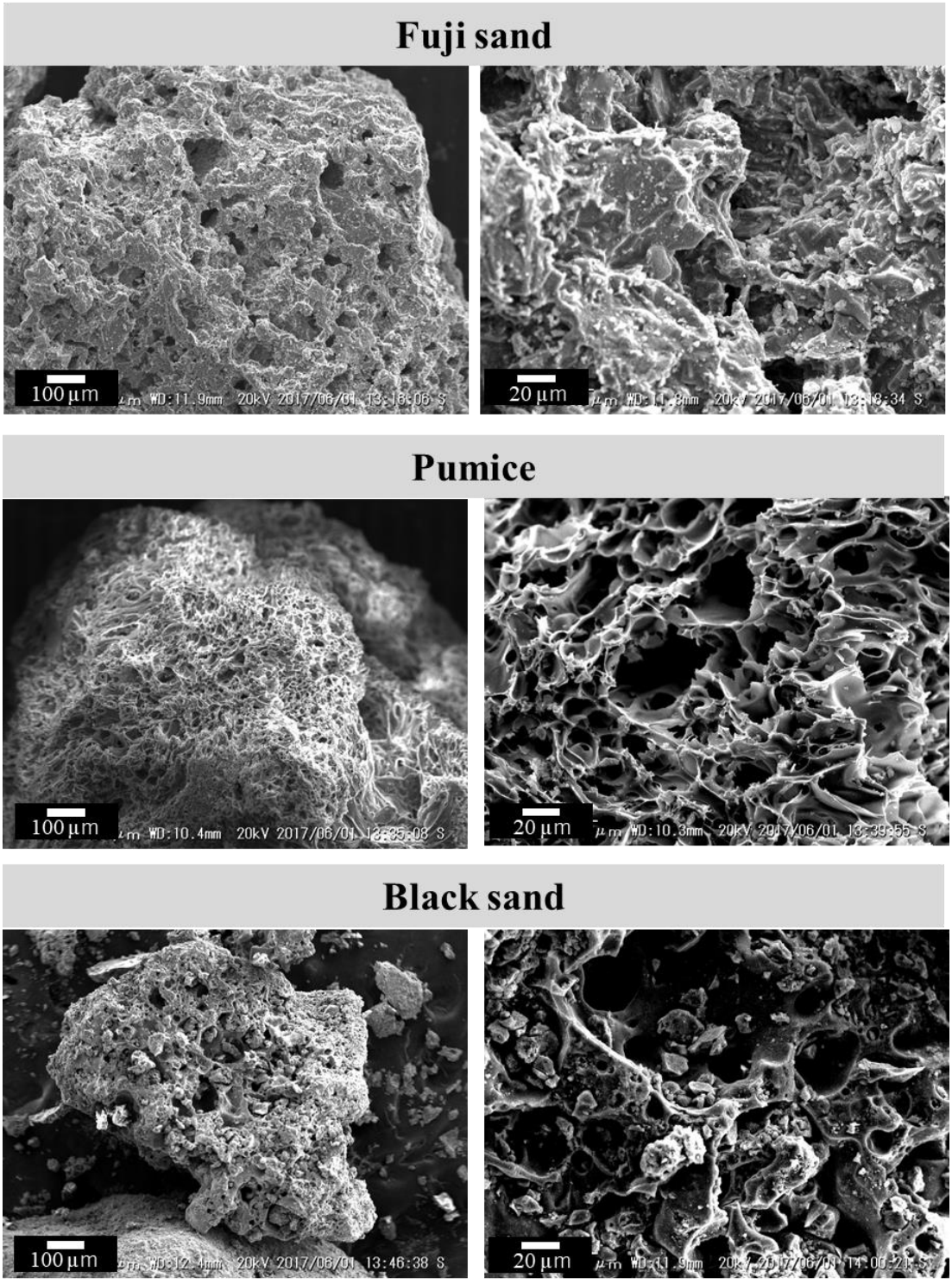

Figure 6.2 Secondary electron images of bacteria-supporting materials at magnification of 100x and 500x.

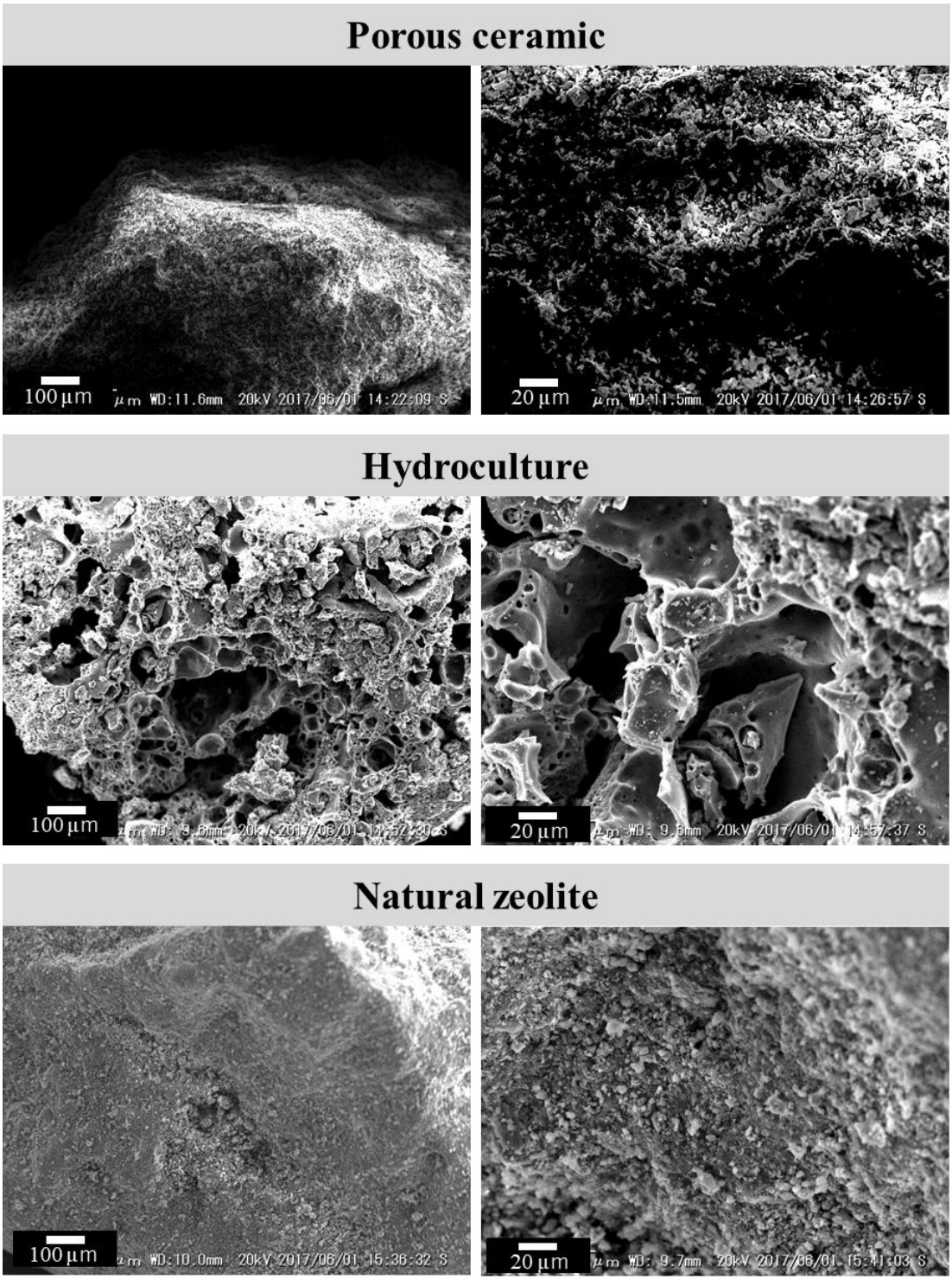

Figure 6.2 *(continued)*

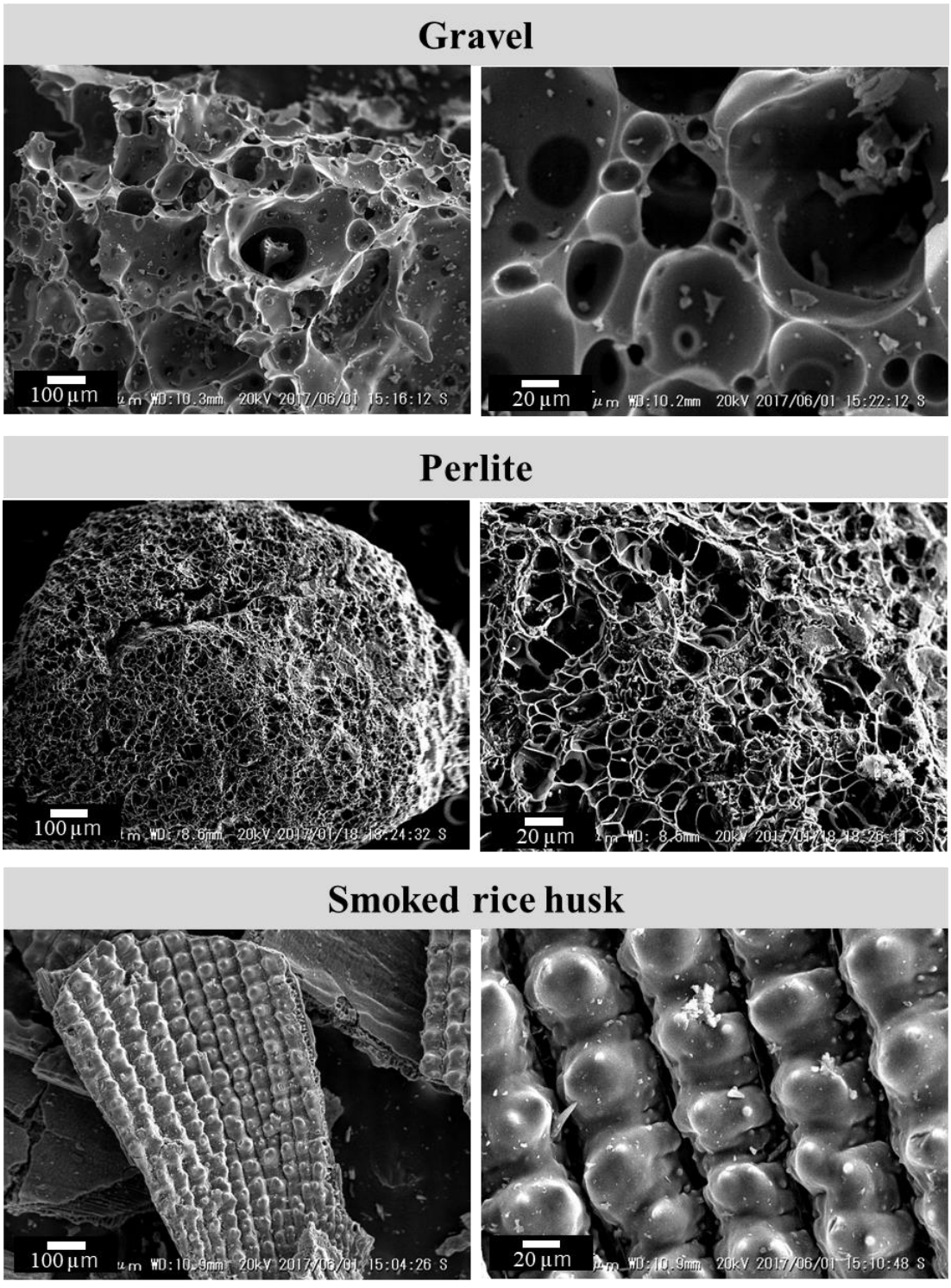

Figure 6.2 *(continued)*

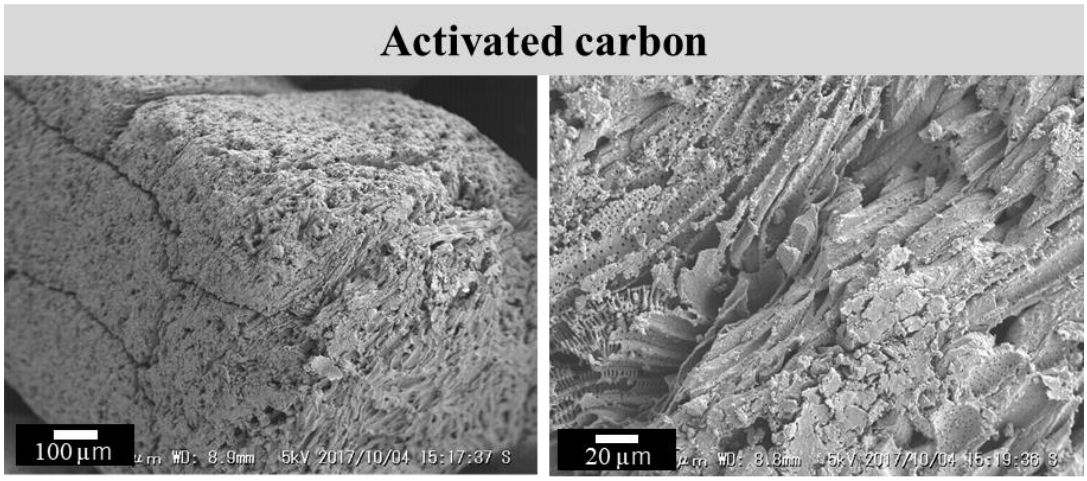

Figure 6.2 *(continued)*

Table 6.1 Surface properties of bacteria-supporting materials

Bacteria-supporting material	**Surface area (m^2/g)**	**Zeta potential at pH 7.0 (mV)**
Gravel	0.3	-50
Black sand	0.5	-45.6
Hydroculture	0.7	-51.5
Fuji sand	3.3	-46.2
Porous ceramic	3.3	-47.1
Perlite		-71
Pumice	4.4	-56.2
Smoked rice husk	126	-56.9
Natural zeolite	246	-45.6
Activated carbon	1280	-29.5

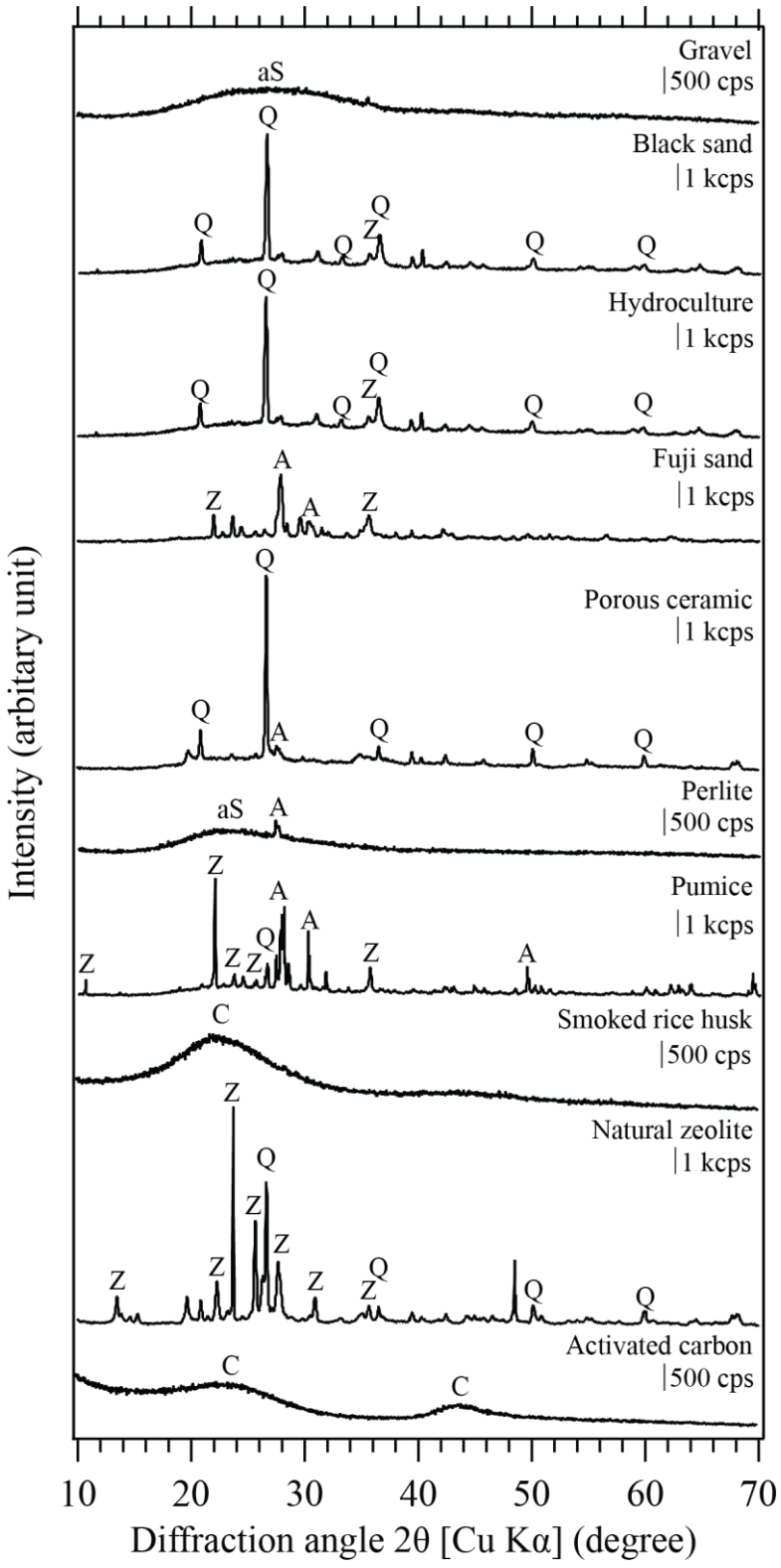

Figure 6.3 X-ray diffraction pattern of bacteria-support material tested in this study. A; anorthite ($CaAl_2Si_2O_8$; JCPDS 41-1486), aS (amorphous silica), C; carbon (JCPDS 82-1691), Q; quartz (JCPDS 46-1045), Z; zeolite (JCPDS 43-016

6.3.2 Cycle Mn(II)-oxidative removal

Figure 6.4 showed the changes in Mn concentration, pH, and planktonic cell density during cycle Mn(II)-oxidative removal test. After 20 hours of incubation, there was no sign indicated bacterial Mn(II)-oxidation yet (no black precipitate formed and stable pH). Slightly change in Mn concentration (<20%) was observed in all materials except activated carbon (>90%). Within 70 hours of incubation, 56%, 90.67%, 100%, and 100% Mn(II) was removed in the presence of pumice, porous ceramic, zeolite and perlite, respectively (Fig. 6.4a). For fuji sand, black sand, hydroculture, gravel, smoked rice husk, Mn(II) was removed 100%, 74.6%, 100%, 7.86%, and 100%, respectively (Fig. 6.4a').

After replacing new medium, Mn removal speed was significantly increased in the presence of most materials. This may due to the accumulation of biogenic birnessite on the surface of the materials from 1st cycle. Birnessite ($Mn^{III,IV}O_2$) could facilitate Mn(II)-oxidation via synproportionation reaction resulting in the formation of $Mn^{III}_2O_3$ (Zhao et al., 2016).

In 3rd cycle, Mn removal speed was improved in all materials except gravel (Fig 6.4 a, a'). There might be some inhibitory factor released from this material which prevented Mn(II)-oxidation activity.

Mn removal efficiencies in each cycle were summarized in Fig 6.5. The removal efficiency was low in most materials (fuji sand, pumice, black sand, hydroculture, gravel, and perlite). Sharp increase of Mn removal efficiency in fuji sand, black sand, and hydroculture (2nd cycle) indicated their potential as a support for biogenic birnessite.

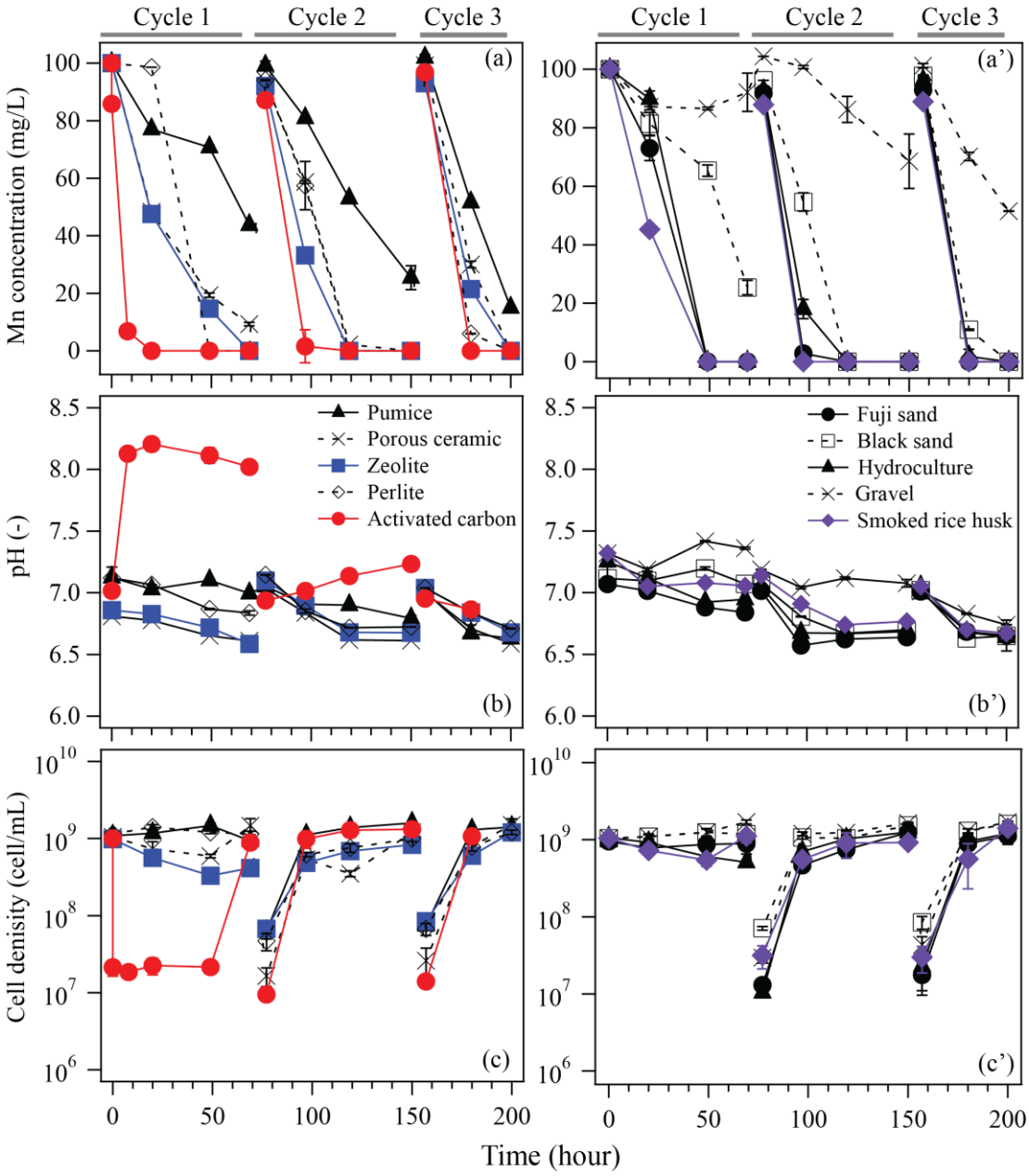

Figure 6.4 Cycle Mn(II)-oxidative removal in the presence of various bacteria-supporting materials and *Pseudomonas* sp. strain SK3 showing Mn concentration (a, a'), pH (b, b'), and planktonic cell density (c, c'). After each cycle, the spent media were replaced with fresh sterilized media without re-inoculation of cells. Symbol indicators: (a, b, c) pumice (▲), porous ceramic (×), zeolite (■), perlite (◇), activated carbon (●). (a'. b', c') fuji sand (●), black sand (□), hydroculture (▲), gravel (×), smoked rice husk (♦).

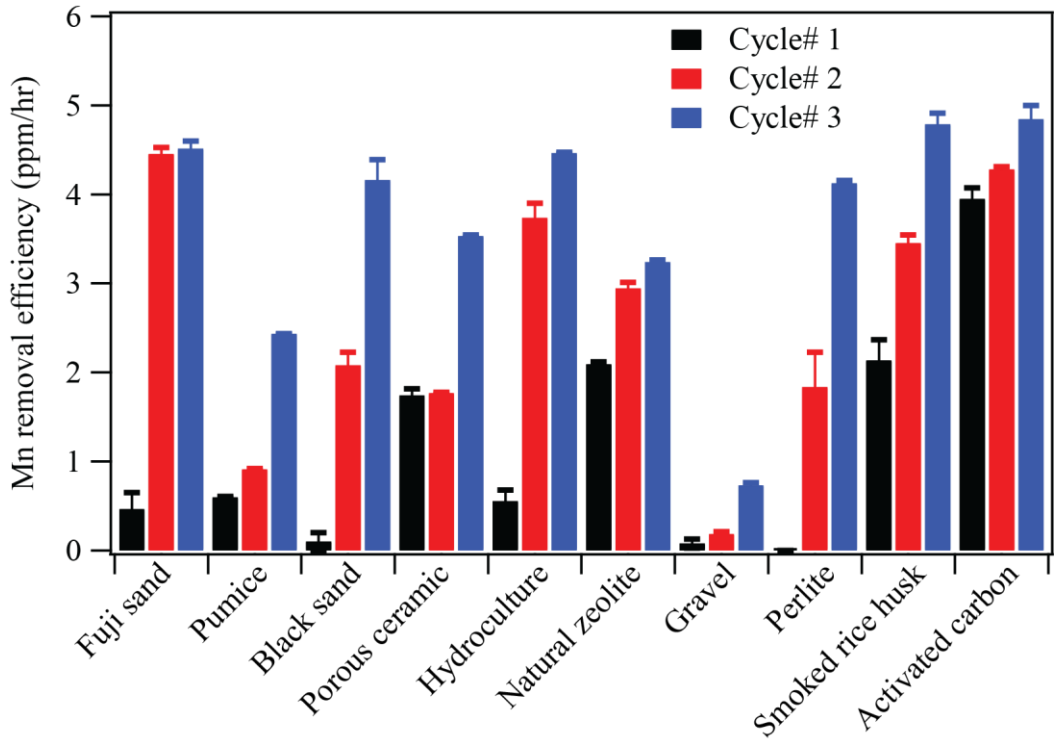

Figure 6.5 Mn removal efficiency in the presence of various bacteria-supporting materials and *Pseudomonas* sp. strain SK3. The values were calculated from Mn removed at a fixed time interval of 20 hours.

6.3.3 Characterization of bacteria-supporting materials after cycle Mn(II)-oxidative removal experiment

After 3 successive cycles Mn(II)-oxidative removal test, spent bacteria-supporting materials were collected and washed for further analysis. With the naked eye, the materials become darker in color due to the attachment of biogenic birnessite.

SEM images comparing before and after showed that biogenic birnessite was accumulated inside the material's pore (Fig. 6.6). In the case of gravel, a significantly lesser amount of Mn-oxide was observed which corresponded to liquid analysis (only 50% oxidized, Fig. 6.4a').

The changes in zeta potential value of bacteria-supporting materials were shown in table 6.2. Zeta potential value of the materials seemed to shift to the positive side and this might due to the attachment of biogenic birnessite (-33 mV).

Table 6.2 Zeta-potential of bacteria-supporting materials before and after cycle Mn(II)-oxidative removal

Bacteria-supporting materials	Zeta-potential at pH 7.0	
	Before	**After**
SiO_2-based material		
Fuji sand	-46.2 mV	-46 mV
Pumice	-56.2 mV	-46 mV
Black sand	-45.6 mV	-41.4 mV
Porous ceramic	-47.1 mV	-47.1 mV
Hydroculture	-51.1 mV	-41 mV
Natural zeolite	-45.6 mV	-38.9 mV
Gravel	-50 mV	-40.5 mV
Perlite	-71 mV	-47 mV
Carbon-based material		
Smoked rice husk	-56.9 mV	-44.8 mV
Activated carbon	-29.5 mV	-32.4 mV

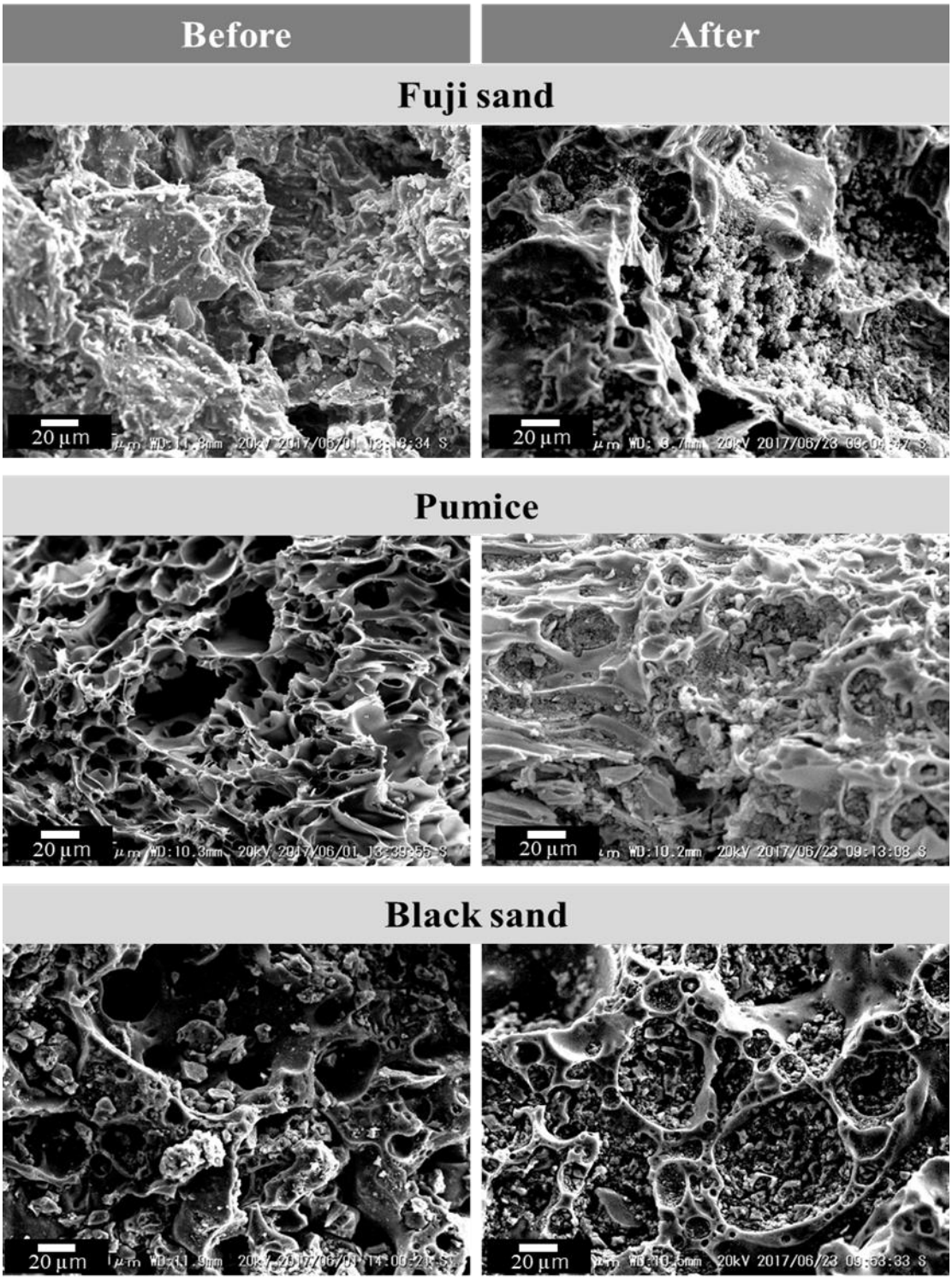

Figure 6.6 Secondary electron images of bacteria-supporting materials before and after cycle Mn(II)-oxidative removal

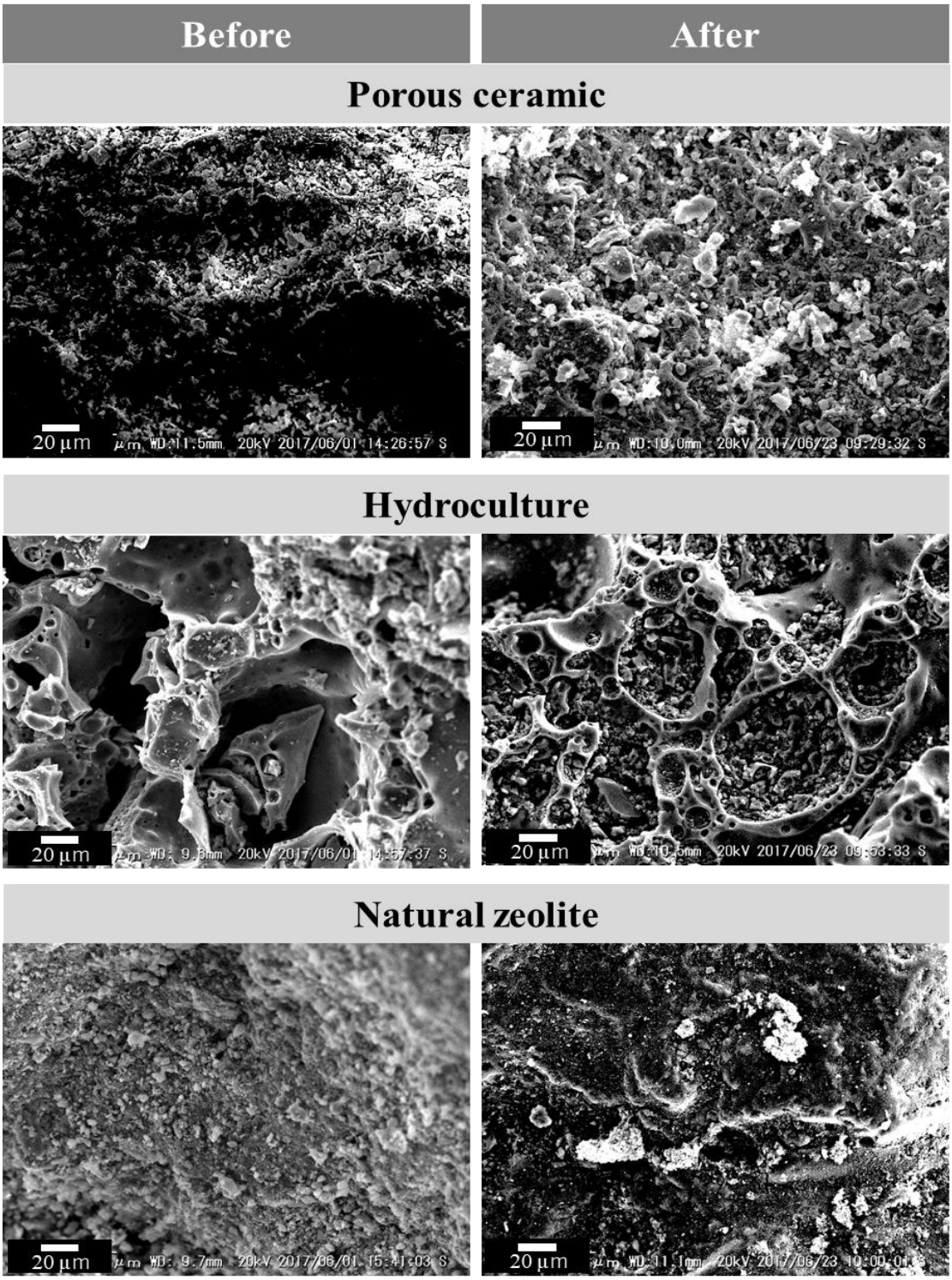

Figure 6.6 *(continued)*

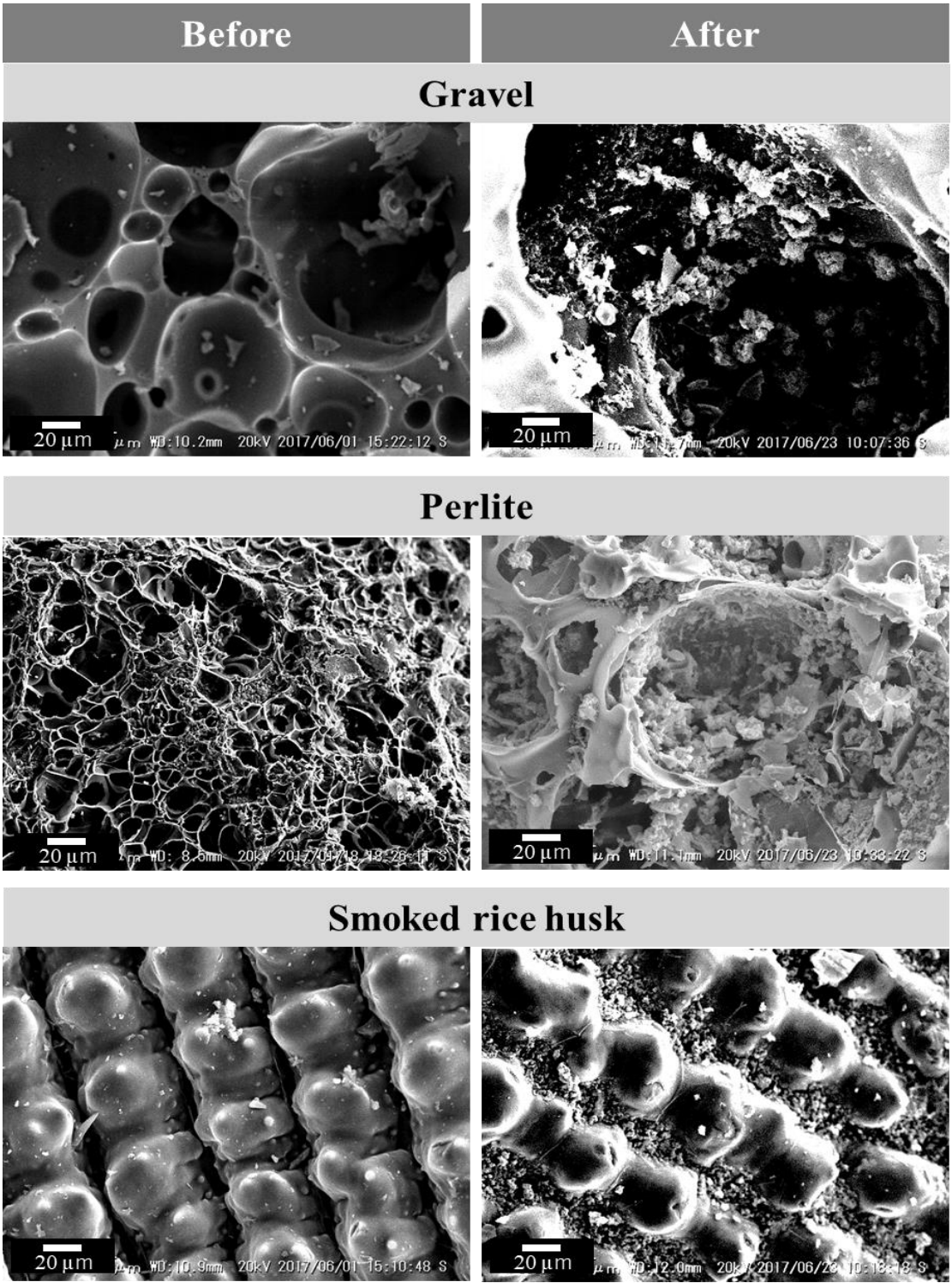

Figure 6.6 *(continued)*

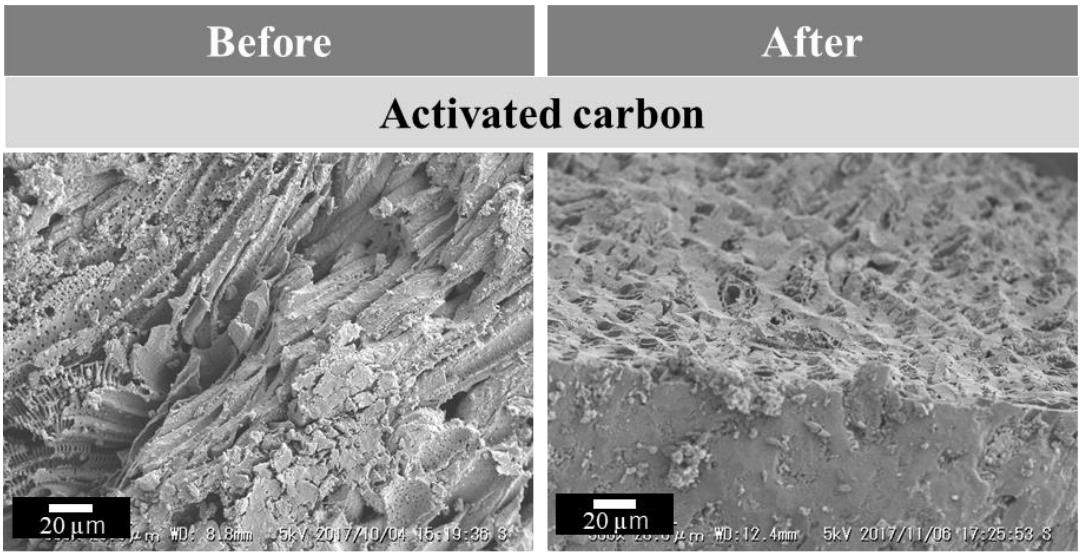

Figure 6.6 *(continued)*

6.3.4 Evaluation of bacteria-supporting materials

After cycle experiment, bacteria-supporting materials were evaluated for their ability to support Mn(II)-oxidizing bacteria (*Pseudomonas* sp. SK3) as well as its biogenic birnessite. The results were summarized in table 6.3.

The attachment of bacteria and biogenic birnessite were evaluated by planktonic cell density counting after medium refreshment and shift of zeta-potential, respectively. Sharp increasing of Mn removal efficiency was observed in fuji sand and smoked rice husk indicating that biogenic birnessite produced by strain SK3 was attached on their surface.

The ideal characteristics of the filler material in the biofilter column are to retain Mn(II)-oxidizing bacteria and its biogenic birnessite. According to the evaluation results, smoked rice husk and activated carbon are candidate materials for further biofilter column test.

Table 6.3 Evaluation of bacteria-supporting materials based on cycle Mn(II)-oxidative removal experiment and physical characterization

Bacteria-supporting materials	Mn(II) removal efficiency (at 0-20 hr) (ppm/hr)			Attachment of bacteria*1	Attachment of biogenic birnessite*2
	Cycle 1	Cycle 2	Cycle 3		
SiO_2-based materials					
Fuji sand	0.47	4.45	4.51	▲	◎
Pumice	0.60	0.91	2.43	○	△
Black sand	0.10	2.1	4.16	◎	○
Porous ceramics	1.74	1.8	3.53	○	△
Hydroculture	0.55	3.7	4.46	▲	○
Natural zeolite	2.09	2.9	3.24	◎	▲
Gravel	0.08	0.2	0.73	○	△
Perlite	0	1.8	4.12	◎	○
Carbon-based materials					
Smoked rice husk	2.0	3.45	4.28	○	◎
Activated carbon	3.95	4.28	4.84	○	○

*1 Evaluated by the planktonic cell density counting after medium refreshment

*2 Evaluated the shift of zeta-potential value to positive side after cycle Mn(II)-oxidative removal experiment and increasing of Mn(II) removal efficiency between cycle

6.3.5 Mn(II) oxidative removal by activated carbon at a different pulp density

Previous experiment (section 6.3.2) showed that in the presence of activated carbon, Mn(II) was readily removed at high speed from the 1st cycle. In order to clarify the involvement of Mn(II)-oxidizing bacteria, control experiments using only AC were carried out.

Single batch experiment at higher AC pulp densities (1.25-10%) indicated that AC alone was capable of chemically removing Mn(II) via adsorption and oxidation. Mn(II) initially 100 mg/L was removed 10%, >60%, >99%, 99% in the presence of 1.25%, 2.5%, 5%, and 10% AC, respectively (Fig 6.7a). Chemical Mn(II)-oxidative removal leading to precipitation of $Mn^{II,III}{}_3O_4$ (1.25% AC) and $Mn^{III}{}_2O_3$ (2.5-5% AC) (Fig 6.7c). Use of higher AC pulp densities increased both pH and Eh, precipitating Mn-oxides of higher oxidation states.

Use of lower AC pulp densities (0.25-1.0%) allowed only <20% Mn(II) removal (1% AC) and this was partly due to an inadequate increase of pH for Mn precipitation. At 0.25-0.5% AC, no Mn removal observed (Fig 6.8a). The presence of Mn(II)-oxidizing bacteria, *Pseudomonas* sp. SK3 cells enabled Mn(II) to be microbially oxidized and completely removed even with lower AC pulp densities.

XRD pattern indicated that the phase of Mn-oxide produced in the presence of Mn(II)-oxidizing bacteria are birnessite. In the case of sterile control, $Mn^{II,III}{}_3O_4$ was formed instead (Fig. 6.8d).

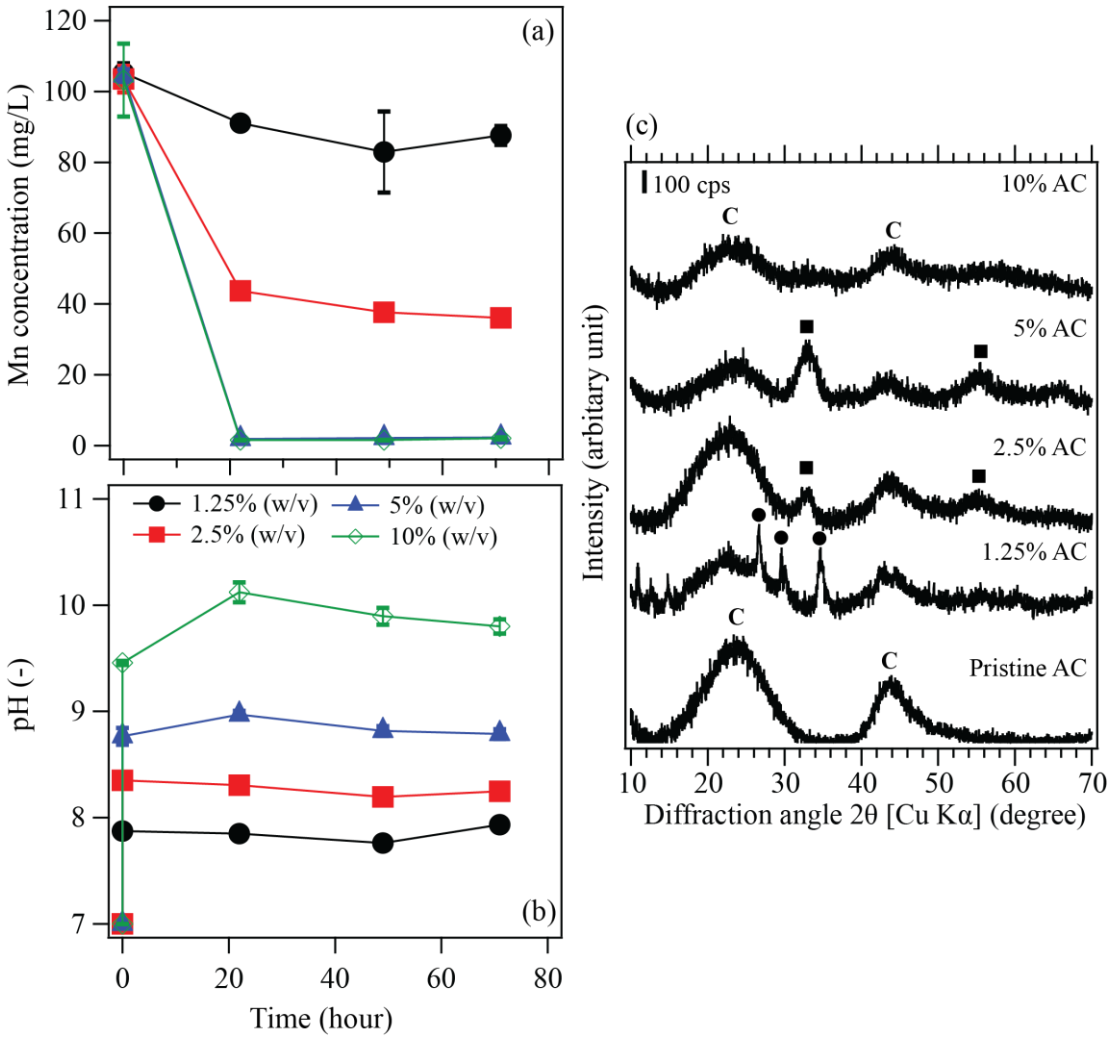

Figure 6.7 Changes in Mn concentration (a) and pH (b) in the presence of activated carbon at 1.25, 2.5, 5, and 10% (w/v). X-ray diffraction pattern of spent activated carbon collected after experiment showing different Mn-oxide formed (c). ●: Mn_3O_4/C JCPDS 00-24-0734, ■: Mn_2O_3 JCPDS 41-1442, C: carbon JCPDS 75-1621.

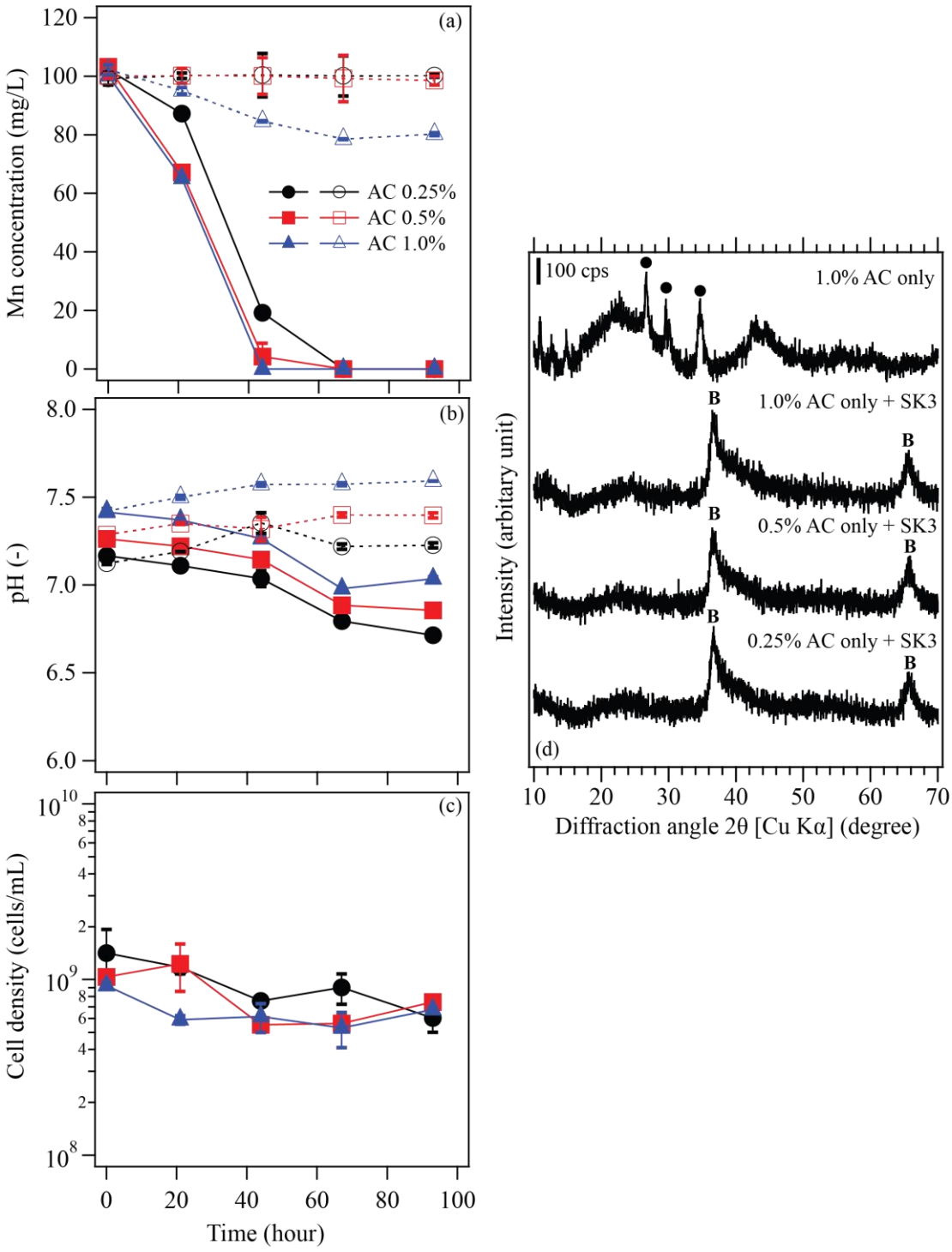

Figure 6.8 Changes in Mn concentration (a) and pH (b) and cell density (c) in the presence of activated carbon at 0.25, 0.5, and 1% (w/v). X-ray diffraction pattern of spent activated carbon collected after experiment showing different Mn-oxide formed (d). ●: Mn_3O_4/C JCPDS 00-24-0734, B: birnessite JCPDS 43-1456.

6.3.6 Cycle Mn(II)-oxidative removal in the presence of bio-AC

From last section (6.3.5), 5% (w/v) seemed to be an optimal AC pulp density to oxidize Mn(II) and mineralize Mn_2O_3.

In the first cycle, 100 mg/L Mn(II) was completely removed at high speed regardless of the presence of Mn(II)-oxidizing bacteria (Fig. 6.9). After medium refreshing, Mn removal efficiency in sterile control decreased significantly and diminished in the 3rd cycle; whereas, those in the presence of *Pseudomonas* sp. SK3 still maintained. The decrease of Mn removal efficiency might due to the formation of a passivation layer of $Mn^{III}_2O_3$ which incapable of facilitating chemical Mn(II) oxidation via synproportionation.

XRD analysis of the spent activated carbon after each cycle indicated the different Mn oxide phase formed between bio-AC and AC. In the presence of Mn(II)-oxidizing bacteria, mixed phases $Mn^{III,IV}_2O_3$ and birnessite type of Mn-oxide was formed after the 1st cycle. This showed that both chemical and biological reaction contributed to Mn(II)-oxidative removal. After 2nd and 3rd cycles, only birnessite type Mn-oxide was formed indicating that the main reaction occurred was enzymatic Mn(II)-oxidative removal. On the other hand, lesser precipitates formed after each medium refreshment and $Mn^{III,IV}_2O_3$ peak gradually disappeared in sterile control (fig. 6.8d'') in agreement with liquid analysis data (Fig 6.9a).

SEM images of cross-sectioned bio-AC revealed that *Pseudomonas* sp. SK3 cells were colonized inside AC with its biogenic birnessite (Fig. 6.10).

Previously, carbon fiber was utilized to enhance Mn(II) oxidation speed by a fungus, *Phoma* sp., isolated from watercourse in Hokkaido prefecture of Japan. Without fungi, carbon fiber was unable to oxidize Mn(II) but the fiber facilitates enzymatically Mn(II)-oxidation through the stimulation of Mn peroxidase enzyme release or

participating in the kinetic process (Sasaki et al., 2004). In this experiment, AC alone could oxidize and precipitated Mn(II) as Mn_3O_4 or Mn_2O_3 depend on solution pH and Eh which refer to the amount of AC added (Fig. 6.7).

Proposed mechanism of Mn(II)-oxidative removal by activated carbon in the presence/absence of Mn(II)-oxidizing bacteria, *Pseudomonas* sp. SK3 was shown in Fig 6.11. Three reactions including (I) chemical reaction, (II) enzymatic reaction, and (III) synproportionation were occurred and synergistically promote Mn(II) oxidative removal. Chemical Mn(II)-oxidation resulted in the deposition of Mn_2O_3 on AC and might passivate on its surface; thus, Mn(II) removal speed was deteriorated.

Oppositely, in the presence of Mn(II)-oxidizing bacteria colonized in AC, biogenic birnessite was continuously produced. Mn^{IV} in birnessite could react with Mn(II) via synproportionation. As a result, the reaction speed was kept maintained at a high level throughout 3 cycles.

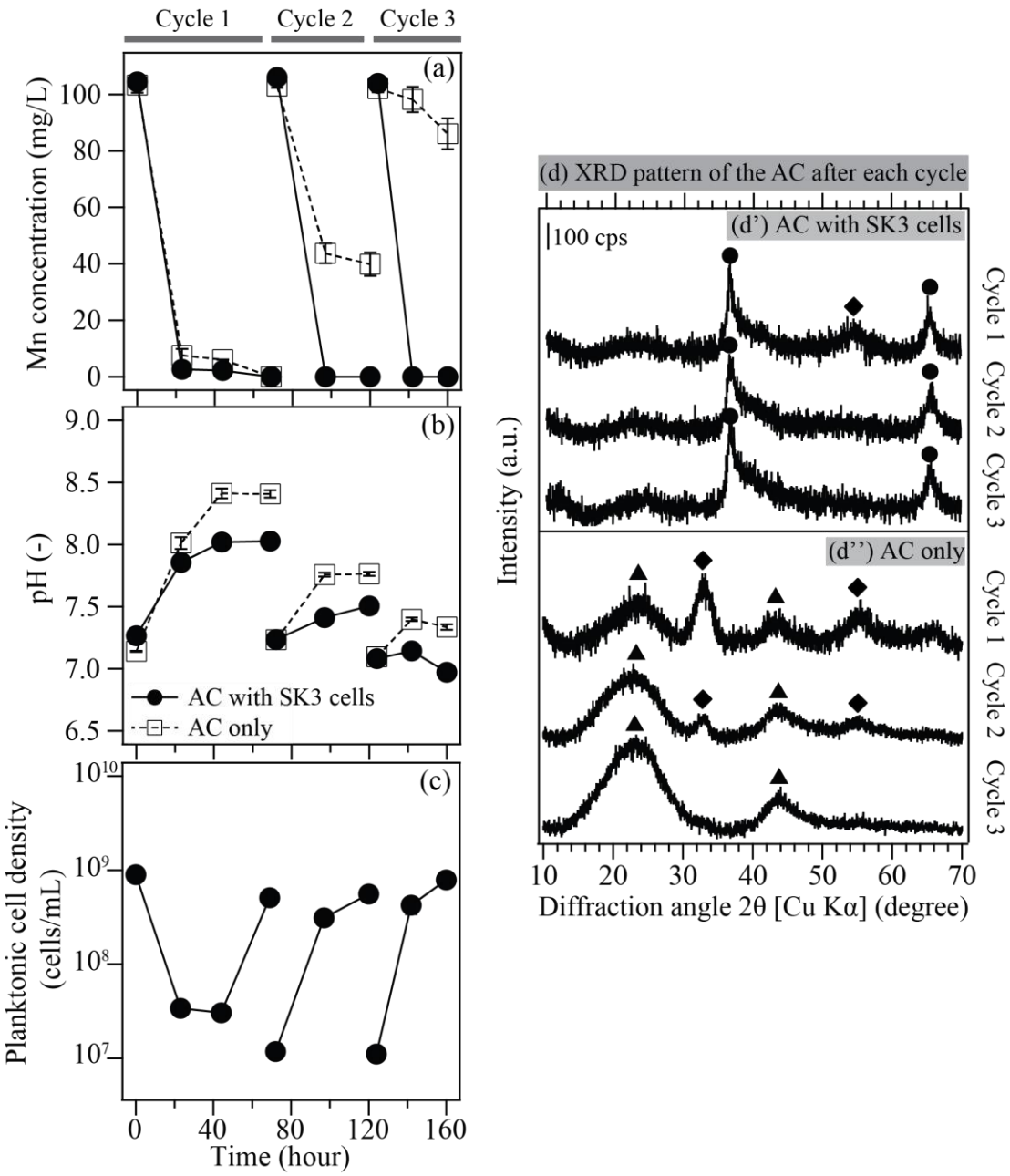

Figure 6.9 Changes in Mn concentration (a) and pH (b) and planktonic cell density (c) in the presence of activated carbon at 5% (w/v) during cycle Mn(II) oxidative removal. Sterile control was showed in open symbol. X-ray diffraction pattern of spent activated carbon collected after each cycle showing different Mn-oxide formed (d). ●: birnessite JCPDS 43-1456, ♦: Mn_2O_3 JCPDS 41-1442, ▲: carbon JCPDS 75-1621.

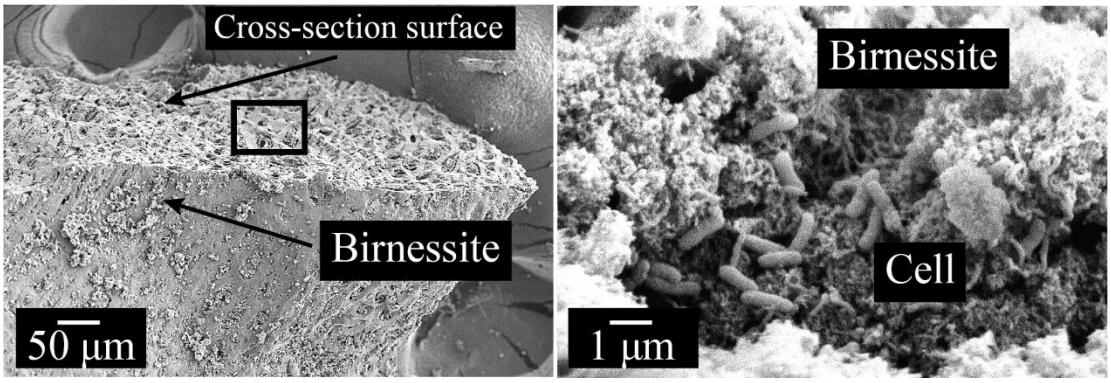

Figure 6.10 SEM images of activated carbon collected after 3rd cycle showing Mn(II)-oxidizing bacteria, *Pseudomonas* sp. SK3 colonized inside activated carbon with biogenic birnessite.

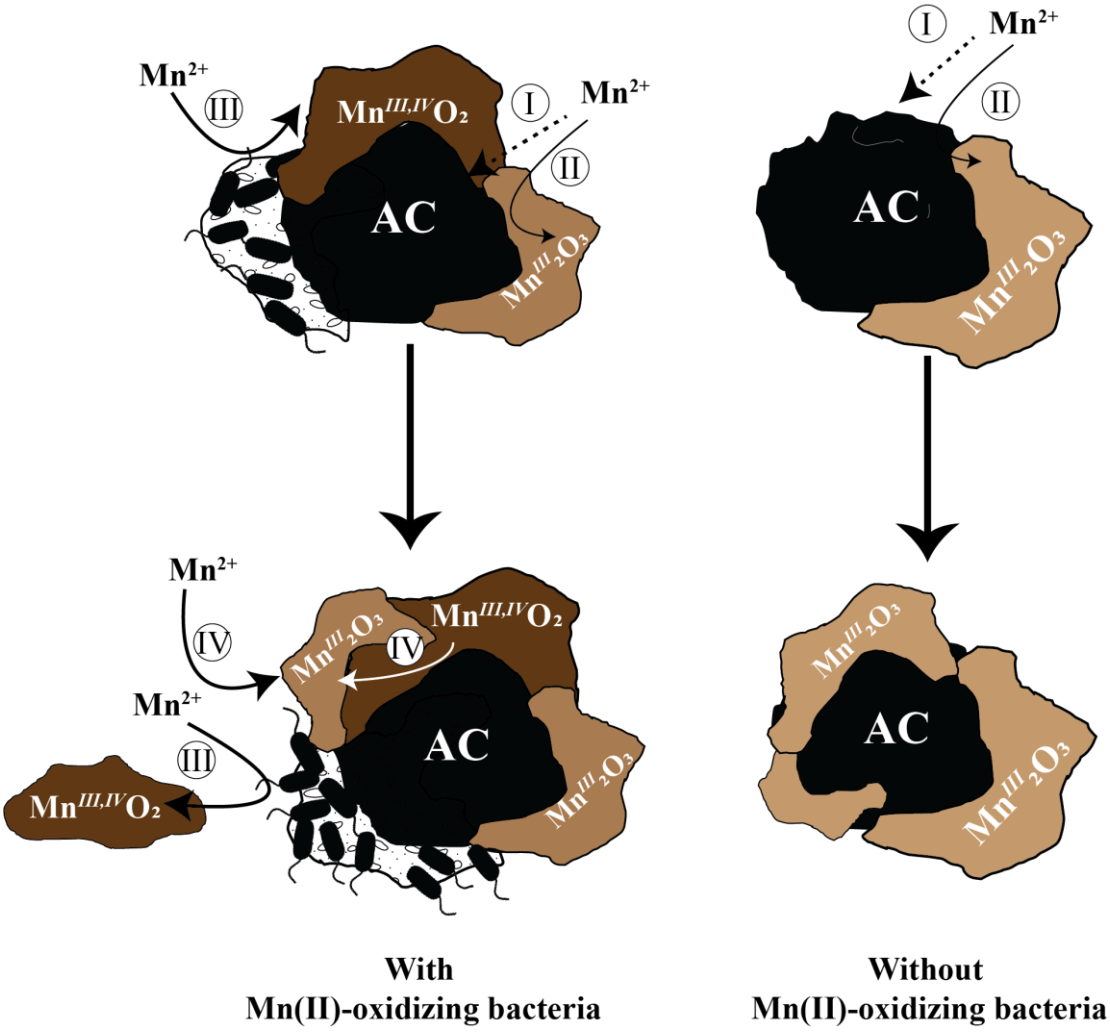

Figure 6.11 Proposed mechanism for cycle Mn(II)-oxidative removal in the presence of absence of Mn(II)-oxidizing bacteria

6.4 Conclusions

- Physical characteristics of ten different bacteria-supporting materials were compared; eight of them are SiO_2-based material whereas the other two are carbon-based material.

- The criteria for good bacterial-supporting material for biofilter column application included; (1) Does not release toxic substances upon water contact, (2) provide a site for bacteria attachment and (3) good attachment for biogenic birnessite.

- Cycle Mn(II)-oxidative removal together with physical characterization could be used to evaluate the bacteria-supporting materials. Sharp increase in Mn(II) removal speed after medium refreshment indicated that biogenic birnessite was attached on the surface of the supporting material. According to the evaluation results, activated carbon is the most appropriate material for Mn-removal biofilter column application. The combination of Mn(II)-oxidizing bacteria and AC promote synergistic Mn(II)-oxidative removal via (i) enzymatic Mn(II)-oxidation, (ii) synproportionation reaction between attached biogenic birnessite and Mn(II), (iii) adsorption and chemical Mn(II)-oxidation by AC. The maintaining of high Mn(II)-oxidative removal efficiency throughout 3 cycles marks the importance of the presence of active Mn(II)-oxidizing bacteria.

- The biofilter column filled with bio-AC for Mn(II)-oxidative removal from metal-refinery wastewater will be tested and discussed in the next chapter.

References

Cruz, I., Bashan, Y., Hernàndez-Carmona, G., and de-Bashan, L.E. (2013). Biological deterioration of alginate beads containing immobilized microalgae and bacteria during tertiary wastewater treatment. *Applied Microbiology and Biotechnology* 97(22), 9847-9858. doi: 10.1007/s00253-013-4703-6.

Kitjanukit, S., Takamatsu, K., and Okibe, N. (2019). Natural Attenuation of Mn(II) in Metal Refinery Wastewater: Microbial Community Structure Analysis and Isolation of a New Mn(II)-Oxidizing Bacterium Pseudomonas sp. SK3. *Water* 11(3), 507.

Pluemsab, W., Fukazawa, Y., Furuike, T., Nodasaka, Y., and Sakairi, N. (2007). Cyclodextrin-linked alginate beads as supporting materials for Sphingomonas cloacae, a nonylphenol degrading bacteria. *Bioresource Technology* 98(11), 2076-2081. doi: https://doi.org/10.1016/j.biortech.2006.08.009.

Pujol, R., Hamon, M., Kandel, X., and Lemmel, H. (1994). *Biofilters: Flexible, reliable biological reactors*.

Sasaki, K., Konno, H., Endo, M., and Takano, K. (2004). Removal of Mn(II) ions from aqueous neutral media by manganese-oxidizing fungus in the presence of carbon fiber. *Biotechnology and Bioengineering* 85(5), 489-496. doi: 10.1002/bit.10921.

Wang, J.Z., Summers, R.S., and Miltner, R.J. (1995). Biofiltration performance: part 1, relationship to biomass. *Journal - American Water Works Association* 87(12), 55-63. doi: 10.1002/j.1551-8833.1995.tb06465.x.

Zhao, H., Zhu, M., Li, W., Elzinga, E.J., Villalobos, M., Liu, F., et al. (2016). Redox Reactions between Mn(II) and Hexagonal Birnessite Change Its Layer Symmetry. *Environ Sci Technol* 50(4), 1750-1758. doi: 10.1021/acs.est.5b04436.

Chapter 7

Mn(II) oxidative removal from metal-refinery wastewater using biofilter column packed with bio-activated carbon

Abstract

In this chapter, the biofilter column packed with bio-AC was tested for continuous Mn(II) removal from metal-refinery wastewater. Pre-colonization of Mn(II)-oxidizing bacteria on AC before packed in the column could reduce the lengthy ripening to 4-5 days. Column supplemented with yeast extract showed greater Mn removal efficiency (65-90%) compared with control (20-40%). The fluctuation of yeast extract concentration (0.005-0.01%) did not significantly affect the removal efficiency. Low level of nutrient would rather gradually alter the growth of bacteria and eventually negatively affect Mn removal efficiency. The short-pass problem could be prevented by mixing pulverized AC with bio-AC, allowing 5-10% improve in the removal efficiency.

After backwashing, the efficiency dropped dramatically to 50-60% and this probably due to washed-out of bacteria and biogenic birnessite from the column. The efficiency was recovered back to 80% after approximately 1 week. Apparently, flow speed does matter when higher Mn(II) concentration was spiked in the feed water. Only about 60% of Mn(II) was removed when HRT (hydraulic retention time) was set to 20 min. However, it was gradually improved to 85% after increasing HRT to 40 min.

7.1 Introduction

Mn(II) removal using biofilter column requires filler which could hold and support Mn(II)-oxidizing bacteria as well as its biogenic birnessite. According to the evaluation results in **chapter 6**, activated carbon (AC) was selected as filter media for the biofilter column test.

As mention in **chapter 1**, there are several factors affecting Mn(II) removal efficiency of the column. For examples: nutrient enhancement, filter media, and retention time. This experiment aimed to develop a biofilter column for removing Mn(II) from actual metal-refinery wastewater.

As the target wastewater is directly from the neutralization process, colonization of indigenous Mn(II)-oxidizer is more difficult than in groundwater. The filter media was first pre-colonized with Mn(II)-oxidizing bacteria and packed into a column. By so doing, the lengthy ripening time should be ideally shortened.

7.2 Materials and methods

7.2.1 Mn(II)-oxidizing bacteria

Pseudomonas sp. strain SK3 (Kitjanukit et al., 2019) was maintained and routinely sub-cultured in LB medium (pH 7.0). The strain was pre-grown overnight, washed, and harvested by centrifugation prior to use in the following experiment

7.2.2 Collection and analysis of tailing dam wastewater

Mn(II)-containing tailing dam and post-neutralized wastewater samples were collected from the metal-refinery wastewater treatment facility. The concentration of metals, $NH_4^{+,}$ and TOC (total organic carbon) were determined by ICP-OES (iCAP 6500, Thermo Scientific), ion chromatography (Dionex ICS1000, Thermo Scientific), and TOC analyzer (TOC-5000A, Shimadzu).

7.2.3 Preparation of bio-AC and bio-zeolite

Activated carbon (Kuraray coal) or natural zeolite (5% (w/v)) were added into modified PYG medium (pH 7.0) and autoclaved (120℃, 20 min). Mn(II) (100 mg/L), Cu(II) (3 μM) and glucose (1 mM) were aseptically added prior to inoculation of *Pseudomonas* sp. strain SK3 to the final cell density of 10^9 cells/mL. After 3 days, the spent medium was replaced with fresh sterilized PYG medium containing 100 mg/L Mn(II), 3 μM Cu(II) without re-inoculation of bacteria cells. The cycles were repeated for 3 times.

7.2.4 Preparation of pulverized activated carbon (plvAC)

Activated carbon (Kuraray coal) was crushed and ground using ball mill (Fritsch, Pulverizer P-6) for 15 min, 300 rpm.

7.2.5 Preliminary experiment: Batch Mn removal experiment from actual wastewater by activated carbon, bio-activated carbon, zeolite, or bio-zeolite

7.2.5.1 Batch cycle experiment; PYG-1 medium and tailing dam wastewater $[Mn(II)]_{ini}$ *= 100 mg/L*

Activated carbon or natural zeolite (5% (w/v)) and pre-grown cells of *Pseudomonas* sp. SK3 cells (10^9 cell/mL) were added into 300 mL Erlenmeyer flasks containing 100 mL PYG-1 medium (pH 7.0). Initial Mn(II) concentration was set to 100 mg/L (added as $MnSO_4$). After certain incubation time (48 hours), spent medium was replaced with fresh pre-sterilized PYG-1 medium supplemented with 100 mg/L without re-inoculation of Mn(II)-oxidizing bacteria. After three consecutive cycle, PYG-1 medium was replaced with tailing dam wastewater. In addition to ~2 mg/L Mn(II) originally presented in tailing dam wastewater, initial Mn(II) was adjusted to 100 mg/L (added as $MnSO_4$) and supplemented with 0.01% yeast extract. Again, spent tailing dam wastewater was replaced with fresh one without re-inoculation of Mn(II)-oxidizing bacteria.

7.2.5.2 Batch experiment; tailing dam wastewater $[Mn(II)]_{ini}$ *= 5 mg/L*

Activated carbon or natural zeolite (25, 50, 100% (v/v)) was added into 300 mL Erlenmeyer flasks containing 100 mL of tailing dam wastewater (table 7.2).

7.2.5.2 Batch cycle experiment; tailing dam wastewater $[Mn(II)]_{ini}$ *= 5 mg/L*

Activated carbon (AC), natural zeolite, bio-AC, or bio-zeolite (25, 50, 100% (v/v)) was added into 300 mL Erlenmeyer flasks containing 100 mL of tailing dam wastewater (table 7.2). Yeast extract concentration was set to 0, 0.0025, or 0.01% (w/v). Contact time was set to 5 or 10 min per cycle.

7.2.6 Column experiment

7.2.6.1 Apparatus

Glass chromatography tube with 0.03 m diameter and 0.3 m long was packed with teflon wool as a support (0.05 m) and bio-AC as a filter media (0.1 m) (Fig. 7.1 right)

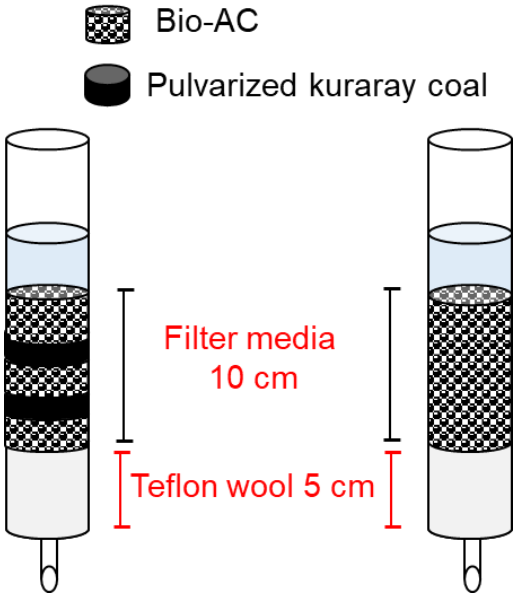

Figure 7.1 Packing of bio-AC into glass chromatography tube

7.2.6.2 Design of column experiment

Table 7.1 Column technical information

Type of filtration	Down flow
Type of filter media	Bio-activated carbon or bio-AC/plvAC
Filter height	0.1 m
Filter area	0.0007 m^2
Filter volume	0.00007 m^3
Flow per filter	0.0002 or 0.0001 m^3/hr
Hydraulic retention time	21 min or 42 min

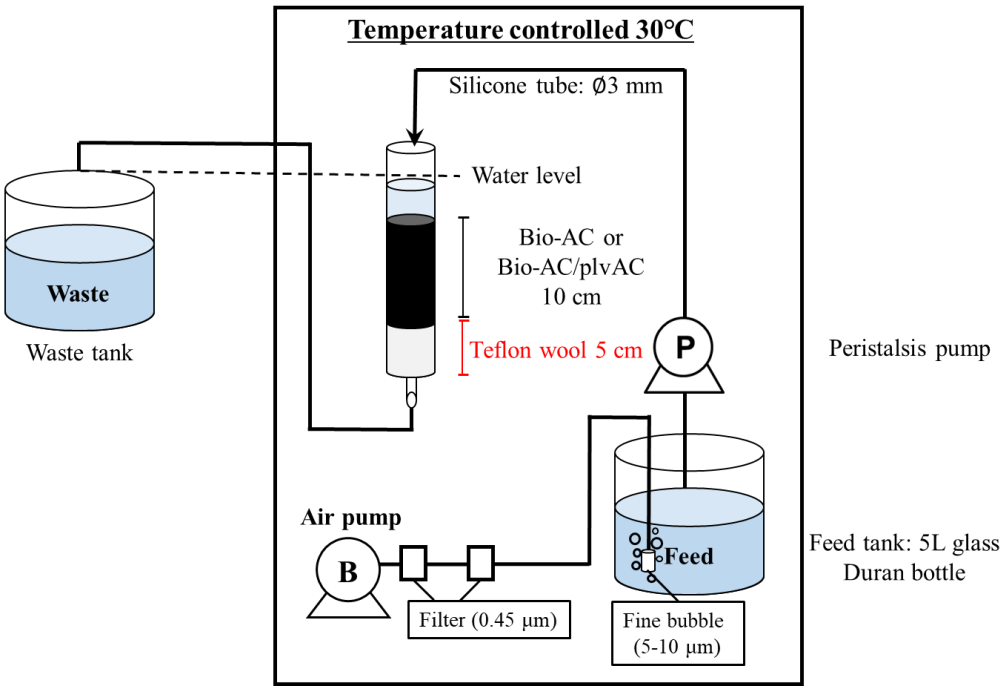

Figure 7.2 Schematic diagram of the bio activated carbon column reactor

7.2.5.3 Effect of additional organic carbon on the removal of Mn(II) from tailing dam wastewater by means of biofilter column packed with bio-AC

Bio-AC column reactor was set up as mentioned in section 7.4.2.2. Tailing dam wastewater was filtered (0.45 µm) and fed into a column reactor with a flow speed of 0.0002 m^3/hr. Yeast extract was added as organic carbon at 0 or 0.01%. Samples from feed and column effluent were routinely withdrawn to monitor pH and Mn concentration (ICP-OES).

7.2.6.4 Reduction of short-pass by addition of plvAC

In addition to bio-AC, pulverized AC (8.5 µm) (Fig. 7.3) was mixed at a ratio of 7:3 and packed into column reactor (total filter height 0.1 m) (Fig. 7.1 left). Yeast extract was added at 0.01% and fluctuated between 0.01%-0.05% throughout the column operation. Samples from feed and column effluent were routinely withdrawn to

monitor pH and soluble Mn concentration (formaldoxime method; (Majestic et al., 2007)). Total dissolved Mn concentration was confirmed again using ICP-OES.

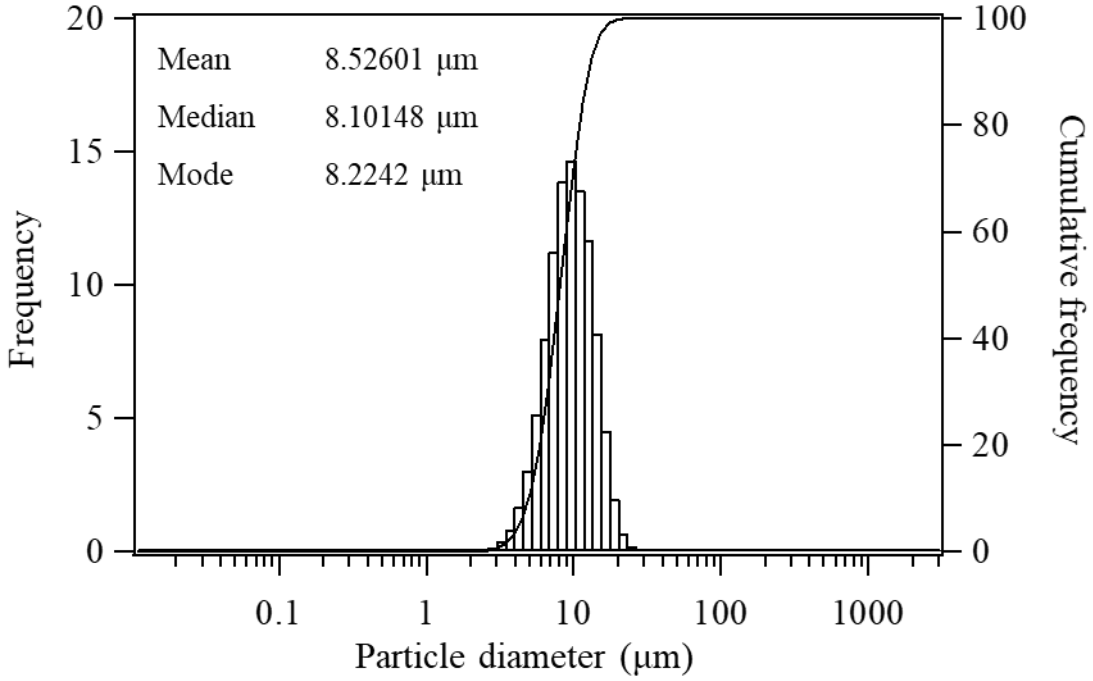

Figure 7.3 Particle size distribution of pulverized activated carbon prepared by ball mill

7.3 Results and discussion

7.3.1 Characteristics of tailing dam wastewater sample

The characteristics of tailing dam wastewater collected from a metal-refinery wastewater treatment facility are shown in table 7.2. Compared with other heavy metals, Mn(II) concentration is the highest (1.n ~ 2.3 mg/L); whereas the most abundant ions in this wastewater is sulfate (SO_4^{2-}; 780 mg/L) as one of the main components of metal-refinery wastewater. Noticeable TOC value might be derived from those plants or microbes living in an open pool of tailing dam.

Table 7.2 Composition of tailing dam wastewater from the metal-refinery wastewater treatment facility

Composition	
Mn	1.n ~ 2.3 mg/L
Cu	0.008 mg/L
Ni	0.035 mg/L
Ca	510 mg/L
Si	5.1 mg/L
Mg	150 mg/L
S (as SO_4^{2-})	780 mg/L
N (as NH_4^+)	3.6 mg/L
Org. N	1.3 mg/L
Total P	< 0.01 mg/L
TOC	16 mg/L
pH	6.9-7.3

7.3.2 Mn(II)-removal from tailing dam wastewater using zeolite, bio-zeolite, AC, or bio-AC; [Mn(II)] = 100 mg/L

This experiment divided into 2 parts; colonization period (PYG-1 medium) and Mn(II)-oxidative removal from tailing dam wastewater.

During the colonization period (PYG-1 medium), Mn(II) was completely removed (bio-AC) and nearly completed (bio-zeolite). Most of the biogenic birnessite was found separated from zeolite indicating its poor Mn-oxide supporting property compared with AC. After replacing with tailing dam wastewater, Mn(II) removal efficiency dropped in both bio-AC and bio-zeolite. Approximately, 70.8%, 69.4, and 84% were obtained as final Mn(II) removal from tailing dam wastewater by bio-AC after 50 hours (1^{st} cycle), 48 hours(2^{nd} cycle), and 100 hours (3^{rd} cycle), respectively. Due to its poor biogenic birnessite support property, only 37%, 34.2, and 55.8% were obtained as final Mn(II) removal after 50 hours (1^{st} cycle), 48 hours(2^{nd} cycle), and 100 hours (3^{rd} cycle), respectively (Fig. 7.4a). Dramatically dropped in pH resulted from rapid Mn(II)-oxidation via both enzymatic activity and synproportionation consequently inhibited both reaction and this might due to the absence of buffering agent (PIPES) (Fig. 7.4b)

Zeolite could remove about 10% of Mn(II) via adsorption, whereas AC effectively removed Mn(II) completely owing to chemical oxidation. After 1^{st}, 2^{nd}, and 3^{rd} cycles, Mn(II) was removed 100%, 51%, 23.6% respectively in the case of AC (Fig. 7.5). The results were similar to those observed in **chapter 6** (section 6.3.6), where the AC surface was passivated by Mn_2O_3.

X-ray diffraction pattern showed the different in the form of immobilized Mn products between inoculated and sterile control (Fig. 7.6 and 7.7). In the presence of Mn(II)-oxidizing bacteria, Mn(II) was oxidized and precipitated enzymatically as

biogenic birnessite; whereas, AC oxidized and precipitated Mn(II) as Mn_2O_3. After the 3rd cycle, no Mn-oxide peak appeared in XRD pattern of spent AC corresponding to liquid analysis (<10% Mn(II) removed) (Fig. 7.4a).

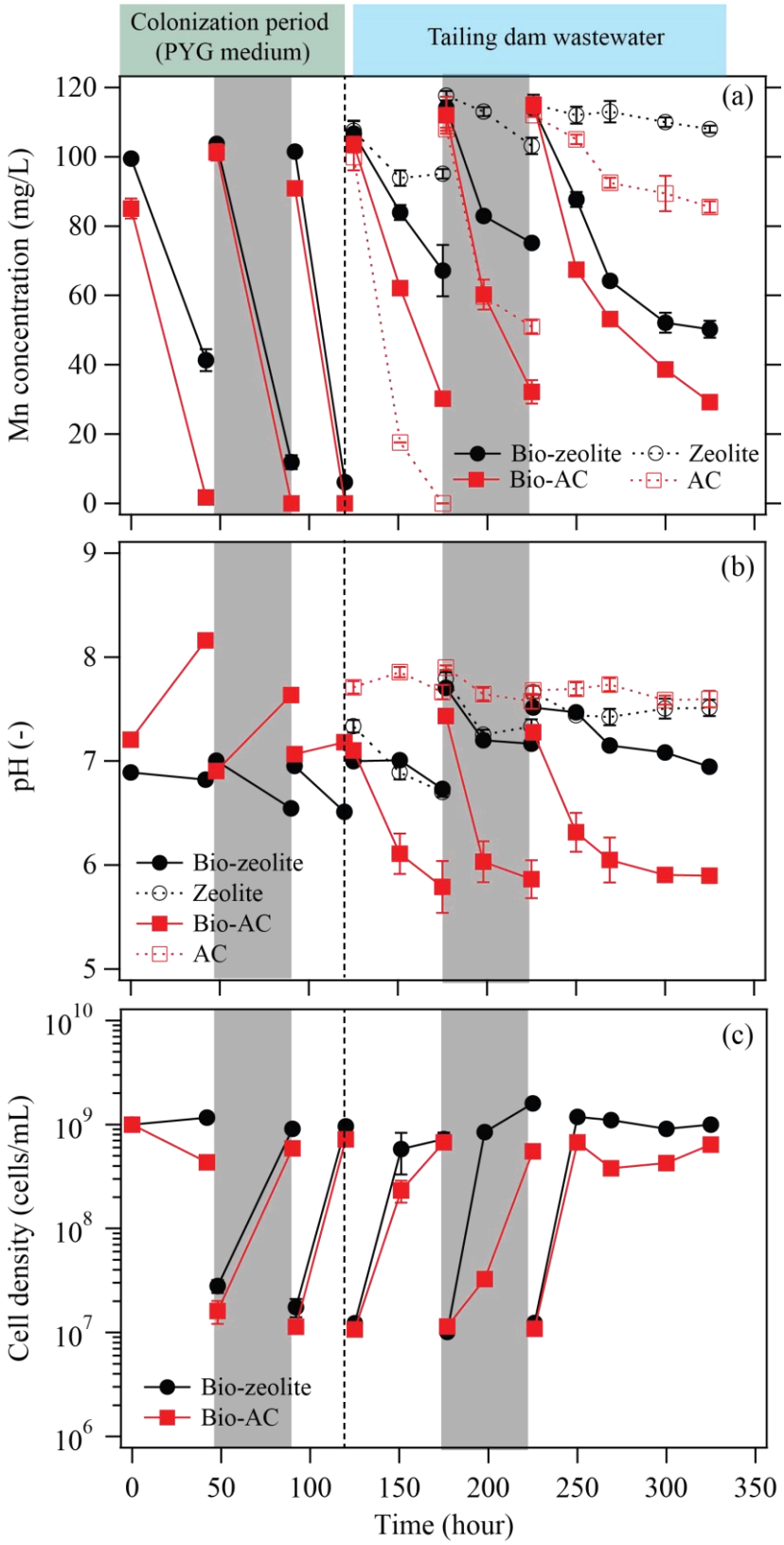

Figure 7.4 Changes in Mn concentration (a), pH (b), and cell density (c) during Mn(II) oxidative removal from tailing dam wastewater in the presence of bio-zeolite (●), zeolite (○) bio-AC (■), and AC (□)

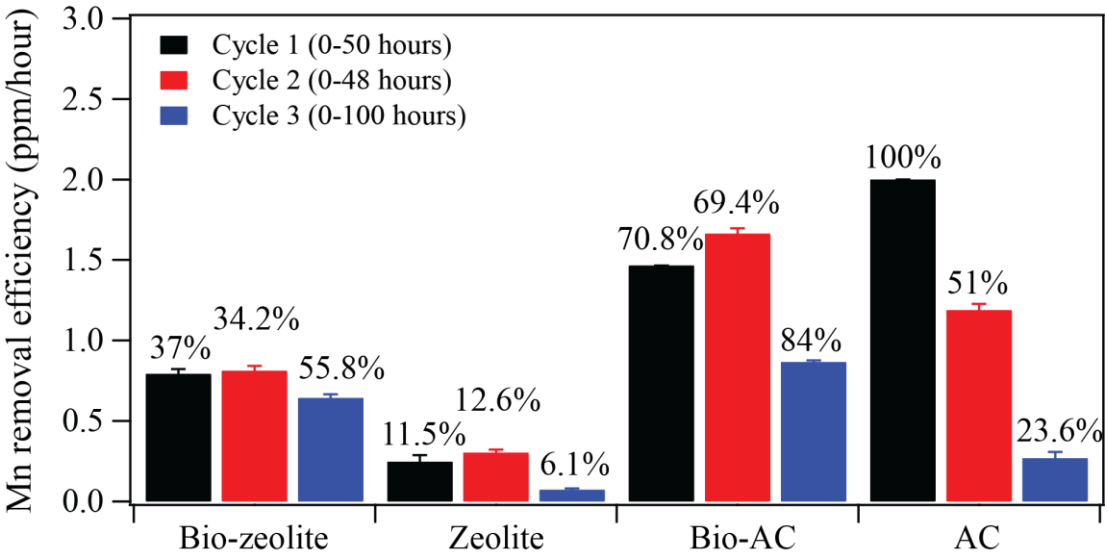

Figure 7.5 Mn removal efficiency from tailing dam wastewater in the presence of zeolite, bio-zeolite, AC, or bio-AC. The value calculated from fixed incubation time of 50, 48, and 100 hours for cycle 1, 2, and 3, respectively.

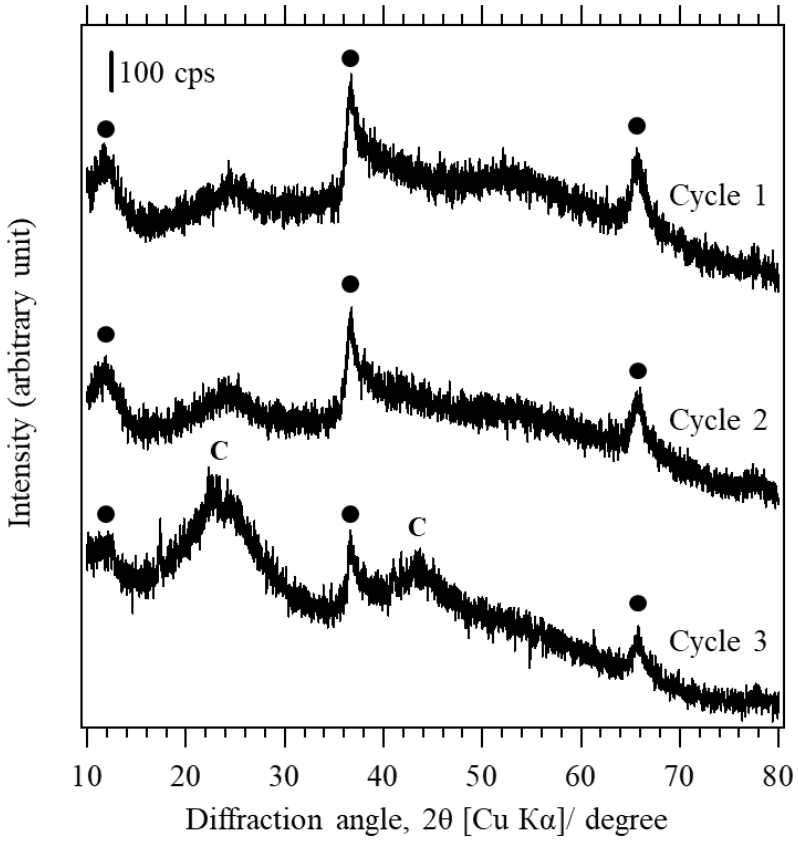

Figure 7.6 X-ray diffraction pattern of the spent bio-AC collected after each cycle of Mn(II)-oxidative removal from tailing dam wastewater. ●: birnessite (JCPDS 43-1456), C: carbon (JCPDS 75-1621)

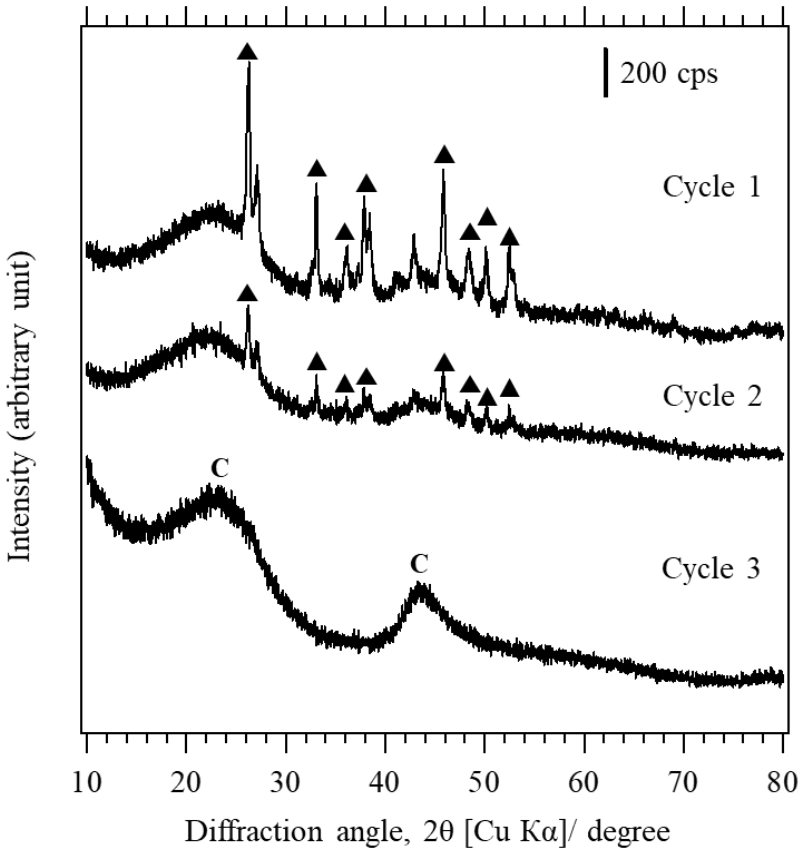

Figure 7.7 X-ray diffraction pattern of the spent AC collected after each cycle of Mn(II)-oxidative removal from tailing dam wastewater. ▲: Mn_2O_3 (JCPDS 41-1442), C: carbon (JCPDS 75-1621).

7.3.3 Mn(II)-removal from tailing dam wastewater using zeolite, bio-zeolite, AC, or bio-AC; $[Mn(II)]_{ini}$ = 5 mg/L

Changes in Mn concentration and pH over time in the presence of zeolite, bio-zeolite, AC, or bio-AC were shown in Fig. 7.8. In the presence of zeolite, the adsorption reached equilibrium after 2 hours. The pH of the solution decreased over time due to the release of acidic substances presented originally in the natural zeolite. Activated carbon behaved differently due to their catalytic activity. More than 90% of initial Mn(II) was removed from the solution after 30 min (Fig .7.8a).

In the cases of bio-zeolite or bio-AC, pH of the solution slightly changed and this might due to washed out of alkaline/acidic substances during bio-zeolite/bio-AC preparation. Within short contact time (10-30 min), no significant difference between zeolite and bio-zeolite observed but the latter managed to completely remove Mn(II) after 24 hours. The combination of Mn(II)-oxidizing bacteria and chemical Mn(II)-oxidation (from AC and attached biogenic birnessite) in bio-AC synergistically promoted Mn removal rate. More than 90% of initial Mn(II) was removed after 10 min contacted with bio-AC (Fig. 7.8)

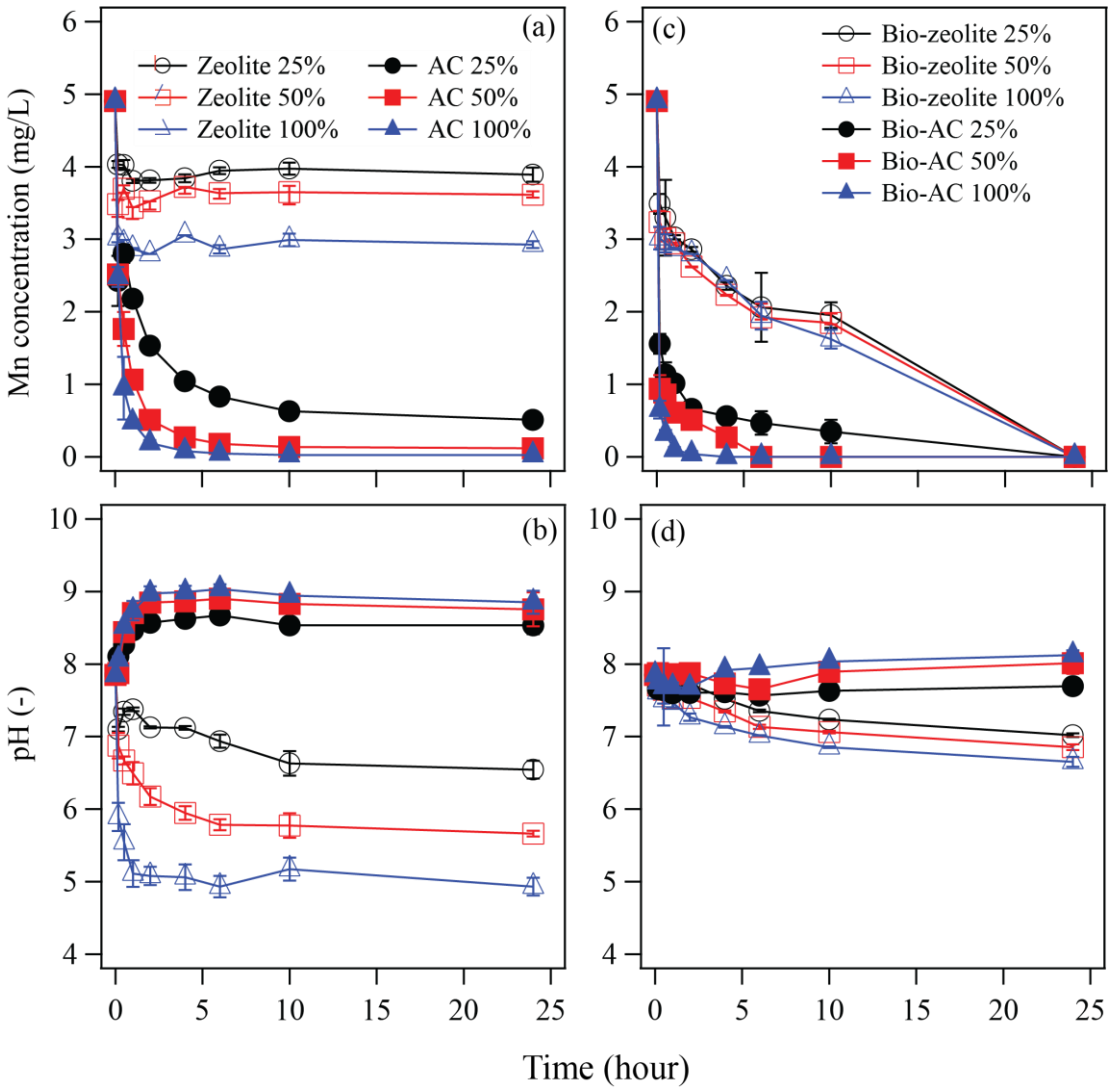

Figure 7.8 Changes in Mn concentration (a, c) and pH (b, d) in the presence of zeolite, activated carbon, bio-zeolite, or bio-activated carbon at different pulp densities of 25%, 50% and 100% (v/v)

7.3.4 Cycle Mn(II)-oxidative removal; tailing dam wastewater ($[Mn]_{ini}$ = 5 mg/L)

In order to confirm the advantage of having Mn(II)-oxidizing bacteria colonized on the AC, cycle experiments (with different contact time and yeast extract concentration) were conducted. The changes in Mn concentration, removal efficiency, and pH during cycle experiment with different contact time and yeast extract concentration were shown in Fig. 7.9. Mn(II) was effectively removed (>90%) from tailing dam wastewater in the first 3 cycles but gradually become poorer after shortening the contact time from 10 min to 5 min. Regardless of the presence of yeast extract, Mn(II) could be removed via synproportionation with attached biogenic birnessite (Fig. 7.9a). However, the importance of having active Mn(II)-oxidizing bacteria was emphasized by the difference in removal efficiency after the 5^{th} cycle.

Decreasing of pH after contacted with bio-AC indicated Mn(II)-oxidation either from synproportionation or enzymatic activity (Fig. 7.9c). When the concentration of Mn(II) in the feed was reduced from 5 to 2 mg/L, the removal efficiency becomes poorer. Bacteria washed-out during feed refreshment might accountable for decreasing of removal efficiency; therefore, retaining of bacteria on the support is crucially important.

Nevertheless, the addition of yeast extract is marked as an important factor to enable the oxidation activity from Mn(II)-oxidizing bacteria, which consequently resulted in the maintaining of high removal efficiency.

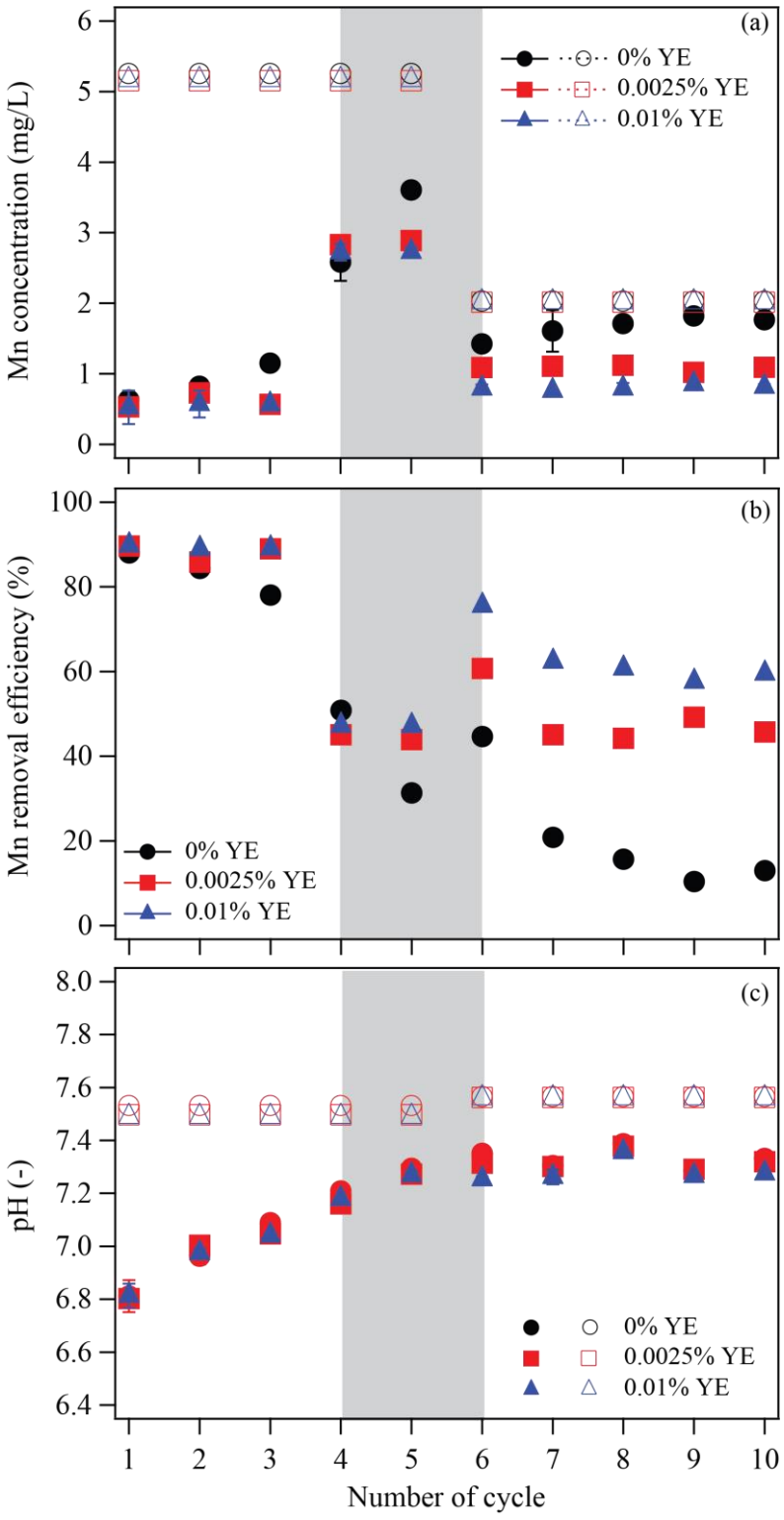

Figure 7.9 Changes in Mn concentration (a), Mn removal efficiency (b), and pH (c) in the presence of bio-AC (100% (v/v)) supplemented with different yeast extract concentration. Close and open symbol indicated value for output and feed, respectively. Contact time was fixed to 10 min (gray shade indicated cycles with 5 min contact time)

7.3.5 Mn(II)-oxidative removal from tailing dam wastewater using biofilter column

7.3.5.1 Effect of additional organic carbon

In the column test, Mn(II)-contaminating tailing dam wastewater as a feed was flowing into a column packed with bio-AC. Mn(II) in the feed supplemented with yeast extract was removed with more efficiency compared with control. This clearly indicated the addition of organic carbon is necessary to enable Mn(II)-oxidation activity as well as supporting the growth. Approximately 50-80% of Mn was removed during the start-up period of the filter and gradually increased to reach more than 90% after 5 days. Pre-colonization of Mn(II)-oxidizing bacteria and its biogenic birnessite onto the filter media could shorten the filter ripening time which generally took 2-3 weeks (Bruins et al., 2015). When yeast extract was lowered from 0.01% to 0.005% at day 9-12, it seemed that the removal efficiency was decreased. After increase the concentration back to 0.01%, the efficiency still not significantly improved (Fig. 7.11). The fluctuation of yeast extract concentration (0.005%-0.01%) did not significantly affect Mn removal directly; however, low level of nutrient would rather gradually alter the growth of Mn(II)-oxidizing bacteria and consequently negatively affect Mn removal efficiency. Figure 7.10 illustrated 3 main Mn(II)-removal reactions by bio-AC. Lacking of nutrient could altered enzymatic Mn(II)-oxidation and subsequently affected the synproportionation since the regeneration of Mn^{IV} was ceased.

Correlation between Mn removal efficiency and initial Mn concentration was plotted (Fig.7.12). Here, it is clearly seen that column without yeast extract could only remove about 20-40% of Mn(II) at an initial Mn concentration of 0.8-1.3 mg/L. At an early stage (before maturation), initially 1.1-1.3 mg/L of Mn(II) was removed around

60-80%; whereas, Aat middle stage, Mn was effectively removed (70-90%; 0.9-1.1 mg/L $Mn(II)_{ini}$) regardless of yeast extract concentration (Fig. 7.12)

Silicone tube from the column supplement with yeast extract was found coated with blackish brown Mn-oxide after 5 days of running. High magnification SEM micrograph revealed that bacteria cells are associated with Mn-oxide (Fig.7.13). This further suggested the importance of nutrient enrichment. Despite high Mn removal efficiency (>90%) was obtained from the bio-AC column, reduction of the short-pass problem might further improve the efficiency. Addition of pulverized AC to the column will be investigated in the next section.

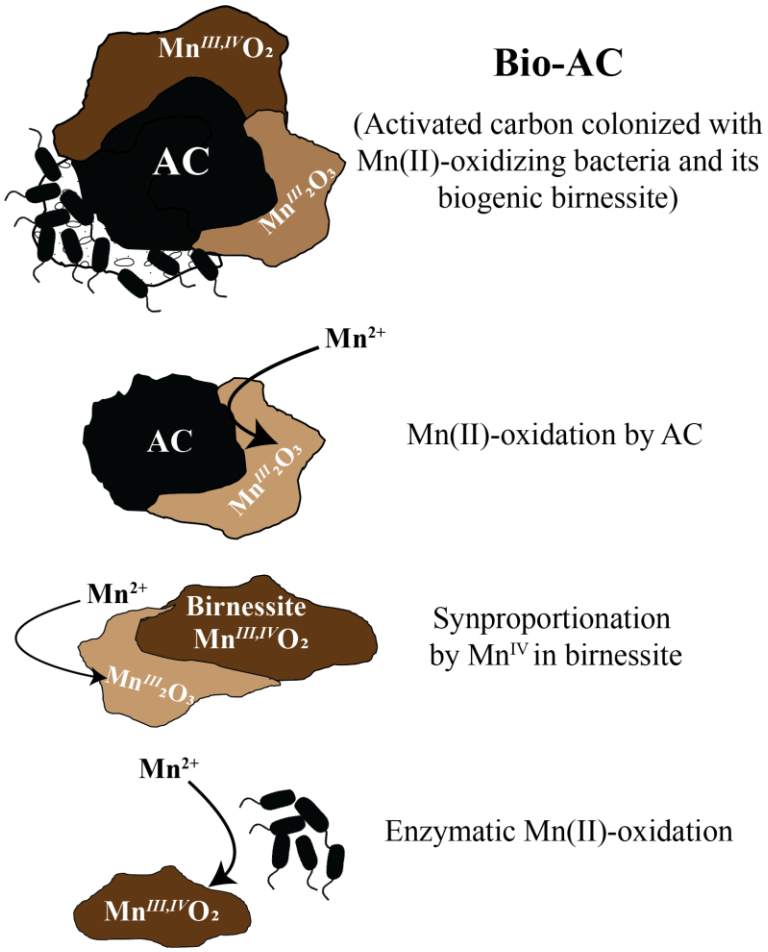

Figure 7.10 Three main Mn(II) removal reaction occurred by bio-AC.

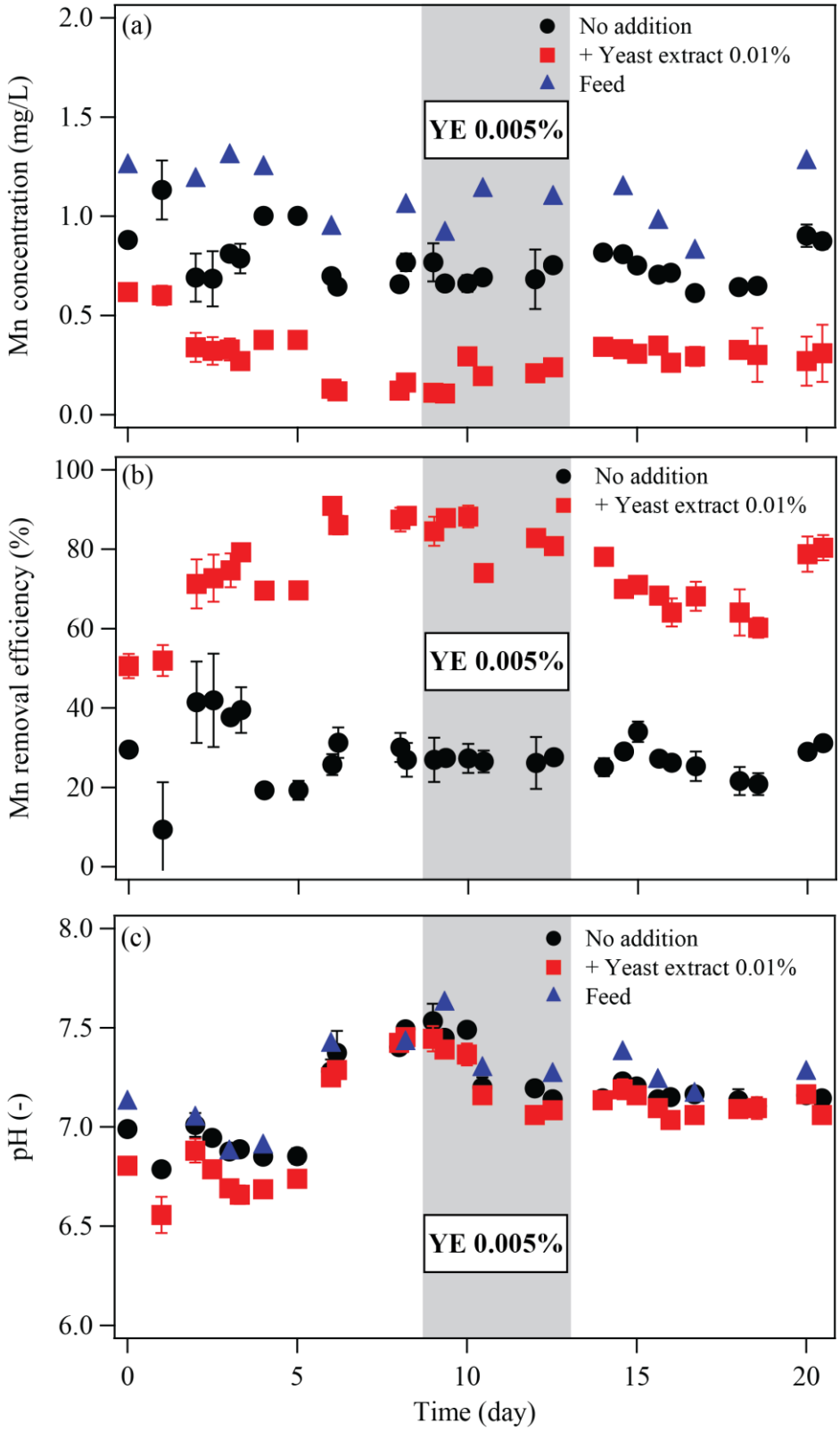

Figure 7.11 Changes in Mn concentration (a), Mn removal efficiency (b), and pH (c) in wastewater feed and column effluents in the presence of yeast extract (■) and without (●).

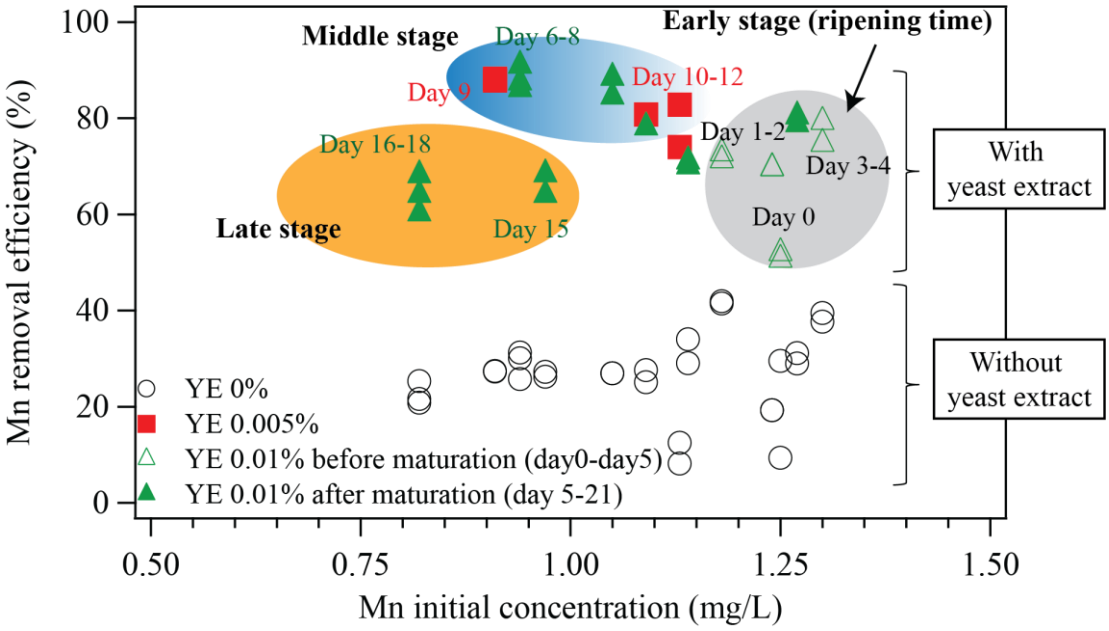

Figure 7.12 Correlation between Mn removal efficiency and Mn initial concentration in the presence of different concentration of yeast extract

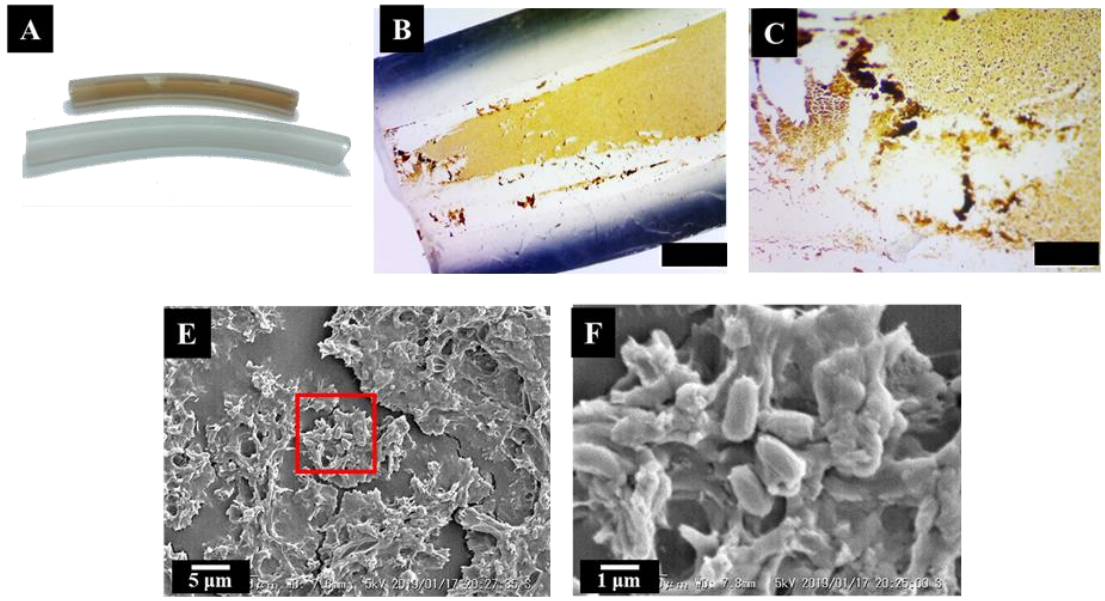

Figure 7.13 Photograph (a; above) and stereoscope micrograph (B and C) showing biogenic Mn-oxide coated on silicone tube surface. SEM micrograph (E and F) revealed that bacteria cells are associated with Mn-oxide

7.3.5.2 Effect of addition of pulverized activated carbon, reduction of short-pass and aeration

Second column test investigated the effect of additional pulverized AC (plvAC) for reduction of short-pass and improve the removal efficiency.

The difference between Mn concentration in the effluent from the column packed with bio-AC only and bioAC/plvAC is only 5-10% during early and middle stage. In this test, the filter material was matured faster. The concentration of yeast extract was increased to 0.05% after day 9 and no significantly different in the removal efficiency. It seemed that column packed with bioAC/plvAC could maintain high removal efficiency than the one packed with bioAC (Fig. 7.14a and b).

After the introduction of the bubbling system to the feed, a noticeable improvement of the removal efficiency of the bioAC/plvAC column was observed.

Sufficient amount of dissolved oxygen is necessary for complete removal of Mn(II) biologically (Abu Hasan et al., 2013a; Abu Hasan et al., 2013b)

$$[O_2] = 0.14[Fe^{2+}] + 0.29[Mn^{2+}] + 4.57[NH_4^+] \quad \text{(eq. 7.1)}$$

In this case, no Fe^{2+} and NH_4^+ were presented in the feed water; therefore, oxygen will be consumed mainly by Mn(II)-oxidation and bacteria respiration.

Next, backwashing was done by washing the bioAC on the sieve and re-packing in the column supported with clean teflon wool. After backwashing, both columns were rested overnight. Mn removal efficiency dropped dramatically in both column and this may due to washed-out of biogenic birnessite as well as Mn(II)-oxidizing bacteria that attached on the filter media. The efficiency was gradually recovered back to approximately 60% in 5 days. At day 37, the feed water was changed from tailing dam wastewater to neutralized refinery wastewater. Higher Mn(II) was spiked into the feed water (5 mg/L) causing a dropped in removal efficiency. This wastewater also

contained high concentration of SO_4^{2-} ion (1400 mg/L), which might alter enzymatic Mn(II) oxidation activity by *Pseudomonas* sp. SK3 (Kitjanukit et al., 2019).

Only 60% of Mn(II) was removed when the hydraulic retention time (HRT) was set to 20 min. When the flow speed was lowered half (HRT = 40 min), the removal efficiency gradually increased to >80% (bioAC/plvAC). This indicated that longer retention time is required to completely remove higher initial Mn(II) concentration.

Re-inoculation of the cell suspension (at day 73) was done by incubating cell suspension of strain SK3 overnight. However, the removal efficiency was stable at around 85-90%. Apparently, this indicated that when treating higher initial Mn(II) concentration, flow speed (retention time) strongly affected the Mn removal efficiency of the column. Nonetheless, maintaining of actively Mn(II)-oxidizing bacteria in the system was crucial in order to enable 3 main Mn(II)-removal reaction (Fig. 7.10)

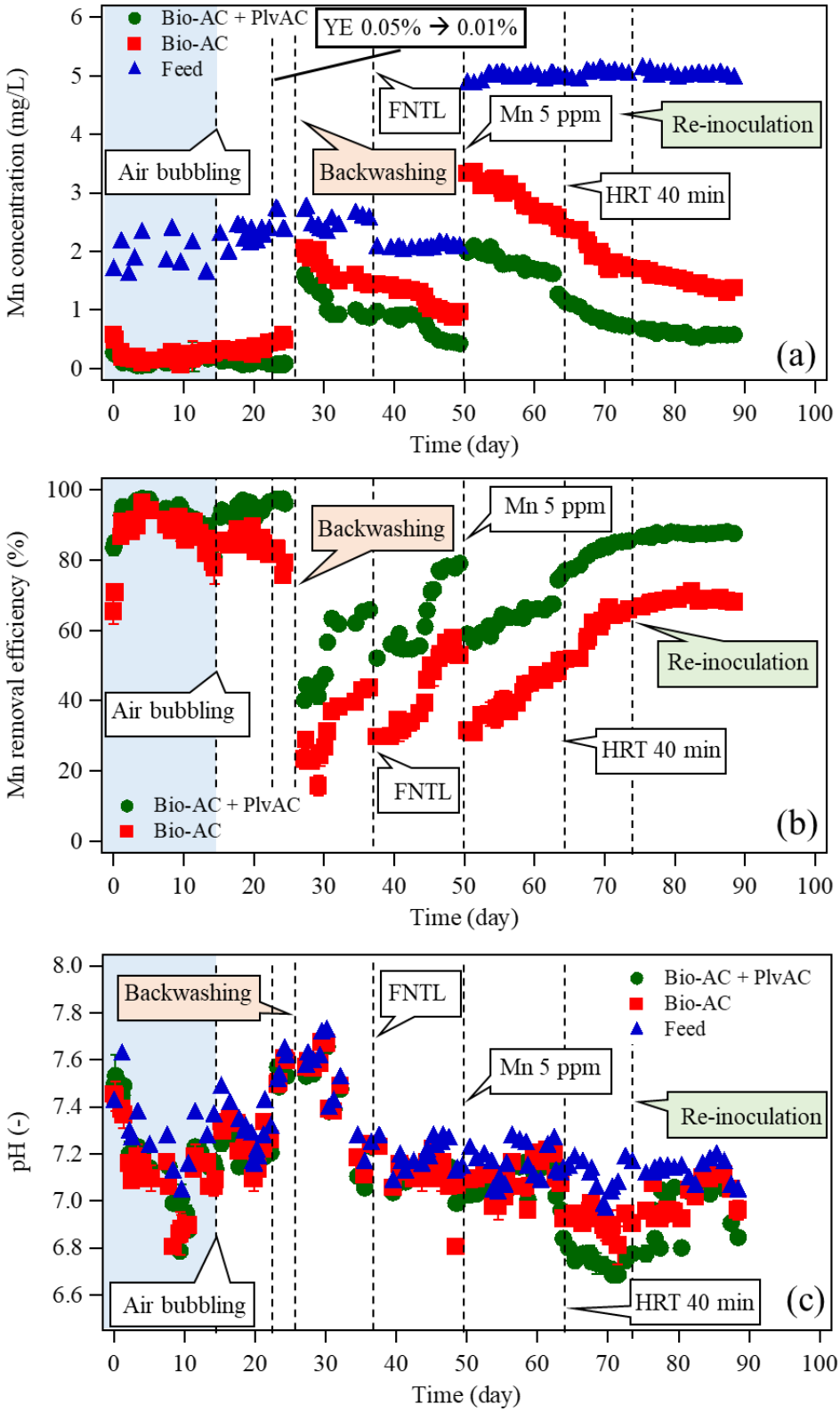

Figure 7.14 Changes in Mn concentration (a), Mn removal efficiency (b), and pH (c) in wastewater feed (▲) and column effluent (● and ■). ● and ■ indicate column packed with bioAC/plvAC and bioAC, respectively.

7.4 Conclusions

- Approximately, 70.8%, 69.4, and 84% were obtained as final Mn(II) removal from tailing dam wastewater by bio-AC after 50 hours (1st cycle), 48 hours(2nd cycle), and 100 hours (3rd cycle), respectively.
- Due to the poor biogenic birnessite support property of zeolite, only 37%, 34.2, and 55.8% were obtained as final Mn(II) removal after 50 hours (1st cycle), 48 hours(2nd cycle), and 100 hours (3rd cycle), respectively.
- Activated carbon could remove 90% of 5 mg/L Mn(II) within 30 min, whereas 40% was removed with zeolite after 24 hours.
- The combination of Mn(II)-oxidizing bacteria and chemical Mn(II)-oxidation (from AC and attached biogenic birnessite) in bio-AC synergistically promoted Mn removal rate. More than 90% of initial Mn(II) was removed after 10 min contacted with bio-AC.
- Cycle Mn(II) oxidative removal from tailing dam wastewater marked the important of yeast extract to enable the oxidation activity from Mn(II)-oxidizing bacteria, which consequently resulted in the maintaining of high removal efficiency.
- Pre-colonization of Mn(II)-oxidizing bacteria and its biogenic birnessite on activated carbon before packing in the column greatly reduced the lengthy ripening time.
- The fluctuation of yeast extract concentration did not promptly affect the Mn(II) removal efficiency but rather altered the growth of Mn(II)-oxidizing bacteria, which will eventually negatively affected the efficiency.
- By mixing bioAC with plvAC, the short-pass problem could be reduced and improved Mn(II) removal efficiency by 5-10%.

- Longer retention time (slower flow speed) is necessary when treating higher initial Mn(II) concentration

References

Abu Hasan, H., Sheikh Abdullah, S.R., Kamarudin, S.K., and Tan Kofli, N. (2013a). On–off control of aeration time in the simultaneous removal of ammonia and manganese using a biological aerated filter system. *Process Safety and Environmental Protection* 91(5), 415-422. doi: https://doi.org/10.1016/j.psep.2012.10.001.

Abu Hasan, H., Sheikh Abdullah, S.R., Kamarudin, S.K., Tan Kofli, N., and Anuar, N. (2013b). Simultaneous NH4+-N and Mn2+ removal from drinking water using a biological aerated filter system: Effects of different aeration rates. *Separation and Purification Technology* 118, 547-556. doi: https://doi.org/10.1016/j.seppur.2013.07.040.

Bruins, J.H., Petrusevski, B., Slokar, Y.M., Huysman, K., Joris, K., Kruithof, J.C., et al. (2015). Reduction of ripening time of full-scale manganese removal filters with manganese oxide-coated media. *Journal of Water Supply: Research and Technology-Aqua* 64(4), 434-441. doi: 10.2166/aqua.2015.117.

Kitjanukit, S., Takamatsu, K., and Okibe, N. (2019). Natural Attenuation of Mn(II) in Metal Refinery Wastewater: Microbial Community Structure Analysis and Isolation of a New Mn(II)-Oxidizing Bacterium Pseudomonas sp. SK3. *Water* 11(3), 507.

Majestic, B.J., Schauer, J.J., and Shafer, M.M. (2007). Development of a Manganese Speciation Method for Atmospheric Aerosols in Biologically and Environmentally Relevant Fluids. *Aerosol Science and Technology* 41(10), 925-933. doi: 10.1080/02786820701564657.

Chapter 8

Arsenite oxidative removal using biogenic manganese oxide

Abstract

In this chapter, biogenic birnessite produced by enzymatic Mn(II)-oxidation activity of *Pseudomonas* sp. SK3 was test for their As(III)-oxidation ability. Approximately 2-fold of the required amount is necessary to completely oxidized 0.2 mM As(III) with bioBir. This might due to synproportionation between Mn^{IV} in bioBir and Mn(II) (released upon As(III) oxidation), in which bioBir was passivated. As(III) was oxidized more effectively by the combination of 0.2% (w/v) bioBir and strain SK3 (0.02 mM/hour) than solely bioBir (0.0049 mM/hour). This is owing to Mn^{IV}-oxide regeneration by enzymatic Mn(II)-oxidation; thus, the As(III) oxidation persisted with high speed and made bioBir reusable. However, the As removal was poorer in the presence of strain SK3 (12%) compared with the control (75.5%). This might due to the EPS (exopolymeric substances) produced by the bacteria blocked the adsorption sites or alteration of the bioBir structure by enzymatic Mn(II)-oxidation. Nevertheless, according to TCLP test of immobilization product, As(V) should be separated from the spent birnessite and immobilized by either co-precipitation with Ca^{2+} (as calcium arsenate; $CaAsO_4$ under alkaline condition) or with Fe^{3+} (as scorodite; $FeAsO_4$ under acidic condition) instead.

8.1 Introduction

Mn-oxide minerals are robust oxidants that play an important role in many redox processes in the natural environment, such as oxidation of arsenite As(III)) and chromite (Cr(III)). Layered Mn-oxide minerals (i.e. phyllomanganate and birnessite) are more reactive for the oxidation of As(III) than other types of Mn-oxides.

To treat As-contaminating wastewater (contain mostly As(III)), oxidation of As(III) to As(V) is crucial to decrease its mobility. In this case, biogenic Mn-oxide (birnessite) derived directly from Mn(II)-contaminating wastewater treatment could be ideally utilized for As(III) oxidation. Mechanism of As(III) oxidation by Mn-oxides is complex because it involves several simultaneous reactions.

$$2H^{+} + MnO_2 + H_3AsO_3 \rightarrow Mn^{2+} + H_3AsO_4 + H_2O\ldots \text{ (Eq. 8.1)}$$

The overall reaction is shown in eq. 8.1. Upon oxidation of As(III), Mn(II) and As(V) is produced. First, Mn(II) was adsorbed onto the MnO_2 vacancy site and As(V) was sorbed at edge sites (Fig. 8.1).

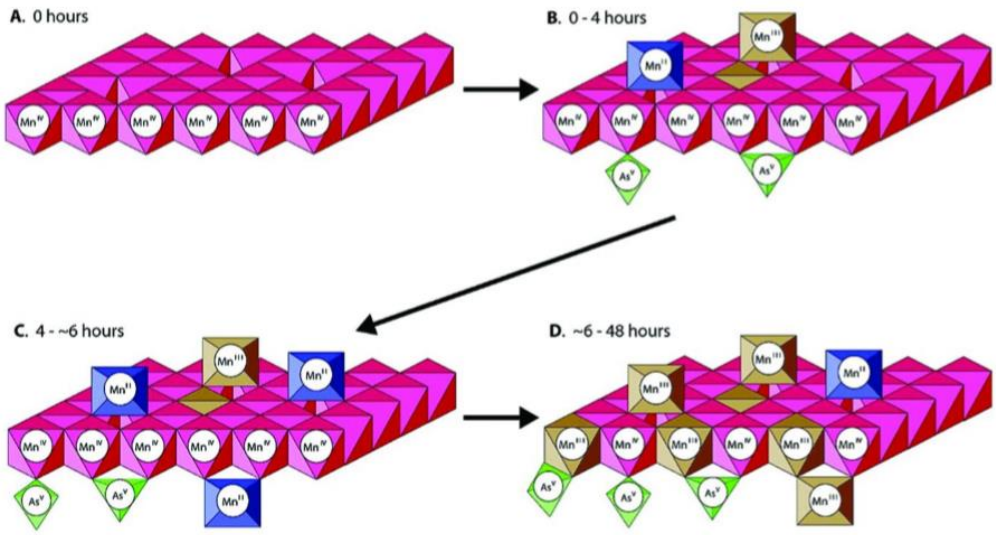

Figure 8.1 Proposed mechanisms for As(III) oxidation by δ-MnO_2 over 48 hours (Fischel et al., 2015)

Some study claimed that oxidation of As(III) by MnO_2 attributed to Mn^{2+} release, forming more Mn vacancy site, which makes the adsorption site more active. Overall As removal decreased significantly when arsenic wastewater contained As(V) more than As(III) (Hou et al., 2017). However, at pH above 6.0 Mn(II) could also react with MnO_2 via synproportionation (Eq. 8.2)

$$Mn^{IV}O_2(s) + Mn^{2+} + H_2O \rightarrow Mn^{III}_2O_3(s) + 2H^+ \quad \text{Eq. 8.2}$$

$Mn^{IV}O_2$ mineral might get passivated by $Mn^{III}_2O_3$ mineral and inhibited As(III) oxidation. Another possible As(III)-oxidation pathways are defined by one As(III) reacted with two Mn^{IV} reactive site or with one Mn^{III} and one Mn^{IV} reactive sites.

In **chapter 5**, the addition of Mn(II)-oxidizing bacteria was shown to synergistically improve Mn(II)-oxidative removal via regeneration of Mn^{IV}-oxide. With the expectation that the combination of Mn(II)-oxidizing bacteria and Mn-oxide could synergistically oxidize As(III), this study tested the oxidation capability of crystalline natural Mn oxide (NMO) and biogenic birnessite in the presence of *Pseudomonas* sp. SK3.

8.2 Materials and methods

8.2.1 Mn(II)-oxidizing bacteria

Pseudomonas sp. strain SK3 (Kitjanukit et al., 2019) was maintained and routinely sub-cultured in LB medium (pH 7.0). The strain was pre-grown overnight, washed, and harvested by centrifugation prior to use in the following experiment

8.2.2 Natural-occurring Mn oxide

Crystalline MnO_2 collected from metal-refinery wastewater treatment facility contained mainly Mn(IV) 84% (with 13% Mn(III) and 3% Mn(II)) with an average oxidation state of 3.75. The sample was washed with ethanol and deionized water, freeze-dried overnight to remove the effects from indigenous microbial activity.

8.2.3 Preparation of biogenic birnessite

Pseudomonas sp. strain SK3 was inoculated in modified PYG-1 medium pH 7.0 (as described in **chapter 2**) containing 100 mg/L Mn(II) (as $MnSO_4$) and 3 μM Cu(II) (as $CuCl_2$). After incubated for 3-4 days, biogenic birnessite was collected and washed thoroughly (10,000 rpm, 15 min) and then freeze-dried overnight.

8.2.4 As(III)-oxidation and removal

In all cases, duplicate flasks were set up and incubated at 25℃ with shaking at 120 rpm.

8.2.4.1 Natural Mn-oxide

Pre-grown *Pseudomonas* sp. SK3 cells (10^9 cells/mL) and pre-sterilized natural Mn-oxide (0.02, 0.05, 1% (w/v)) was aseptically added into 300 mL Erlenmeyer flasks containing 100 mL PYG-1 medium at pH 7.0. As(III) concentration was set to 1.2 mM (added as $NaAsO_2$).

8.2.4.2 Biogenic birnessite

8.2.4.2.1 Effects of pulp density and initial pH

Biogenic birnessite (0.125, 0.25, or 0.5% (w/v)) was aseptically added into 100 mL Erlenmeyer flasks containing 30 mL deionized water (pH 7.0). As(III) concentration was set to 0.2 mM (added as $NaAsO_2$). To study the effect of initial pH (3.0, 4.0, 5.0, 6.0, or 7.0), biogenic birnessite was added to the final pulp density of 1.25% (w/v).

8.2.4.2.2 Effects of the presence of Mn(II)-oxidizing bacteria

Pre-grown *Pseudomonas* sp. SK cells (10^9 cells/mL) and biogenic birnessite (0.1 or 0.2% (w/v)) was added into 100 mL Erlenmeyer flasks containing 50 mL PYG-1 medium (pH 7.0). As(III) concentration was set to 0.2 mM (added as $NaAsO_2$)

8.2.4.3 Analytical method

Samples were routinely withdrawn to monitor cell density (bacterial counting chamber), pH, Eh, As(III) (molybdenum blue method), total As, and total Mn (ICP-OES). Precipitates after the experiment were selectively collected by short spin (5000 rpm, 10 sec), washed and freeze-dried overnight. Solid sample was analyzed for its mineralogy by XRD (Rigaku, Ultima IV).

8.2.5 Reusability of biogenic birnessite; cycle As(III)-oxidation experiment

Biogenic birnessite (0.1% (w/v)) and pre-grown *Pseudomonas* sp. SK3 cells (10^9 cells/mL) were aseptically added into 100 mL Erlenmeyer flasks containing 30 mL PYG-1 medium (pH 7.0). As(III) concentration was set to 0.2 mM (added as $NaAsO_2$) plus 3 μM Cu(II) (added as $CuCl_2$). After 24 hours of incubation, spent medium was replaced with fresh pre-sterilized PYG-1 medium containing 0.2 mM As(III) and 3 μM Cu(II). The cycles were repeated for three times. Sterile control was also conducted in parallel.

8.2.6 Regeneration of Mn-oxide from spent medium as biogenic birnessite

Spent medium from scorodite crystallization using MnO_2 containing Mn(II), As(V), and Fe(III) was subjected to Mn-oxide regeneration experiment using Mn(II)-oxidizing bacteria.

Pre-grown *Pseudomonas* sp. SK3 cells (10^9 cells/mL) and biogenic birnessite seed crystals (0.1% (w/v)) were aseptically added into 300 mL Erlenmeyer flasks containing 100 mL of 15x diluted spent medium (table 8.1) supplemented with 0.01% yeast extract, 0.01% peptone, and 1 mM glucose. Initial pH was adjusted to 3.0, 4.0, 5.0, or 7.0. In the case of acidic pH (3.0-5.0), α-MnO_2 was added as seed crystals instead.

Duplicate flasks were set up and incubated at 25℃ with shaking at 120 rpm. Samples were regularly withdrawn to monitor pH and total Mn concentration (ICP-OES).

Table 8.1 Concentration of Total As, Fe, and Mn in the spent medium from scorodite crystallization before and after dilution

	Total As	Total Fe	Total Mn
Before dilution	1.5 mM	0.5 mM	21 mM
After dilution	0.09 mM	0.04 mM	1.4 mM

8.2.7 Biogenic Fe-oxide production from Fe(II)-Mn(II) containing solution

Pre-grown *Pseudomonas* sp. SK3 cells (10^9 cells/mL) were aseptically added into 300 mL Erlenmeyer flasks containing 100 mL PYG-1 medium (pH 7.0). Mn(II) concentration was set to 1.8 mM (added as $MnSO_4$) and Fe(II) concentration was set to 0.9, 1.8, or 3.6 mM (added as $FeSO_4$) to set the Fe:Mn molar ratio to 0.5, 1, or 2, respectively. Cu(II) was also added to the final concentration of 3 μM (added as $CuCl_2$). Samples were regularly withdrawn to monitor pH, Eh, cell density, Fe(II) concentration (*o*-phenanthroline method), total Mn and Fe concentration (ICP-OES). The precipitate was collected after the experiment, washed thoroughly (centrifugation; 10,000 rpm, 15 min), and freeze-dried overnight prior to analyze with XRD.

8.3 Results and discussion

8.3.1 As(III) oxidation by natural Mn-oxide

The changes in As(III) concentration, total As, total Mn, and pH were shown in Fig. 8.2 and summarize of the data was shown in table 8.2. As(III) was oxidized more efficiently by a combination of Mn(II)-oxidizing bacteria and NMO. Approximately, 0.5 mM of As(III) was rapidly oxidized at an early stage and gradually become slower (Fig. 8.2b). This may result from mineral passivation cause by either sorption of Mn(II) and As(V) produced from oxidation reaction or formation of Mn_2O_3 (Scott and Morgan, 1995; Nesbitt et al., 1998; Manning et al., 2002). Stoichiometrically, 0.02, 0.05, or 0.1% (w/v) of NMO could oxidize 0.17, 0.43, or 0.87 mM of As(III) based on eq. 8.1. As(III) oxidation by Mn-oxides is complex, involving several simultaneous reactions, a difference in observed and calculated values is prevalence.

Regeneration of Mn^{IV}-oxide as biogenic birnessite by Mn(II)-oxidizing bacteria was expected in this experiment; however, *Pseudomonas* sp. SK3 might not be able to tolerate this concentration of arsenic. This was illustrated by the increasing of Mn concentration even in the presence of *Pseudomonas* sp. SK3. Nevertheless, the bacteria managed to oxidize a certain amount of Mn(II) according to XRD pattern of precipitates selectively collected after experiment indicated that birnessite was formed only in the presence of Mn(II)-oxidizing bacteria.

Although As(III) was oxidized more efficiently in the presence of Mn(II)-oxidizing bacteria, As sorption was poorer compared with NMO alone (Fig. 8.2a). Previously, As(III)-oxidizing bacteria and δ-MnO_2 were used in combination to oxidize As(III) (Jones et al., 2012). MnO_2 mineral surface was passivated by bacteria EPS, which have phosphate functional groups that could compete with As for sorption sites (Parikh et al., 2010; Huang et al., 2011).

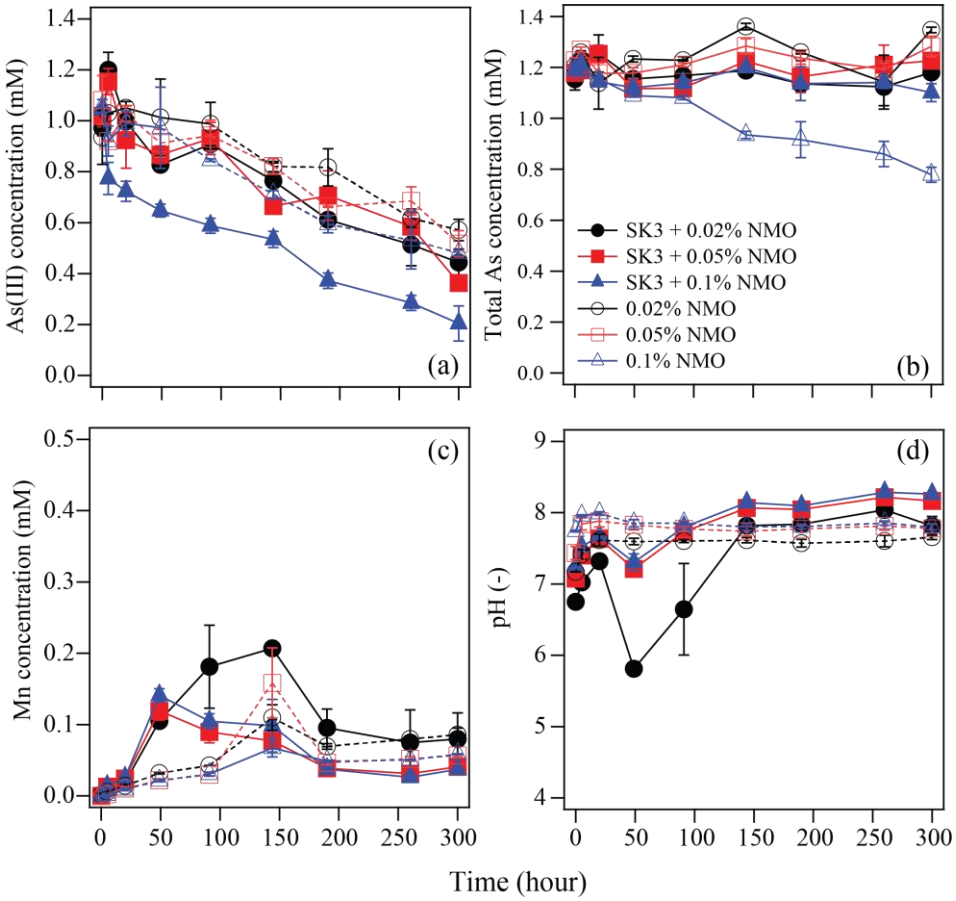

Figure 8.2 Changes in total As concentration (a), As(III) concentration (b), solution pH (c), and Mn concentration (d) during As(III) oxidation in the presence of 0.02% (●, ○), 0.05% (■, □), and 0.1% (▲, △) natural Mn-oxide (NMO) and the Mn(II)-oxidizing bacteria, *Pseudomonas* sp. strain SK3 (solid symbol, solid line) and sterile control (open symbol, broken line).

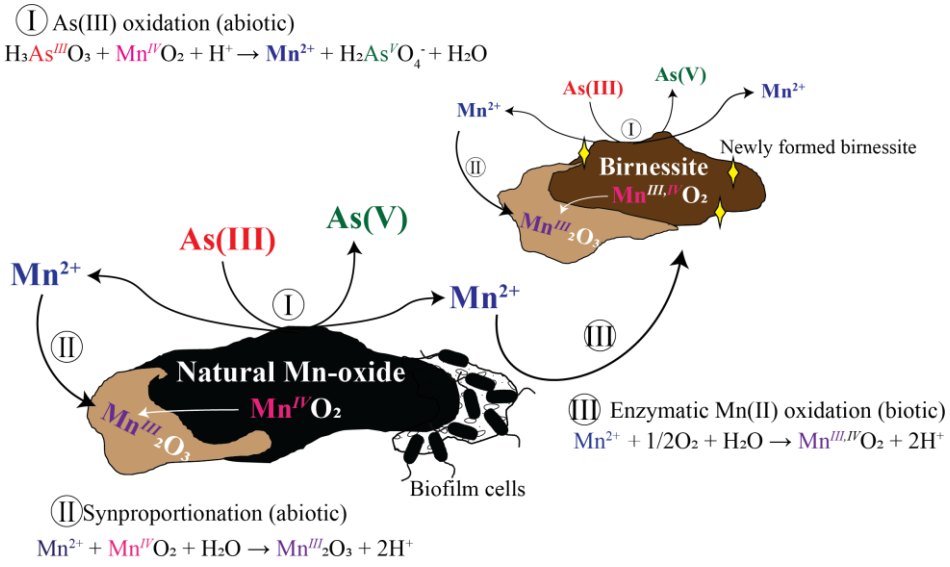

Table 8.2 As(III) oxidation and removal by natural Mn-oxide (NMO) at different pulp density. Data from cell-free control are indicated in parentheses.

	0.1% NMO	***0.05% NMO***	***0.02% NMO***
As(III) oxidized (mM)	0.84 (0.50)	0.65 (0.56)	0.53 (0.36)
As removed (%)	7.5 (35.8)	<1 (<1)	<1 (<1)
Mn(II) leached (mM)	0.037 (0.06)	0.04 (0.057)	0.08 (0.085)

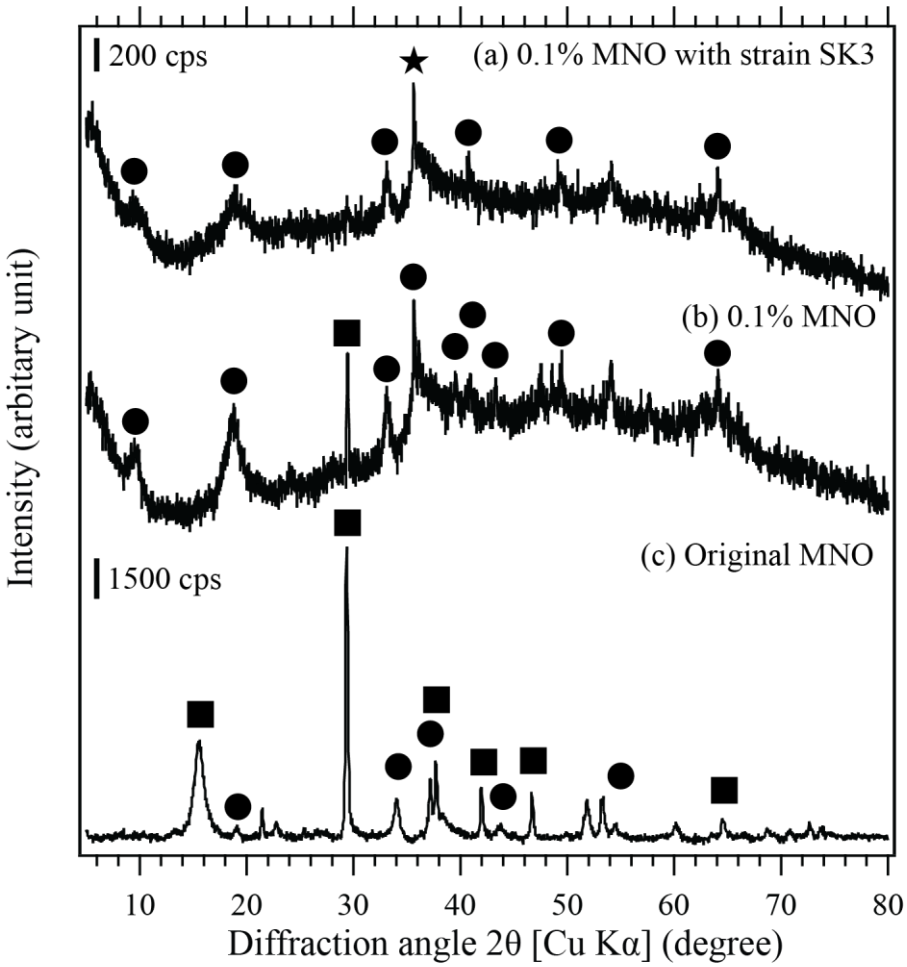

Figure 8.3 X-ray diffraction pattern of precipitate selectively collected after As(III) oxidation in the presence of natural Mn-oxide (NMO) and *Pseudomonas* sp. strain SK3. ■: α-MnO_2 (JCPDS 44-141), ●: Mn_2O_3 (JCPDS 41-1442), and ★; birnessite (JCPDS 43-1456)

8.3.2 As(III) oxidation by biogenic birnessite

8.3.2.1 Effects of pulp density and initial pH

The changes in As(III) concentration, total As, total Mn, and pH were shown in Fig. 8.3. As(III) was oxidized by Mn^{IV} in biogenic birnessite (Fig 8.4a) and the speed of the oxidation is higher as biogenic birnessite pulp density increased. The concentration of soluble Mn increased over time upon oxidation of As(III) (fig . 8.4d). Based on eq. 8.1, the molar ratio of soluble Mn and As(V) should be 1:1; however, due to the adsorption of As(V) onto natural Mn-oxide and synproportionation reaction between soluble Mn (Mn^{2+}) and Mn^{IV}, the actual molar ratio was prevalence.

When initial pH was set to 3.0, a sudden increase of pH and Mn concentration was observed (Fig. 8.5) and this might due to the dissolution of Mn^{2+} from the birnessite. Mn was kept in insoluble form due to synproportionation reaction until 8 hours of incubation. Approximately 7.6%, 20%, 17.6%, 24.9% or 34.4% of As was adsorbed onto biogenic birnessite at pH 3.0, 4.0, 5.0, 6.0, or 7.0, respectively (Fig. 8.5b).

8.3.2.2 Effects of the presence of Mn(II)-oxidizing bacteria

In the case of inoculated culture, the solution pH was unchanged compared to those of sterile control (Fig. 8.6d). Owing to the proton-consuming As(III) oxidation reaction by MnO_2 (Eq. 8.1), pH was raised significantly. In the presence of *Pseudomonas* sp. SK3, enzymatic proton-generating Mn(II) oxidation occurred and solution pH was kept stable (Eq. 8.3).

$$Mn^{2+} + 1/2O_2 + H_2O \rightarrow MnO_2 + H^+ \text{ (Eq. 8.3)}$$

Regardless of the presence of bacteria, approximately 0.3 mM of Mn dissolved from birnessite after 8 hours of incubation owing to As(III) oxidation reaction (Fig. 8.6c).

The significant difference in Mn concentration between inoculate culture and sterile control was observed after 24 hours of incubation.

However, the concentration of Mn in sterile control exceeded the stoichiometric value for completely oxidized 0.2 mM As(III). Considering the amount of As adsorbed onto birnessite in the case of sterile control, it might additionally cause the dissolution of Mn(II) (Fig. 8.5b). Apart from birnessite mineral passivation effect by bacteria EPS, ion exchanging between As(V) and adsorbed Mn(II) could be hypothesized. Figure 8.6 summarized the changes in molar ratio of soluble Mn and As in the solution.

According to TCLP test of As-immobilization product, prevention of As(V) adsorption onto birnessite by addition of Mn(II)-oxidizing bacteria has notably advantage because As(V) should be immobilized via either scorodite crystallization or calcium arsenate precipitation for better stability.

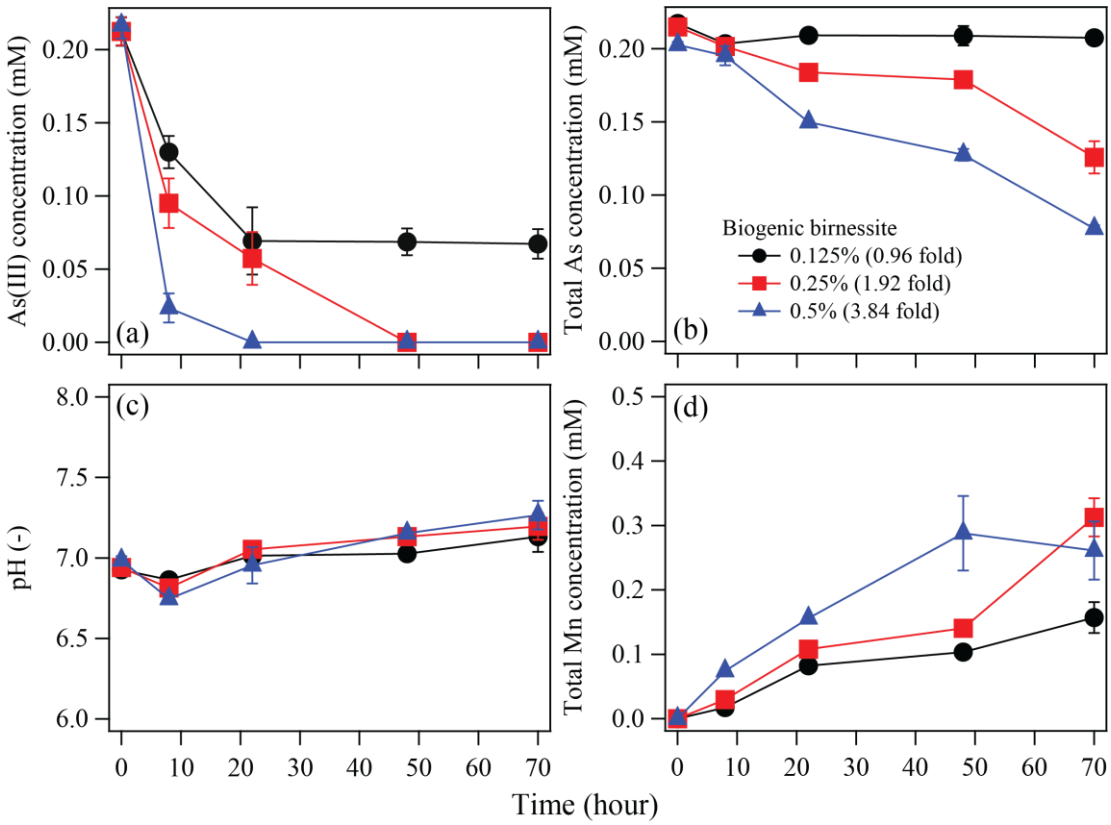

Figure 8.4 Changes in As(III) concentration (a), total As concentration (b), solution pH (c), and Mn concentration (d) during As(III) oxidation in the presence of 0.125% (●), 0.25% (■), and 0.5% (▲) biogenic birnessite.

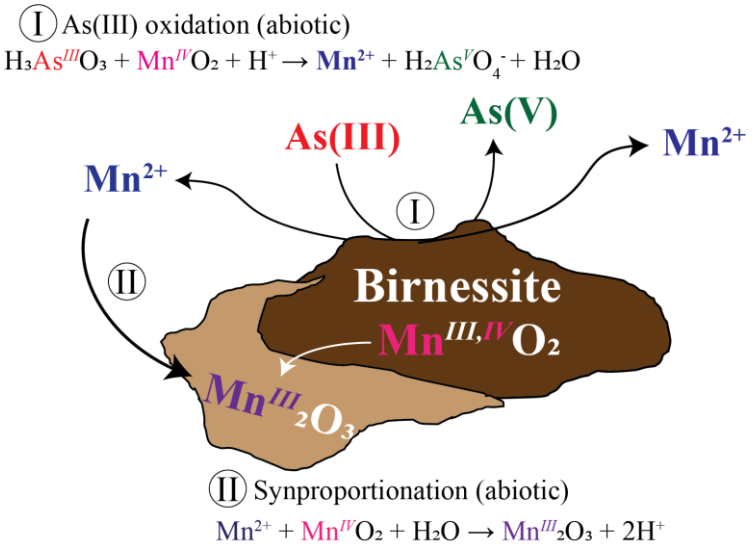

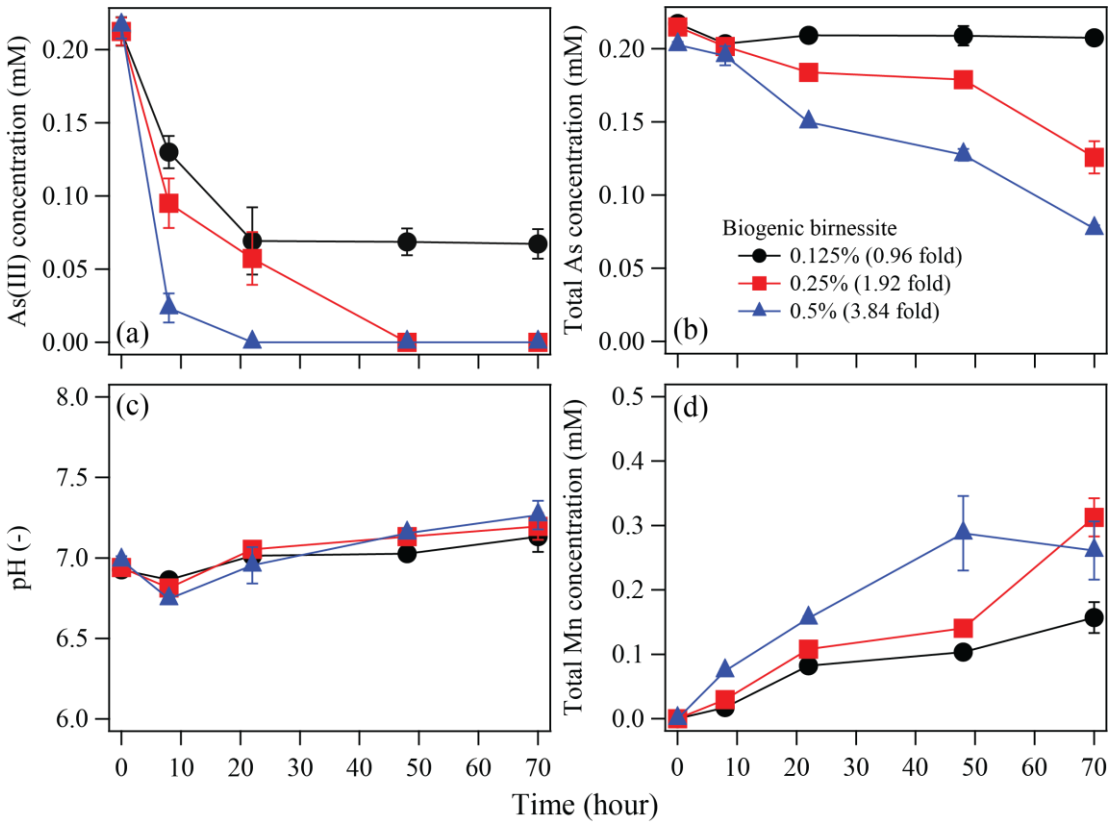

Figure 8.5 Changes in As(III) concentration (a), Total As concentration (b), Mn concentration (c), and pH (d) during As(III) oxidation in the presence of 0.1% biogenic birnessite (0.96 fold) at initial pH of 3.0, 4.0, 5.0, 6.0, 7.0.

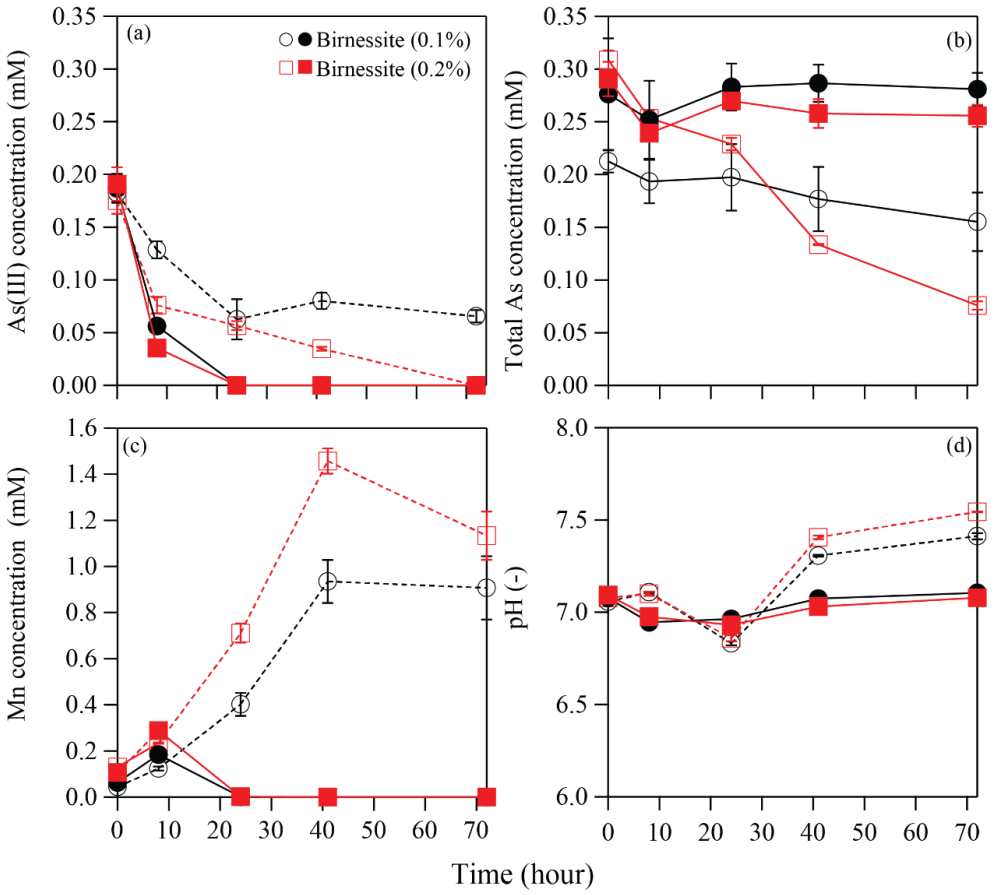

Figure 8.6 Changes in As(III) concentration (a), Total As concentration (b), Mn concentration (c), and pH (d) during As(III) oxidation in the presence of 0.1% (●,○) or 0.2% (■, □) biogenic birnessite. Open and close symbols indicated the sterile control and the presence of Mn(II)-oxidizing bacteria, respectively.

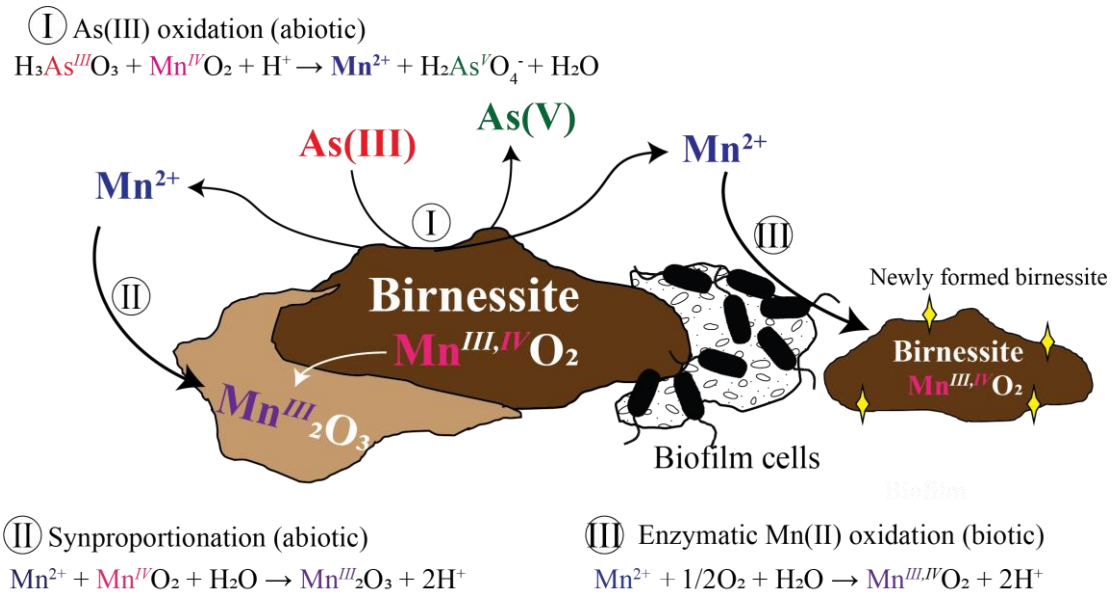

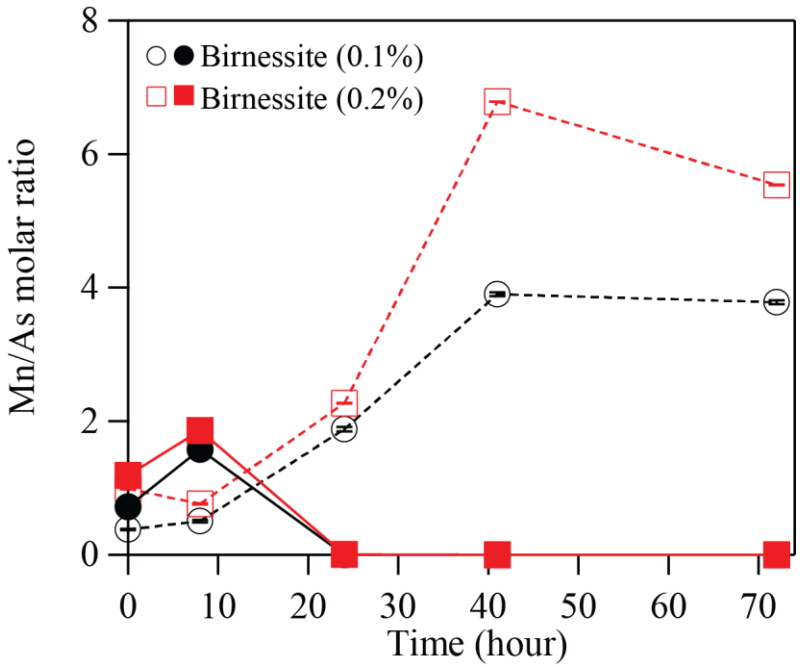

Figure 8.7 Changes in Mn/As molar ratio during As(III) oxidation in the presence of 0.1% (●,○) or 0.2% (■, □) biogenic birnessite. Open and close symbols indicated the sterile control and the presence of Mn(II)-oxidizing bacteria, respectively.

8.3.3 Reusability of biogenic birnessite; cycle As(III)-oxidation experiment

According to the above finding, the combination of Mn(II)-oxidizing bacteria and biogenic birnessite (bioBir) could oxidize As(III) more effective than the latter alone. Since fresh birnessite was regenerated via bacterial Mn(II)-oxidation, the spent bioBir could be ideally reused for another As(III)-oxidation. This experiment tested the reusability of spent bioBir in the presence and absence of Mn(II)-oxidizing bacteria, *Pseudomonas* sp. SK3.

In consistent with previous result, As(III) was oxidized faster with bioBir and strain SK3. As(III) oxidation speed increased dramatically after medium refreshment. Approximately, 58.8% and 64.4% of As(III) was oxidized right after spent bioBir suspension was added in the 2nd and 3rd cycle, respectively (Fig. 8.8a). This might due to the accumulation of Mn^{IV} (and cells) between each cycles since Mn was kept in insoluble form (Fig. 8.8c).

the In the absence of Mn(II)-oxidizing bacteria, the dissolution of Mn from bioBir become lower after each cycle indicated the cease of As(III)-oxidation activity (Fig. 8.8c). Only about 22% and 20% of As(III) was oxidized in the 2nd and 3rd, respectively (Fig. 8.8a). In 3rd cycle, the sudden decrease and increase of As(III) might due to adsorption and desorption when considered the total As concentration (Fig. 8.8a and b).

No significantly different in the changes of solution pH, redox potential, and cell density after each cycle (Fig. 8.8d, e, and f).

Apparently, the presence of Mn(II)-oxidizing bacteria marked its importance for both As(III)-oxidation efficiency and reusability of bioBir.

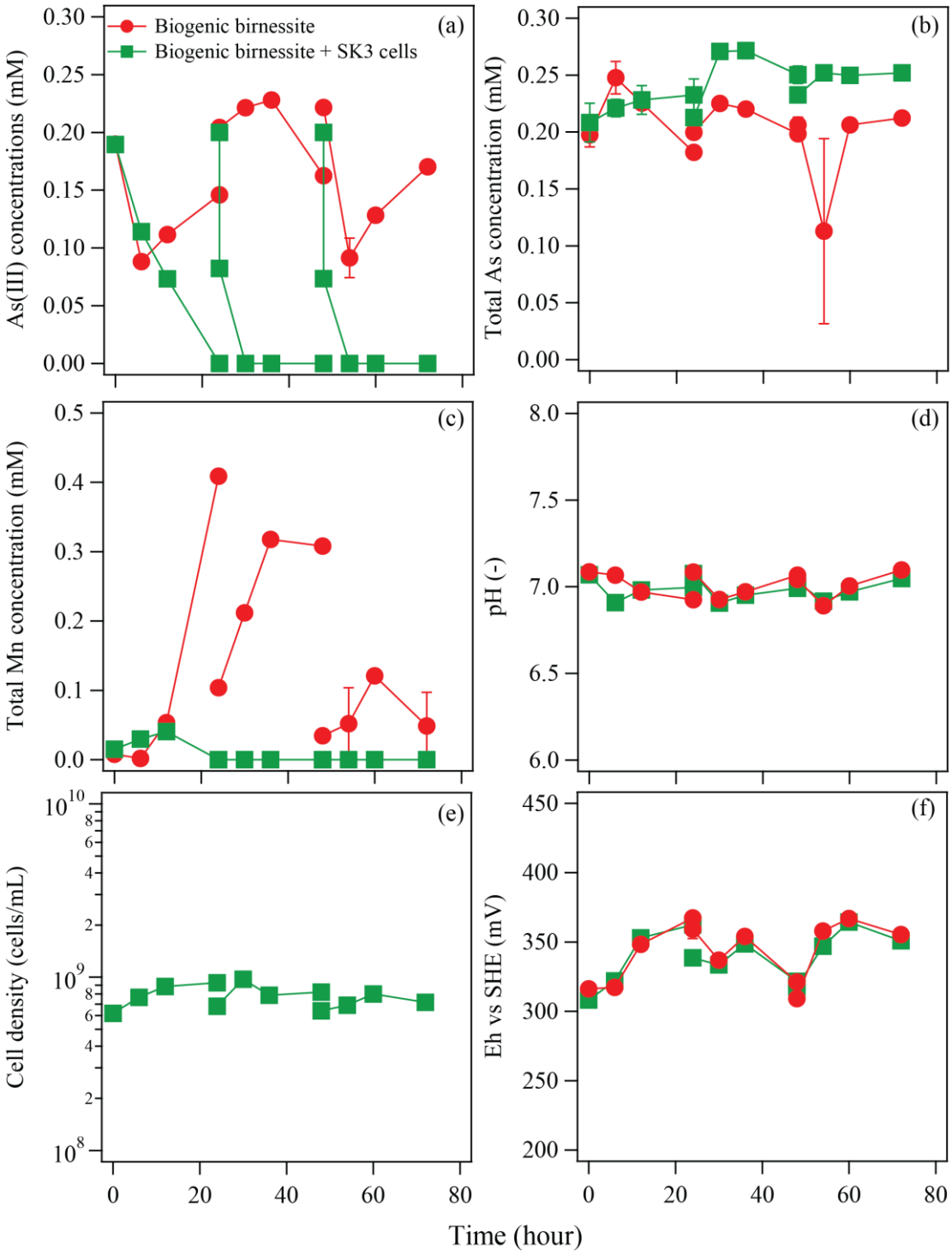

Figure 8.8 Changes in As(III) concentration (a) , total As concentration (b), total Mn concentration (c), pH (d), cell density (e), and redox potential (f) during cycle As(III)-oxidation using 0.1% biogenic birnessite. ● and ■ indicate sterile control and inoculated culture (*Pseudomonas* sp. SK3), respectively

8.3.4 Regeneration of Mn-oxide from the spent medium as biogenic birnessite

The use of MnO_2 to facilitate the crystallization of scorodite from As(III) and Fe(II)-containing wastewater, resulting in of dissolution of Mn(II). Either upon oxidation of As(III) and Fe(II) reaction or acid dissolution, Mn(II) should be ideally re-oxidized back to Mn-oxides for the Mn recycling purpose.

First, pre-grown cells of *Pseudomonas* sp. strain SK3 plus biogenic birnessite seed crystals were tested for Mn(II) recovery from the diluted spent medium. The changes in cell density, pH and Mn concentration were shown in Fig. 8.9. Planktonic SK3 cells could not manage to oxidize Mn(II) back to birnessite. Even though at pH 7.0, strain SK3 could completely oxidize 1.8 mM of Mn(II) within 48 hours (Kitjanukit et al., 2019).

Interestingly, when biogenic birnessite was added together as a seed crystal, Mn(II) in the spent medium was completely oxidized within 140 hours (Fig. 8.9a). Addition of biogenic birnessite could promote synproportionation reaction and only about 43% of Mn(II) was oxidized. Stoichiometrically, 0.1% (w/v) of birnessite seed added is 0.96 fold of amount required to completely oxidize Mn(II) via synproportionation (Eq. 8.2). Due to mineral passivation, the reaction then slowed down and consequently halted. Addition of birnessite seed could have provided strain SK3 with a surface to colonize biofilm forming. This may have enabled cells to be less affected by the inhibitory effect of As(V). Regardless of the additional yeast extract, combination of strain SK3 and birnessite could completely recover Mn(II) as newly formed birnessite. There might be a certain amount of organic carbon left in the spent scorodite crystallization medium and in birnessite seed, which SK3 could utilize. When initial pH was set to 5.0, the speed of reaction was slowed down because Mn(II)-oxidation activity of SK3 was activated when pH raised above 6.5 owing to the dissolution of

Mn from birnessite (Kitjanukit et al., 2019). After 96 hours of incubation, 90% of Mn was recovered as new biogenic birnessite (Fig. 8.9).

Our challenge in this study was to set the initial pH for Mn-oxide regeneration as low as possible because originally the spent medium was extremely acidic (pH 1.5-2.0). Since biogenic birnessite is not stable at pH lower than 5.0, poorly crystalline α-MnO_2 was added as seed crystals instead. Solution pH was raised to above 5.0 owing to the dissolution of Mn(II) from MnO_2 and this enabled synproportionation reaction. Approximately, 30% of Mn(II) was recovered after 300 hours of incubation. In the case of pH 3.0 initially, Mn concentration increased while solution pH was still lower than 4.0 and no synproportionation reaction observed (data not shown). According to the results, the seed crystals fed into that acidic spent medium should be dissolved to allow the rise of pH and consequently enable both synproportionation and enzymatic Mn(II)-oxidation.

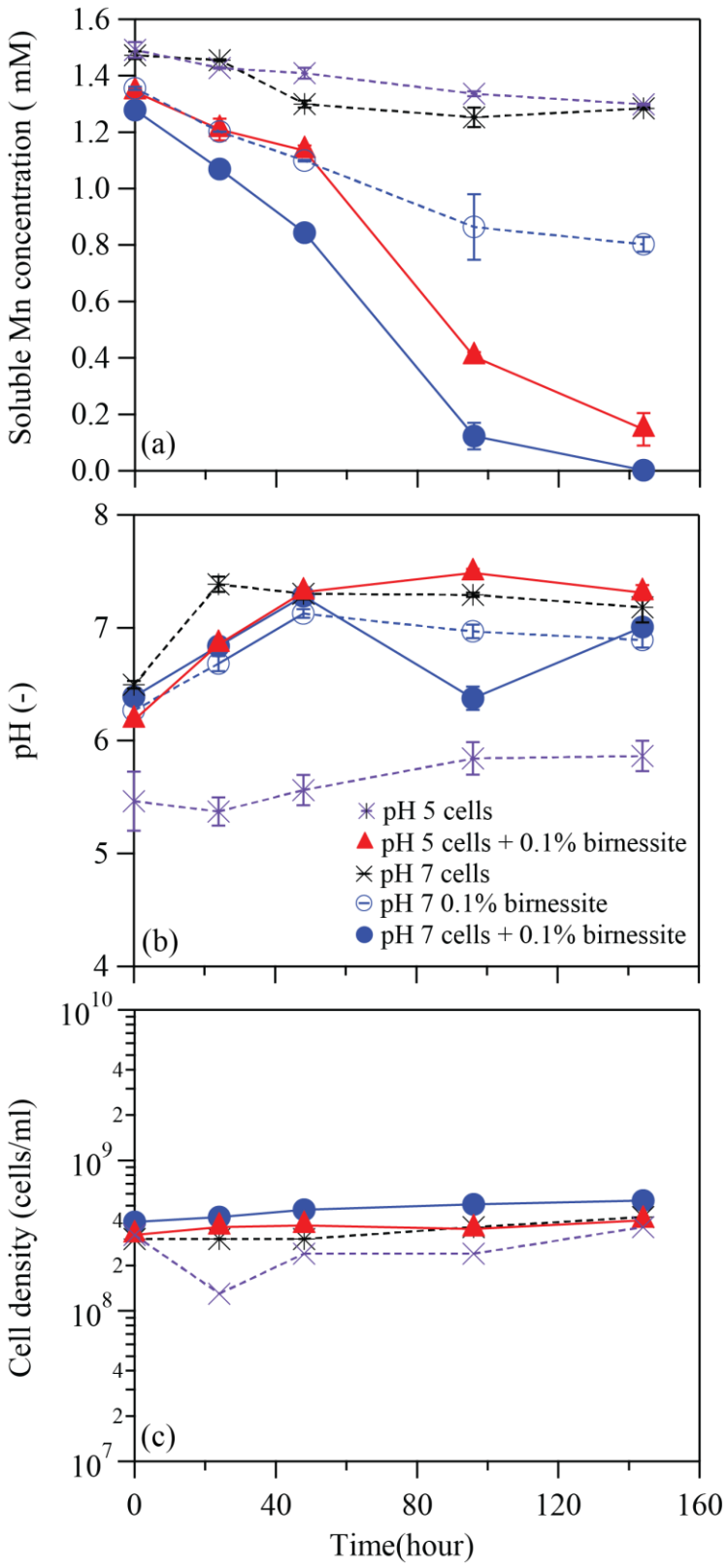

Figure 8.9 Changes in soluble Mn concentration (a), pH (b), and cell density (c) during Mn(II)-oxidation from Mn(II)-containing spent medium for Mn-oxide regeneration purpose.

8.3.5 Mn(II)-oxidative removal from Fe(II)-Mn(II) containing solution and formation of biogenic Fe-Mn oxide

Due to the high affinity between Fe-oxide and arsenic, it has been widely used to immobilize As(V) via adsorption. Particularly, arsenic occurred as As(III) which has higher mobility; hence, oxidation of As(III) to As(V) is necessary for further treatment. However, Fe-oxide alone could not facilitate oxidation of As(III). Earlier in this chapter, biogenic birnessite has been demonstrated for its As(III)-oxidation capability.

The previous study also showed that biogenic Fe-Mn oxide formed in situ adsorbed As(V) better than biogenic Mn-oxide (Bai et al., 2016). In the Fe-Mn oxide system, As(III) was oxidized by Mn-oxide and the resulting As(V) was adsorbed by Fe-oxide.

This experiment investigated the formation of biogenic Fe-Mn oxide from Fe(II)-Mn(II) containing solution using Mn(II)-oxidizing bacteria, which will be utilized later for As(III)-oxidative removal.

Upon addition of Fe(II) into PYG-1 medium, it was rapidly oxidized, precipitated to a hydrous ferric oxide and solution pH dropped. At Fe:Mn molar ratio of 0.5, 1, 2 and , strain SK 3 could oxidized 100%, 76.5%**,** and 11.7% of Mn(II), respectively (Fig. 8.10)

From visual observation, the orange-brown precipitate (ferric oxide) turned blackish brown after 74 (Fe: Mn = 0.5) and 117 hours (Fe: Mn = 1), indicating biogenic birnessite formation. This lagging period for initiation of enzymatic activity might be due to lower pH and the presence of ferric oxide.

In the presence of Mn(II)-oxidizing bacteria, mixed phase of Fe^{III}-oxide and birnessite was formed at Fe: Mn molar ratio of 0.5 and 1 (Fig. 8.11). Since there is no Mn(II)-oxidation at a high molar ratio, the precipitate consisted only Fe^{III}-oxide.

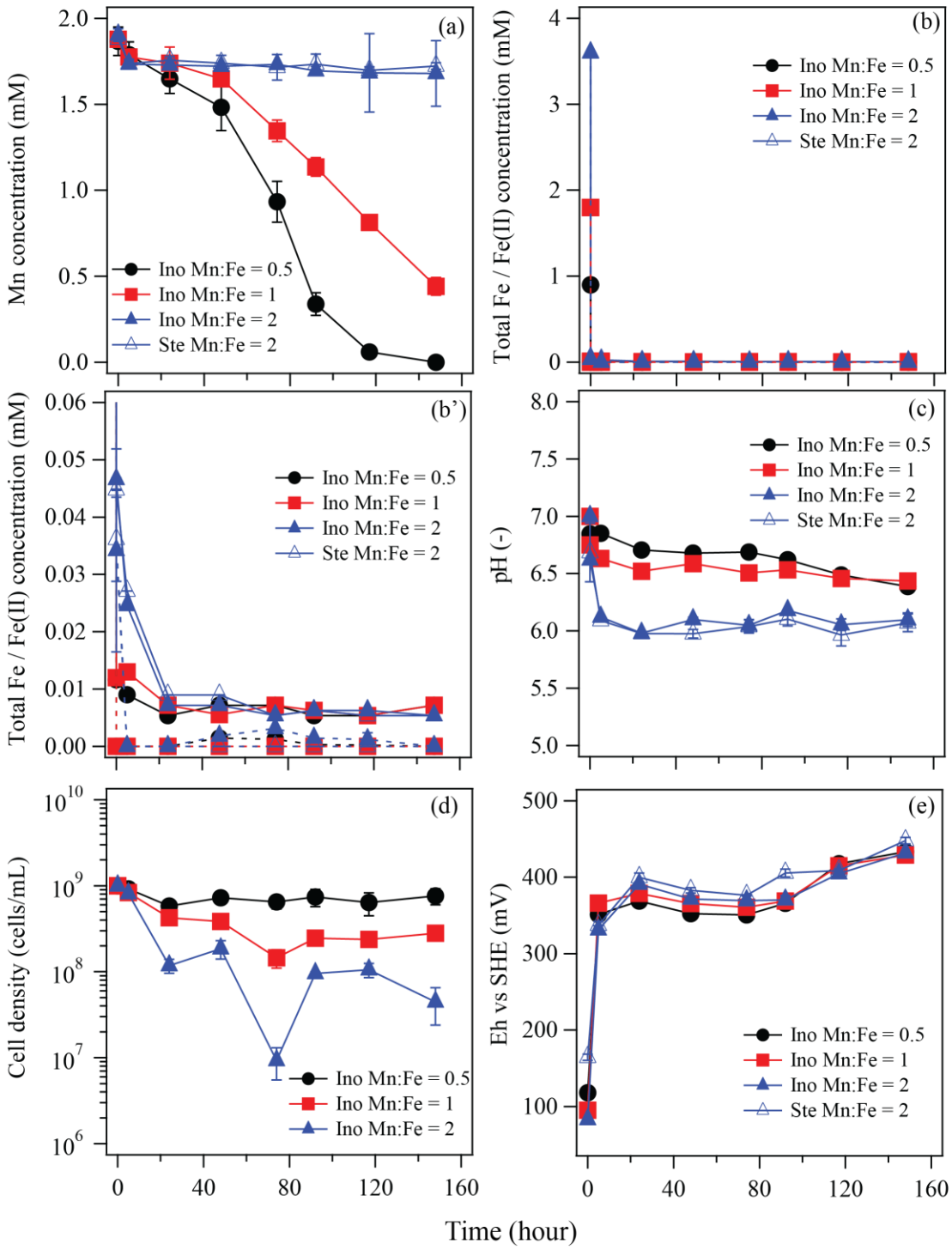

Figure 8.10 Changes in Mn concentration (a), total Fe/Fe(II) concentration (b,b'), pH (c), cell density (d), and Eh (e) during Mn(II) oxidation in Fe(II)-Mn(II) containing solution

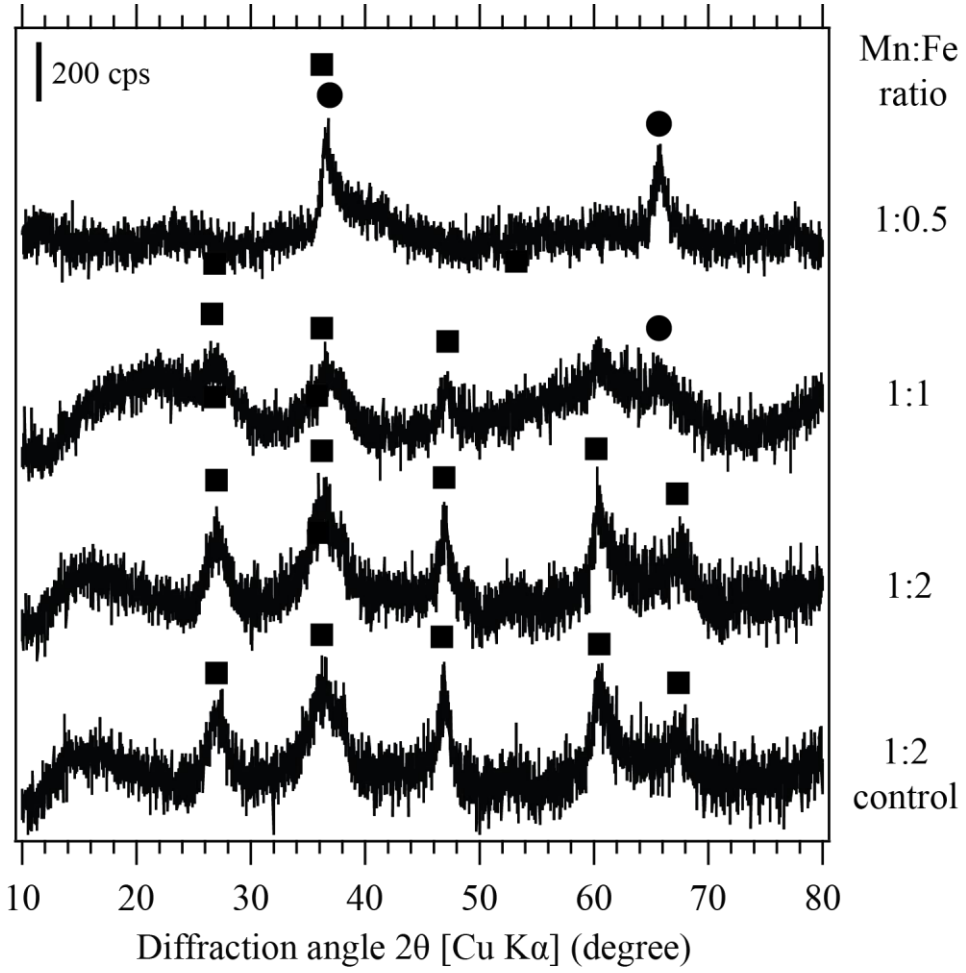

Figure 8.11 X-ray diffraction pattern of the precipitates formed after Mn(II)-oxidation in Fe(II)-Mn(II) containing solution experiment. ●; birnessite JCPDS 43-1546, ■; lepidocrocite PDF 00-044-1414.

8.4 Conclusions

- As(III) was oxidized better by layered Mn^{IV}-oxide (i.e. birnessite) than α-MnO_2.

- Approximately 2-fold of the stoichiometric amount of Mn^{IV}-oxide is necessary to completely oxidized 0.2 mM of As(III). This might due to the consumption of Mn^{IV} from synproportionation and mineral passivation.

- The presence of Mn(II)-oxidizing bacteria greatly improved the As(III)-oxidation by bioBir via the regeneration of fresh Mn-oxide from Mn(II); thus, the reaction speed was maintained.

- Spent bioBir could be reused to oxidize another batch of As(III) with interestingly increased speed owing to accumulation of Mn^{IV} and cell density after each cycle.

- The combination of bioBir seed crystals and Mn(II)-oxidizing bacteria could recovered Mn(II) from spent scorodite crystallization wastewater as newly formed bioBir about 90% and 100% when the initial pH was set to 5.0 and 7.0, respectively.

- Biogenic Fe-Mn oxide could be produced when Fe(II): Mn(II) molar ratio was set to 0.5 or 1.0 according to XRD analysis.

References

Bai, Y., Yang, T., Liang, J., and Qu, J. (2016). The role of biogenic Fe-Mn oxides formed in situ for arsenic oxidation and adsorption in aquatic ecosystems. *Water Research* 98, 119-127. doi: https://doi.org/10.1016/j.watres.2016.03.068.

Fischel, J.S., Fischel, M.H., and Sparks, D.L. (2015). "Advances in Understanding Reactivity of Manganese Oxides with Arsenic and Chromium in Environmental Systems," in *Advances in the Environmental Biogeochemistry of Manganese Oxides*. American Chemical Society), 1-27.

Hou, J., Luo, J., Song, S., Li, Y., and Li, Q. (2017). The remarkable effect of the coexisting arsenite and arsenate species ratios on arsenic removal by manganese oxide. *Chemical Engineering Journal* 315, 159-166. doi: https://doi.org/10.1016/j.cej.2016.12.115.

Huang, J.-H., Elzinga, E.J., Brechbuehl, Y., Voegelin, A., and Kretzschmar, R. (2011). Impacts of Shewanella putrefaciens Strain CN-32 Cells and Extracellular Polymeric Substances on the Sorption of As(V) and As(III) on Fe(III)-(Hydr)oxides. *Environmental Science & Technology* 45(7), 2804-2810. doi: 10.1021/es103978r.

Jones, L.C., Lafferty, B.J., and Sparks, D.L. (2012). Additive and competitive effects of bacteria and Mn oxides on arsenite oxidation kinetics. *Environ Sci Technol* 46(12), 6548-6555. doi: 10.1021/es204252f.

Kitjanukit, S., Takamatsu, K., and Okibe, N. (2019). Natural Attenuation of Mn(II) in Metal Refinery Wastewater: Microbial Community Structure Analysis and Isolation of a New Mn(II)-Oxidizing Bacterium Pseudomonas sp. SK3. *Water* 11(3), 507.

Manning, B.A., Fendorf, S.E., Bostick, B., and Suarez, D.L. (2002). Arsenic(III) Oxidation and Arsenic(V) Adsorption Reactions on Synthetic Birnessite. *Environmental Science & Technology* 36(5), 976-981. doi: 10.1021/es0110170.

Nesbitt, H.W., Canning, G.W., and Bancroft, G.M. (1998). XPS study of reductive dissolution of 7Å-birnessite by H3AsO3, with constraints on reaction mechanism. *Geochimica et Cosmochimica Acta* 62(12), 2097-2110. doi: https://doi.org/10.1016/S0016-7037(98)00146-X.

Parikh, S.J., Lafferty, B.J., Meade, T.G., and Sparks, D.L. (2010). Evaluating Environmental Influences on AsIII Oxidation Kinetics by a Poorly Crystalline Mn-Oxide. *Environmental Science & Technology* 44(10), 3772-3778. doi: 10.1021/es903408g.

Scott, M.J., and Morgan, J.J. (1995). Reactions at Oxide Surfaces. 1. Oxidation of As(III) by Synthetic Birnessite. *Environmental Science & Technology* 29(8), 1898-1905.

doi: 10.1021/es00008a006.

The results in this chapter were cooperated by Mr. Ryohei Nishi (Master's 2nd year student in fiscal year 2019) and Mr. Kohei Nonaka (Master's 1st year student in fiscal year 2019).

Chapter 9

Conclusions and future recommendation works

9.1 Conclusions

Mn(II) could be oxidized and precipitate as Mn-oxide more effective by an enzyme-mediated reaction of microorganisms at circumneutral pHs (without the addition of chemical oxidizing agents). Therefore, a vast cost of neutralizing agents is needed for conventional Mn(II) removal process could be reduced. Mn(II)-contaminating metal-refinery wastewater problem is challenging due to its acidic characteristic and other contaminants containing.

In order to search for useful Mn(II)-oxidizing bacteria for the treatment of those wastewaters, the phenomenon of natural attenuation of dissolved Mn level on site was investigated (**chapter 3**). Mn(II) concentration was found noticeably lowered from 1-n to 0.n mg/L after the wastewater traveled through a long pipe. The inner pipe was found to be heavily encrusted with dark-brown deposits, which was characterized as mixed phases of crystalline $Mn^{IV}O_2$, $Mn^{III}_2O_3$, and Fe_2O_3. This Mn-oxide has an average oxidation state (AOS) of 3.75 and consisted of 84% Mn(IV), 13% Mn(III), and 3% Mn(II), based on linear combination fitting of Mn K-edge XANES spectra. Due to the high activation energy of Mn(II)-oxidation, the microbial-mediated reaction was suspected to involve in this phenomenon, rather than a spontaneous chemical reaction.

Next-generation sequencing based on 16S rRNA revealed that the photoheterotroph (*Porphyrobacter* sp.; 52%) and facultative autotroph budding bacteria (*Hyphomicrobium* sp.; 22.1%) were dominated the community of classified sequences and the presence of putative Mn(II)-oxidizing bacteria (*Pseudomonas* sp. (0.03%) and *Bacillus* sp. (0.18%)) was implied based on previous studies. The formation of Mn-deposit in the wastewater pipe might start from the colonization of those photoheterotroph and autotroph owing to their ability to harness energy

carbon-independently. Owing to hyphal filament produced by the hyphomicrobia, it could establish both structural and nutritional scaffolds to support secondary colonization of Mn(II)-oxidizer against continuous water flow. The above finding motivated us to isolate new strain Mn(II)-oxidizer which could withstand such conditions in metal-refinery wastewater. Following the culture enrichment of Mn-deposit and selective screening, *Pseudomonas* sp. strain SK3 was isolated and characterized (**chapter 4**). Its closest relative was shown to be *Pseudomonas resinovorans* (98.4% homologous; 1398 bp), which is so far unknown as Mn(II)-oxidizer. This finding suggested that Mn(II)-oxidizing ability might be more diversely present across the genus *Pseudomonas*, rather than just in *Ps. putida* group. The new isolate SK3 was tested for Mn(II) oxidation at several conditions targeting metal-refinery wastewater characteristics. A trace amount of Cu(II) ions was found to facilitate Mn(II) oxidation (implying the involvement of multicopper oxidase enzyme), enabled strain SK3 to exhibit more stable Mn(II)-oxidation activity. The new isolate also exhibited remarkable resistance to high $MgSO_4$ dose (2400 mg/L), which completely stopped Mn(II) oxidation by *Ps. putida* MnB1. Biogenic Mn-oxide was characterized as poorly-crystalline birnessite (XRD) with high Mn(IV) fraction of 0.86 and AOS of 3.8.

Natural Mn-oxide is known as one of the strongest oxidant found in nature, capable of oxidizing various organic and inorganic compounds. Therefore, a combination of natural Mn-oxide (NMO) collected from the metal-refinery wastewater treatment facility and the isolate SK3 was tested for Mn(II)-oxidative removal under various conditions in **chapter 5.** When only sterilized NMO was provided, Mn(II)-oxidation proceeded only to a limited extent by chemical synproportionation ($Mn^{2+} + Mn^{IV}O_2 + H_2O \rightarrow Mn^{III}_2O_3 + 2H^+$; Eq. 2) even 2.5 fold of

stoichemically required amount of NMO was added. This was due to surface passivation of NMO with $Mn^{III}_2O_3$. The presence of SK3 cells further oxidized Mn(II) and formed Mn^{IV}-oxide as birnessite, which could also catalyze synproportionation; thus, this enabled synergistic Mn(II)-oxidative removal. Addition of NMO also provided a site for SK3 cells to colonize via biofilm, which allowed it to take less effect from inhibitory effects of $MgSO_4$ and temperature. Utilization of the proton-consuming reactions of Mn(II) and alkaline substances dissolution from NMO, enabled treatment of acidic Mn(II)-solution. Overall, the results illustrated the applicability of synergistic Mn(II)-oxidative removal in the upstream of the metal-refinery wastewater treatment system to deal with a Mn(II) contaminant coexisted with $MgSO_4$ at slightly acidic pH values.

Nevertheless, in order to oxidize and remove Mn(II) effectively, both Mn(II)-oxidizing bacteria and Mn-oxide (i.e. biogenic birnessite) should be retained actively in the treatment system. This leads to application studies on the development of Mn(II)-oxidative removal using a biofilter column in **chapter 6 and 7**.

In **chapter 6**, screening of bacterial-supporting material to find the best match to the isolate SK3 was conducted. Ten different materials including SiO_2- and carbon-based were subjected to cycle Mn(II)-oxidative removal test, which done by decantation of the spent medium and replaced with the fresh one without re-inoculation of bacteria. According to the results, activated carbon (AC) is the most suitable material, capable of supporting both Mn(II)-oxidizing bacteria and its biogenic birnessite. At an optimal amount, AC could promote chemical Mn(II)-oxidation in addition to adsorption, resulting in synergistic Mn(II) removal.

Finally, the laboratory-scale AC-packed biofilter column test was conducted in **chapter 7**, using two types of actual metal-refinery wastewaters (downstream water [Mn^{2+}] 2 mg/L, [SO_4^{2-}] 780 mg/L; upstream water [Mn^{2+}] 2-5 mg/L, [SO_4^{2-}] 1500 mg/L). The results obtained from this chapter were expected to offer improvement suggestions for the on-going pilot-scale test column constructed at the mental-refinery site. This *on-site* pilot-scale column was packed with zeolite with the current Mn-removal of around 40%. The advantage of using AC instead of SiO_2-based zeolite as column-carrier was reconfirmed in this test, as the contact time required for the complete Mn-removal was shortened with the former. Before starting the water flow (at the hydraulic retention time (HRT) of 20 min), AC granules pre-colonized with actively Mn-oxidizing SK3 cells were packed in the column, in order to kick-start the Mn-removal. The importance of organic supply was clearly indicated, since Mn-oxidation was catalyzed by heterotrophic bacteria: In fact, the addition of the minimum amount of yeast extract (0.01%) was essential to maintain high Mn-removal efficiency (65-90%, compared to 20-40% in control). For the treatment of upstream water with higher Mn^{2+} and SO_4^{2-} contents, the addition of pulverized AC to granule AC (at 3:7 ratio) promoted Mn-oxidation by 5-10%, resulting in about 85% final Mn-removal at HRT 40 min, even after a harsh backwashing process. Overall results obtained in this chapter suggest that the following factors should be considered to improve performance of the *on-site* pilot-scale column; type of column-carrier, installation of pre-colonization step, the supply of suitable organic nutrient, optimization of HRT.

In **chapter 8**, biogenic birnessite (bioBir) produced by the isolate SK3 was investigated for As(III)-oxidation capability. Approximately 2-fold of the required amount is necessary to completely oxidized 0.2 mM As(III) with bioBir. This might

due to synproportionation between Mn^{IV} in bioBir and Mn(II) (released upon As(III) oxidation), in which bioBir was passivated. As(III) was oxidized more effectively by the combination of 0.2% (w/v) bioBir and strain SK3 (0.02 mM/hour) than solely bioBir (0.0049 mM/hour). This is owing to Mn^{IV}-oxide regeneration by enzymatic Mn(II)-oxidation; thus, the As(III) oxidation persisted with high speed and made bioBir reusable. However, the As removal was poorer in the presence of strain SK3 (12%) compared with the control (75.5%). This might due to the EPS (exopolymeric substances) produced by the bacteria blocked the adsorption sites. Also, the birnessite structure might be altered by bacterial Mn(II)-oxidation resulting in poorer As(V) adsorption.

From overall findings obtained in this study, a possible flow of practical processes was elucidated in Fig. 9.1 and Fig. 9.2. The flow started from the treatment of acidic Mn(II)-containing metal-refinery wastewater. As acidophilic Mn(II)-oxidizer has not been found yet, those acidic wastewater will be treated by neutralization (addition of limestone). This proposed bioprocess could reduce the vast cost of limestone for raising pH from 2.0 to 9.0 to circumneutral pHs (7.0-8.0). The wastewater then passed through settling tank or tailing dam to separate particulate Fe-oxide and $MnCO_3$ prior to entering column reactor packed with bio-AC (activated carbon colonized with Mn(II)-oxidizing bacteria and biogenic birnessite). This could reduce the backwashing frequency and enlonged column lifespan. Since bacterial Mn(II)-oxidation required nutrient to activate, digested local products (ex: coconut shell and maize) could be utilized as organic carbon sources. A monitoring system is placed after the column monitor column efficiency as well as Mn(II) concentration. If the effluent Mn(II) concentration is less than 0.05 mg/L, the wastewater could be discharged or reused. The second column reactor is setup if further treatment is

required. In Fig. 9.2, bioreactor utilizing Mn(II)-oxidizing bacteria and local products (as nutrient source) was purposed to treat higher concentration of Mn(II) (50-100 mg/L). In this case, the birnessite seed crystals could be fed back to improve Mn(II)-removal efficiency. Moreover, the biogenic birnessite (bioBir) derived directly from the bioprocess could be utilized for the treatment of As(III)-contaminating groundwater (As(III) = 10 mg/L, circumneutral pH). After As(III) was oxidized to As(V) by bioBir, it will be separated from the mineral and immobilized by either scorodite or calcium arsenate methods. By doing so, bioBir could be utilized as the self-regenerating oxidant source for As(III) treatment.

With the aim to encourage future sustainability, this thesis demonstrated the utilization of resource produced from waste to treat another waste using biotechnology.

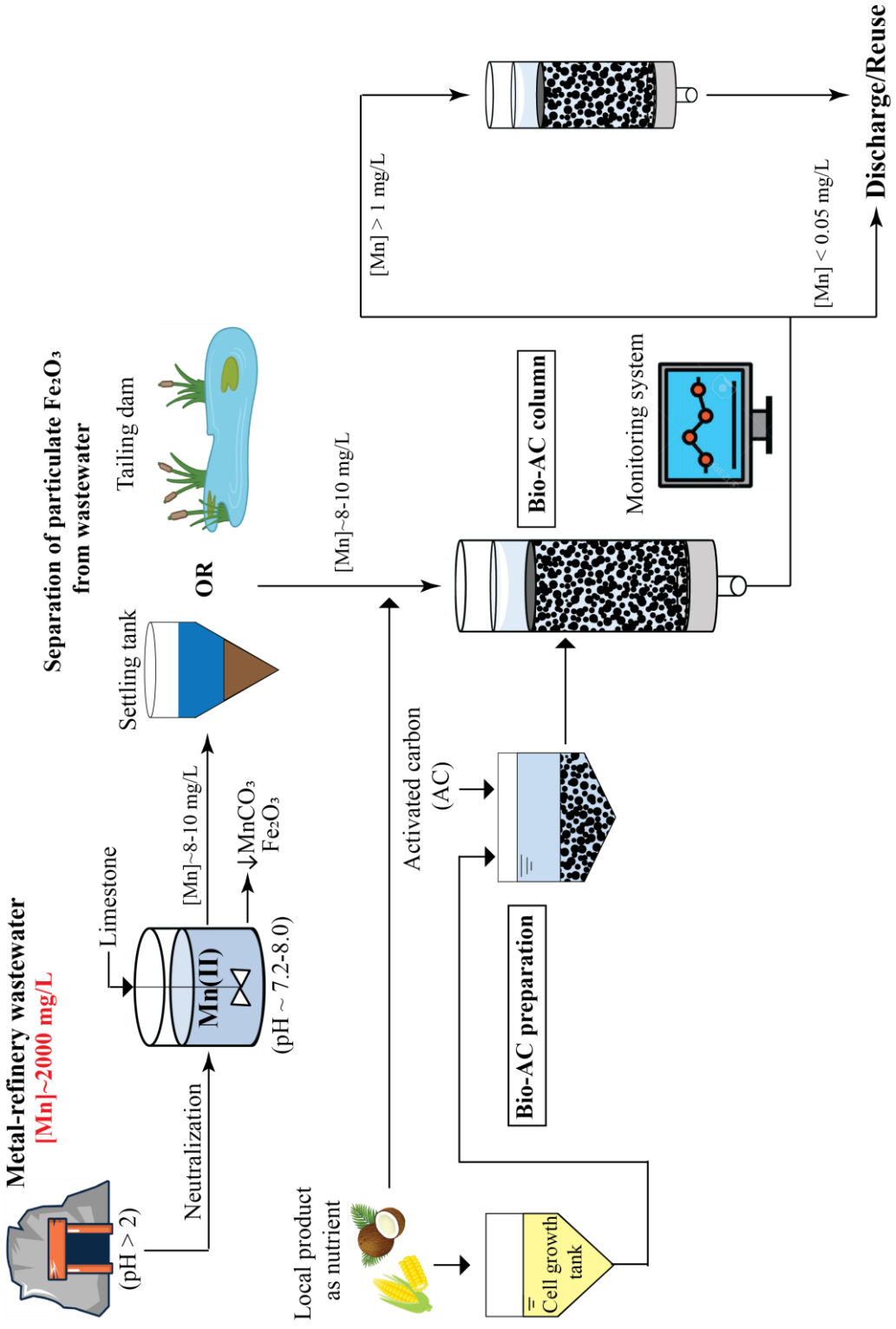

Figure 9.1 Proposed flowsheet of bioprocess for Mn(II)-contaminating metal-refinery wastewater treatment using biofilter column

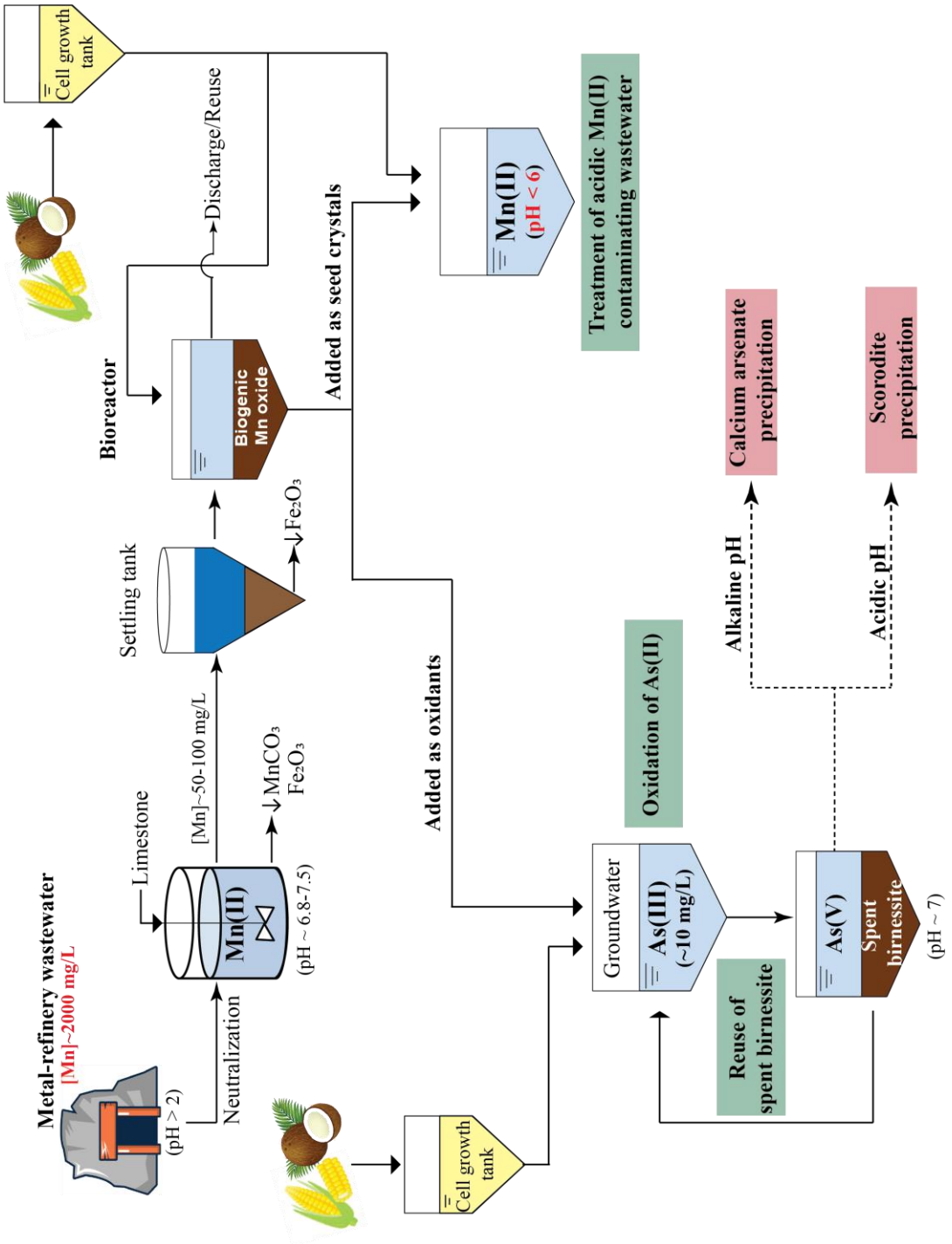

Figure 9.2 Proposed flowsheet of bioprocess for Mn(II)-contaminating metal-refinery wastewater treatment and utilization of derived biogenic birnessite for As(III)-oxidation processes.

9.2 Future recommendation works

9.2.1 Mn(II)-oxidative removal under acidic condition

- Search and isolation of moderately acidophilic Mn(II)-oxidizing microorganisms
- Feeding of biogenic birnessite seed crystals

9.2.2 Mn(II)-oxidative removal by biofilter column

- Utilization of digested local products (ex: coconut shell or maize) as nutrient for Mn(II)-oxidizing bacteria.
- To reduce the addition of organic carbon to the feed, colonization of mixed cultures of autotrophic bacteria might be mandatory to derive nutrient for Mn(II)-oxidizing bacteria.
- Optimization of the ratio of particulate bio-AC and pulverized AC to improve Mn(II)-oxidative removal efficiency.
- Trial for up-flow biofilter column system to improve contact between wastewater and bio-AC.

9.2.3 As(III)-oxidation by biogenic birnessite

- In order to utilize biogenic birnessite in wider pH range, aging/transformation into more stable Mn-oxide phase is required.
- To improve the stability as well as keeping the oxidizing power, optimization of the ratio of layered and tunnel Mn-oxide mix phases is necessary.

Acknowledgements

First of all, I would like to show my greatest appreciation to my supervisor, associate Prof. Naoko Okibe, for her enormous supports and invaluable suggestions throughout the course of my Master's and Ph.D. courses. She spent much of her precious time and efforts teaching me not only research but life's lesson. She ignored my broken Japanese and even encouraged me to use it to speak with her. I might not success job hunting without her support. I am honored to be her first international student.

Besides, I would like to express my sincerely thanks to my thesis committee, Prof. Takahiro Kuba and Prof. Keiko Sasaki, for their important suggestions, invaluable comments, and constant encouragements. They provided me with critical advice for understanding the results obtained from my experiments.

My appreciation also goes to Prof. Tsuyoshi Hirajima, associate Prof. Hajime Miki, and assistant Prof. Moriyasu Nonaka for their technical advice and insightful comments. Mrs. Makiko Semba for her technical supports and arrangement in the lab's activity.

I would like to show my appreciation to Dr. Sabrina Hedrich, Dr. Axel Schipper, Dr. Ruiyong Zhang from Bundesanstalt fur Geowissenschaften und Rohstoffe (BGR), Germany. Dr. Naoaki Kataoka, Dr. Takao Hagino, Mr. Sen Shimamoto and Mr. Suzuki from Swing corporation for accepting me as an internship student and for taking care of me.

I would like to thank the Advanced Graduate Program in Global Strategy for Green Asia. This educational program provided me with meaningful opportunities to learn and understand the relationship between technologies and society. I am also grateful for the financial support provided by the program.

My appreciation also goes to Assist. Prof. Takahiro Funatsu, Ms. Miwa Hirashima, and Ms. Minako Matsue (as secretaries) in Advanced Graduate Program in Global Strategy for Green Asia education center, who gave me kind supports and encouragement.

The XAFS experiments were performed at Kyushu University Beamline (Saga-LS /BL06, No. 2016IIIK006) under the supervision of associate Prof. Takeharu Sugiyama.

I have great pleasure in acknowledging my heartful thanks to Lab. Members in Mineral Processing, Recycling and Environmental Remediation Laboratory as follows; Dr. Sayo Moriyama, Dr. Mohsen M. Farahat, Dr. Ahmed M. Elmahdy, Dr. Paulmanickam Koilraj, Dr. Widi Astuti, Dr. Mutia Dewi Yuniati, Dr. Wuhui Luo, Dr. Yusei Masaki, Dr. Gde Pandhe Wisnu Suyantara, Dr. Xiangchun Liu, Dr. Masahito Tanaka, Dr. Intan Nurul Rizki, Dr. Binglin Guo, Shiori Morishita, Taichi Momoki, Osamu Ichikawa, Mari Yoshida, Kojo Twum Konadu, Yuken Fukano, Daisuke Nakayama, Hidekazu Matsuoka, Yu Takaki, Kenta Toshiyuki, Akinobu Iguchi, Katsutoshi Tsutsumi, Takahiro Matsumoto, Keishi Oyama, Tsubasa Oji, Akihiro Inoue, Shugo Nagato, Kazuyoshi Oka, Melisa Pramesti Dewi, Yuta Era, Takeru Fukumori, Taigen Masuyama, Ryota Matsushita, Yusuke Hotta, Kyohei Takamatsu, Yuta Kamura, Yoshikazu Hayashi, Yu hirayama, Yukihiro Muta, Tian Quanzhi, Ryohei Nishi, Haruki Noguchi, Shunsuke Imamura, Shingo Nakama, Shogo Nagano, Chitiphon Chuaicham, Yu Tanaka, Yuya Komori, Yuta Orii, Yuna Watanabe, Kinato Yagi, Wang mengmeng, Diego Moizes Mendoza Flores, Kohei Nonaka, Kaito Hayashi, Ryotaro Sakai, Zenta Shirozu, and Yuki Semoto.

It was great pleasure to be together in the laboratory.

Last but no least, I would also like to express my gratitude to my parents, Thanawat Kitjanukit and Phattharawaran Kitjanukit for their moral supports and warm encouragements. Ensuring that the fire keeps burning and be with me when I required motivation.

September 2019, Santisak Kitjanukit
Kyushu University
Fukuoka, Japan